Thermally Stable Polymers from 1,4,5,8-Naphthalenetetracarboxylic Acid and Aromatic Tetraamines

R. L. VAN DEUSEN, O. K. GOINS, and A. J. SICREE,
*Air Force Materials Laboratory, Nonmetallic Materials Laboratory,
Polymer Branch, Wright-Patterson Air Force Base, Ohio 45433*

Synopsis

Polycondensations of 1,4,5,8-naphthalenetetracarboxylic acid (NTCA) with both 3,3'-diaminobenzidine (DAB) and 1,2,4,5-tetraaminobenzene tetrahydrochloride (TAB) in polyphosphoric acid (PPA) were found to produce soluble polymers which exhibit excellent thermal stabilities. Polymer structures were deduced from infrared, thermal, and elemental analyses of model compounds and polymers. Polymer derived from TAB had a ladder-type structure. Polymers with solution viscosities near 1 or above (determined in H_2SO_4) were obtained from polymerizations near 200°C., and analysis showed these to possess a very high degree of completely cyclized benzimidazobenzophenanthroline structure. Less vigorous reaction conditions gave polymers with lower solution viscosities which appeared to be less highly cyclized. Low-viscosity polymer was also prepared from DAB and NTCA by solid-phase polycondensation. Some advancements in the solution viscosities of polymers synthesized from DAB in PPA were caused by second staging in the solid phase.

INTRODUCTION

The superior thermal stabilities exhibited by polybenzimidazoles[1] and polyimides[2,3] have been known for some time. Polymers with more highly fused benzimidazole-benzimide type structures have since been found to have outstanding thermal stabilities.[4-6] Another class of highly fused polymers which are remarkably heat stable are the polybenzimidazobenzophenanthrolines synthesized in this laboratory.[7] This paper describes the preparation and some properties of these latter polymers. Synthesis is based upon condensation of 1,8-dicarboxynaphthalene compounds with aromatic amines which have been well known for many years and utilized in the dye industry.[8] Extension of these types of condensations by using tetrafunctional acids and tetrafunctional amines has been utilized to obtain tractable polymers.

EXPERIMENTAL

Model Compounds

N-Phenylnaphthalimide (I) was prepared from 1,8-naphthalic anhydride and aniline in ethyl alcohol according to the method of Jaubert.[9] The crude

product was precipitated in aqueous HCl and washed with hot aqueous Na$_2$CO$_3$ and water. Recrystallization from ethyl alcohol gave colorless needles, m.p. 204–205°C. (lit. m.p., 202°C.).

ANAL. Calcd. for C$_{18}$H$_{11}$NO$_2$: C, 79.11%; H, 4.06%; N, 5.13%. Found: C, 78.64%; H, 4.15%; N. 5.10%.

N-(2-Aminophenyl)naphthalimide (II) was synthesized from 1,8-naphthalic anhydride and o-phenylenediamine as reported previously.[10] The product was successively extracted with ethanol and acetone. Recrystallizations from anhydrous acetone gave crystals, m.p. 308–311°C. (dec.) (lit. m.p., 300°C, dec.).

ANAL. Calcd. for C$_{18}$H$_{12}$N$_2$O$_2$: C, 74.99%; H, 4.20%; N, 9.72%. Found: C, 74.88%; H, 4.15%; N, 9.67%.

7H-Benzimidazo(2,1-a)benz(de)isoquinolin-7-one(III) was prepared (a) by the method of Okazaki[10] involving intramolecular condensation of N-(2-aminophenyl)naphthalimide(II) obtained from above and (b) by direct condensation of 1,8-naphthalic anhydride with o-phenylenediamine under conditions similar to those used for polymerizations:

(a) N-(2-Aminophenyl)naphthalimide was refluxed in glacial acetic acid for 16 hr. The product was isolated and recrystallized from ethyl alcohol, m.p., 211–212°C. (lit. m.p., 203–204°C.).

ANAL. Calcd. for C$_{18}$H$_{10}$N$_2$O: C, 79.99%; H, 3.73%; N, 10.36%. Found: C, 80.10%; H, 3.85%; N. 10.12%.

(b) Equimolar quantities of 1,8-naphthalic anhydride and o-phenylenediamine were reacted in PPA (0.02 mole/100 ml. PPA) at 160°C. for 16 hr. under nitrogen. Precipitation of the product in water and washing several times with water gave crude product yields of approximately 70%. This was purified by successive extractions with aqueous Na$_2$CO$_3$, water, and ethanol followed by recrystallizations from ethanol, m.p. 209–211°C. Mixed melting point determinations with III obtained from (a) above and comparisons of infrared spectra confirmed the identity of these compounds.

Monomers

1,4,5,8-Napthalenetetracarboxylic acid (NTCA) (Aldrich Chemical Co.) was reprecipitated several times with aqueous HCl from aqueous KOH solution following hot filtrations in the presence of activated carbon.

3,3'-Diaminobenzidine (DAB) was furnished by Narmco Research and Development Div., Whitaker Corp. This was analyzed and used as received.

1,2,4,5-Tetraaminobenzene tetrahydrochloride (TAB·4HCl) was prepared by the reduction of 1,3-dinitro-4,6-diaminobenzene and purified as the hydrochloride salt by the Dayton Laboratory of Monsanto Research Corporation. The tetrahydrochloride was used as received.

Polycondensations

Solution polymerizations were carried out in polyphosphoric acid (82–84% P_2O_5). Most favorable results were obtained when equimolar mixtures of monomers were stirred in warm PPA (previously purged with nitrogen at 100°C.) for a few minutes until the liquid became mobile and the solids appeared to be homogeneously dispersed. These mixtures were then gradually heated to specified reaction temperatures for varying lengths of time. The polycondensations were terminated by partially cooling the reaction solutions and pouring them onto crushed ice or into cold, aqueous alkali carbonate solutions. Due to the swollen nature of these polymers, it was expeditious to collect the solids by centrifugation and decantation as opposed to filtration. The wet solids were extracted with DMAC and/or methyl alcohol prior to final washing with ether. Polymers obtained by this treatment did not appear to be swollen. These were dissolved in an excess of concentrated H_2SO_4, reprecipitated in water, and successively extracted with water and absolute methyl alcohol. Yields were usually determined on the basis of polymer recovered after one such reprecipitation. Details of some representative solution polycondensations are given below.

Solid-phase reactions were carried out in a straightforward manner. Either equimolar mixtures of monomers of samples of previously isolated polymer were heated under nitrogen (after evacuation and flushing with nitrogen) or heated entirely *in vacuo*. After specified heating periods, the solids were cooled under nitrogen and reprecipitated from concentrated H_2SO_4 as above. An example is given below.

Secondary PPA reactions on previously isolated polymers amounted to dissolving the solids in the hot acid and stirring at temperatures near 200°C. The resulting polymers were isolated and reprecipitated in the manner described above.

Polymerization of NTCA and DAB in Solution. Under an atmosphere of nitrogen a mixture of 11.12 g. of NTCA, 8.06 g. of DAB and 350 ml. of PPA was stirred at 60°C. for 10 min. The temperature was gradually increased over a period of 7 hr. to 180°C. and maintained at 180–190°C. for 20 hr. The resulting polymer was isolated in water, extracted with DMAC and MeOH, reprecipitated from concentrated H_2SO_4, and dried for several hours at 100–120°C. *in vacuo*. The yield was 90% of soluble polymer which did not soften at 425°C. under a load of 1000 g./cm.². Prior to analysis, the product was heated for an additional 114 hr. at 165–185°C. *in vacuo;* $[\eta] = 1.15$ in concentrated H_2SO_4 (30°C.).

ANAL. Calcd. for $C_{26}H_{10}N_4O_2$: C, 76.09%; H, 2.46%; N, 13.65%; O, 7.80%. Found C, 72.58%; H, 3.29% (residue, 0.91%); N, 13.47%; O, 1.99%.

Extraction of this polymer for several hours with water followed by heating at 310–312°C. *in vacuo* caused an increase in intrinsic viscosity to 1.43. A sample of the product was reprecipitated from concentrated aqueous NaOH and resubmitted for analysis.

ANAL. Found: C, 73.62%; H, 2.72% (residue, 1.36%); N, 12.49%; O, 8.12%; P, 0.0%; S, 0.0%.

Emission spectrographic analysis showed Pb, 0.5; Si, 0.15; Al, 0.1; Fe, 0.1; Ni, 0.1; Cu, 0.1; Mg, 0.1; Sn, 0.005; Mn, 0.001; P and K, <1; Na and Zn, <0.1.

Polymerization of NTCA and DAB in Solid Phase. A reaction tube containing a mixture of NTCA (1.57 g.) and DAB (1.08 g.) was successively evacuated and purged with nitrogen. The mixture was heated under a small positive nitrogen pressure at a rate of approximately 5°C./min. Evolution of water was observed at 160–200°C. Heating above 200°C. was continued at approximately 1°C./min. to 285°C. and maintained at 285–295°C. for 4 hr. The reaction mixture was cooled under nitrogen and dissolved in concentrated H_2SO_4. Upon reprecipitation, the resulting polymer was found to have an inherent viscosity of 0.22 dl./g. measured at 0.54 g./dl. in concentrated sulfuric acid.

ANAL. Found: C, 73.89%; H, 3.02% (residue, 0.65%); N, 12.08%; O, 10.10%.

Polymerization of NTCA and TAB in Solution. Under nitrogen 5.90 g. of NTCA and 5.49 g. of TAB·4HCl were mixed with 300 ml. of PPA and stirred for 1 hr. near 75°C. to permit controllable evolution of hydrogen chloride. At a rate slightly above 1°C./min., the mixture was heated to 180°C. and maintained at 180–190°C. for 20 hr. The resulting polymer was isolated in the usual manner and dried under reduced pressure for several hours at 160–180°C. (83% yield). The soluble product was reprecipitated from concentrated H_2SO_4 and an inherent viscosity of 0.63 dl./g. was measured at a concentration of 0.15 g./dl. in the acid. A sample was heated at 350°C. for 4 hr. *in vacuo* prior to elemental analysis.

ANAL. Calcd. for $C_{26}H_6N_4O_2$: C, 71.86%; H, 1.81%; N, 16.75%; O, 9.57%. Found: C, 70.97%; H, 2.13% (residue 0.0%); N, 14.47%; O, 12.15%; P, 0.0%.

This sample was heated again for 1 hr. *in vacuo* at 475°C.

ANAL. Found: C, 71.55; H, 2.17; N, 14.65; O, 11.54.

Some spectra changes due to heating were observable only in the region near 6–7 μ (See Fig. 8 below).

Solution viscosities in concentrated H_2SO_4 were determined on polymer samples previously reprecipitated from concentrated H_2SO_4. The data was obtained at 30°C. in Ubbelohde dilution viscometers. Solution concentrations were calculated on the basis of quantitative dilutions. Extrapolations of the data to zero concentrations to obtain intrinsic viscosities given in Table II were straightforward with no unusual effects.

TGA measurements were obtained through G. F. L. Ehlers, AF Materials Laboratory, from 0.2 g. samples on a Chevenard thermobalance. A heating rate of 150°C./hr. to 900°C. was employed for determinations in both nitrogen and air atmosphere.

Softening point determination was performed on an automatic Vicat-type heat-distortion and softening-range apparatus in this laboratory.

DISCUSSION

The primary objective of our work was to incorporate bisbenzimidazo-benzophenanthroline structure into linear polymer backbone:

 or
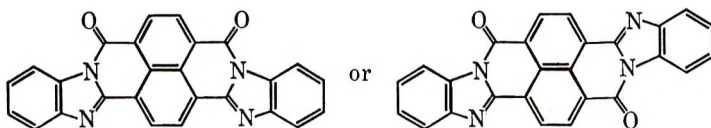
Polymers possessing this structure were prepared in polyphosphoric acid (PPA) from reactions of 1,4,5,8-naphthalenetetracarboxylic acid with 3,3′-diaminobenzidine and 1,2,4,5-tertaaminobenzene tetrahydrochloride. Although evidence indicating the probable presence of some incompletely cyclized structure was obtained, complete conversions to polymer can be represented by eqs. (1) and (2).

$$(1)$$

BBB

$$(2)$$

BBL
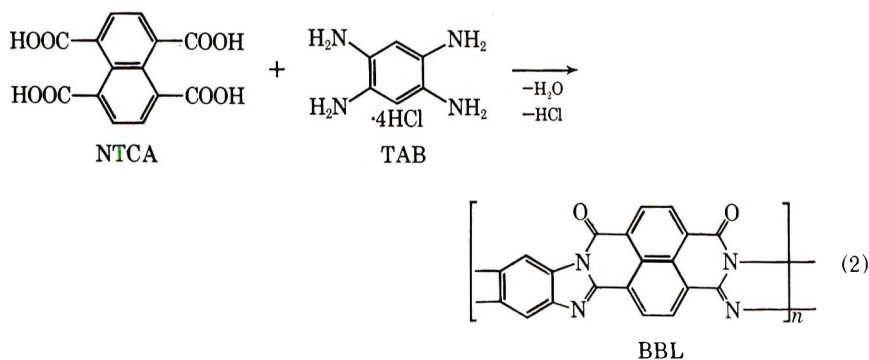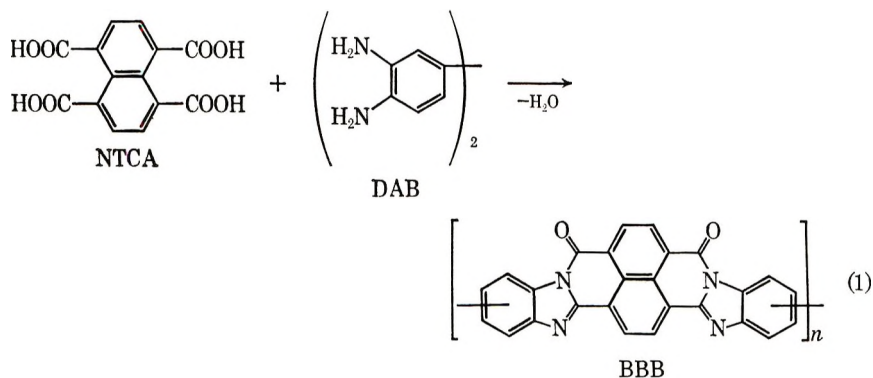
With reference to the representative structures given for BBB (the bisbenzimidazobenzophenanthroline polymer) and for BBL (the benzimidazo-benzophenanthroline-ladder polymer) only the *cis* isomers are depicted. All possible *cis* and *trans* isomers can be expected to occur, and this adds to the complexity of an already cumbersome nomenclature. As indicated earlier,[7] the benzimidazobenzophenanthroline (BB) system of naming is recommended for these types of polymers; i.e., poly(6,9-dihydro-6,9-dioxo-

bisbenzimidazo [2,1-_b_ : 1′,2′-_j_]benzo [1mn] [3,8]phenanthroline-2,13-diyl) for the BBB structure shown and poly(6,9-dihydro-6,9-dioxobisbenzimidazo-[2,1-_b_ : 1′,2′-_j_]benzo [1mn] [3,8]phenanthroline-2,3,12,13-tetrayl for the BBL structure shown.

The extent to which complete or perfect cyclization occurred, particularly in the case of the ladder-structured BBL, has not been established although the analytical results indicate the conversion to be very high. Imperfect structure could arise from incomplete cyclohydration, nonlinear branching, or incorporation of monomer contaminants such as triamine or triacid. BBL ladder propagation may be hindered to some extent by restricted rotational freedom of prepolymer backbone, whereas BBB propagation would be expected to be more facile. Nevertheless, crosslinking was not extensive in any of these solution polycondensations since polymerization reaction products were soluble to a very large extent. Very few polymer solvents could be found however, and concentrated polymer solutions were unattainable in most cases. Sulfuric acid solutions of low concentrations could be prepared for comparing the solution viscosities of polymers which were synthesized under different reaction conditions.

Model Compounds

Some condensation products which may arise from the reaction of 1,8-naphthalene dicarboxylic acid with _o_-phenylenediamine or aniline are shown (I–IV). During the course of this investigation, model compounds I, II and III were prepared and their infrared characteristics examined (Figs. 1–3). By the synthetic procedures used (see Experimental section) neither imidazol-acid (IV) nor intermediate amide condensates (V and possibly VI) were isolated as model compounds. Particular attention was given to spectra obtained from I and II as compared with III in the 6 μ region. Here it was noted that model compounds I and II, the incompletely cy-
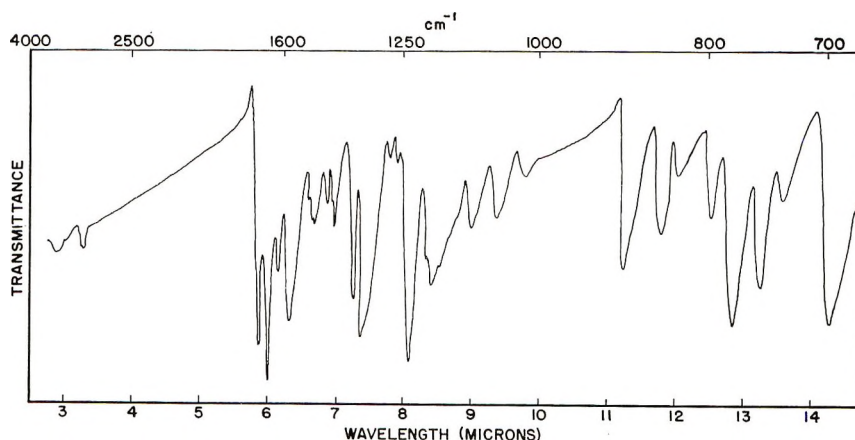

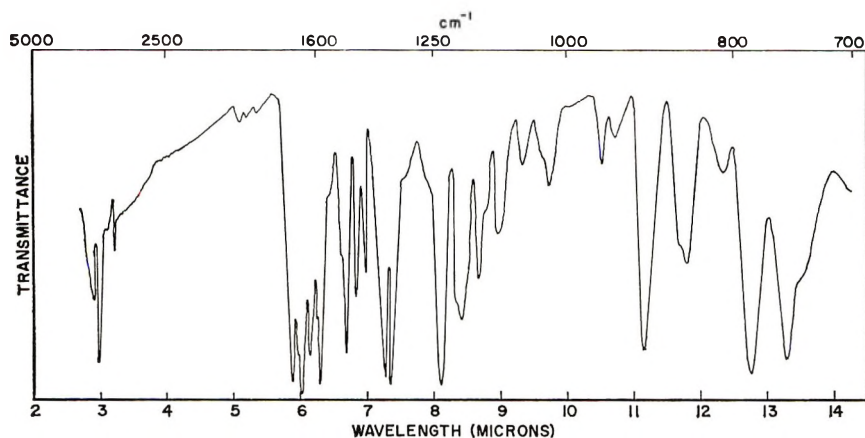Fig. 1. Analytical infrared spectrum of _N_-phenylnaphthalimide (model compound I).

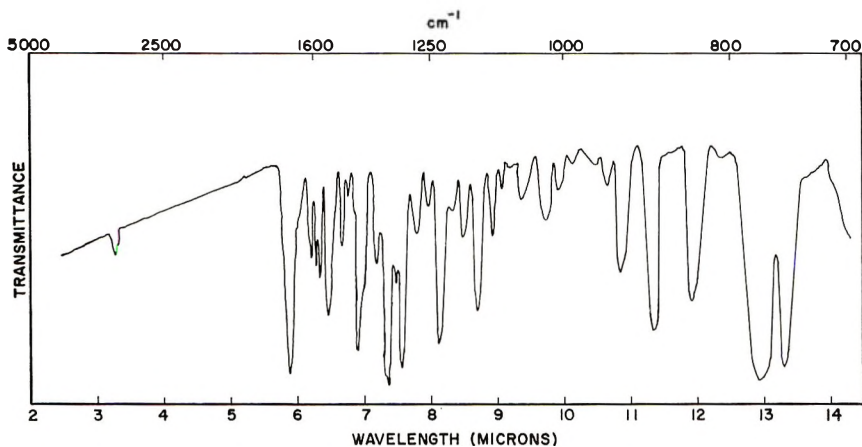Fig. 2. Analytical infrared spectrum of N-(2-aminophenyl)naphthalimide (model compound II).

Fig. 3. Analytical infrared Spectrum of 7H-benzimidazo(2,1-a)benz(de)isoquinolin-7-one (model compound III).

clized structures, absorbed intensely between 6.0 and 6.1 μ. The fully cyclized model compound III differed significantly, since it did not exhibit these pronounced absorption characteristics. This difference proved to be very useful in establishing that desired structures analogous to III were obtained in polymers.

The polybenzimidazobenzophenanthrolines were prepared at high reaction temperatures in PPA. Under these reaction conditions, isolation of initial polyamide condensates analogous to V and VI were not expected. Further, evidence described in the following sections support the idea that intermediate or prepolymer structures analogous to II or IV preferentially underwent continued intramolecular cyclodehydration to the highly fused BBB and BBL structures.
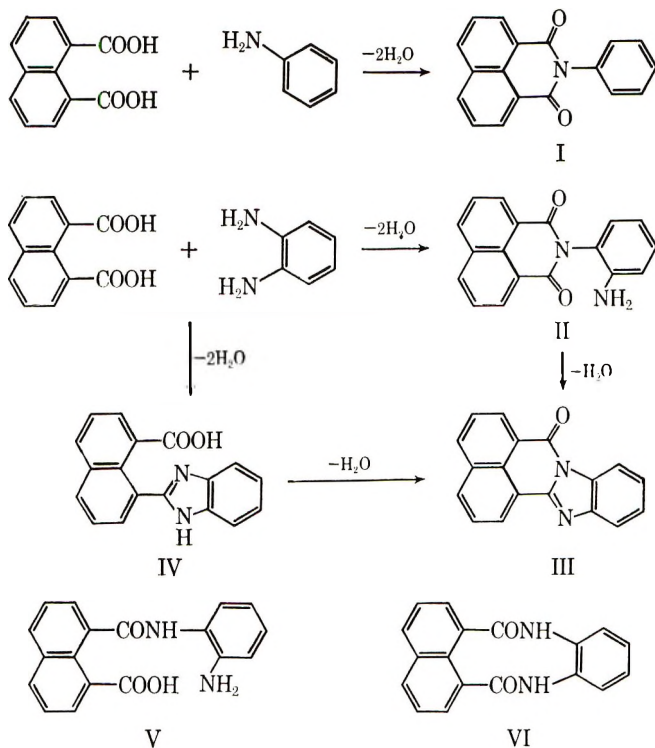
Polymer Structure

Comparisons of infrared spectra obtained on polymer samples with those spectra obtained from model compounds gave substantial evidence that polycondensations had produced cyclized backbone structures.   Spectra of high-viscosity (i.e., 1.0 or greater) BBB closely resembled the spectra of model compound III in the 5.9–6.5 μ region (Fig. 4).   Unresolved absorption maxima near 6.2 and 6.3 μ of polymer spectra appear to be resolved into pairs of peaks in this region for III (Fig. 3).   Intense absorptions in the 6.0–6.1 μ region which were found to be typical for incompletely cyclized model compounds I and II (Figs. 1 and 2) were not apparent in the polymer spectra.   These characteristics are summarized in Table I.

TABLE I
Infrared Absorption Characteristics in Region of 5.9–6.5 μ

	Peaks[a]				
	5.9 μ	6.0–6.1 μ	6.2 μ	6.3 μ	6.4–6.5 μ
Model I	X	M	XX	XX	—
Model II	X	M	XX	XX	—
Model III	X	—	XX	XX	X
High η BBB	X	—	X	X	X

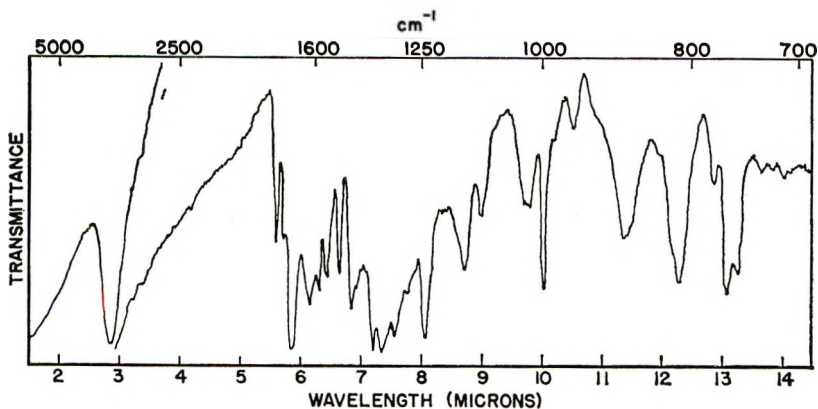[a]Peaks designated as X (single), XX (double), and M (multiple).

Fig. 4. Representative analytical infrared spectrum of high-viscosity BBB polymer prepared in PPA.
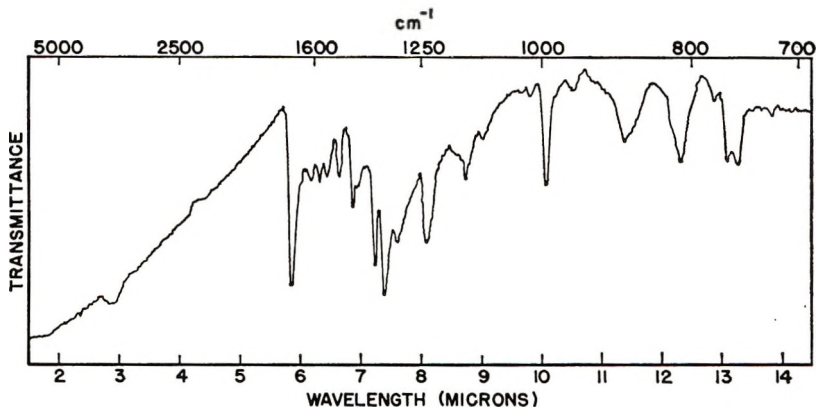

Fig. 5. Representative analytical infrared spectrum of low-viscosity BBB polymer prepared by solid-phase reaction.

Low-viscosity BBB polymers (i.e., less than 0.5 dl./g.) gave spectra typically represented by Figure 5 of the polymer prepared in the solid phase. These spectra contained bands not normally found for higher viscosity BBB (Fig. 4). Evidence of absorption in low-viscosity samples in the 5.6–5.8 and 3 μ regions are believed to be due to anhydride endgroups or incomplete cyclization, i.e., imide carbonyl.[2,6] Clear indication of incomplete cyclization by 6.0–6.1 μ absorption is not observed, possibly due to poor resolution, although absorption between 3.0 and 3.4 μ may suggest the presence of incompletely cyclized imidazole-acid (IV) in low-viscosity BBB.

In a few instances, 5.6 and 5.8 μ absorptions in low polymers appeared to be decreased in intensity by second-stage heating in the solid phase. These observations were not satisfactorily substantiated however, due to difficulties in obtaining reproducibility in spectral resolution.

As expected, spectra of BBL (Fig. 7) had characteristics similar to those of BBB, the 5.9 μ carbonyl absorption being the most striking. In the
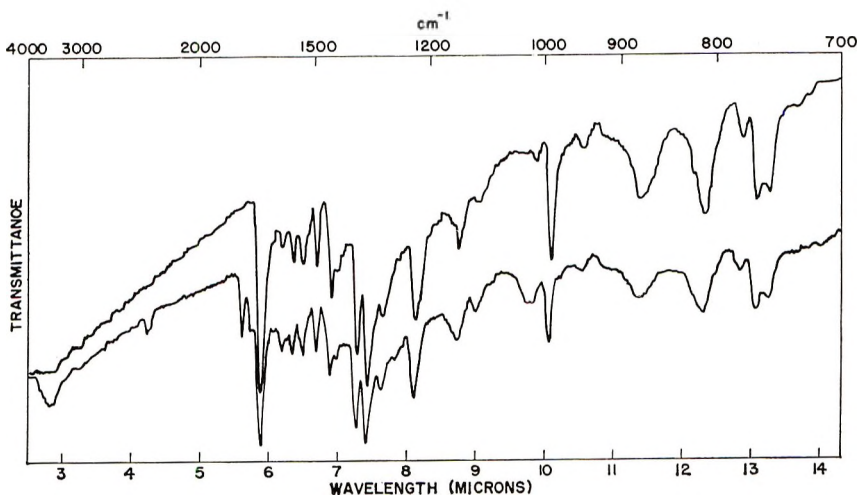
Fig. 6. Comparison of spectra obtained on products from secondary PPA reaction of BBB polymer: (top) insoluble BBB polymer product; (bottom) soluble BBB polymer product.
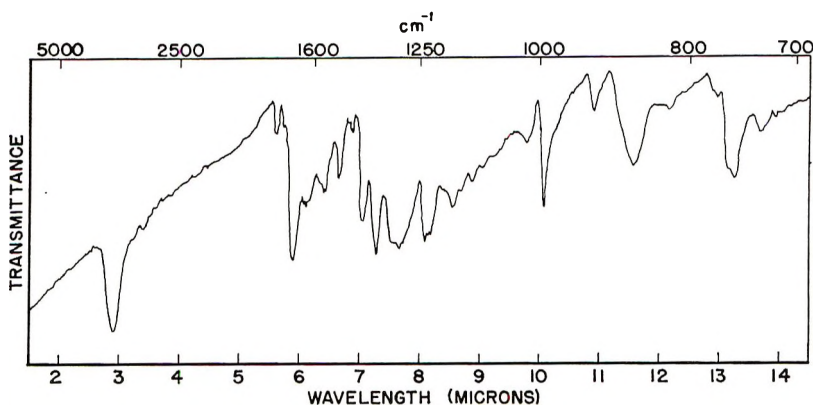

Fig. 7. Representative analytical infrared spectrum of low-viscosity BBL polymer prepared in PPA.

region of 6.0–6.4 μ, it is noticeable that BBL differs by exhibiting absorption maxima (unresolved peaks) nearer to 6.1 and 6.4 μ than to the maxima near 6.2, 6.3, and 6.4 μ found for BBB. Much like the low-viscosity BBB discussed above, low-viscosity BBL exhibited peaks likely indicating incompletely cyclized structure or endgroups. Sufficient evidence to indicate continued cyclization upon post heating of BBL was not obtained although some indication that structural changes may occur was suggested by small differences in spectra (Fig. 8) and elemental analysis (see Experimental section) after heating to 475°C.

By nature the polymers are intensely colored and difficult to grind so that information from infrared spectra was difficult to obtain. Nevertheless,
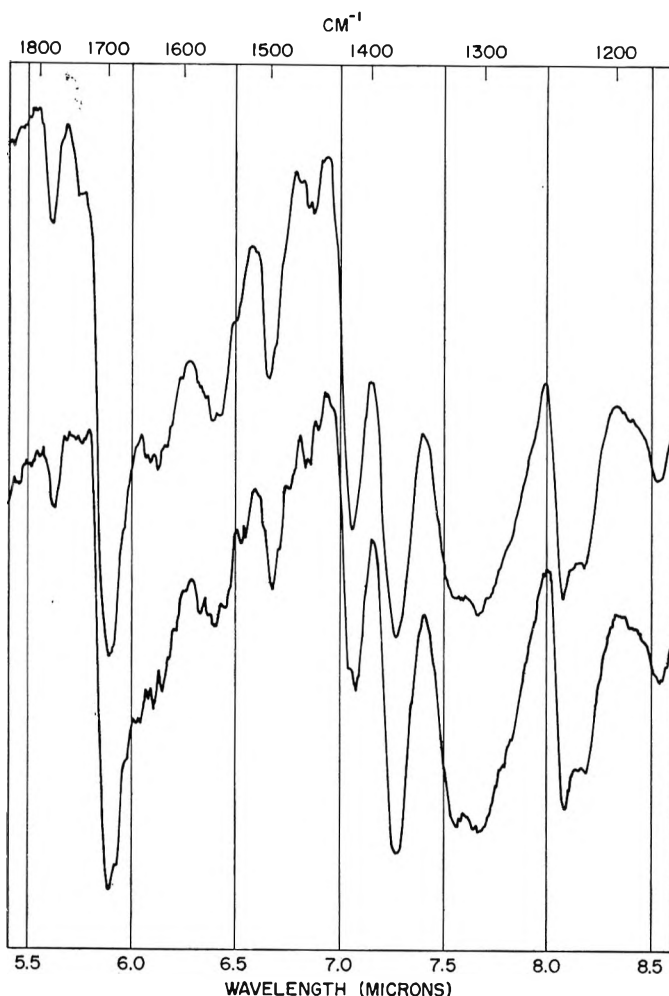
Fig. 8. Effects of post heating upon the 6.0–8.0 μ region of BBL spectra: (bottom) polymer heated at 350°C. for 4 hr. *in vacuo* followed by (top) heating at 475°C. for 1 hr. *in vacuo*.

considering the evidence available, it appears that polymers do indeed possess the BBB and BBL structures. That the extent of cyclization tends to be complete for the high-viscosity BBB polymers seems to be quite certain. This conclusion is further substantiated by results from thermal and elemental analysis. As previously mentioned, the presence of poly-amide type structures analogous to V or VI is very unlikely due to the high-temperature procedures used here. In fact polymer stabilities (Fig. 9) exceed those of unsubstituted aromatic polyamides.[11] Even if this were not the case, amide analogs would be expected to lose weight by branching or intramolecular cyclization reactions at temperatures well below 300°C. This is not the case, as is verified by the fact that BBB polymerization in the
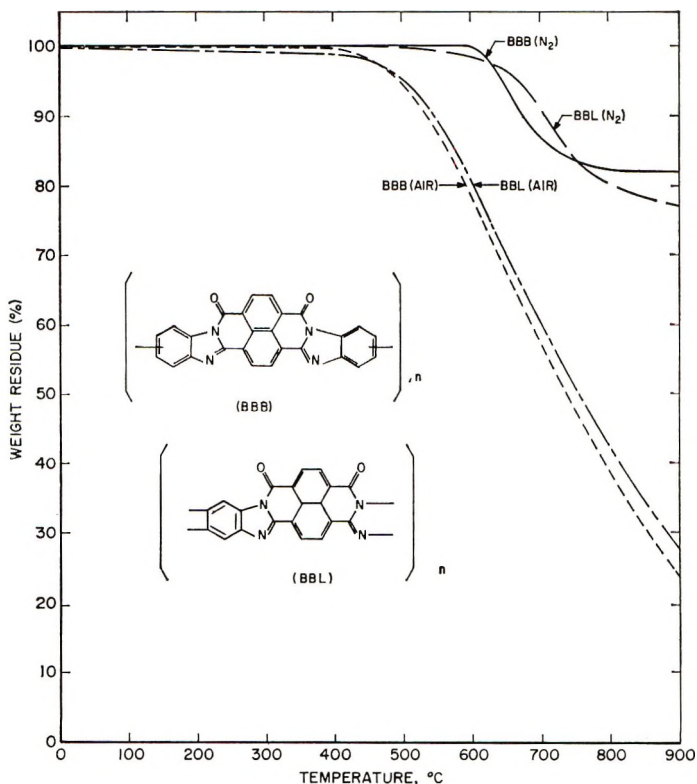
Fig. 9. TGA Comparison of BBB and BBL.   Heating rate = 150°C./hr.

solid phase gave completely soluble, low-viscosity polymer (Fig. 5) below 300°C. which was found to show only 3% weight loss up to 600°C. by TGA under nitrogen.   Further, results of elemental analysis did not indicate the presence of amide when compared with theoretical values calculated for various degrees of cyclization.   It should be pointed out that elemental analyses were not in complete agreement with calculated values for fully cyclized structures.   This is not uncommon for highly fused aromatic-heterocyclic polymers.   Also emission spectroscopy revealed the presence of metallic impurities probably scavenged from the acid solvents.   In this light, the results of analyses appear to substantiate very well the predominance of completely cyclized structures.   It is noteworthy that even the short, low-temperature polycondensations did not appear to have been interrupted at a prepolymer stage.   The properties of these low polymer products indicated the presence of extensive cyclization as above.

Polymer Properties

Polybenzimidazobenzophenanthrolines varying in solution viscosities were obtained.   For typical dilute solution BBB polycondensations (Table II), more vigorous reaction conditions tended to produce polymers with

TABLE II
Comparisons of Some Typical Equimolar
Polycondensations in PPA

Type reaction	Monomer concentration, mole/l.[a]	Reaction Conditions		Viscosity (H₂SO₄)[b]
		Temp., °C.	Time, hr.	
BBB	0.40	110–120	18	0.57
BBL	0.20	100–130	18	0.28
BBB	0.22	180–190	20	1.35
BBL	0.18	180–190	20	0.63
BBB	0.40	200–220	3.5	0.75
BBL	0.19	200–220	4.5	0.34
BBL	0.13	190–195	24	0.90

[a] Total concentration of both monomers in PPA.
[b] η_{inh}, 30°C.; BBB concn. 0.5 g./dl.; BBL conc., 0.2 g./dl.

higher solution viscosities. Similar effects were noted for BBL polymerizations, although significantly lower viscosities were obtained under comparable conditions. Valid comparisons of these viscosities to reflect relative degrees of polymerization between BBB and BBL cannot be made, however, since the effects of the molecular structure differences upon the observed solution properties have not been established. BBB's with inherent viscosities less than 0.5 dl./g. were prepared in PPA under milder conditions. Reactions of short duration near 100°C. were found to produce products which were somewhat easier to dissolve and had inherent viscosities of the order of 0.1–0.2 dl./g. in sulfuric acid 30°C. Monomers were also condensed in the solid phase to produce low BBB polymer which was completely soluble (η_{inh} = 0.2). A solid-phase BBL experiment to determine the feasibility of using tetraaminobenzene hydrochloride salt for melt condensation gave negative results.

All polymers appeared black although acid solutions were intensely colored red. Aqueous alkali solutions were dark brown. Of many solvents examined, BBB and BBL polymers were found to be soluble in concentrated sulfuric acid, polyphosphoric acid, methanesulfonic acid, benzenesulfonic acid, methylene sulfate dimer, 85% phosphoric acid, and concentrated aqueous sodium or potassium hydroxide. The polymers were insoluble in many other organic solvents such as DMAC, HMP, cresol, formic acid, and numerous others. The casting of films and the determination of molecular weights have not been accomplished due to the lack of suitable solvents. BBB polymers were less difficultly soluble than BBL but several days of stirring were required to prepare BBB sulfuric acid solutions of 1–2% concentration at room temperature. Solutions of 5–10% concentration were obtainable by heating near 100°C. This polymer has fiber-forming properties and is sufficiently soluble in the acid to be spun into multifilament yarn.[12] With BBL, solutions of 0.2 g./dl. or less were obtained after approximately two weeks of mixing. Nevertheless, attempts to achieve

solution concentrations of 0.5 g./dl. were unsuccessful with the use of BBL which had been previously dissolved completely and reprecipitated from a large excess of sulfuric acid. Incompletely dissolved materials were detectable upon filtration, so that meaningful solution viscosities could not be determined on these samples. All viscosities reported in this paper were determined at concentrations where samples were completely soluble.

Polymer species which exist in solutions have not been determined. Although intrinsic viscosity data do not give evidence of polyelectrolyte effects, the presence of ionic species are likely. Polymers have been reprecipitated from all of the solvents found to dissolve them with no apparent alteration in structure of the polymer recovered. For example, no changes were noted in infrared spectra of polymers reprecipitated from 15–20M KOH after heating near 100°C. for several hours. Similar stability was observed in sulfuric acid. The intrinsic viscosity of a BBB sample, 0.80, was unchanged after reprecipitation from concentrated sulfuric acid solution which had been heated up to 70–80°C. for approximately 16 hr. Polymers were routinely extracted in boiling water for many hours as a means of removing impurities with no evidence of hydrolysis detected.

Inherent viscosities of low BBB polymers were found to be affected to some extent by secondary reactions. A sample dried at 135–145°C. for 65 hr. under reduced pressure had an inherent viscosity of 0.18 dl./g. in concentrated sulfuric acid (0.5 g./dl. at 30°C.). This was advanced to 0.24 dl./g. by more vigorous second staging: 18 hr. at 275–290°C. followed by 5.5 hr. at 300–335°C. under nitrogen. Similar results were obtained on other low-viscosity BBB samples. These small increases in viscosity may have resulted from chain extension reactions although other things such as further intramolecular cyclization to increase chain "stiffness" could alter solution properties. In another instance, a 0.12 dl./g. inherent viscosity BBB polymer was subjected to a secondary reaction in PPA for 4 hr. at 210–240°C. Approximately one-half of the recovered product was found to be insoluble in concentrated sulfuric acid probably indicating that further reaction had taken place to produce a network structure. After being reprecipitated and dried for 24 hr. near 200°C., the acid-soluble portion of the product was found to have an inherent viscosity of 0.29 dl./g. This was a greater than twofold increase from the original value, although it is unlikely that this increase reflects the full extent of advancement caused by secondary reaction. The spectrum of the 0.29 viscosity polymer (Fig. 6) was analogous to that of the original polymer of 0.12 viscosity. Absorption peaks commonly found for all low viscosity BBB polymers at 5.6 and 5.8 μ (Fig. 5) were readily apparent in both. The spectrum of the insoluble portion of the secondary reaction product (also shown in Fig. 6) did not exhibit prominent 5.6 and 5.8 μ absorptions. Differences are also noted in the 8.8 and 9.8 μ regions. In fact, the insoluble polymer spectrum closely resembled spectra (Fig. 5) found for soluble, high-viscosity BBB polymers. Thus, this routine examination by infrared did not provide evidence for postulating a crosslinking process.

Proof that linear polycondensation could occur in the solid phase was established by slowly heating BBB monomers to temperatures approaching 300°C. under nitrogen. Water evolution was observed. The resulting polymer was found to be completely soluble with an inherent viscosity of 0.22 dl./g. The infrared curve was typical of low-viscosity BBB (Fig. 5). Considering the results obtained on polybenzimidazoles,[1] one might expect that use of the phenyl ester of monomer acid would give higher viscosity BBB in solid phase reactions.

The higher BBB polymers prepared in PPA also exhibited increases in solution viscosities as a result of secondary reactions in the solid phase. For example, a 0.49 intrinsic viscosity polymer exhibited an overall twofold increase on second-stage heating, although higher molecular weight polymers did not appear to be affected to this great an extent (Table I). This

TABLE III
Effects of Solid-Phase Heating (*in Vacuo*) Upon
Intrinsic Viscosities of BBB Polymers[a]

Intrinsic viscosity		
100–120°C. 16 hr. (or more)	165–185°C. 114 hr.	300–350°C. 4–5 hr.
0.49	0.60	1.01
0.80[b]	—	1.03[c]
—	1.15	1.43

[a] Reprecipitated from H_2SO_4 prior to $[\eta]$ determination in H_2SO_4 (30°C.).
[b] $[\eta]$ in benzenesulfonic acid = 1.29.
[c] 36 hr. at 200°C. (N_2).

possibly provides some indication of the levels of cyclization, although definitive evidence such as exact changes in spectral and solubility characteristics was lacking.

As mentioned above, BBL is completely soluble only at very low concentration. This poor solubility property has thus far limited examination of secondary reaction effects. The ladder-type structure would be expected to be more rigid and less readily soluble. The inherent viscosities listed in Table II for BBL polymers were measured on solutions considered to be of near maximum concentration for room temperature solubility. More recently however, it has been found in our laboratory that the ease of polymer solubility can be improved by freeze-drying wet polymer.[13] Ordinarily, polymers were reprecipitated in aqueous media. Water was then removed from the wet polymers by methanol extractions followed by ether washings. This methanol–ether treatment caused dramatic shrinking of the wet swollen polymers. Conversely, removal of water from wet polymer by using freeze-drying procedure appears to eliminate this shrinking and render fluffy polymer which is more readily dissolved.

A BBB polymer sample ($[\eta] = 0.8$) was examined by x-ray diffraction, and no evidence of crystallinity was found. An attempt to determine the
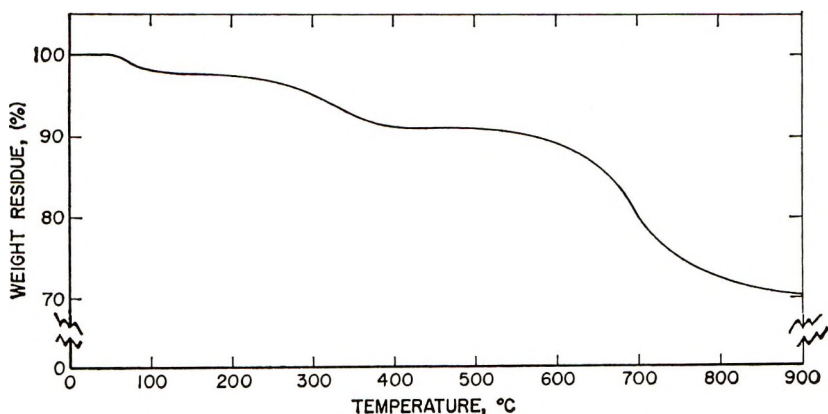
Fig. 10. TGA of insoluble BBB polymer prepared by secondary reaction in PPA of BBB polymer of 0.12 inherent viscosity.   Heating rate = 150°C./hr.
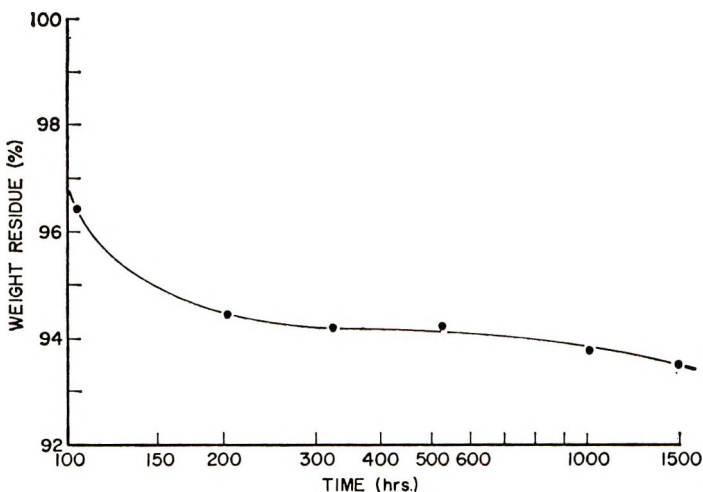

Fig. 11. Isothermal aging of BBB polymer: (600°F. in air).

softening point of this amorphous material gave no indication of softening up to 425°C., the temperature limit of the apparatus.   Thermally decomposed polymer residues retrieved from thermal gravimetric analysis (150°C./hr. to 900°C.) were found to be free-flowing powders which did not appear to have been fused.   These observations suggest that polybenzimidazobenzophenanthrolines may not undergo transitions prior to decomposition.

The thermal stability of BB polymers appeared to be excellent.   For example, the 0.80 and 1.15 intrinsic viscosity samples of BBB shown in Table III exhibited no weight loss by thermal gravimetric analysis (TGA) in nitrogen to 600°C.   Other BB polymers listed in Tables II and III showed less than 2% weight loss by this technique.   BBL polymers typically exhibited weight losses of 2–4% under similar analysis, although catastrophic decomposition appeared to occur above 600°C.   Heating in

air at 150°C./hr. normally caused weight losses of the order of 5% up to 500°C. for both type polymers. Examples of TGA curves are shown in Figure 9.

In view of the previously discussed conclusions reached by examining viscosities, infrared absorption characteristics and elemental compositions, it does not seem unreasonable to find initial weight losses occurring earlier for BBL than for high viscosity BBB. The evidence indicates that less perfect structure was achieved in the ladder-type polymer.

It is of some interest to note the TGA curve obtained from the insoluble BBB polymer produced by the secondary PPA reaction (discussed above). This differed significantly from other TGA curves of soluble polymers (Fig. 10). The insoluble polymer appeared to degrade in a stepwise fashion to a lower weight residue which qualitatively tends to support the idea that weaker bonds (such as might be expected for crosslinks) are present in the polymer.

Preliminary results of an isothermal aging test (Fig. 11) of BBB polymer indicated weight losses to be less than 10% at 315°C. after 1500 hr. in air.[14] The maximum rate of decomposition for this polymer was found to be in the region of 610–620°C. when determined by DTA at a heating rate of 10°C/min. in air.

References

1. H. Vogel and C. S. Marvel, *J. Polymer Sci.*, **50**, 511 (1961); *J. Polymer Sci. A*, **1**, 1531 (1963).

2. G. M. Bower and L. W. Frost, *J. Polymer Sci. A*, **1**, 3135 (1963).

3. C. E. Scroog, A. L. Endrey, S. V. Abramo, C. E. Berr, W. M. Edwards, and K. L. Olivier, *J. Polymer Sci. A*, **3**, 1373 (1965).

4. F. Dawans and C. S. Marvel, *J. Polymer Sci. A*, **3**, 3549 (1965).

5. V. L. Bell and G. F. Pezdirtz, *J. Polymer Sci. B*, **3**, 977 (1965).

6. J. Colson, R. Michel, and R. Paufler, *J. Polymer Sci. A-1*, **4**, 59 (1966).

7. R. L. Van Deusen, *J. Polymer Sci. B*, **4**, 211 (1966).

8. H. A. Lubs, *The Chemistry of Synthetic Dyes and Pigments*, Reinhold, New York, 1955, p. 475.

9. G. F. Jaubert, *Ber.*, 360 (1895).

10. M. J. Okazaki, *J. Soc. Org. Chem. Japan*, **13**, 80 (1955); *Chem. Abstr.*, **51**, 27452 (1957).

11. J. Preston, *J. Polymer Sci. A-1*, **4**, 529 (1966).

12. W. H. Gloor, *J. Polymer Sci.*, in press; *Polymer Preprints*, **7**, No. 2, 819 (1966).

13. T. E. Helminiak, Air Force Materials Laboratory, Wright-Patterson Air Force Base, Ohio, private communication.

14. H. H. Levine, Whittaker Corporation, Narmco Research and Development Division, San Diego, California, private communication.

Retardation of Discoloration of Poly(vinyl Chloride) and Decolorization of Discolored Poly(vinyl Chloride) with Diimide
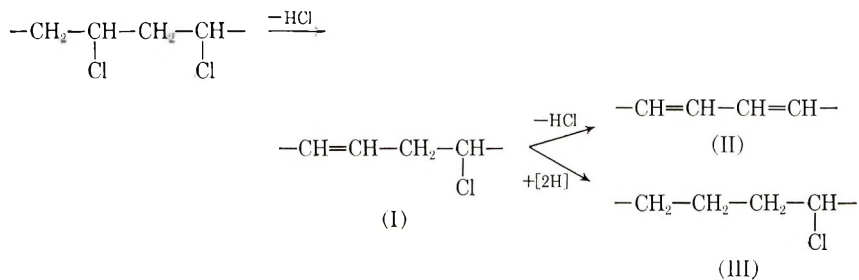
TSUTOMU NAKAGAWA, *Industrial Arts Institute of the Japanese Government, Shimomaruko, Oota-ku, Tokyo, Japan*, and MAKOTO OKAWARA, *Research Laboratory of Resources Utilization, Tokyo Institute of Technology, Ookayama, Megro-ku, Tokyo, Japan*

Synopsis

Retardation of discoloration of poly(vinyl chloride) with diimide was studied in dimethylformamide at 130°C. with the use of p-toluenesulfonylhydrazide (PSH) as a source of diimide. A process was proposed that involved prolonging the induction periods of discoloration by inhibiting the development of conjugated polyene structure. The optimum proportion of PSH was one fourth of the poly(vinyl chloride), the best results. Furthermore, poly(vinyl chloride) discolored by thermal degradation in o-dichlorobenzene or gamma-ray irradiation under vacuum was decolorized in solution at 130°C. by addition of PSH. The decolorized poly(vinyl chloride) thus obtained was thermally stable compared with that obtained by oxidative methods.

INTRODUCTION

Improvement of the thermal stability is one of the most important and practical modifications of poly(vinyl chloride), or PVC. The deterioration of PVC is known to proceed through a rapid and sequential elimination of hydrogen chloride along a length of polymer chain, giving rise to a chromophoric and easily oxidizable polyene structure. The ease of formation of the 1,3 diene structure (II), once a double bond has formed at a weak point of PVC (I), is readily understood in terms of the allylic effect of an olefinic group upon an adjoining chlorine-bearing carbon atom. Thus the polyene structure might be developed by this zipperlike elimination.

$$-CH_2-\underset{\underset{Cl}{|}}{CH}-CH_2-\underset{\underset{Cl}{|}}{CH}- \quad \xrightarrow{-HCl}$$

$$-CH=CH-CH_2-\underset{\underset{Cl}{|}}{CH}- \underset{(I)}{} \begin{array}{l} \xrightarrow{-HCl} -CH=CH-CH=CH- \quad \text{(II)} \\ \xrightarrow{+[2H]} -CH_2-CH_2-CH_2-\underset{\underset{Cl}{|}}{CH}- \quad \text{(III)} \end{array}$$

Accordingly, it is reasonable to expect that a reagent that can either inhibit the introduction of such an olefinic structure or, if such a structure is already present, alter it to a saturated structure, can thus serve to stabilize the polymer. The catalytic effect of a trace of hydrogen chloride, arising from PVC, on the following dehydrochlorination has been postulated,[1] and many investigations have been carried out in order to fix the hydrogen chloride generated.[2] Recently, however, another report has described that the effect of $(RCOO)_2SnR_2$ is ascribed to the substitution in PVC of carboxylate radicals[3] for labile chlorine. On the other hand, if the degraded PVC is saturated by reduction, the retardation of the development of conjugated polyene structure can be expected. Although there are various methods of saturating C=C double bonds with hydrogen, such as hydrogenation under high pressure and alkali metal reduction in ammonia (Birch's method), they are not available in the processing of PVC. The decolorization method for discolored PVC, the post chlorination method,[4] and the bleaching method with oxygen[5] have been reported. Furthermore, the free radicals, arising from α,α'-azobisisobutyronitrile,[6] peroxides, and solvents containing peroxides,[7] have been known to be effective for the decolorization. The oxidative decolorization, however, might be considered to result in the formation of unstable structures in decolorized PVC. On the other hand, the reductive decolorization might not cause changes in the inherent structures and properties of PVC, except that a small quantity of chlorine of PVC is substituted for with hydrogen.

Diimide (HN=NH) has been used to hydrogenate unsaturated compounds of low molecular weight,[8] and the mechanism has been postulated to involve the transition state, such as (IV).[9] If diimide hydrogenates C=C double bonds in the conjugated system, the discolored PVC is also expected to be decolorized by this method. The first purpose of our present work was to retard the discoloration of PVC; the second, to decolorize the discolored PVC, using the reductive method with diimide. p-Toluenesulfonylhydrazide, which is widely used as a blowing agent in the plastic industry, was used as a source of diimide throughout this work.
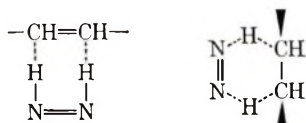
(IV)

EXPERIMENTAL

Reagents and Materials

PSH was purified by recrystallization from aqueous methanol. Dimethylformamide (DMF) and o-dichlorobenzene (ODB) were purified by distillation, and hexamethylphosphorictriamide (HMPA), which was supplied by Nippon Oil Seal Co., Ltd., was used without further purifica-

tion. A commercial PVC manufactured by Sumitomo Chemical Co., Ltd. (average degree of polymerization, 600) was purified by repeated precipitations with methanol from dioxane solutions and dried under vacuum.

Discolored PVC

The discolored PVC's used in these experiments were homogeneously prepared by the following methods.

(1) The purified PVC (9.4 g.) was dissolved in 300 ml. of ODB and heated to reflux at 180°C. under a nitrogen atmosphere. The color of the solution changed into black-brown in a few hours. After heating until a small amount of gel-like polymer appeared, 150 ml. of dioxane was added. This solution was filtered, the filtrate was poured into 4 liters of methanol, and the pale, brownish polymer that precipitated was filtered and immersed in fresh methanol overnight, filtered again, and dried under vacuum. The pale-brown powders thus obtained were coded PVC(T-1 to T-3). As shown in Table I, products having the same degree of discoloration were difficult to obtain.

TABLE I
Discolored PVC

Discolored PVC	Method of discoloration	E^a
PVC(T-1)	Heating in ODB at 180°C.	0.060
PVC(T-2)	Heating in ODB at 180°C.	0.041
PVC(T-3)	Heating in ODB at 180°C.	0.024
PVC(γ-T)	Heating at 98°C. after gamma-ray irradiation under vacuum	0.237
PVC(D-1)	Heating in DMF at 100–120°C.	0.270
PVCl$_2$(A)^b	Heating in aniline at 60°C.	0.096

^{a} $E = \log I_0/I = Ecl$, where c is concentration in g./l. and l is thickness of the cell in cm.

^{b} Vinylidene chloride–vinyl chloride copolymer (80:20 molar).

(2) Commercial PVC (30 g.), unpurified, was dissolved in 300 ml. of DMF and heated at 100–120°C. for about 2 hr. under a nitrogen atmosphere. The solution turned black-brown and was poured into 3 liters of methanol. The brown precipitate produced was filtered and washed thoroughly with methanol and dried under vacuum [PVC(D-1)].

(3) PVC film prepared by casting from tetrahydrofuran solution was irradiated to 20 Mrad under vacuum at room temperature by gamma-rays from a ^{60}Co source. After irradiation the film, which turned pale yellow, was heated at 98°C. for about 15 hr. to give a reddish-purple film [PVC(γ-T)].

(4) Film of vinylidene chloride–vinyl chloride copolymer (80:20 mole ratio) was heated in aniline at 60°C. for about 6 days, and the reddish-brown film was extracted with ether until the film did not contain aniline

[PVCl$_2$(A)]. The infrared absorption of ν_{NH} and the organic analysis of primary aromatic amine were used for determining the absence of free aniline in the film. That the aniline combined with the polymer was confirmed by the elementary analysis of nitrogen and by the infrared spectra, which showed the absorptions due to the aromatic ring and the C=N group.

The absorbances at 500 mμ of discolored polymers prepared by these methods are summarized in Table I.

Measurement of Degree of Discoloration

For measurement of the discoloration degree of the polymer about 4 ml. of solution was withdrawn from the reaction vessel at various time intervals, and measurements of the electronic spectra were carried out with a Hitachi EPS Type-2 Spectrophotometer and quartz cell (1 cm. thickness). The grades of discoloration of polymers in solutions were expressed by per cent transmission or absorbance at the wavelength of 500 mμ. The measurements of the ODB–PSH system were carried out in a range of temperatures high enough to dissolve PSH.

Gas Measuring Unit

A four-necked flask equipped with a thermometer, a glass tube, through which nitrogen gas was let in, and another tube connected to the gas buret. The side of the main neck had a rod inserted in it, on which a small dish filled with the weighed PSH was supported. The buret was connected to a leveling bulb, and both were filled with water. The flask containing the required volume of solvent was flushed with nitrogen gas and immersed in a constant-temperature bath. Magnetic stirring was used in these experiments. After dropping PSH with the dish into the solvent, the volume of gas evolved was recorded at various time intervals. Rapid stirring was used to obtain reaction rates independent of the rate of agitation.

RESULTS AND DISCUSSION

Formation of Diimide from PSH in Solution

For ascertaining the decomposition of PSH in various solvents, the behavior of the gas evolution was examined. The results of measurement of the volumes of gas evolved are shown in Figure 1, in which the volumes are plotted against time. Only nitrogen was detected in the evolved gas by gas chromatography in each case, except for a trace of hydrogen in HMPA and DMF at 130°C.

These results suggest that PSH is decomposed in these solvents into diimide and p-toluenesulfinic acid and that then the diimide alone disproportionates to nitrogen and hydrazine, following the mechanism proposed by Hünig et al.[10] for the case of benzenesulfonyl hydrazide in ethylene glycol monomethyl ether at 120°C. Furthermore, the solvent effect on the
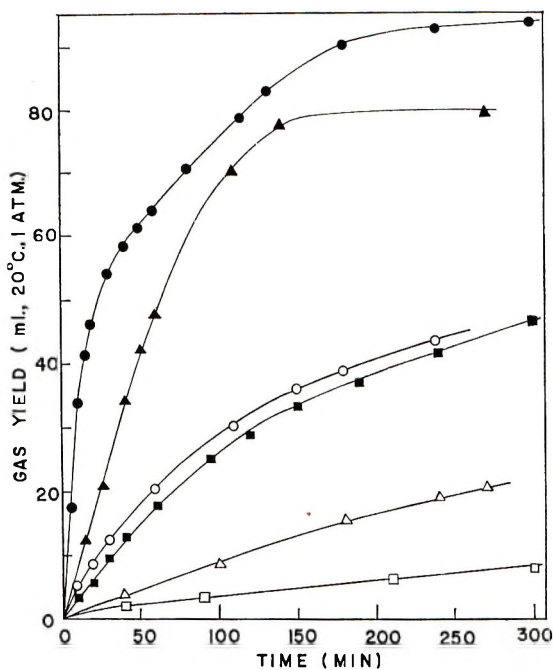
Fig. 1. Gas evolution by thermal decomposition of PSH in various solvents; 0.60 g. of PSH, 40 ml. of solvent: (●) HMPA, 130°C.; (○) HMPA, 100°C.; (▲) DMF, 130°C.; (△) DMF, 100°C.; (■) ODB, 130°C.; (□) ODB, 100°C.

decomposition of PSH was observed as shown in Figure 1. Dipolar solvents such as HMPA (DC 34) and DMF (DC 36.7) accelerate the decomposition of PSH to diimide and p-toluenesulfinic acid because of the greater polarization of the transition-state compound (V):

(V)
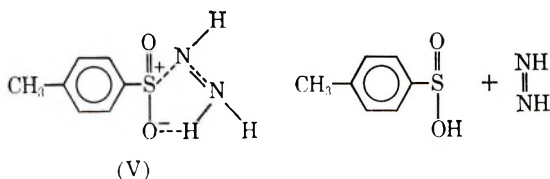
The apparent activation energies for the decomposition of PSH in HMPA and DMF were 15.8 and 17.4 kcal./mole, respectively, which were estimated from the initial rates of gas evolution. These values are smaller than the 20.9 kcal./mole in ethylene glycol monomethyl ether and the 23.5 kcal./mole in ethylene glycol monomethyl ether containing ethanolamine.[10] On the other hand, the activation energy in ODB was somewhat larger, about 34 kcal./mole.

Retardation of Discoloration of PVC with PSH

It has been well known that PVC is readily discolored in DMF by heating.[11] In our preliminary experiment it was observed that the rates
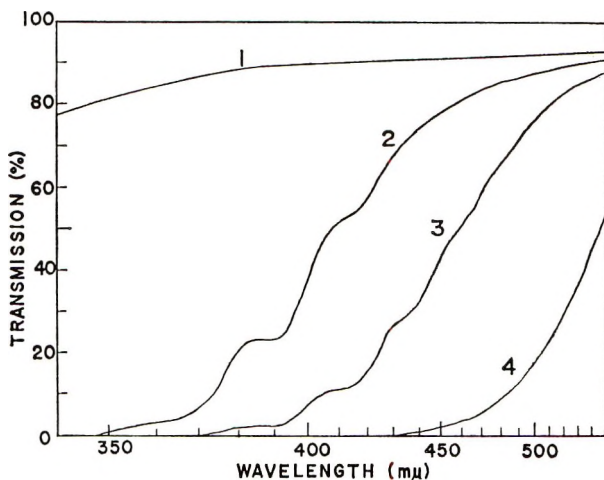
Fig. 2. Electronic spectra of discolored PVC in DMF; 1.0 g. of PVC, 50 ml. of DMF at 130°C.: (1) original colorless PVC; (2) 0.33 g. of PSH, for 90 min.; (3) 0.16 g. of PSH, for 90 min.; (4) without PSH, for 70 min.
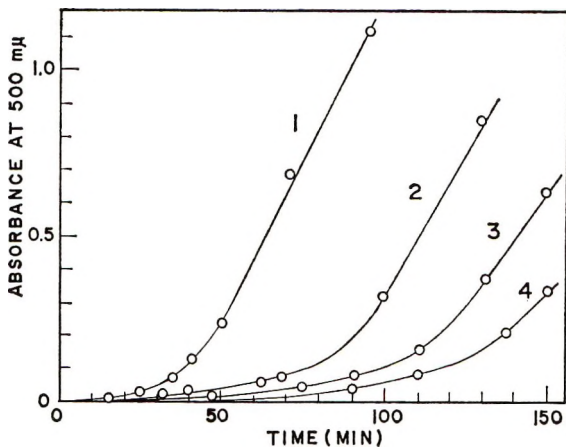

Fig. 3. Effect of PSH on the rate of discoloration of PVC; 1.0 g. of PVC, 5 ml. of DMF at 130°C: (1) without PSH; (2) 4.5 g. of PSH; (3) 0.16 g. of PSH; (4) 0.75 g. of PSH.

of discoloration were dependent upon the degree of purification of PVC. For example, the purified polymer did not show any discoloration in DMF at 100°C., but PVC of the commercial grade without purification was readily discolored in DMF at 100°C. in 2 hr. For reproducible results a purified PVC was used in this work.

Figure 2 shows the electronic spectra of PVC in DMF, which was discolored at 130°C. in the same solvent under a nitrogen atmosphere with or without PSH. The absorptions spread from the ultraviolet to the visible area in the case of the absence of PSH, whereas the appearance of absorptions in the visible area is remarkably retarded in the case of the presence of PSH.

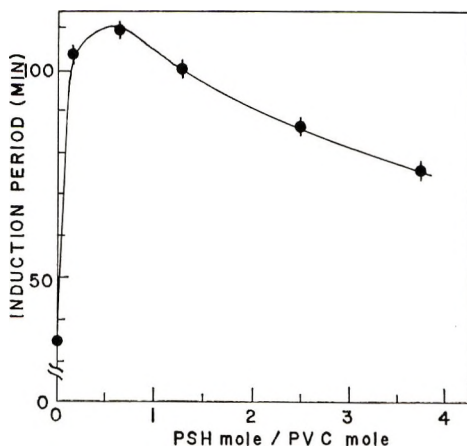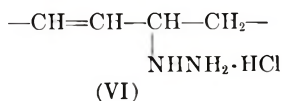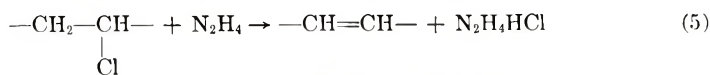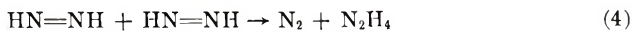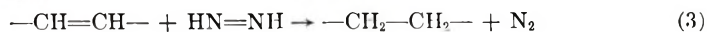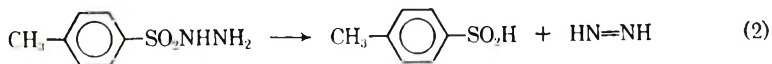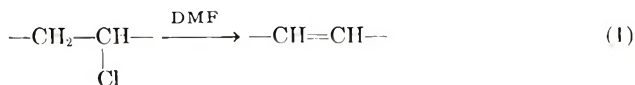The rates of discoloration in the presence of different concentrations of

Fig. 4. Induction period of discoloration vs. mole ratio PSH /PVC (monomer unit).

PSH are shown in Figure 3. This figure indicates the following facts: in the presence of PSH longer induction periods of discoloration are observed and when the concentrations of PSH are increased over a definite range, the induction period decreases. This is amply demonstrated in Figure 4, in which the induction periods are plotted against the molar ratio of PSH to PVC (monomer unit). It is observed in this figure that the induction period attains a maximum when the mole ratio of PSH to PVC is about 0.25. A possible process of the appearance of the maximum in Figure 4 may be deduced as follows.

The amounts of double bonds formed by eq. (1) might be extremely small, whereas the rate of decomposition of PSH in DMF at 130°C. was rather fast, as shown in Figure 1. Therefore, when the larger amounts of PSH were used, the disproportionation of diimide shown in eq. (4) might proceed vigorously to give hydrazine, which further reacts with PVC to produce the discolored PVC containing the structures of chromophore, such as conjugated C=C double bonds or (VI), or both, shown in eq. (5). At the maximum point shown in Figure 4 the hydrogenation reaction described by eq. (3) would predominate over the undesirable reaction described by eq. (5).

$$\underset{\overset{|}{Cl}}{-CH_2-CH-} \xrightarrow{DMF} -CH=CH- \qquad (1)$$

$$CH_3-\!\!\!\bigcirc\!\!\!-SO_2NHNH_2 \longrightarrow CH_3-\!\!\!\bigcirc\!\!\!-SO_2H + HN=NH \qquad (2)$$

$$-CH=CH- + HN=NH \rightarrow -CH_2-CH_2- + N_2 \qquad (3)$$

$$HN=NH + HN=NH \rightarrow N_2 + N_2H_4 \qquad (4)$$

$$\underset{\overset{|}{Cl}}{-CH_2-CH-} + N_2H_4 \rightarrow -CH=CH- + N_2H_4HCl \qquad (5)$$

$$\underset{\overset{|}{NHNH_2 \cdot HCl}}{-CH=CH-CH-CH_2-}$$

$$(VI)$$

Decolorization of Discolored PVC

Solvents that have high boiling points (at least 100°C.) and good solubility for both polymer and PSH were required in this work.   Dioxane was considered suitable in these respects.   Dioxane itself, however, even after being passed through a column of activated alumina, showed the decolorization behavior of discolored PVC under a nitrogen atmosphere, presumably owing to a trace of peroxide.   Decolorization of discolored PVC with peroxide (oxidative decolorization) has been known and reported in the literature.   In fact, the lightening effect of PSH on the discolored PVC could not be observed in dioxane solution.   DMF also showed a similar behavior at 100°C.   Although ODB did not have good solubility for PSH at room temperature, it dissolved more than 5% of the PSH above 50°C., and the decolorization effect of ODB was found to be negligible.   Finally, ODB was chosen as the most suitable for studying the decolorization during our experiments.   HMPA was also used, which has a high dielectric constant; it decomposed PSH more rapidly than ODB and also showed no decolorization effect by itself.

Decolorization of β-carotene

Dewey et al.[12] have reported that the isolated C=C double bonds in low molecular weight compounds were hydrogenated in 70–98% yields with PSH at refluxing temperature in diglyme under a nitrogen atmosphere.
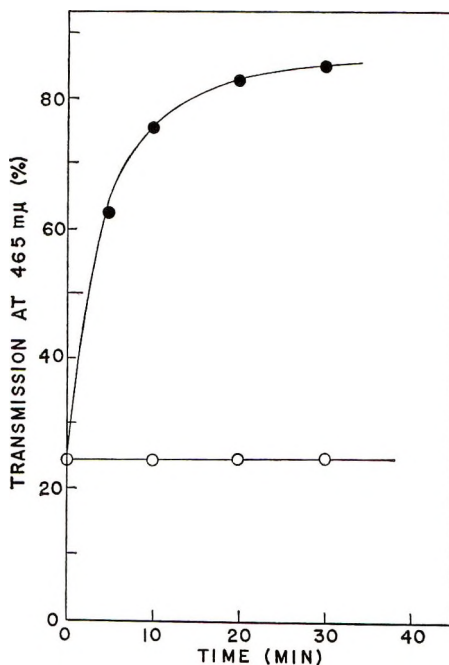

Fig. 5. Decolorization of β-carotene with PSH; β-carotene, 2.6×10^{-6} mole per 20 ml. ODB, 0.3 g. of PSH at 130°C.; (O) without PSH.

However, no study has been made of the reduction of unsaturated macro-molecular compounds or of compounds containing long, conjugated double bonds. Therefore, as one of the corresponding model compounds of discolored PVC, β-carotene was selected, which has 11 conjugated double bonds. The per cent transmission at 465 mμ was used as a measure of decolorization. Although β-carotene is rather unstable and is readily decolorized by oxidation or irradiation by light, it was confirmed that β-carotene was stable enough at 130°C. under a nitrogen atmosphere in the absence of PSH in the dark. When PSH was added to this system, the decolorization of β-carotene began rapidly, as shown in Figure 5.

Decolorization of Discolored PVC

Decolorization behavior according to the per cent transmission of various discolored polymers is shown in Figure 6. The histories of the discolored polymers are found to have a great effect on both the decolorization rate and the degree of decolorization in the final stages. PVC(T-1 to T-3) and PVC(γ-T), which were assumed to have 6 or 7 and more than 10 conjugated double bonds, respectively,[13,14] were greatly decolorized by this method. PVC(D-1), showing a rather slow decolorization rate, contained 0.6% nitrogen from its elemental analysis. This suggests that its discoloration was not based simply on the conjugated double bonds, but on a small amount of nitrogen-containing groups, which seemed to accentuate the
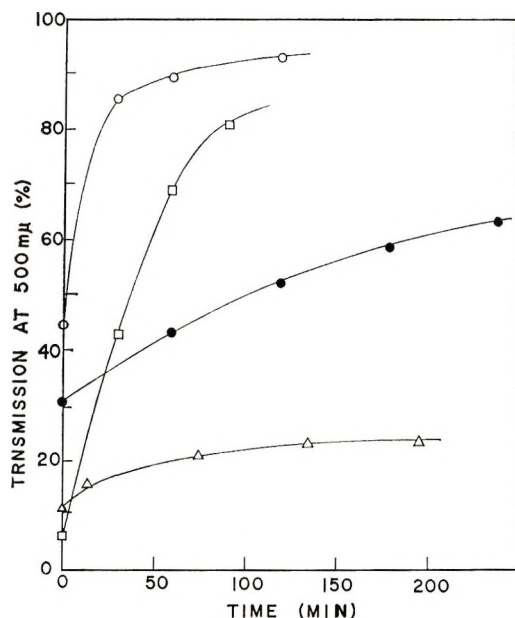
Fig. 6. Decolorization of discolored PVC with PSH in ODB at 130°C.: (○) 0.30 g. of PVC(T-3), 0.6 g. of PSH, 20 ml. of ODB; (●) 0.33 g. of PVC(D-1), 0.6 g. of PSH, 20 ml. of ODB; (□) 0.05 g. of PVC(γ-T), 0.15 g. of PSH, 10 ml. of ODB; (△) 0.10 g. of PVCl₂(A), 0.3 g. of PSH, 10 ml. of ODB.
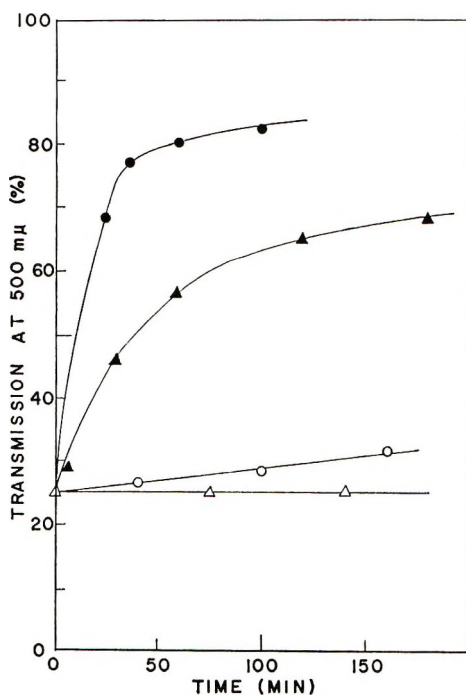
Fig. 7. Decolorization in various temperatures with PSH; 0.3 g. of PVC(T-2), 20 ml. of ODB: (△) without PSH, at 100°C.; (▲) 0.6 g. of PSH, at 100°C.; (○) without PSH, at 130°C.; (●) 0.6 g. of PSH at 130°C.
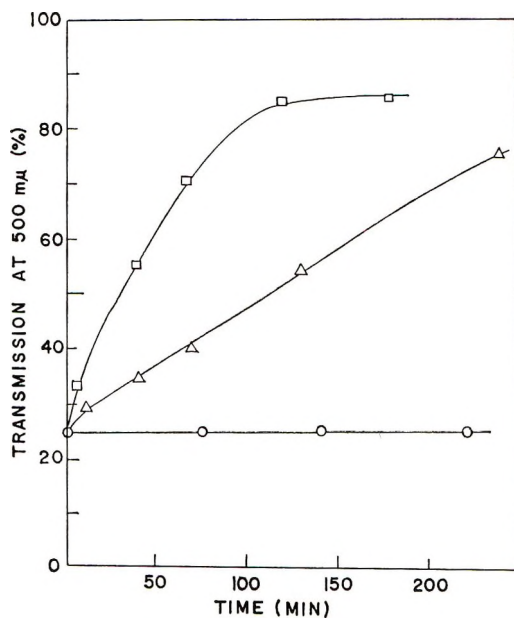
Fig. 8. Decolorization with various amounts of PSH in ODB at 100°C., 0.5 g. of PVC(T-1), 50 ml. of ODB: (○) without PSH; (△) 0.75 g. of PSH; (□) 1.50 g. of PSH.

Fig. 9. Decolorization in HMPA with PSH; 0.3 g. of PVC(T-2), 20 ml. of HMPA: (●) without PSH, at 100°C.; (○) 0.6 g. of PSH, at 100°C.; (▲) without PSH, at 130°C.; (△) 0.6 g. of PSH, at 130°C.

discoloration. Hydrogenation with diimide has been reported to be very difficult in unsymmetrical multiple bonds.[8] It may be possible to assume that nitrogen-containing groups would obstruct the diimide reduction by either an electronic or a steric effect. In the case of PVCl₂(A) the discoloration of the polymer was considered to be based on the structure (VII),[15,16] and the difficulty in decolorization of this polymer may be attributed to its unsymmetrical double bonds and a steric hindrance of a chlorine substituent.

$$-CH_2-\underset{\underset{\bigcirc}{\overset{\|}{N}}}{C}-CH=\underset{\overset{|}{Cl}}{C}-CH=\underset{\overset{|}{Cl}}{C}-CH_2-$$

(VII)

By a pyridine sulfate–dibromide method[17,18] an estimation of the C=C double bonds of PVC(T-3) before and after treatment with PSH in ODB showed that the value of 0.58 per 100 monomer units of PVC decreased to 0.15 of colorless polymer after treatment for 6 hr., corresponding to 0.13 of the original colorless PVC. The intrinsic viscosities of the same polymer in cyclohexanone at 30°C. was shown to be 0.692 for PVC(T-3) and 0.697 after diimide reduction. This result implies that the diimide reduction of discolored PVC does not change the degree of polymerization. Figure 7

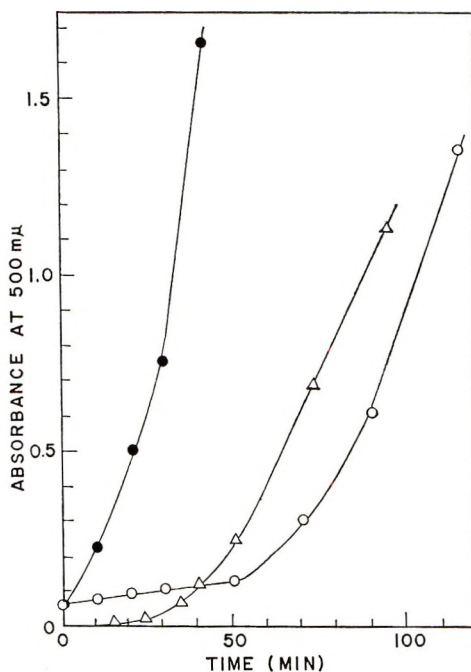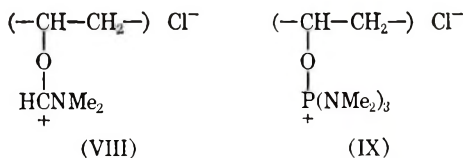Fig. 10. Rediscoloration of decolorized PVC in DMF at 130°C.; 0.30 g. of PVC, 15 ml. of DMF: (O) decolorized PVC with diimide; (●) decolorized PVC with oxygen; (△) original PVC.

shows the effect of temperature on the rate of decolorization of PVC(T-2). As may be seen from Figure 7, in the region of 100–130°C. this is consistent with the effect of temperature on the decomposition of PSH. The poor solubility of PSH in ODB restricts the variation of the concentration of PSH, so that the existence of the maximum point, such as in the case of Figure 4, could not be examined in this case. Within the concentration shown in Figure 8 the rate of decolorization was accelerated as the amount of PSH increased.

The result of the diimide reduction in HMPA with PSH is shown in Figure 9. It is seen from this figure that PVC(T-2) was further discolored even at 100°C., and remarkably so at 130°C. in the absence of PSH. In the presence of PSH a very rapid decolorization took place initially, but this was followed by a rapid rediscoloration. The rapid decolorization might be attributed to the fact that PSH was rapidly decomposed in HMPA at this temperature. The rapid discoloration in the absence of PSH and rediscoloration after a maximum decolorization at 130°C. might also be attributed to the large dielectric constant of HMPA.

Rapid discoloration of PVC in DMF is well known, and the extraordinary ease of nucleophilic substitution on PVC by dithiocarbamate anion in DMF has also been reported.[19] In the case of alkyl halides of low molecular weight it has been reported by Moobery[20] and Yoneda et al.[21] that they

are partly dissociated and show the electric conductivity. We have assumed the presence of ion-pair structure (VIII) for PVC in DMF, and the situation may be true of PVC in HMPA, as illustrated by (IX) below.

$$(-CH-CH_2-) \; Cl^- \qquad (-CH-CH_2-) \; Cl^-$$
$$| \qquad\qquad\qquad |$$
$$O \qquad\qquad\qquad O$$
$$| \qquad\qquad\qquad |$$
$$HCNMe_2 \qquad\qquad P(NMe_2)_3$$
$$+ \qquad\qquad\qquad +$$
$$\text{(VIII)} \qquad\qquad \text{(IX)}$$

Thermal Stability of Decolorized PVC in DMF

The thermal stability of two types of PVC, decolorized by the diimide reduction at 100°C. for 4 hr. (A) and decolorized by oxygen bubbling in dioxane at 100°C. for 4 hr. (B) were compared with that of the original PVC at 130°C. in DMF. As shown in Figure 10, the induction period of the discoloration for (A) was longer than for (B), as expected, and somewhat longer than that for the original PVC. In the PVC decolorized by the diimide reduction the C=C double bonds formed by dehydrochlorination at the most labile chlorine atoms of PVC (tertialy or allylic) were saturated with hydrogen and so were the most stabilized.

References

1. L. Scarbrough, W. L. Kellner, and P. W. Rizzo, *Polymer Degradation Mechanisms*, Natl. Bur. Std., Circular 525, 1953, p. 95.
2. L. H. Wartman, *Ind. Eng. Chem.*, **47**, 1013 (1955).
3. A. H. Frye, R. W. Horst, and M. A. Paliobagis, *J. Polymer Sci. A*, **2**, 1765, 1785, 1801 (1964).
4. C. S. Marvel, J. H. Sample, and M. F. Roy, *J. Am. Chem. Soc.*, **61**, 3241 (1939).
5. Y. Landler and P. Lebel, *J. Polymer Sci.*, **48**, 477 (1960).
6. Y. Nakamura and M. Saito, *Kobunshi Kagaku*, **20**, 245 (1966).
7. G. T. Atchison, *J. Polymer Sci.*, **49**, 385 (1961).
8. E. E. van Tamelen, R. S. Dewey, and R. J. Timmons, *J. Am. Chem. Soc.*, **83**, 3725 (1961).
9. E. J. Corey, D. J. Pasto, and W. L. Mock, *J. Am. Chem. Soc.*, **83**, 2957 (1961); S. Hünig, H. R. Müller, and W. Thier, *Tetrahedron Letters*, **1961**, 353.
10. S. Hünig, H. R. Müller, and W. Thier, *Angew. Chem.*, **77**, 368 (1965).
11. C. Sadron, J. Parrod, and J. P. Roth, *Compt. Rend.*, **250**, 2206 (1960).
12. R. S. Dewey and E. E. van Tamelen, *J. Am. Chem. Soc.*, **83**, 3729 (1961).
13. K. Hirayama, *Nippon Kagaku Zasshi*, **75**, 27, 667 (1954).
14. S. Ohnishi, Y. Nakajima, and I. Nitta, *J. Appl. Polymer Sci.*, **6**, 629 (1962).
15. W. Fuchs and D. Louis, *Makromol. Chem.*, **22**, 1 (1957).
16. T. Nakagawa, unpublished data.
17. K. W. Rosenmund and B. Laukwitz, *Angew. Chem.*, **37**, 58 (1924).
18. H. Mizutani, *Kobunshi Kagaku*, **8**, 75, 181 (1951).
19. M. Okawara, G. Morishita, and E. Imoto, *Kogyo Kagaku Zasshi*, **69**, 761 (1966).
20. D. D. Moobery, Ph.D. Thesis, Purdue University, 1954.
21. S. Yoneda, Z. Yoshida, I. Morishima, and K. Fukui, *Kygyo Kagaku Zasshi*, **68**, 1074 (1965).

Effects of Metal Salts on Polymerization.
Part V: Polymerization of *N*-Vinylcarbazole
Initiated by Sodium Chloroaurate

SHIGEO TAZUKE, MICHIHIKO ASAI, and SEIZO OKAMURA,
Department of Polymer Chemistry, Kyoto University, Kyoto, Japan

Synopsis

The polymerization of *N*-vinylcarbazole (VCZ) initiated by sodium chloroaurate ($NaAuCl_4 \cdot 2H_2O$) in nitrobenzene was studied at 30°C. The rate of polymerization (R_p) is proportional to $[Au^{III}][VCZ]$ after a short induction period. When reducing agents (ascorbic acid, ferrocene, or mercury metal) are added to the system, the rate of polymerization in the dark increases. The R_p is relatively unaffected by addition of water and *N*-ethylcarbazole, but the polymerization is completely inhibited in the presence of ammonia. Oxygen and DPPH act as neither inhibitors nor retarders. Kinetic treatments based on the assumption that the active initiating species is Au^{II} produced by reduction of Au^{III} by VCZ and other reducing agents explain the experimental results very well.

INTRODUCTION

Polymerization induced directly by oxidizing metal salts could proceed either by a cationic or by a radical mechanism, depending upon the kind of monomer used.[1] For the radical polymerization of vinylpyridine initiated by cupric acetate the interpretation is straightforward, assuming electron-transfer initiation.[2] However, with respect to *N*-vinylcarbazole (VCZ) there are several possible explanations of the initiation of a cation-like polymerization induced by oxidizing metal salts. We have already reported that various oxidizing metal salts, such as cupric, ferric, and ceric salts, initiate the polymerization of VCZ.[3] Although the initiation seems to be an electron-transfer reaction, alternative possibilities could not be completely rejected. These metal salts are oxidizing but also acidic. Consequently, they might act as Lewis acids instead of oxidizing agents or even produce protons as a result of hydrolysis.

We found that sodium chloroaurate as initiator of the polymerization of VCZ in nitrobenzene was excellent for studying the kinetics and mechanism of the initiation reaction. This metal salt has been briefly mentioned by Bawn et al.[4] as an initiator of the thermal polymerization of VCZ in acetonitrile. Its advantage is that the gold ion exists as a negatively charged tetrachloro complex, so that action as a Lewis acid would be much weaker

than that of ferric or cupric salts.   Another feature is its extreme sensitivity to photoirradiation.[5]   Details of the photopolymerization will be published elsewhere in the near future.

EXPERIMENTAL

Materials

N-Vinylcarbazole (Koch Light Laboratories Ltd.) was recrystallized from *n*-hexane and dried *in vacuo;* m.p. 65.2°C.

Nitrobenzene, used as solvent for the polymerization, was washed and dried rigorously over barium oxide and then distilled twice *in vacuo* in the dark.   The purified nitrobenzene did not cause a spontaneous polymerization of the VCZ in the dark.

Commercial sodium chloroaurate (NaAuCl$_4$·2H$_2$O, purity better than 99%) was used without further purification.   Since this salt is extremely sensitive to light and moisture, it was divided into small portions and kept in sealed ampules in the dark.   The required amount was weighed immediately before use.

Tetrahydrofuran (THF) was purified by fractional distillation after being dried over calcium hydride.

Polymerization

All polymerizations were carried out at 30°C. in the dark.   The rate of polymerization was measured by a dilatometer and also by weighing the polymer after precipitation in methanol.   The monomer and catalyst solutions were prepared separately and kept in the dark at reaction temperature.   The two solutions were then mixed, and the reaction mixture was immediately transferred to a dilatometer or made to react in the mixing vessel.   All polymerizations proceeded homogeneously.   Sodium chloroaurate, monomer, and additives, except mercury and ascorbic acid, were completely soluble in nitrobenzene.   All operations were carried out under dry-nitrogen atmosphere, but no special care was taken to eliminate dissolved air from reaction mixture.   The effect of a trace amount of water was found to be negligible, and later the polymerization was carried out in an open system.   Identical results were obtained from polymerizations in dry atmosphere and in air.

The molecular weight of the polymer was determined by viscosity measurement according to the equation[6] $[\eta] = 3.35 \times 10^{-4}M^{0.58}$, at 25°C. in benzene.

RESULTS

Polymerization

The polymerization of VCZ initiated by sodium chloroaurate began after a short induction period, as shown in Figure 1.   Excluding the induction period, the time–conversion curves can be fitted to a linear plot (Fig. 2),
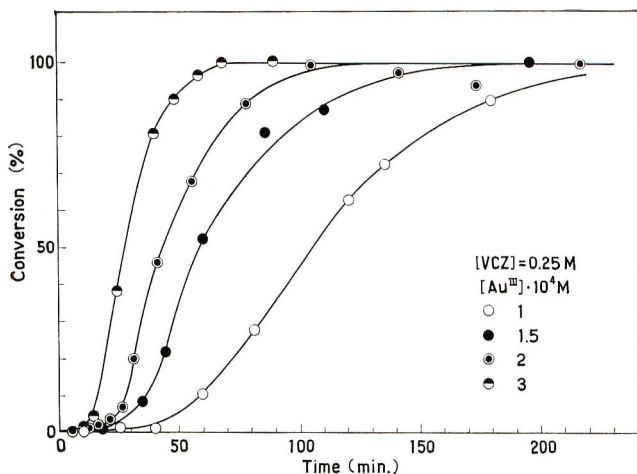
Fig. 1. Polymerization of VCZ by NaAuCl₄·2H₂O in nitrobenzene in the dark.
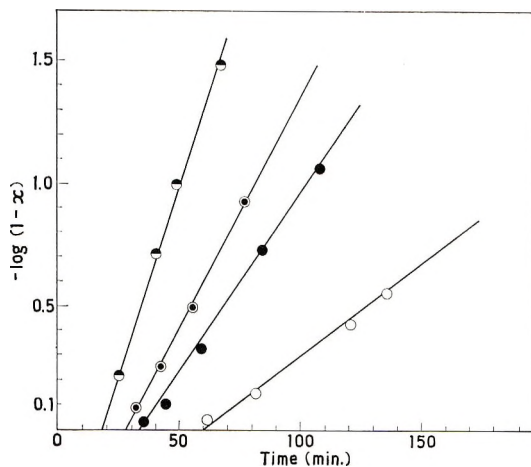

Fig. 2. Linear plots of time versus conversion for polymerization in the dark.   Conditions of polymerization and symbols are same as in Figure 1.

which indicates that the rate of polymerization is proportional to the monomer concentration.   Reproducibility of the gradient of the linear plot is excellent.   However, when the gold salt from a different production lot was used, some difference in the duration of the induction period was observed; this is probably due to some different photochemical history of the gold salt during production and storage.   The photochemical acceleration of the polymerization is remarkable, as has been briefly reported.[5] The present authors confirmed that the presence of VCZ is not necessary for the photochemical production of active species, since a marked acceleration is observed when the catalyst solution alone is irradiated prior to the addition of VCZ.   Details of the photochemical process will be published elsewhere.
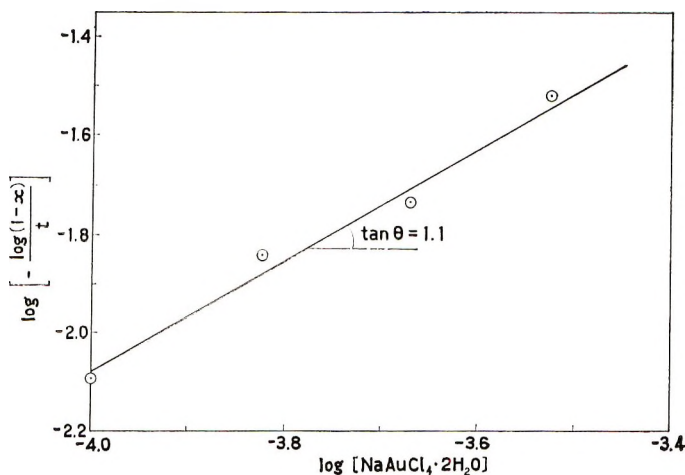
Fig. 3. Dependence of R_p on initiator concentration for polymerization in the dark
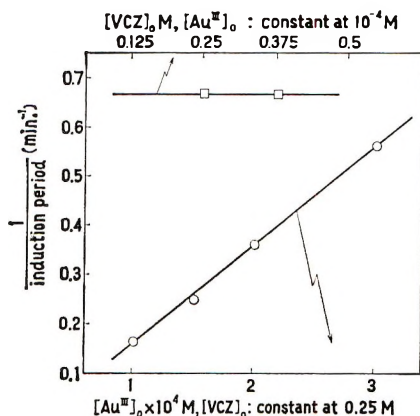

Fig. 4. Reciprocal of induction period versus monomer and initiator concentrations:
($\square$) 1/(induction period) versus [VCZ]; ($\bigcirc$) 1/(induction period) versus [Au^{III}].

The rate of polymerization (R_p) is nearly proportional to the catalyst concentration, as shown in Figure 3. The reciprocal of the induction period is also proportional to the catalyst concentration but seemed to be independent of the initial monomer concentration; see Figure 4. The induction period seems to be the time required for the building up of active species in the reaction between gold salt and monomer, since the second polymerization proceeds without an induction period when monomer is freshly added to the polymerization mixture after completion of the polymerization; see Figure 5. The rates of the first and second polymerizations are almost identical.

The presence of monomer is absolutely necessary to produce the active species, since the lapse of time between dissolving of the initiator in nitrobenzene and mixing of the initiator solution with monomer solution does not
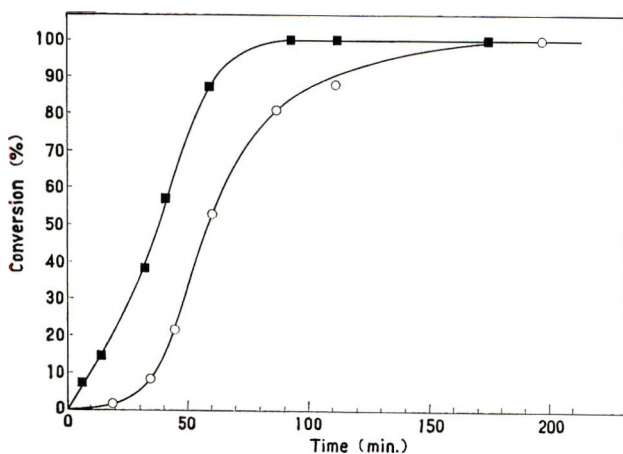
Fig. 5. Addition of monomer after first polymerization is completed, polymerization in the dark: (O) first polymerization, [VCZ] = 0.25M, [Au^{III}] = 1.5 × 10^{-4}M; (■) second polymerization, [VCZ] = 0.25M in the presence of 0.25M of poly VCZ, [Au^{III}] = 1.5 × 10^{-4}M.
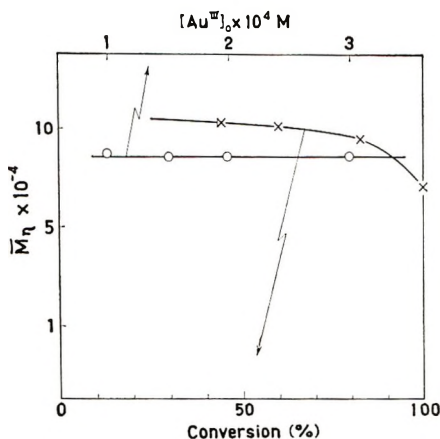
Fig. 6. Dependence of molecular weight of poly VCZ on initiator concentration and conversion for polymerization in the dark: (×) $\overline{M}_\eta$ versus conversion; (O) $\overline{M}_\eta$ versus [Au^{III}]$_0$, conversion = 90%.

influence the R_p and induction period at all, when the solution is kept in the dark.

The use of nitrobenzene as solvent is not a necessary condition. However, available solvents which can stably dissolve the initiator are very limited. For instance, although polymerization proceeds rapidly in THF, the initiator is quite unstable in this solvent, so that the solid salt should be added to the solution of monomer. When the salt was dissolved in THF, the yellow color of the Au^{III} disappeared immediately, and soon afterward a white precipitate formed. This solution was no longer capable of initiating the polymerization of VCZ.

The degree of polymerization is independent of the initiator concentration and slightly decreases with conversion; see Figure 6.

Effect of Additives on Polymerization

Water. Adding water in amounts up to 10^3 times that of the initiator did not affect the R_p (Fig. 7), although the degree of polymerization was considerably reduced. The insensitivity of R_p to the amount of water present has also been observed by Pác and Plesch[7] in a polymerization initiated by tetranitromethane in nitrobenzene.

Ammonia. Polymerization was completely inhibited by ammonia.

2,2-Diphenyl-1-picrylhydrazyl (DPPH). An unexpected acceleration was noticed. This is at least evidence against radical polymerization.

The findings for these three additives suggest that the polymerization is very cationic.

N-Ethylcarbazole. Since VCZ takes part in the formation of initiating species, N-ethylcarbazole was added to the polymerization mixture, to increase the concentration of carbazyl group; it was expected that this would influence the initiation rate, but the effect was slight.

It is almost certain that some redox or electron-transfer process is involved in the initiation step. On the assumption that the intermediate valency state of gold is very active, several reducing agents were added to the polymerization system with the intention of producing the divalent state of gold.

Reducing Agents. The accelerating effect of reducing agents is marked. Metallic mercury and ascorbic acid are insoluble, whereas ferrocene is soluble and a very strong activator. The shape of the time–conversion
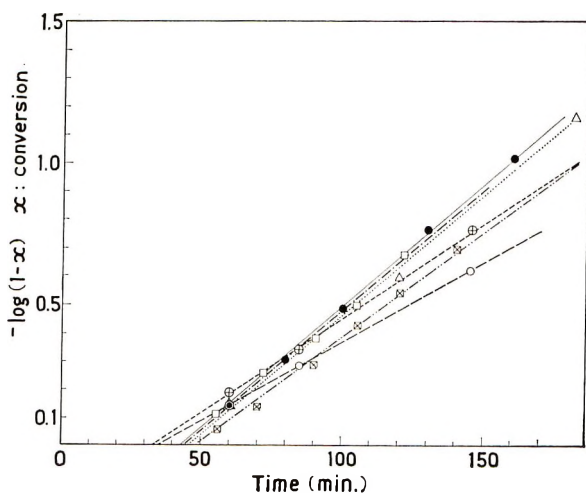

Fig. 7. Effect of various additives on rate of polymerization of VCZ in the dark, $[Au^{III}] = 1.0 \times 10^{-4} M$, $[VCZ] = 0.25 M$: (●) no additive; (△) oxygen bubbled through; (⊕) N-ethylcarbazole, $0.125 M$; (○) N-ethylcarbazole, $0.25 M$; (□) water, $0.01 M$; (⊠) water, $0.1 M$.
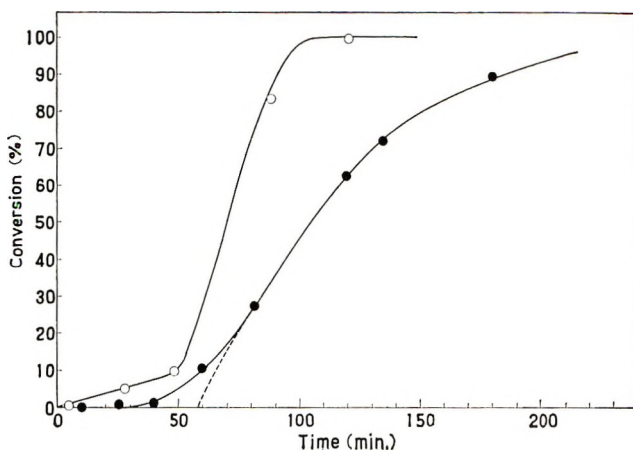
Fig. 8. Effect of mercury on polymerization in the dark, [VCZ] = 0.25M, [sodium chloroaurate] = 1.0 × 10^{-4}M: (●) without mercury; (○) mercury added.
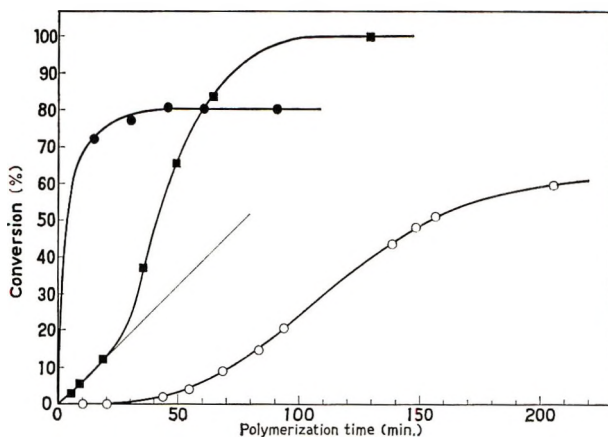
Fig. 9. Effect of ferrocene on polymerization in the dark, [VCZ] = 0.25M. Sodium chloroaurate concentration: (○) 5.0 × 10^{-1}M, without ferrocene; (■) 5.0 ×10^{-5}M, [ferrocene] = 2.5 × 10^{-5}M; (●) 1.0 × 10^{-4}M, [ferrocene] = 1.0 × 10^{-3}M.

curve differs considerably from that in the absence of reducing agents. In the presence of reducing agents the initial part of the curve, which is otherwise still in the induction period, is straight; see Figures 8 and 9.

The reducing agents (mercury, ferrocene, and ascorbic acid) were definitely unable to initiate polymerization either in the dark or in the light in the absence of gold salt.

The results of polymerization in the presence of various additives are shown in Figures 7, 8, and 9 and Table I. Although reducing agents could greatly accelerate the polymerization, an excess of an agent efficient in reducing the salt seems to lower the maximum conversion attainable, as shown in Figure 9. A strong reducing agent such as ferrocene would reduce the active Au^{II} to the Au^{I} species before the Au^{II} species

could react with the VCZ. Consequently, the greater part of the Au^{III} is inactivated by the reducing agent, resulting in saturation of the time–conversion curve owing to consumption of the initiator. Figure 10 shows the
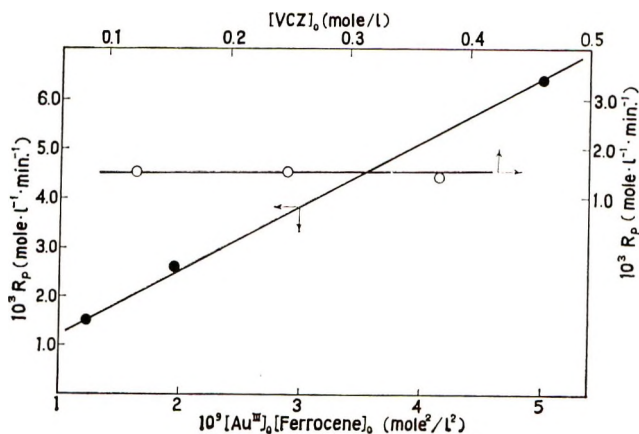

Fig. 10. Dependence of initial R_p on monomer concentration and product of ferrocene and initiator concentrations. (O) R_p versus [VCZ], with [sodium chloroaurate] and [ferrocene] kept constant at $5.0 \times 10^{-5}M$ and $2.5 \times 10^{-5}M$, respectively; (●) [sodium chloroaurate] [ferrocene], with [VCZ] kept constant at $0.25M$.

dependence of R_p on the concentration of Au^{III}, ferrocene, and monomer. Different concentrations of both Au^{III} and ferrocene were examined.

Oxygen. No changes in R_p were observed when pure oxygen was bubbled through the reaction mixture during polymerization.

TABLE I
Polymerization of VCZ in the Presence of Various Additives[a]

Additive	Polymn. time, min.	Convsn., %	Avg. mol. wt.
None (standard)	120	67.5 ± 5	98,000; see Figs. 1 and 6
Ammonia, 10^{-2} to $10^{-3}M$	120	0	
Water, $10^{-2}M$	160	≈ 90	66,000
Water, $10^{-1}M$	180	≈ 90	35,000
N-Ethylcarbazole, $0.125M$	80	50	94,000
N-Ethylcarbazole, $0.25M$	90	50	90,000
Ascorbic acid[b]	120	100	
Mercury metal[b]	120	100	
Ferrocene, $5 \times 10^{-5}M$	30	100	
DPPH, $10^{-4}M$	90	96	

[a] $[VCZ] = 0.25M$, $[NaAuCl_4 \cdot 2H_2O] = 1.0 \times 10^{-4}M$; solvents, nitrobenzene.
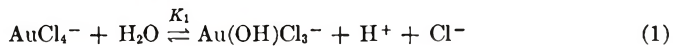[b] Additive is insoluble.

DISCUSSION

Initiation Process

There seems to be little doubt that the polymerization proceeds by a cationic mechanism. The inability of DPPH, nitrobenzene, and oxygen to inhibit the polymerization, the inhibitory effect of ammonia, the decreased molecular weight of the polymer in a wet system, all favor a cationic mechanism.

Another mechanism may be a polymerization by mesomeric polarization, proposed by Ellinger.[8] However, Ellinger's mechanism is less probable from the kinetic standpoint; this will be discussed later. An intensive study of the copolymerization reactivity of VCZ, initiated by various charge-transfer initiators, might provide a definitive answer to the question of the nature of the propagating species.

Two possible kinds of cationic initiation with sodium chloroaurate may be considered as follows.

First, the gold salt might act as a proton source. However, the hydrolysis constant K_1 of the gold salt is of the order of 10^{-6}, as measured in aqueous solution at 20°C., $\mu \rightarrow 0$.[9] (μ is ionic strength.)

$$\text{AuCl}_4^- + \text{H}_2\text{O} \overset{K_1}{\rightleftharpoons} \text{Au(OH)Cl}_3^- + \text{H}^+ + \text{Cl}^- \tag{1}$$

$$K_1 = K_1'[\text{H}_2\text{O}] = [\text{Au(OH)Cl}_3^-][\text{H}^+][\text{Cl}^-]/[\text{AuCl}_4^-] \tag{2}$$

Consequently, assuming the same value of K_1' in nitrobenzene, the concentration of protons is less than $10^{-5}M$ under the present experimental conditions; that is, $[\text{Au}^{III}] = 1 \times 10^{-4}$ and $[\text{H}_2\text{O}] = 2 \times 10^{-4}M$. This proton concentration is apparently too low to bring about the large polymerization rate observed in the present work. The rate of polymerization of VCZ ($0.25M$) in nitrobenzene in the presence of $10^{-5}M$ hydrogen chloride is very low; see Figure 11. The conversion after 210 min. of polymerization in the dark at 30°C. was only 10% and, moreover, the time–conversion curve was completely linear during the 210 min. and without a sign of an induction period. A similar slow polymerization of VCZ by protonic acid
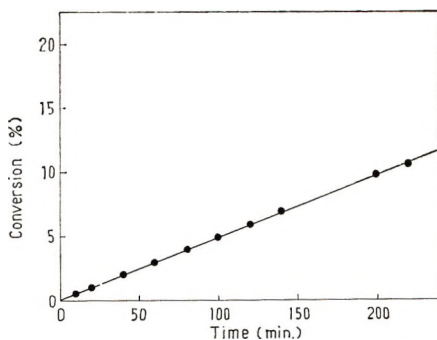

Fig. 11. Polymerization of VCZ by hydrogen chloride in nitrobenzene; [VCZ] = 0.25M and [HCl] = $10^{-5}M$, at 30°C.

has been observed also in dioxane.[3]   Furthermore, it is not possible to explain the accelerating effect of the reducing agents, the presence of the induction period, and the finding that the R_p is not affected by the amount of water added.

The second possibility is an ordinary cationic initiation by gold salt; however, this would be difficult to reconcile with the ESR signal observed during polymerization.   It is also unlikely that the salt of a Group IB element could act as an active cationic catalyst like a Lewis acid or a Friedel-Crafts catalyst.
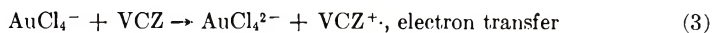
A third possibility is redox initiation.   The gold salt is known to be a strong oxidant that is reduced stepwise to the Au^I state.   So far redox reactions of the gold salt have not been studied systematically.   More than ten years ago Rich and Taube[10] studied the redox reaction between the gold salt and ferrous ion and postulated the presence of the Au^{II} state as an intermediate state.   More recently the redox potential of Au^{III}–Au^{II} in dimethylformamide was measured by polarography.[11]   In addition the solid Au^{II} species was isolated in the form of square planar complex, and confirmed by ESR spectroscopy.[11,12]

The direction of the electron-transfer reaction may be controlled by the relative magnitude of the redox potentials of the reacting species.   Redox potentials of relevant species are listed in Table II, although the values

TABLE II
Standard Redox Potentials of Relevant Compounds

Redox pair	$E°$, v.	Determination
$AuCl_4^-/AuCl^{II}$	-0.5 to -0.96	estimation from redox reaction,[10] polarography in DMF[11]
$AuCl^{II}/AuCl_2^{2-}$	> -1.4	estimation from redox reaction[10]
$VCZ^+·/VCZ$	-1.3	polarography in DMF[14]
Ferrocene$^+$/ferrocene	$+0.56$	emf in alcohol[15]
$Hg_2^{2+}/Hg(1)$	-0.792	emf[9b]
Ascorbic acid	$+0.1$ to $+0.3$	emf[16]

were not determined under identical conditions and consequently are not suitable for precise comparison.   From these values the electron transfer from VCZ to Au^{II} is considered to occur readily from the energetic viewpoint, whereas that from VCZ to Au^{III} would be slower.   An alternative reduction of Au^{III} may be a ligand-transfer process:

$$AuCl_4^- + VCZ \rightarrow AuCl_4^{2-} + VCZ^+·, \text{ electron transfer} \qquad (3)$$

or

$$AuCl_4^- + VCZ \rightarrow AuCl_3^- + Cl-VCZ·, \text{ ligand transfer} \qquad (4)$$
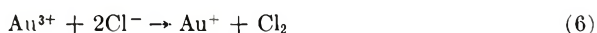
The formation of both $AuCl_4^{2-}$ and $AuCl_3^-$ was postulated by Rich and Taube.[10]

Still another possibility involving a charge-transfer process may be the initiation of polymerization by a chlorine atom,[13] produced during the decomposition of the gold salt:

$$2Au^{3+} + 2Cl^- \rightarrow 2Au^{2+} + Cl_2 \tag{5}$$

or

$$Au^{3+} + 2Cl^- \rightarrow Au^+ + Cl_2 \tag{6}$$

This mechanism is, however, highly unlikely, since the gold salt dissolved in nitrobenzene does not decompose spontaneously in the absence of VCZ, reducing agents, or light, as was confirmed by the initiating activity of the salt solution in nitrobenzene after aging in the dark for different periods. Moreover, the mechanism does not agree with Rich and Taube's observation[10] that chlorine atoms are not generated during the redox reaction of the gold salt.

On the assumption that the Au^{II} state is the effective initiating species, the complicated features of the polymerization may be interpreted. The induction period is then understood as the time required to accumulate the Au^{II} species either by ligand transfer or by electron transfer between VCZ and the gold salt. The induction period disappears when reducing agents are added. The reducing agents are much quicker than VCZ in reducing the Au^{III} state to the active Au^{II} state, which would immediately initiate polymerization. The active species thus formed seems to have a fairly long life, since an induction period is not observed in the second polymerization (Fig. 5).

The initiation process seems to be greatly influenced by the ligands coordinated to gold. When potassium cyanoaurate, $K[Au(CN)_4]\cdot 2H_2O$, was used in place of sodium chloroaurate, no polymerization was induced either in the dark or in the light. Although this cyano complex is poorly soluble, polymerization should be initiated if a redox reaction takes place. Cyanide ion has much stronger ligand field and is a stronger electron acceptor than chloride. As pointed out by Gray,[17] charge transfer of charge in the $Au(CN)_4^-$ complex is from Au^{III} to CN^-, whereas its direction in $AuCl_4^-$ is from Cl^- to Au^{III}. The higher oxidation state of gold is therefore more stabilized in the cyanide complex than in the chloride complex.

The solvent effect is also remarkable. The stability of the gold salt depends very much on the nature of the solvent. When the gold salt is unstable in solution, the initiating ability deteriorates rapidly, as in THF. The deterioration occurs also in the polymerization of vinyl ethers. The dead-end nature of the polymerization indicates that the active initiating species are inactivated before they can initiate polymerization. The present indications are that media having donor oxygen are not favorable to polymerization.

Electron Spin Resonance Spectroscopy

A clear singlet in the ESR spectrum was observed in the VCZ–NaAuCl₄·2H₂O-nitrobenzene system; an example is shown in Figure 12. Since the g value of the spectrum is very close to that of free spin (i.e., $g = 2.00$),

the spectrum would be attributed to delocalized ion–radicals; it is consequently obvious that electron transfer occurs between the carbazyl group and Au^{III}. The ESR signal, however, does not necessarily mean the ion–radical is the active species in polymerization. Nonpolymerizing N-ethyl-carbazole shows a similar singlet when the compound reacts with strong oxidizing agents such as ceric salt.[3]

$g = 2.00$

$\Delta H_{msl} = 9.5$ Gauss
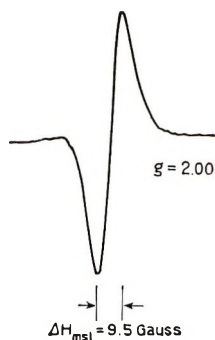
Fig. 12. Electron spin resonance spectrum of VCZ–NaAuCl$_4$·2H$_2$O–nitrobenzene system, made at 77°K. after reaction at room temperature; [VCZ] = 0.5M and [Au^{III}] = $7.5 \times 10^{-3}M$.

ESR spectroscopic data taken under conditions comparable to those of the polymerization experiments and a quantitative comparison between the spin density and kinetic data are needed.

KINETIC CONSIDERATIONS

Rate Expression

The preceding discussion indicates that the polymerization is most probably initiated by Au^{II} produced by the reduction of Au^{III}. Kinetic equations were derived from the following elementary reactions, in which it is assumed that the active initiating species is Au^{II} and that termination of the chain carrier is by monomer, probably through quaternization of nitrogen:[7]

Initial process:
    in the dark,

$$Au^{III} + M \underset{k_{-1}}{\overset{k_1}{\rightleftharpoons}} [Au^{III}\text{–}M] \tag{7}$$

$$(I)$$

$$(I) \xrightarrow{k_2} Au^{II} + X \tag{8}$$

in the presence of reducing agents,

$$Au^{III} + Red \xrightarrow{k_r} Au^{II} + Ox \tag{9}$$
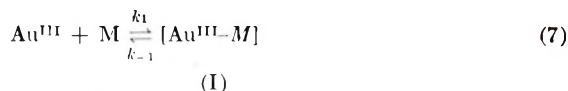
Initiation, propagation, and termination:

initiation, $Au^{II} + M \xrightarrow{k_i} Au^{I} + M^*$ (10)

propagation, $M^* + M \xrightarrow{k_p} P^*_1$ (11)

$P_n^* + M \rightarrow P^*_{n+1}$

termination: $P^* + M \xrightarrow{k_t} P$ (12)
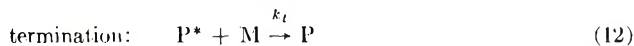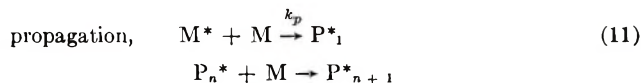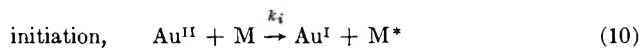
By applying the assumption of stationary concentrations for $[P^*]$, $[Au^{II}]$, and $[Au^{III}-M]$, the following rate expressions were obtained.

For polymerization in the absence of reducing agents (after induction period):

$$-d[M]/dt = [k_1 k_2 k_p / k_t (k_2 + k_{-1})][Au^{III}][M]   (13)$$

For polymerization in the presence of reducing agents and during the induction period in the absence of reductant:

$$-d[M]/dt = (k_p k_r / k_t)[Au^{III}][Red]   (14)$$

After the induction period:

$$-d[M]/dt = (k_p/k_t)\{k_1 k_2 [M]/(k_2 + k_{-1}) + k_r[Red]\}[Au^{III}]   (15)$$

From the kinetics viewpoint the same kinetic expressions are derived if the initiation, eq. (10), is replaced with the noncharge-transfer initiation by Au^{II}. It is, however, difficult to consider ordinary cationic initiation by Au^{II} species, which are probably complexed anions, as shown in eqs. (3) and (4).

These kinetic expressions explain the experimental results very well. The rate of polymerization in the dark is proportional to $[Au^{III}]$ and also to [VCZ], in agreement with eq. (13). When a reducing agent is added, the time–conversion curve is straight during the initial period, in agreement with the rate expression eq. (14); see Figures 8 and 9. The initial R_p is exactly proportional to $[Au^{III}]$[ferrocene] but independent of [VCZ], as expected from eq. (14); see Figure 9. When the direct reaction between VCZ and Au^{III} begins to influence the polymerization, the R_p increases in a manner expressed by eq. (15).

Interpretation of Induction Period of Polymerization in Dark

The physical meaning of the induction period is somewhat obscure when the induction period changes over continuously to a stationary state, as in the present system. The linear plot (Fig. 5) was extrapolated to zero conversion, and the intercept of the time coordinate was taken as the induction period. At the end of the induction period the concentration of active species Au^{II} was assumed to reach a certain definite value, $[Au^{II}]_i$. Since the concentration of Au^{II} is a function of time t during the initial nonstationary state, the induction period could be defined as the time

required to accumulate active species up to the critical concentration $[Au^{II}]_i$.

The following differential equations are derived from nonstationary-state kinetics:

$$d[Au^{III}\text{--}M]/dt = k_1[M][Au^{III}] - (k_2 + k_{-1})[Au^{III}\text{--}M] \tag{16}$$

$$d[Au^{II}]/dt = k_2[Au^{III}\text{--}M] - k_i[M][Au^{II}] \tag{17}$$

Since the change in $[M][Au^{III}]$ is negligible during the induction period the solution is given by

$$[Au^{II}] = \frac{k_1 k_2[M][Au^{III}]}{(k_2 + k_{-2})} \frac{1}{k_i[M]} - $$

$$\frac{\exp\{-(k_2 + k_{-1})t\}}{k_i[M] - (k_2 + k_{-1})} (1 - \exp\{-k_i[M]t\}) \tag{18}$$

On the assumption that the initiation of polymerization by Au^{II} is much faster than the decomposition of $[Au^{III}\text{--}M]$, that is, $k_i[M] >> k_2 + k_{-1}$, the solution is simplified to

$$[Au^{II}] \approx (k_1 k_2/k_i)[Au^{III}]t \tag{19}$$

Then the relation between the induction period and the initiator concentration is given by the following, which explains the experimental results in Figure 4:

$$t_i \approx [Au^{II}]_i k_i/k_1 k_2 (1/[Au^{III}]) \equiv C(1/[Au^{III}]) \qquad C = \text{constant} \tag{20}$$

If it is assumed that the reaction product of VCZ and Au^{III} could initiate polymerization as well, the reciprocal of the induction period is given by the following,

$$t_i \approx C(1/[Au^{III}][M]) \tag{21}$$

which contradicts the experimental findings.

Kinetic Quantities Derived from Molecular Weight

The change in molecular weight of the polymer as a function of conversion was analyzed on the assumption of four unit reactions that decide the chain length:

$$P^*_{n-1} + M \overset{k_p}{\rightarrow} P_n^* \tag{11}$$

$$P_n^* + M \overset{k_t}{\rightarrow} P_{n+1} \quad \text{(quaternization of nitrogen)} \tag{12}$$

$$P_n^* + M \overset{k_{tr}M}{\longrightarrow} P_n + M^* \tag{22}$$

$$P_n^* + Y \overset{k_{tr}Y}{\longrightarrow} P_n + Y^* \quad \text{(Y is chain-transfer agent)} \tag{23}$$
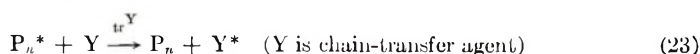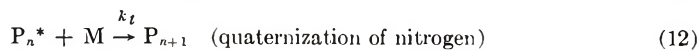
Fig. 13. Kinetic interpretation of dependence of average degree of polymerization on conversion. Calculation based on data of Figure 6.

By considering Y (probably solvent or water) a constant quantity, the following is derived:

$$1/\overline{DP} = (k_t + k_{tr}{}^M)/k_p + k_{tr}{}^Y[Y]/k_p(\log [M]_0 - \log [M])/$$

$$([M]_0 - [M]) \tag{24}$$

From the plot of $1/\overline{DP}$ versus $(\log [M]_0 - \log [M])/([M]_0 - [M])$, as shown in Figure 13 the kinetic quantities presented in Table III are determined.

These kinetic quantities agree well with the values obtained by Pác and Plesch[7] for the polymerization of VCZ initiated by tetranitromethane in nitrobenzene. It is interesting to note that the kinetic quantities obtained for polymerizations initiated by completely different initiators are nearly equal, since an identity of kinetic quantities would be a good indication of the indentity of chain carriers in the systems. If Ellinger's mechanism,[8] which involves the activation of monomer by mesomeric polarization, is valid, the chain carriers and also the incoming monomer molecule should be strongly controlled by the initiator and, consequently, the kinetic quantities should depend on the kind of initiator.

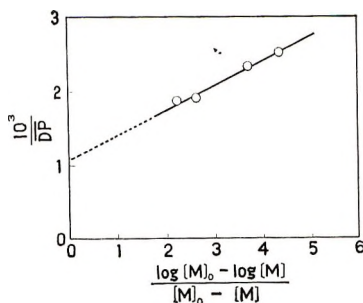We are therefore inclined to consider the chain carrier of the polymerization initiated by tetranitromethane and by sodium chloroaurate to be cationic in both cases, although the initiation process is most likely to be charge-transfer reaction. These are not surprising results. The ion–radical-initiated polymerization could be cationic or radical or both, since an ion–radical would be separated as an ordinary radical and a carbonium ion after the addition of a second monomer. Under the present experimental conditions, in the presence of nitrobenzene, the radical would be scavenged, and the cation alone should survive for propagation.

TABLE III
Comparison of Kinetic Quantities with Published Data

	$(k_t + k_{tr}{}^M)/k_p$	$k_{tr}{}^Y[Y]/k_p$, moles/l.
Present work	1.0×10^{-3}	1.5×10^{-4}
Pác and Plesch[7]	1.16×10^{-3}	10^{-4}

CONCLUSION

The active initiating species in the polymerization of VCZ with sodium chloroaurate is probably divalent gold formed in the reduction of trivalent gold by monomer and other reducing agents. The chain carrier is probably a cation, although the formation of ion–radicals is evidenced by ESR spectroscopy.

References

1. S. Tazuke, K. Nakagawa, and S. Okamura, *J. Polymer Sci. B*, **3**, 923 (1965).

2. S. Tazuke and S. Okamura, *J. Polymer Sci. A-1*, **4**, 141 (1966).

3. S. Tazuke, T. B. Tjoa, and S. Okamura, *J. Polymer Sci. A-1*, **5**, 1911 (1967).

4. C. E. H. Bawn, L. Ledwith, and Y. Shin-Lin, *Chem. Ind. (London)*, **1965**, 769.

5. S. Tazuke, M. Asai, S. Ikeda, and S. Okamura, *J. Polymer Sci. B*, **5**, 453 (1967).

6. K. Ueberreiter and J. Springer, Z. *Physik. Chem.*, **36**, 299 (1963).

7. J. Pác and P. H. Plesch, *Polymer*, **8**, 237 (1967).

8. L. P. Ellinger, *Polymer*, **5**, 559 (1964).

9. Stability Constants, *Chem. Soc. (London)*, *Spec. Publ.*, **17**, (1964): (a) p. 289 (1964), (b) p. 21.

10. R. L. Rich and H. Taube, *J. Phys. Chem.*, **58**, 6 (1954).

11. T. Vänngard and S. Åkerström, *Nature*, **184**, 183 (1959).

12. J. H. Waters and H. B. Gray, *J. Am. Chem. Soc.*, **87**, 3534 (1965).

13. H. Scott, G. A. Miller, and M. M. Labes, *Tetrahedron Letters*, **17**, 1073 (1963).

14. L. P. Ellinger, *J. Appl. Polymer Sci.*, **9**, 3939 (1965).

15. J. A. Page and G. W. Willkinson, *J. Am. Chem. Soc.*, **74**, 6149 (1952).

16. I. Tachi, "Polarography" (Iwanami Shoten) pp. 380 (1954).

17. H. B. Gray, Transition Metal Chemistry, Vol. I, R. L. Carlin, Ed., Marcel Dekker, New York, 1965, p. 239.

Cationic Polymerization of the Geometrical Isomers of β-Methylstyrene and Anethole*

A. MIZOTE, T. HIGASHIMURA, and S. OKAMURA

Department of Polymer Chemistry, Kyoto University, Kyoto, Japan

Synopsis

Cationic polymerization of the geometrical isomers of β-methylstyrene and anethole (p-methoxy-β-methylstyrene) was studied in order to clarify the relation between the geometrical structure of the α,β-disubstituted olefins and their monomer reactivities, subsequent to previous work. Polymerization was carried out in toluene or ethylene dichloride with stannic chloride at 0°C. trans-β-Methylstyrene was 1.3 to 1.5 times more reactive than cis-β-methylstyrene to the styrene carbonium ion; copolymerization between the trans and the cis isomers of β-methylstyrene showed little difference in monomer reactivity. By contrast, the cis anethole was 1.5–2.0 times more reactive than the trans, according to copolymerization between the two isomers together. The lower reactivity of the cis-β-methylstyrene could be explained by steric hindrance in the cis isomer, proposed by Overberger et al.

INTRODUCTION

In contrast to radical polymerization, there have been few studies on the monomer reactivities of the geometrical isomers, especially in cationic polymerization. In previous papers, the monomer reactivities of the geometrical isomers of n-butyl propenyl ether[1] and other alkyl propenyl ethers[2] were discussed, and it was reported that the cis isomer was more reactive than the trans isomer.

Overberger et al.[3] studied the cationic copolymerization of some β-alkylstyrene derivatives and found that the trans isomer of β-methylstyrene was more reactive than the cis isomer. The relations between the monomer reactivity and the geometrical structure of the monomer seemed to be different for styrene derivatives and vinyl ether derivatives.

Thus, in order to clarify this relation, the monomer reactivities of the geometrical isomers of β-methylstyrene and anethole (p-methoxy-β-methylstyrene) were studied further in their cationic copolymerization with styrene and also in copolymerization between the trans and the cis isomers. The gas chromatographic technique was used to measure the residual monomers in the reaction mixture during the copolymerization.

In the case of β-methylstyrene the trans isomer was found to have a higher reactivity than the cis isomer in copolymerization with styrene.

* This is the sixth in a series of papers, "Cationic Polymerization of α,β-Disubstituted Olefins."

However, in the case of anethole, which is more reactive than β-methyl-styrene, the *cis* isomer was found to have a higher reactivity than the *trans* isomer in copolymerization with styrene and in copolymerization between the *trans* and *cis* isomers.

EXPERIMENTAL

Monomers

β-Methylstyrene and anethole were prepared from α-methylcinnamic acid derivatives by heating with copper dust and quinoline. The crude monomers were washed with dilute hydrochloric acid and water and then sodium hydroxide and water. The organic layer was extracted with *n*-hexane and dried over sodium sulfate.

After the *n*-hexane was distilled off, further distillation through a short Vigreux column gave a mixture of the geometrical isomers, rich in *cis* isomer (*cis*, 60-70%; *trans*, 40-30%), for both β-methylstyrene and anethole.

The geometrical isomers of β-methylstyrene were separated by gas chromatography (column, polyethylene glycol + dioctylphthalate at 150°C.). Anethole was used without separation of the geometrical isomers. The physical constants of these monomers are listed in Table I.

TABLE I
Physical Properties of β-Methylstyrene and Anethole

Monomer	B.p., °C., and press., mm. Hg	n_D^{25}	d	Isomeric purity, %	Ref.
β-methylstyrene:					
cis isomer	—	1.5397	—	97	Present work
	64.5, 20	1.5400	0.9107 (25°)	100	4
trans isomer	—	1.5465	—	98	Present work
	73.5, 20	1.5473	0.9019 (25°)	100	4
Anethole:					
cis/trans mixture	110–115, 15	1.5530	—	*cis*70, *trans* 30	Present work
trans isomer	108–109, 11.5	1.5564	0.9788 (30°)	100	Present work
	112–114, 15	1.5614 (21°)	0.9936 (15°)	100	5

Procedure

Polymerization was carried out in ethylene dichloride and in toluene with stannic chloride, trichloroacetic acid being used as a cocatalyst, at 0°C. under nitrogen atmosphere. Trace amounts of water in the these poly-

merization systems were no more than 5 mmoles/l.   The polymerization systems with β-methylstyrene contain a certain amount of monochlorobenzene as an internal standard substance for the gas chromatographic analysis.   p-Nitrotoluene was used for this purpose in the polymerization system with anethole.

An aliquot of the reaction mixture was drawn out at certain intervals of reaction time, and the polymerization was stopped by the addition of methanol.   Then the residual monomers in the aliquot were analyzed on the gas chromatograph.   Thus the relative monomer reactivities of the geometrical isomers in the copolymerization were determined from the time–conversion curves by the Fineman-Ross-Sakurada method.[1]

RESULTS

β-Methylstyrene

cis-β-Methylstyrene was copolymerized with styrene in ethylene dichloride with stannic chloride at 0°C.   Figure 1 shows the time–conversion curves of each comonomer.   The rate of consumption of styrene is greater than that of cis-β-methylstyrene.   From the time–conversion curves in Figure 1 the monomer reactivity ratios were calculated according to the Fineman-Ross-Sakurada equation.[1]   A plot of the equation is shown in Figure 2, where M_1 and M_2 represent styrene and cis-β-methylstyrene, respectively.   It was found that r_1 was 1.95 ± 0.1 and r_2 was 0.03 ± 0.05.

The relative monomer reactivity of trans-β-methylstyrene in copolymerization with styrene was determined in a similar way.   The time–conversion curves and Fineman-Ross-Sakurada plot are shown in Figures 3 and 4, respectively.   It was found that r_1 was 1.4 ± 0.15 and r_2 was 0.2 ± 0.1; M_1 and M_2 represent styrene and trans-β-methylstyrene, respectively.

Comparing the relative monomer reactivities of the two copolymerizations the trans isomer of β-methylstyrene was found to be 1.5 times more

Fig. 1. Time–conversion curves of (a) styrene and (b) cis-β-methylstyrene in copolymerization: monomer concentration (mole/l.), St 0.44, cis-β-M, 0.38; solvent (CH₂Cl)₂; catalyst SnCl₄·CCl₃COOH (1:0.5), 5 mmole/l.; at 0°C.
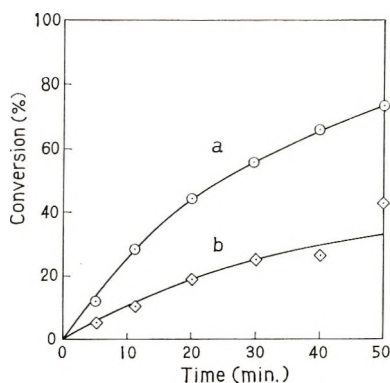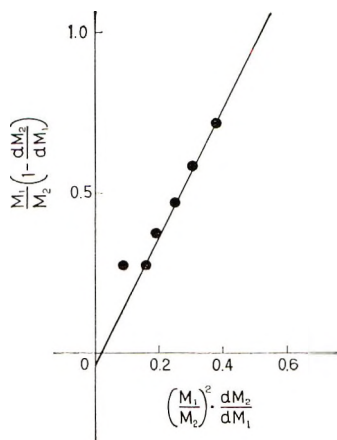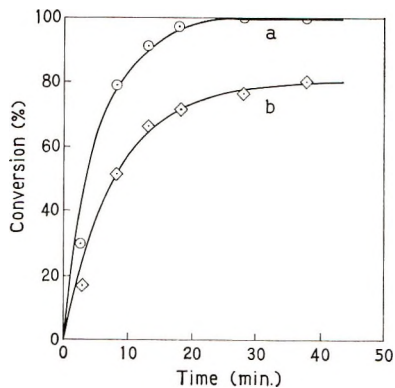
Fig. 2. Fineman-Ross-Sakurada plot from Figure 1.

Fig. 3. Time–conversion curves of (a) styrene and (b) *trans-β*-methylstyrene in co-polymerization: monomer concentration (mole/l.), St 0.44, *trans-β*-M 0.38; solvent $(CH_2Cl)_2$; catalyst $SnCl_4 \cdot CCl_3COOH$ (1:0.5), 10 mmole/l.; at 0°C.
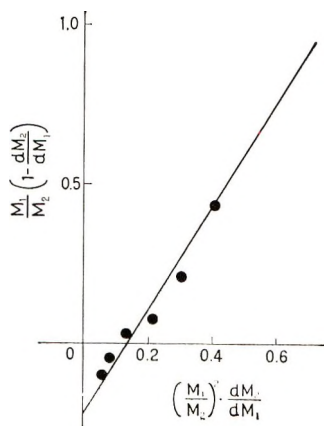
Fig. 4. Fineman-Ross-Sakurada plot from Figure 3.
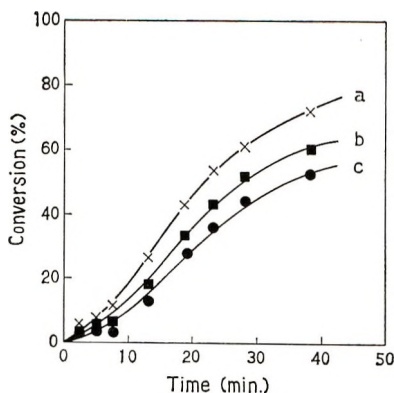
Fig. 5. Time–conversion curves of (a) styrene, (b) *trans*-β-methylstyrene, and (c) *cis*-β-methylstyrene in terpolymerization: monomer concentration (mole/l.), St 0.44, *cis*-β-M 0.27, *trans*-β-M 0.12; solvent $(CH_2Cl)_2$; catalyst $SnCl_4 \cdot CCl_3COOH$ (1:0.5), 5 mmole/l.; at 0°C.
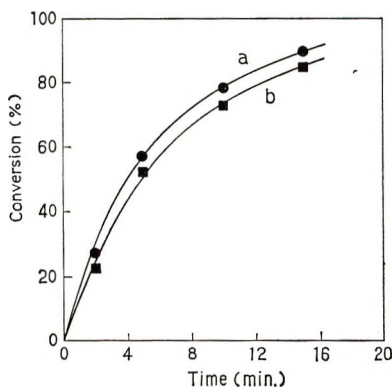
Fig. 6. Time–conversion curves of (a) *cis*-β-methylstyrene and (b) *trans*-β-methylstyrene in copolymerization: monomer concentration (mole/l.), *cis*-β-M 0.54, *trans*-β-M 0.24; solvent $(CH_2Cl)_2$; catalyst $SnCl_4 \cdot CCl_3COOH$ (1:0.5), 50 mmole/l.; at 0°C.

reactive than the *cis* isomer. This conclusion was confirmed in a terpolymerization with styrene and the *cis* and *trans* isomers of β-methylstyrene. Figure 5 shows the time–conversion curves of the three components in the terpolymerization, calculated from the amount of residual monomers. The rates of polymerization in Figure 5 are in agreement with the relative reactivities of the geometrical isomers of β-methylstyrene, obtained in the copolymerization of styrene with either isomer of β-methylstyrene.

The difference between the monomer reactivities of the geometrical isomers may also be estimated from the copolymerization of the *cis* and *trans* isomers. Figure 6 shows the time–conversion curves of this polymerization. As the figure shows, when the *cis* and *trans* isomers of β-methylstyrene were copolymerized, the difference in reactivity between the isomers was small, and the *cis* isomer was found to be a little more reactive

than the *trans* isomer.   This is the opposite of the result obtained in the copolymerization with styrene; it is discussed in a later section of this paper.

Anethole

A mixture of styrene and the geometrical isomers of anethole was terpolymerized in ethylene dichloride.   The time–conversion curves are shown in Figure 7.   The monomer reactivities of the geometrical isomers of anethole to carbonium ions could be estimated qualitatively from these
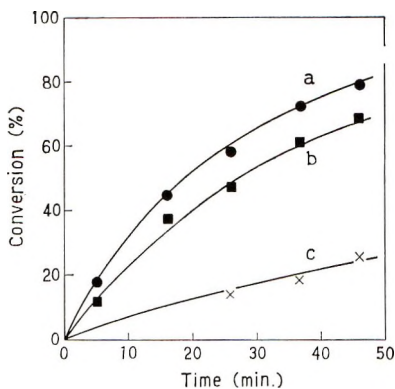
Fig. 7. Time–conversion curves of (a) *cis*-anethole, (b) *trans*-anethole, and (c) styrene in terpolymerization: monomer concentration (mole/l.), St 0.44, *cis*-A 0.23, *trans*-A 0.10; solvent $(CH_2Cl)_2$; catalyst $SnCl_4 \cdot CCl_3COOH$ (1:0.5), 2 mmole/l.; at 0°C.
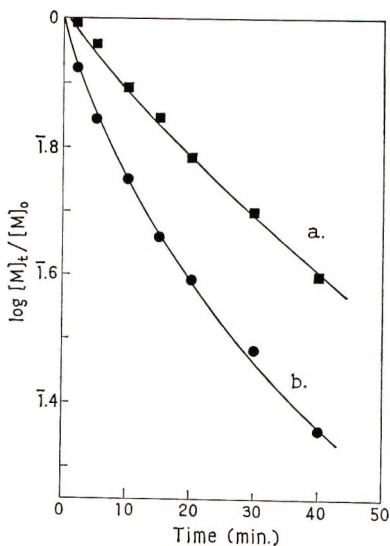
Fig. 8. First-order plot of copolymerization of (a) *trans*-anethole and (b) *cis*-anethole: monomer concentration (mole/l.), *cis*-A 0.46, *trans*-A 0.20; solvent toluene; catalyst $SnCl_4 \cdot CCl_3COOH$ (1:0.5), 30 mmole/l.; at 0°C.

curves.   That is, in the case of anethole the *cis* isomer was found to be more reactive than the *trans* isomer in ethylene dichloride in the terpolymerization.

Figure 8 shows first-order plots of each monomer in a mixture of the *trans* and *cis* isomers of anethole, polymerized in toluene with stannic chloride.   The rate of consumption of the *cis* isomer was found greater than that of the *trans* isomer.

DISCUSSION

As a summary of the results in this paper the following may be concluded. In the case of β-methylstyrene, when its *cis* and *trans* isomers were copolymerized together, the difference between their monomer reactivities was small, and the *cis* isomer seemed to be more reactive than the *trans*, but in the copolymerization of styrene with either of the isomers the *trans* isomer was the more reactive.   In the case of anethole the *cis* isomer was found to be the more reactive in copolymerization of the two isomers together and also in terpolymerization with styrene.

Concerning the monomer reactivity of the geometrical isomers of β-methylstyrene, Overberger et al.[3] reported the copolymerization of *p*-chlorostyrene and the geometrical isomers of β-methylstyrene with stannic chloride; they found the *trans* isomer to be the more reactive monomer, but the difference was small, consistent with our present results.   They interpreted the difference in reactivity between the *trans* and *cis* isomers of β-methylstyrene as due to steric hindrance in the *cis* isomer, which might reduce the reactivity of the *cis* isomer.   They referred to ultraviolet spectra and the extinction coefficient to show the steric hindrance between the β-methyl group and a hydrogen atom at the *ortho* position in the *cis* isomer.

The olefinic part in the β-methylstyrene monomer is not so reactive that, when the bulky propagating carbonium ion attacks the *cis* isomer, such steric hindrance in the *cis* isomer as proposed by Overberger et al. would play an important role in affecting the monomer reactivity in the polymerization. There is no such steric hindrance in the *trans* isomer and, apparently, the *trans* isomer polymerizes the more easily.   On the other hand, it was found that the *cis* isomer of β-methylstyrene was slightly more reactive than the *trans* isomer in copolymerization of the two together.   The products of copolymerization of the isomers were oily, low molecular weight materials. The rate of monomer consumption in these systems could be controlled not only by the propagation reaction but also, perhaps, by the initiation reaction or the transfer reaction.   Therefore, the higher reactivity of the *cis* isomer in the copolymerization of the isomers together could be attributed to the higher reactivity of its olefinic part, because the attacking ion would not be so bulky as the propagating species so that the steric hindrance would not be important.

In the case of anethole the *cis* isomer always was the more reactive monomer in copolymerization with styrene and also in the copolymerization

between the isomers.   Considering the monomer structure of anethole and β-methylstyrene, the steric hindrance in the *cis* isomer would be almost the same.   Such kind of steric hindrance in the *cis* isomer of anethole might be compensated for by the higher reactivity of the olefinic part.

References

1. A. Mizote, S. Kusudo, T. Higashimura, and S. Okamura, *J. Polymer Sci. A-1*, **5**, 1727 (1967).

2. T. Higashimura, S. Kusudo, Y. Ohsumi, A. Mizote, and S. Okamura, *J. Polymer Sci. A-1*, in press.

3. C. G. Overberger, D. Tanner, and E. M. Pearce, *J. Am. Chem. Soc.*, **80**, 4566 (1958).

4. R. Y. Mixer, R. F. Heck, S. Winstein, and W. G. Young, *J. Am. Chem. Soc.*, **75**, 4094 (1953).

5. L. Bert, *Compt. Rend.*, **213**, 873 (1941).

Effect of Surfactants on the Polymerization of Acrylamide in Aqueous Solutions

J. P. FRIEND and A. E. ALEXANDER, *Department of Physical Chemistry, University of Sydney, Australia*

Synopsis

The polymerization of acrylamide in aqueous surfactant solutions, initiated by potassium persulfate, has been investigated, dilatometry being used to follow the conversion. It has been shown that below the critical micellar concentration (CMC), cationic, anionic and non-ionic surfactants have no effect, while above the CMC only cationic soaps have an effect, lowering both the rate of polymerization and the molecular weight of the resultant polymer.

INTRODUCTION

The role of the surfactant in the polymerization of the more water-soluble monomers (vinyl acetate, methyl acrylate, and acrylonitrile), initiated by persulfate, has been examined in earlier studies in this laboratory.[1-3] Surfactants were found to exert a dominating influence on the very initial stages of the polymerization process, when the insoluble embryos are being formed from a very small number of molecules ("alive" or "dead"). (In these systems the polymer is insoluble in the aqueous phase.) The micelle as such appeared to play no particular role, serving merely as a reservoir of single surfactant molecules.

On the basis of the theory advanced to explain those earlier observations, a polymerizing system in which the polymer does not separate from solution should be unaffected by addition of surfactants, either below or above the critical micellar concentration (CMC).

Accordingly the polymerization of acrylamide by potassium persulfate (the initiator used in earlier studies), was examined in the absence and in the presence of a number of anionic, non-ionic, and cationic surfactants. The reaction in the absence of surfactants was found to agree closely with the published data of Riggs and Rodriguez.[4]

In the presence of both anionic and non-ionic surfactants, below or above the CMC, there was no appreciable effect on the rate of polymerization. (Polymerization was followed to at least 90%.) Cationics below the CMC were also without effect, but above the CMC both the rate of polymerization and the molecular weight of the polymer were reduced. These effects can be most readily explained by assuming that persulfate

ions bound to the surface of a cationic micelle decompose less readily than persulfate ions in aqueous solution.

EXPERIMENTAL

Acrylamide from B.A.L.M. Research Laboratories was recrystallized twice from chloroform and vacuum dried.

Potassium persulfate was recrystallized twice from hot water (60°C.) and vacuum dried.

Dodecyl-, tetradecyl-, and hexadecyltrimethyl-ammonium bromides (DTAB, TTAB, and HTAB, respectively) were made by reacting excess trimethylamine with the appropriate long chain bromide (Eastman) in acetone solution. After ether extraction the compounds were recrystallized from acetone.

Renex 690 [$CH_3C(CH_3)_2CH_2C(CH_3)_2$-$p$-$C_6H_4(OCH_2CH_2)_{10}OH$] was a commercially available non-ionic surfactant.

Sodium dodecyl sulfate (NaDS) was made from Fluka dodecanol by the method of Dreger et al.[5] and was ether-extracted.

Water was doubly distilled, the second time from alkaline permanganate solution.

The kinetics were followed dilatometrically, a dilatometer of volume 91 ml. fitted with a magnetic stirrer and a 2.00 mm. diameter capillary being used.

Reactions were not carried out under deaerated conditions as it has been shown that the only apparent effect of deaeration is to decrease the induction period. This assumption was further supported by the fact that the kinetic data of Riggs and Rodriguez[4] obtained under deaerated conditions agreed very closely with those obtained here.

The specific contraction of polyacrylamide (0.221 ml./g. polymer) reported by Dainton et al.[6] was confirmed. Temperatures were maintained to ±0.1°C. and each run done in duplicate.

For molecular weight determinations polymerization was stopped at the desired level by pouring into ice-cold 0.1% hydroquinone solution. The polymer was precipitated by ethanol, a little aluminum sulfate being added to assist the precipitation of low molecular weight materials.[6] It was purified by a twofold solution and precipitation procedure.

After drying *in vacuo* the viscosity of a series of aqueous solutions was measured in an Ostwald viscometer at 25°C. and the viscometric average molecular weight calculated[6] from the equation,

$$[\eta] = KM^{\alpha}$$

taking $K = 6.84 \times 10^{-4}$, where concentration is in grams/100 ml. and $\alpha = 0.66 \pm 0.05$.

RESULTS AND DISCUSSION

Reaction in Absence of Surfactants

Runs were carried out at 50°C. in unbuffered systems, since the rate was found to be unaffected by pH over the range 4–7. Initiator concentration was varied over a thirtyfold range (1–30mM $K_2S_2O_8$) and monomer concentration over a fourfold range (0.132–0.528M).

From the rate equation

$$-d[M]/dt = k[M]^\alpha[I]^\beta \qquad (1)$$

where M denotes monomer and I initiator, the exponents α and β were found from the plot of log $d[M]/dt$ versus log [M] and log [I], respectively, to be 1.25 and 0.51, in good agreement with those found by Riggs and Rodriguez.[4] (Instantaneous rates were obtained at points on the conversion–time curve by using an OTT derivimeter.)

Classical theory for free-radical polymerization predicts $\alpha = 1$ and $\beta = 1/2$ in eq. (1). Various theories to explain the departure from first-order kinetics with respect to monomer concentration have been advanced, such as the "complex" theory,[7] the "cage effect" theory,[8] the "solvent transfer" theory,[9,10] and various "diffusion control" theories.[7,11-13]

Another possibility is that the monomer solutions deviate increasingly from ideality with increase in concentration (possibly through hydrogen-bond formation as in the case of urea solutions,[14]) and this leads to a slight increase in the propagation constant with increasing monomer concentration.

Reaction in the Presence of Surfactants

With a system containing 0.264M monomer and 10mM potassium persulfate the effect of addition of anionic, non-ionic, and cationic surfactants

TABLE I
Effects of Surfactants on Rate and Molecular Weight of Polymer[a]

Surfactant	Hydrocarbon chain length	Concentration, M	CMC, M	Effect on rate	Molecular weight at 80% conversion
No surfactant	—	—	—	—	2.3×10^5
NaDS	C_{12}	8.7×10^{-4}	8×10^{-3}	None	Not measured
NaDS	C_{12}	3.1×10^{-2}		None	"
NaDS	C_{12}	4.84×10^{-2}		None	"
Renex 690	$C_{10}-C_{11}$	8×10^{-3}	8×10^{-5}	None	"
DTAB	C_{12}	4.84×10^{-2}	1.2×10^{-2}	Reduced	9.6×10^4
TTAB	C_{14}	4.84×10^{-2}	5×10^{-3}	Reduced	Not measured
HTAB	C_{16}	4.84×10^{-2}	8×10^{-4}	Reduced	6.3×10^4

[a] 0.264M monomer; 10mM $K_2S_2O_8$, 50°C.

Fig. 1. Effect of chain length of cationic surfactant on the rate of polymerization (0.264M monomer, 10mM K$_2$S$_2$O$_8$, 50°C.): (1) no added surfactant; (2) 0.0484M DTAB; (3) 0.0484M TTAB; (4) 0.0484M HTAB.

was examined. Rates at 50°C. and molecular weights of polymer at 80% conversion were studied. The results are summarized in Table I.

The CMC's quoted in Table I are literature values for room temperature and salt-free systems. The effect of added monomer (0.264M), added salt (10mM K$_2$SO$_4$, to avoid polymerization) and the higher temperature (50°C.) on the CMC of C$_{14}$ trimethylammonium bromide (TTAB) was found to cause a slight reduction, namely from 5 to 4 × 10^{-3}M. For the present purposes this can be ignored.

Figure 1 shows that as the chain length of the cationic surfactant is increased (at a fixed molar concentration, which in all cases is above the CMC) the rate is progressively reduced. Unlike the blank, however, these curves do not obey a simple kinetic law with respect to monomer concentration. This is shown by the plot of log rate versus log monomer concentration in Figure 2. From eq. (1) it is seen that the exponent α is not constant.

The effect of increasing the concentration of C$_{12}$ trimethylammonium bromide (DTAB) (above the CMC) is also to reduce the rate, as shown in Figure 3.

An experiment was carried out in which equal micellar concentrations of DTAB and TTAB were used (i.e., bulk concentrations of 0.0554M and 0.0484M respectively). Under these conditions TTAB gave a rate ca. 4% lower than the DTAB.

The effect of the concentration and chain length of cationic surfactant upon the induction period is shown in Table II, which also includes some
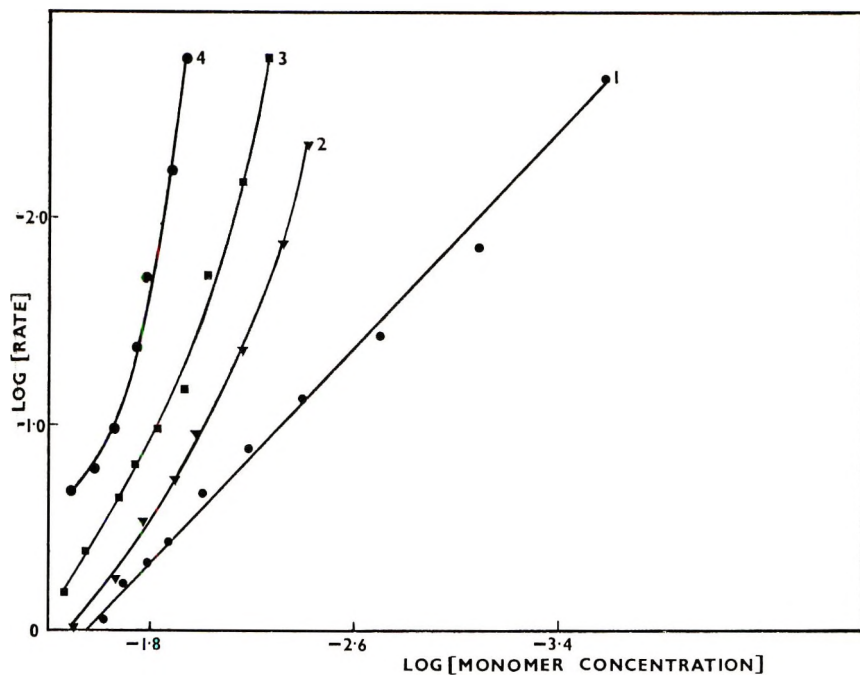
Fig. 2. Plot of log rate of reaction vs. log monomer concentration in absence and presence of cationic surfactants: (1) no added surfactant; (2) 0.0484M DTAB; (3) 0.0484M TTAB; (4) 0.0484M HTAB.
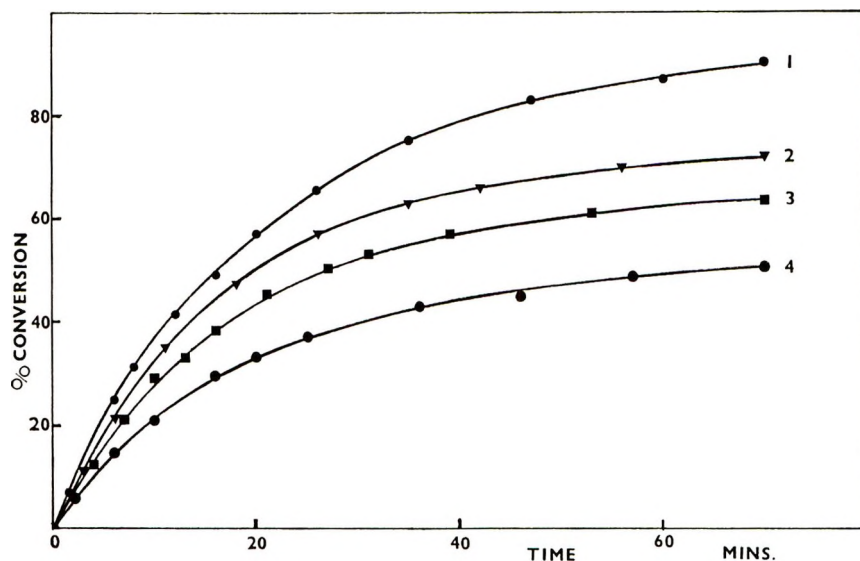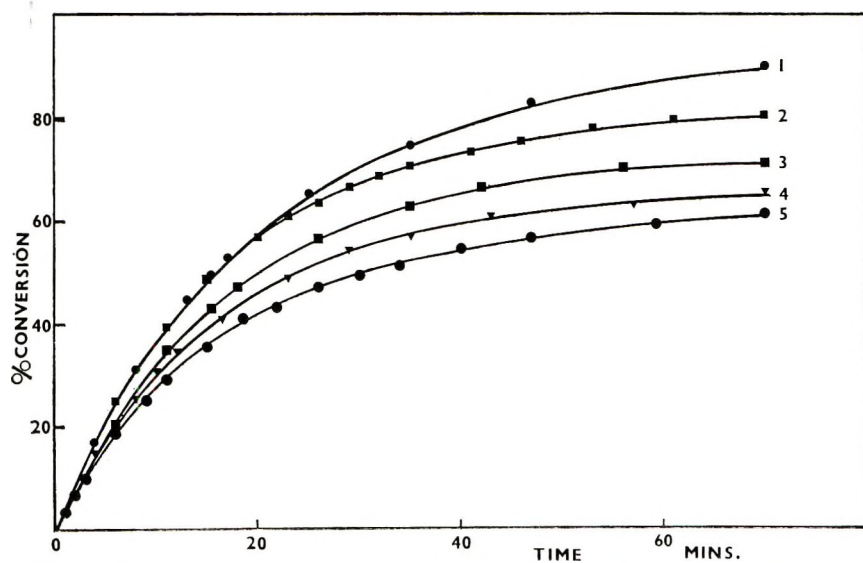

Fig. 3. Effect of concentration of cationic surfactant on the rate of polymerization (0.264M monomer, 10mM K₂S₂O₈, 50°C.): (1) no added surfactant; (2) 0.0323M DTAB; (3) 0.0484M DTAB; (4) 0.0554M DTAB; (5) 0.0800M, DTAB.

TABLE II
Induction Periods with Various Cationic Surfactants

Surfactant	Concn., mM	$K_2S_2O_8$ concn., mM	Induction period, min.
Nil		10	23
DTAB	32.3	"	20
"	48.4	"	29
"	55.4	"	30
"	80.0	"	34
TTAB	48.4	10	37
HTAB	48.4	"	45
Nil		1.25	71
"		2.5	52
"		3.5	41
"		5.0	37
"		7.1	24
"		10	23
"		15	15
"		20	13
"		30	10

ᵃ 0.264M monomer, 50°C. in all.

data for the effect of persulfate concentration in the absence of surfactant.

The effect of the cationic surfactants above the CMC can be most readily explained by assuming that the $S_2O_8^=$ ions are bound to the strongly positively charged micelles in preference to $Br^=$ and that a $S_2O_8^=$ ion so bound decomposes into free radicals at a slower rate than one free in solution. This strong bonding of divalent ions by micelles is well known and in the present case can lead to the precipitation of a stoichiometric complex, e.g., $(HTAB)_2^+ (S_2O_8)^=$, at room temperature. The solubility of this complex increases as the temperature is raised and as the chain length of the
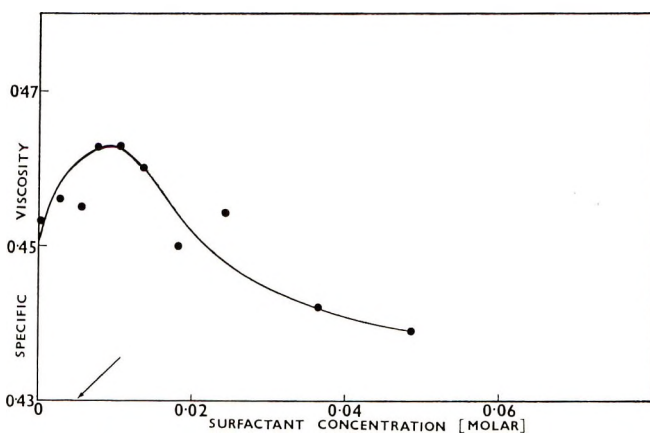
Fig. 4. Effect of added cationic surfactant (TTAB) on the specific viscosity of 0.198% polyacrylamide solution. CMC of surfactant denoted by arrow.

surfactant is decreased. The complex can also be dissolved (or dispersed) by further addition of the original surfactant. Under the conditions used here for polymerizations in the presence of cationic micelles the surfactant is in excess.

The increase in induction period with increasing concentration and increasing chain-length of surfactant could also be ascribed to the adsorbed $S_2O_8^=$ ion decomposing less readily than the $S_2O_8^=$ in solution.

The possibility that the polymer and the cationic soap micelles might interact in some way was examined by measuring the specific viscosity of a 0.198% polyacrylamide solution as a function of TTAB concentration. The results, shown in Figure 4, indicate a small increase in viscosity up to about the CMC followed by a rather more pronounced fall. Some interaction with the cationic micelle is thus indicated, possibly through the sulfate groups at the ends of the polymer chains.

This conclusion, although clearly tentative, could also explain the decrease in molecular weight observed in the presence of the cationic micelles. This decrease is contrary to expectation on the basis of homogeneous polymerization studies, where molecular weight normally increases as the rate decreases. If, however, the polymer chain ("alive" or "dead") is attracted to some degree by the cationic micelle, then clearly the rate of termination will be enhanced, and the molecular weight diminished, relative to the system without micelles.

References

1. D. H. Napper and A. G. Parts, *J. Polymer Sci.*, **61**, 113 (1962).

2. D. H. Napper and A. E. Alexander, *J. Polymer Sci.*, **61**, 127 (1962).

3. C. E. M. Morris, A. E. Alexander, and A. G. Parts, *J. Polymer Sci. A-1*, **4**, 985 (1966).

4. J. P. Riggs and F. Rodriguez, paper presented at American Chemical Society, Div. Polymer Chem., Detroit, Mich., April, 1965. *Polymer Preprints*, **6**, No. 1, 207 (1965).

5. E. E. Dreger, G. I. Keim, G. D. Miles, L. Shedlovsky, and J. Ross, *Ind. Eng. Chem.*, **36**, 610 (1944).

6. E. Collinson, F. S. Dainton, and G. S. McNaughton, *Trans. Faraday Soc.*, **53**, 489 (1957).

7. P. Allen and C. Patrick, *Makromol. Chem.*, **48**, 89 (1961).

8. M. S. Matheson, *J. Chem. Phys.*, **13**, 584 (1945).

9. G. M. Burnett and L. D. Loan, *Trans. Faraday Soc.*, **51**, 214, 219 (1955).

10. P. W. Allen, F. M. Merrett, and J. Scanlan, *Trans. Faraday Soc.*, **51**, 95 (1955).

11. S. Toppet, G. Delzenne, and G. Smets, *J. Polymer Sci. A*, **2**, 1539 (1964).

12. M. G. Baldwin, *J. Polymer Sci. A*, **1**, 3209 (1963).

13. A. Chapiro, P. Cordier, V. K. Hayashi, I. Mita, and J. Sebban-Danon, *J. Chim. Phys.*, **56**, 447 (1959).

14. G. E. Hibberd and A. E. Alexander, *J. Phys. Chem.*, **66**, 1854 (1962).

Polymerization and Copolymerization of α-Methacrylophenone

J. E. MULVANEY, J. G. DILLON, and J. L. LAVERTY,
*Department of Chemistry, The University of Arizona, Tucson,
Arizona 85721*

Synopsis

Under a variety of conditions it has not been possible to induce the free-radical-initiated homopolymerization of α-methacrylophenone (α-MAP). The only product isolated from such efforts was the Diels-Alder dimer of the monomer. A Mayo-Lewis plot of the free-radical copolymerization of α-MAP and styrene shows considerable scatter but the copolymer composition indicates that an α-MAP unit can add to itself. These results have been ascribed to a penultimate effect. α-MAP is homopolymerized by dimsylsodium or n-butyllithium. Attempted copolymerization of α-map and styrene with n-butyllithium produces >95% α-MAP. Unexpectedly, α-MAP does not homopolymerize with lithium dispersion, but does react in the presence of styrene to give product containing a relatively small amount of α-MAP.

INTRODUCTION

In the previous paper[1] an account was given of the polymerization behavior of acrylophenone in anionic polymerizations. α-Methacrylophenone (α-MAP) (I) was examined in the hope that the proton resonance signal of the methyl group of poly-(α-MAP) would be resolved into isotactic, heterotactic, and syndiotactic components

$$CH_2=C \begin{matrix} CH_3 \\ | \\ | \\ C=O \\ | \\ C_6H_5 \end{matrix}$$

I
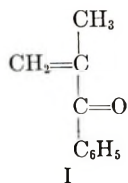
and could thus be used in determination of polymer stereochemistry as a function of reaction variables. This expectation was not realized, but some results concerning the polymerization behavior of this monomer are reported here.

There are apparently no reports in the literature concerning the polymerization or copolymerization of α-MAP.

RESULTS AND DISCUSSION

Free-radical homopolymerization of α-MAP was first investigated under a variety of conditions (Table I). In contrast to the behavior of acrylo-

TABLE I

Attempted Free-Radical Polymerizations of α-Methacrylophenone

Run no.	Initiator[a]	Amount of initiator, mole-%	Temp., °C.	Time, hr.	Solvent	Conversion, wt.-%
1	BP	1	80	24	Bulk	0
2	BP	3	80	48	Toluene	0
3	TBP	3	100	24	Bulk	0
4	AIBN	3	60	24	Bulk	0
5	AIBN	1	60	48	Benzene	0
6	AIBN	3	75	144	Bulk	53.8 dimer (II)
7	None	—	85	117	Bulk	52.0 "
8	None	—	80	187	Bulk	73.4 "
9	None	—	90	304	Bulk	94.5 "
10	Ultraviolet[b]	—	30	34	Bulk	0
11	"	—	−50	6	Bulk	0
12	" (0.05% benzoin)		−50	5	Bulk	0
13	" (0.05% benzoin)		−50	5	Toluene	0
14	BPO (N,N-dimethyl-aniline)		25	138	Bulk	0.2

[a] BP = benzoyl peroxide; TBP = tert-butyl peroxide; AIBN = azobisisobutyronitrile.

[b] A degassed sample of monomer was irradiated through glass by using a 450 w. Hanovia high-pressure lamp.

phenone,[1] it was never possible to obtain more than a trace of polymer at temperatures ranging from $-50°C$. to $100°C$. In addition to recovered monomer, the only product isolated was the Diels-Alder dimer II(runs 6–9, Table I) which was shown to have the expected[2]

$$2\ CH_2=\overset{\overset{\displaystyle CH_3}{|}}{\underset{\underset{\displaystyle C_6H_5}{|}}{\underset{C=O}{|}}}\ \longrightarrow\ \text{(structure)} \tag{1}$$

head-to-head structure by analysis and NMR. No oligomers were found upon distillation of the reaction mixture.

Photochemical initiation of this monomer also failed to produce polymer, whereas acrylophenone is readily polymerized by ultraviolet irradiation.[1]

The lack of reactivity in radical polymerization is in contrast to anionic polymerization (Table II). Either n-butyllithium or dimsylsodium $(CH_3SOCH_2^-Na^+)$ afford high yields of solid polymer with inherent viscosities of about 0.1. It should be noted however, that conversions are lower with α-MAP than with similar polymerizations with acrylophenone.

Because anionic homopolymerization of α-MAP may be carried out at $25°C$. to polymers of $\eta_{inh}\sim 0.1$, the failure of low-temperature radical polymerizations (runs 10–14, Table I) can not easily be ascribed to a ceiling temperature phenomenon. However, one could argue that in anionic polymerization the ceiling temperature is considerably higher because of 1,4-propagation [eq. (2)] of the enolate anion, or in any event a mixture of 1,2- and 1,4-propagation. Complete 1,4-propagation is ruled

$$\text{(structure)}\ +\ \text{(structure)}\ \xrightarrow[\text{add'n}]{1,4-}\ \text{(structure)} \tag{2}$$
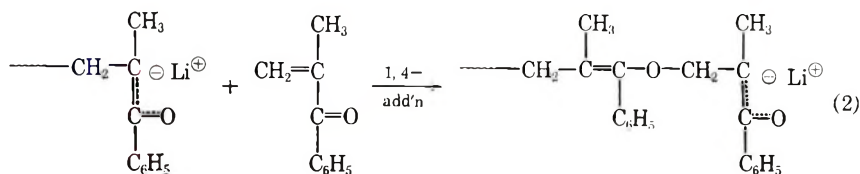
out on the basis of the prominent carbonyl peak in the infrared spectrum $(1675\ cm.^{-1})$. A consequence of even partial 1,4-propagation would be the formation of methylene groups α to oxygen [see eq. (2)] which would give rise to an NMR signal in the vicinity of 6 τ. No such signal is observed, and we conclude that not more than a few per cent 1,4 linkages, if any, occur.

If a polymer chain ending in an α-MAP radical is unable to add to an α-MAP monomer, one would expect the reactivity ratio for α-MAP to be zero. Therefore, α-MAP (M_1) and styrene (M_2) were copolymerized. The data are presented in Table III and shown graphically in Figure 1. Solution of the copolymer composition equation by the Mayo-Lewis method is shown in Figure 2.
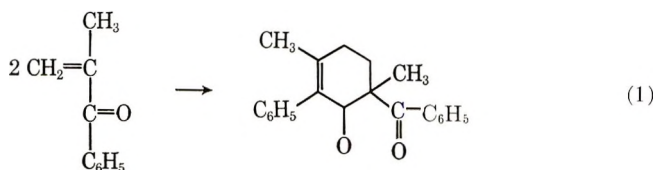
TABLE II
Anionic Polymerizations of α-Methacrylophenone

Run no.	Initiator[a]	Amount of initiator, mole-%	Temp., °C.	Time, hr.	Solvent	Conversion, %	η_{inh}[b]
1	n-BuLi	2	25	1.5	Bulk	37	
2	" "	2	-30	1.5	Bulk	1.9	
3	" "	3	-40	24	Bulk	87	0.12
4	" "	1	-50	24	Pentane	6.9	0.10
5	DS	3	30	12	Bulk	90.0	0.10
6	"	3	-25	-18	Bulk	90.0	0.15

[a] n-BuLi (n-butyllithium); DS (dimsylsodium).
[b] Inherent viscosities in benzene at 30.0°C.; (0.5%).

TABLE III
Free-Radical Copolymerization of α-MAP (M_1) and Styrene (M_2)[a]

Run no.	Mole fraction M_1 in feed, f_1	Time, hr.	Conversion, %	Mole fraction M_1 in polymer, F_1
1	0.17	1.0	3.53	0.30
2	0.20	1.0	3.48	0.32
3	0.25	2.3	3.26	0.37
4	0.33	6.7	3.67	0.47
5	0.50	27.5	1.74	0.53
6	0.75	49.2	0.62	0.63
7	0.83	68.0	0.37	0.65

[a] Polymerization initiated by 0.1 mole-% benzoyl peroxide and carried out in bulk at 75°C.

It is apparent from these two figures that more than 50% α-MAP can be incorporated into the copolymer and that r_1 is not equal to zero ($r_1 = 0.18$–0.5; $r_2 = 0.12$–0.35). The scatter in the Mayo-Lewis plot and the reluctance of α-MAP to homopolymerize under radical conditions suggest that a penultimate effect may be responsible for this behavior. A growing radical chain ending in one α-MAP unit may add to an α-MAP monomer, but a chain ending in two α-MAP units can not effectively add a third or fourth α-MAP monomer because of steric compression in the transition state or product. [Models of poly(α-MAP) indicate more steric compression than models of poly(methyl methacrylate).] Copolymerizations in which penultimate effects are observed do not obey the classical copolymerization equation.[3]

Although the same kind of steric compression in the polymer chain ought to occur in anionic homopolymerization of α-MAP, termination does not occur as readily and, therefore, chains grow, although slowly. (Compare conversions under similar conditions for acrylophenone.[1])
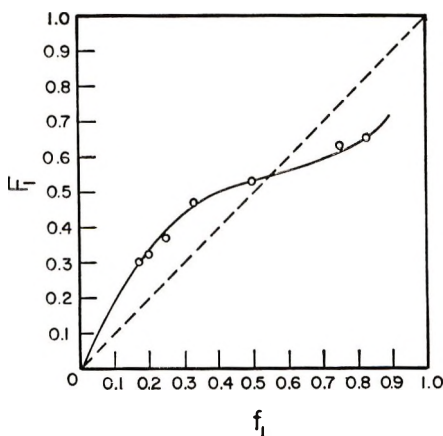

Fig. 1. Feed–copolymer composition plot for α-MAP (M_1) and styrene (M_2).
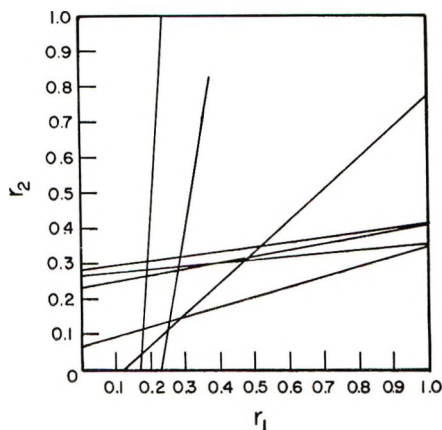
Fig. 2. Mayo-Lewis plot for the copolymerization of α-MAP (M_1) and styrene (M_2).

The n-butyllithium-initiated polymerization of a 1:1 molar ratio of α-MAP and styrene with 3 mole-% n-butyllithium gave a 5% conversion to polymer after 7.5 hr. The product was $96 \pm 5\%$ poly(α-MAP), and thus it appears that just as in the case of acrylophenone[1] a chain ending in an α-MAP carbanion cannot add to styrene monomer, and if any styryl carbanions are formed by an initiation reaction with n-butyllithium, they quickly cross over to α-MAP.

A few preliminary results of the lithium dispersion initiated copolymerization of styrene and α-MAP are presented in Table IV. It should be

TABLE IV

Copolymerizations of α-Methylacrylophenone and Styrene
with Lithium Dispersion in Tetrahydrofuran[a]

α-MAP, mmoles	Styrene, mmoles	Time	Conversion, %	% α-MAP	η_{inh}
30.0	70.0	8 min.	4.03	11.9	0.154
50.0	50.0	10 min.	1.68	5.1	0.192
70.0	30.0	$4^1/_2$ hr.	5.47	14.1	0.092
90.0	10.0	48 hr.	0.00	0.00	—
100	0	48 hr.	0	—	—

[a] Lithium (0.0138 g., 1.99 mmoles). Tetrahydrofuran 40.0 ml. Room temperature.

noted that under these conditions α-MAP does not homopolymerize, and in fact the molar ratio of α-MAP to styrene must be somewhat less than 9:1 in order for polymerization to occur. There is insufficient data at the moment to allow for any quantitative interpretation of these results. The low α-MAP content of the product is interesting in terms of the discussion in the preceding paper.[1] The conversions reported here are low, however, and we may once again be observing preferential initiation on styrene.

EXPERIMENTAL

The experimental details concerning polymerization with n-butyllithium or lithium dispersion are the same as those reported in the previous paper. The per cent α-MAP in polymeric products was determined by quantitative infrared analysis.[1]

Polymerizations with dimsylsodium have also been previously described.[4]

Homopolymers of α-MAP were purified by reprecipitation from either methyl ethyl ketone or benzene into methanol followed by drying overnight *in vacuo* at 60°C. In the infrared spectra poly(α-MAP) showed a carbonyl peak at 1675 cm.$^{-1}$. In a number of different solvents and at temperatures greater than 100°C. the methyl proton NMR signal was not resolved into the triad composition (60 or 100 Mc./sec.). In the methyl region a broad band centered at $\sim 9 \tau$ and a broad methylene band at $\sim 7.5 \tau$ were observed.

ANAL. Calcd. for $(C_{10}H_{10}O)_n$: C, 82.15%; H, 6.84%. Found: C, 82.29%; H, 6.97%.

α-MAP (I)

α-Methacrylophenone was prepared essentially according to the procedure of Burckhalter and Fuson[5] from the corresponding Mannich base. The product had b.p. 70°C. 3.5 mm., n_D^{25} 1.5370.

2,5-Dimethyl-6-phenyl-2-benzoyl-3,4-dihydro-2H-pyran (II)

α-MAP (14.4 g.) was degassed three times followed by heating under a nitrogen atmosphere for 304 hr. at 90°C. Distillation through a Vigreux column yielded 13.6 g. (94%) of II, b.p. 128–131°C./0.04 mm., n_D^{27} 1.5767. Redistillation over calcium hydride gave a product with b.p. 124–125°C./0.05 mm., n_D^{27} 1.5767, λ_{max} 246 mμ (ϵ-13,600). The NMR spectrum (CCl$_4$) of the product showed signals at 1.8–3.5 τ (10 H) assigned to the aromatic protons; 7.2–8.3 τ (complex multiplet, 4H) assigned to methylene groups and 8.4 τ (3H) and 8.5 τ (3H) singlets assigned to the methyl groups. No signals were observed in the region in which protons α to an ether linkage absorb.

ANAL. Calcd. for $C_{20}H_{20}O_2$: C, 82.19%; H, 6.85%; mol. wt. 292. Found: C, 82.00%; H, 6.88%; mol. wt. 282.

Radical Copolymerization of α-MAP and Styrene

The apparatus used was the same as that described for the n-butyllithium experiments. Monomers were degassed three times followed by the addition of 0.1 mole-% benzoyl peroxide. After heating (in nitrogen) at 75°C. the reaction mixture was poured into a large excess of methanol in a Waring Blendor. The copolymer was reprecipitated twice more from benzene into methanol and dried overnight at 60°C. (10 mm.).

References

1. J. E. Mulvaney and J. G. Dillon, *J. Polymer Sci. A-1*, **6,** 1849 (1968).

2. J. Colonge and G. Descotes in *1,4-Cycloaddition Reactions;   The Diels-Alder Reaction in Heterocyclic Synthesis*, J. Hamer, Ed., Academic Press, New York, 1967, p. 220 ff.

3. G. E. Ham, Ed., *Copolymerization*, Interscience, New York, 1964, p. 9 ff.

4. J. E. Mulvaney and R. L. Markham, *J. Polymer Sci. B*, **4,** 343 (1966).

5. J. H. Burckhalter and R. C. Fuson, *J. Am. Chem. Soc.*, **70,** 4184 (1948).
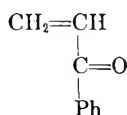
Anionic Polymerization and Copolymerization of Acrylophenone

J. E. MULVANEY and J. G. DILLON, *Department of Chemistry, University of Arizona, Tucson, Arizona 85721*

Synopsis

The *n*-butyllithium-initiated polymerization of a mixture of acrylophenone (AP) and styrene produces only poly(AP), indicating that a chain ending in an AP enolate ion is not sufficiently nucleophilic to add to styrene. Radical copolymerization of AP and styrene yields a polymer containing 65% AP (at 41% conversion). In contrast, lithium dispersion-initiated polymerization of AP and styrene produces a product containing 50-99% AP, depending upon conversion. This observation is discussed in terms of current knowledge concerning alkali metal-initiated polymerization.

This report concerns some anionic polymerization and copolymerization studies of acrylophenone (AP). This monomer was of particular interest

$$CH_2=CH$$
$$|$$
$$C=O$$
$$|$$
$$Ph$$

with respect to its behavior toward anionic initiators. Unusual copolymer compositions have been obtained in certain kinds of anionic polymerizations, and, in particular, the case of styrene–methyl methacrylate–lithium[1-8] has been shown to yield a copolymer containing 30–80% of styrene, depending upon conditions. A purely anionic copolymerization, such as that brought about by *n*-butyllithium, of these two monomers produces nearly pure poly(methyl methacrylate), whereas radical copolymerization yields an alternating copolymer. Careful NMR and fractionation studies have shown that the lithium-initiated copolymer consists of a block of methyl methacrylate and a block of styrene and contains no alternating styrene–methyl methacrylate units in the copolymer.[6,7] The last observation rules out the possibility of any radical propagation with lithium. It has been suggested that the surface of the lithium metal is slightly positive due to the presence of lithium cations which do not immediately discharge into solution. Styrene, having a larger cloud of π electrons than methyl methacrylate could be preferentially adsorbed on the surface, and the initially formed heterogeneously propagated polymer is largely styrene. Copolymerization of AP was studied in order to test the generality of these conclusions.

TABLE I
Polymerizations of Acrylophenone(AP) and Styrene

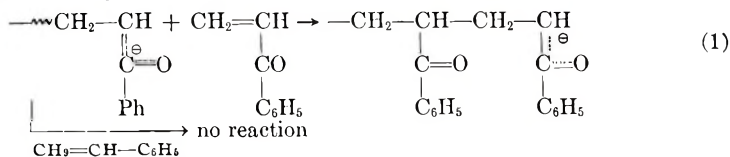| Run no.	AF, mmole	Styrene, mmole	Initiator	Mole-% initiator	Solvent	Temp., °C.	Time, hr.	Conversion, wt.-%	AP in total polymer, %
1	22.7	00.0	n-BuLi	0.3	Bulk	25	1	84	100
2	10	10	"	0.3	Bulk	25	0.75	43	100
3	10	10	"	0.3	THF(25 ml.)	25	2	51	100
4	10	10	AIBN	1.0	Bulk	61	11	40.7	65
5	15	00.0	Ultraviolet[a]	—	Bulk	30	5	25	
6	5	5	"	—	Bulk	30	1.75	15.7	
7	22.7	00.0	Li dispersion	6.6	Bulk	25	10	52.1	
8	10	00.0	Li dispersion	0.3	THF(25 ml.)	25	70	71.5	
9	10	10	None	—	Bulk	25	74	0	
10	10	10	"	—	THF(25 ml.)	25	74	0.9	

[a] A degassed sample of monomer was irradiated (through glass) using a 450 watt Hanovia high pressure lamp.

AP has been homopolymerized by Marvel and Casey[9] with radical as well as anionic initiators to polymers with inherent viscosities in the range of 0.1–0.2. Tsuruta et al.[10] have also reported briefly on the organometallic-initiated polymerization of AP. Apparently the only account of copolymerization is that AP and maleic anhydride give a copolymer with benzoyl peroxide as an initiator.[11]

AP polymerizes quite readily on standing, even under nitrogen. In the experiments reported here, AP monomer contained approximately 1 part in 25,000 of hydroquinone. This quantity of hydroquinone was not sufficient to prevent either anionic or radical homopolymerization or copolymerization (Table I, runs 1–8), but did allow mixtures of styrene and AP to remain unpolymerized in the absence of initiator for as long as 3 days (Table I, runs 9, 10). It should be noted that in an anionic polymerization propagated by R^-M^+, the only effect of the hydroquinone would be to destroy a minute percentage of R^-M^+.

Examination of Table I reveals that AP undergoes radical polymerization (including photo-initiated polymerization) as well as homopolymerization with lithium dispersion or n-butyllithium. A radical copolymerization of a $1:1$ molar ratio of styrene and AP (run 4) produces a copolymer containing 65% AP.

In contrast, attempted copolymerization of styrene–AP in bulk or in tetrahydrofuran with n-butyllithium produced only poly(AP) (Table I, runs 2 and 3). Just as in the case of methyl methacrylate–styrene[12] a chain ending in AP-enolate ion is sufficiently nucleophilic to add to an AP monomer, but not styrene.

$$—\!\!\!\!\wedge\!\!\wedge CH_2\!\!-\!\!CH + CH_2\!\!=\!\!CH \rightarrow —CH_2\!\!-\!\!CH\!\!-\!\!CH_2\!\!-\!\!CH \tag{1}$$

—CH₂—CH + CH₂=CH → —CH₂—CH—CH₂—CH

Copolymerizations of AP were carried out by using lithium dispersion in THF. The time–conversion data are plotted in Figure 1. After a short apparent induction period polymerization proceeds to 40–50% conversion (by weight) in about 8 min.

It is interesting that all of the polymer was soluble, except for a minute fraction too small to weigh or characterize (<1 mg.). This is in contrast to the styrene–methyl methacrylate system in which 0.3–34% of the copolymer which is formed is insoluble and crosslinked.[7] In the latter system, crosslinking must occur by growing polystyryl dianions reacting with ester groups of polymer containing methyl methacrylate units. In the present case this crosslinking reaction does not occur, possibly because of steric repulsions between adjacent phenyl
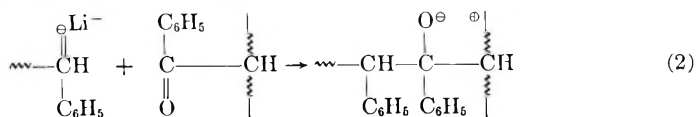
groups in the product [eq. (2)].

Fig. 1. Polymerization of styrene–AP with lithium dispersion: (O) 0.05 mg.-atom; (●) 2.0 mg.-atom. Styrene, 20.0 mmole; AP, 20 mmole; THF, 20.0 ml.; 30°C.

Fig. 2. Polymerization of styrene–AP with lithium dispersion: (O) 0.05 mg.-atom; (●) 2.0 mg.-atom. Styrene, 20.0 mmole; AP, 20.0 mmole; THF, 20.0 ml.; 30°C.

Conversion–inherent viscosity data are shown in Figure 2. Inherent viscosities change only slightly with conversion.

Of particular interest is the polymer composition–conversion data (Fig. 3). At very low conversion the product contains approximately 49% styrene. In the range 15–40% conversion, the polymer contains 95% AP, and at higher conversions the amount of styrene increases again because AP has been depleted.
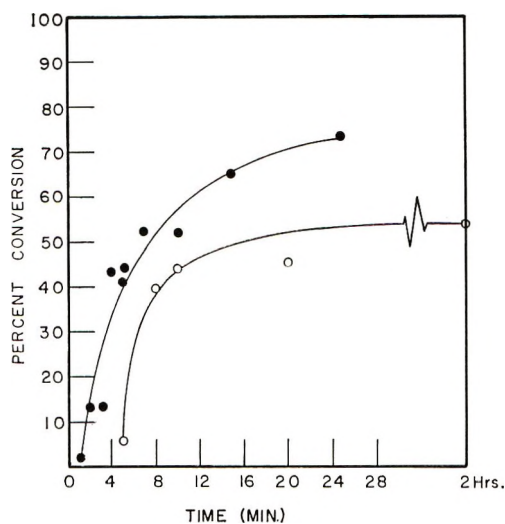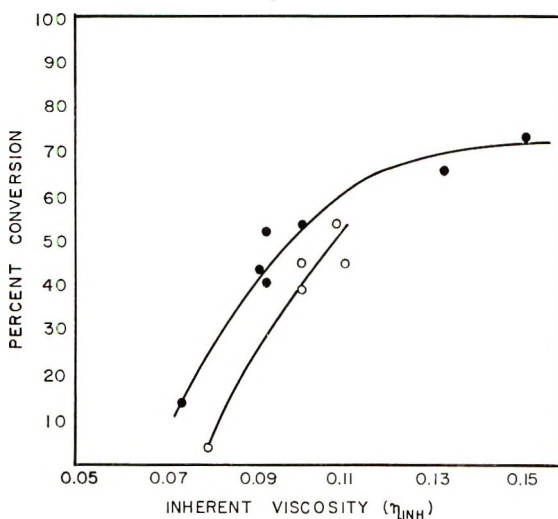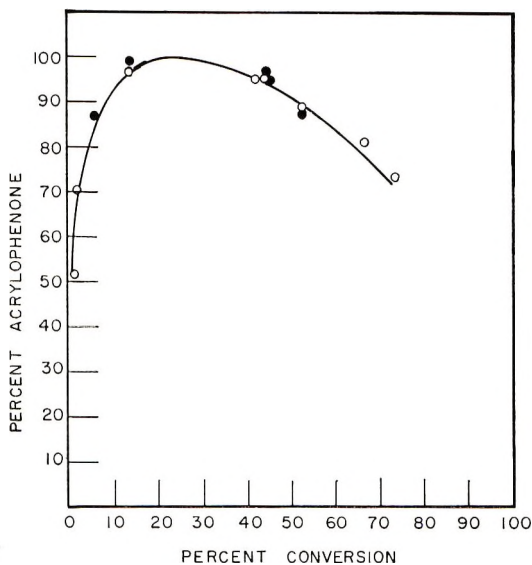
Fig. 3. Polymerization of styrene–AP with lithium dispersion: (●) 0.05 mg.-atom; (○) 2.0 mg.-atom. Styrene, 20.0 mmole; AP, 20.0 mmole; THF, 20.0 ml.; 30°C.

It is clear from these results that neither a homogeneous anionic polymerization nor a purely radical polymerization is occurring in the styrene–AP–lithium system. The former produces pure poly(AP), whereas the latter yields a copolymer containing 65% AP. Because we have not been able, as yet, to determine whether the styrene–AP product is a block copolymer, an alternating copolymer, or a mixture of homopolymers, a definitive conclusion cannot be drawn. However, the high styrene content of the product at low conversion is strongly reminiscent of the styrene–methyl methacrylate case in which propagation was shown to be purely anionic.

It should be pointed out that if propagation is purely anionic, the high styrene content at low conversions would mean that styrene is the monomer preferentially adsorbed on the surface of the lithium metal. One might expect that acrylophenone having a larger π cloud than styrene and a dipole as well, would be the monomer preferentially adsorbed on lithium, and therefore the monomer which would appear to the greatest extent at low conversions. This suggests that the question of preferential initiation and propagation is not only a question of the size of the π cloud of the monomer, but must involve other factors as well.

EXPERIMENTAL

Melting points were determined on a Fisher-Johns melting point apparatus and are uncorrected. NMR spectra were taken with a Varian A-60 spectrometer, tetramethylsilane being used as internal standard.

Microanalyses were performed by Micro-Tech Laboratories of Skokie, Illinois. Viscosities were determined in a Cannon-Fenske viscometer.

Tetrahydrofuran was dried by stirring over calcium hydride for one day and then distilled under dry nitrogen prior to use.

Monomers

Styrene was freed from inhibitor by washing with 10% potassium hydroxide and then with water until the aqueous phase was neutral. The inhibitor-free styrene was stored over anhydrous sodium sulfate overnight and distilled in an inert atmosphere over calcium hydride.

Lithium dispersion in wax (Lithium Corporation of America) was composed of 30% lithium, 68% wax, and 2% oleic acid. n-Butyllithium (Foote Mineral Company) was 1.6M in hexane.

Infrared analysis of the styrene–AP polymers was used to determine the amount of AP present. The area of the carbonyl peak at 1675 cm.$^{-1}$, in the product was compared with that of poly(AP). Solutions (3%) of the polymer in chloroform were used. Results obtained by the above method and by C, H analysis were found to be within ±5% of one another.

Copolymerizations with Lithium Dispersion

In a typical polymerization, 20.0 mmole (2.08 g.) of styrene, 20.0 mmole (2.64 g.) of AP, and 20.0 ml. of freshly distilled tetrahydrofuran were placed in a 50 ml. flask equipped with a magnetic stirring bar. The solution was degassed by three freeze–thaw cycles in liquid nitrogen and, in a dry box previously purged overnight with dry nitrogen, the vacuum was broken, and a weighted amount of lithium dispersion (lithium weighed out in a weighing bottle which was loaded in the dry-box) was added. The flask was closed and placed in a constant temperature bath at 30°C. and stirred. The polymerization was terminated by decanting into 200 ml. of methanol (AR) in a Waring Blendor. The polymer was reprecipitated twice from benzene (AR) into methanol and dried in a vacuum oven at 60°C. 10 mm. Analytical samples were dissolved in benzene, filtered, and freeze-dried.

Copolymerizations with n-Butyllithium

In a typical run, 10 mmole (1.32 g.) AP and 10 mmole (1.04 g.) styrene were placed in a 50 ml. flask equipped with two stopcocks and degassed by three freeze–thaw cycles. Against a flow of nitrogen, 0.3 mole-% (0.0375 ml.) of n-butyllithium solution was injected with a syringe. The solution rapidly became viscous. Polymerization was terminated by pouring into methanol. The white solid was reprecipitated twice from benzene into methanol and dried in a vacuum oven at 60°C. 10 mm.

Acrylophenone (AP)

AP was prepared from the corresponding Mannich base, β-dimethylaminopropiophenone hydrochloride[13] by steam distillation for 20 hr.

Hydroquinone was placed in the still and the receiving flasks. The distillate was extracted with ethyl ether, dried over sodium sulfate, and solvent was removed under reduced pressure. Distillation yielded 41 g. (63%) of AP, b.p. 54°C. 0.15 mm., n_D^{20}, 1.5588, (lit. b.p. 58–60°C. 0.2 mm.,[10] n_D^{20}, 1.5588[9]).

References

1. A. V. Tobolsky, K. F. O'Driscoll, and R. J. Boudreau, *J. Polymer Sci.*, **31**, 115 (1958).

2. A. V. Tobolsky and K. F. O'Driscoll, *J. Polymer Sci.*, **31**, 123 (1958).

3. A. V. Tobolsky and K. F. O'Driscoll, *J. Polymer Sci.*, **37**, 363 (1959).

4. S. B. George and A. V. Tobolsky, *J. Polymer Sci. B*, **2**, 1 (1964).

5. S. Pluymers and G. Smets, *Makromol. Chem.*, **88**, 29 (1965).

6. C. G. Overberger and N. Yamamoto, *J. Polymer Sci. B*, **3**, 569 (1965).

7. C. G. Overberger and N. Yamamoto, *J. Polymer Sci. A-1*, **4**, 3101 (1966).

8. A. A. Korotkov, S. P. Metzengendler, and L. L. Dantzig, *J. Polymer Sci. B*, **4**, 809 (1966).

9. C. S. Marvel and D. J. Casey, *J. Org. Chem.*, **24**, 957 (1959).

10. T. Tsuruta, R. Fujio, and J. Furukawa, *Makromol. Chem.*, **80**, 172 (1964).

11. L. Strzelecki and J. Petit, *Compt. Rend.*, **259**, 3019 (1964).

12. R. K. Graham, D. L. Dunkelberger, and W. E. Goode, *J. Am. Chem. Soc.*, **82**, 400 (1960).

13. C. E. Maxwell, in *Organic Syntheses, Coll. Vol. III*, E. C. Horning, Ed., Wiley, New York, 1955, p. 305.

Retardation of Radical Polymerization by Phenylacetylene and Its *p*-Substituted Derivatives

K. HIGASHIURA and M. OIWA, *Department of Applied Chemistry, Faculty of Engineering, Kansai University, Senriyama, Suita-shi, Osaka, Japan*

Synopsis

Radical polymerizations of styrene and methyl methacrylate in the presence of phenylacetylene and five of its *p*-substituted derivatives were carried out with the use of 2,2'-azobisisobutyronitrile as the initiator at 60°C. The initial overall rates of the polymerizations of styrene and methyl methacrylate in the presence of phenylacetylene were not proportional to the square root of the initiator concentration under the experimental conditions employed. The relationship between the overall polymerization rate and the concentration of the phenylacetylenes could be expressed by the Kice equation for the rate of a radical polymerization in the presence of a terminator. From this relationship the rate constant (k_s) of the reaction of a growing polymer radical with the phenylacetylenes and the constant $C_s = (k_s/k_p)$, where k_p is the propagation rate constant of vinyl monomers, were determined. The C_s value thus obtained agree well with that derived from the relationship between the number-average degree of polymerization and the molar ratio of the phenylacetylenes to the vinyl monomer. Therefore the mechanism of the reaction may be considered as being one in which the growing radical reacts with the ethynyl group of the phenylacetylenes to yield a comparatively stable radical which terminates mainly by reaction with the growing radical, and so apparently the phenylacetylenes retard the vinyl polymerization. The substituent effects on the reaction were discussed on the basis of the following modified Hammett equation proposed by Yamamoto and Otsu: $\log [C_s(p\text{-sub. PA})/C_s(\text{PA})] = \rho\sigma + \gamma E_R$, where PA represents phenylacetylene, σ and E_R are the Hammett polar substituent constant and resonance substituent constant, respectively, and both ρ and γ are reaction constants. The γ value for the polymerization of both styrene and methyl methacrylate was 1.7. The ρ value was 1.0 for the polymerization of styrene and approximately zero for that of methyl methacrylate. These results demonstrate that the reactivity of the phenylacetylenes with the growing chain is influenced by both polar and resonance effects of their *p*-substituents in the degradative copolymerization of styrene and only by the resonance effect in that of methyl methacrylate.

INTRODUCTION

The radical polymerization of vinyl monomers in the presence of phenylacetylene (PA) had been studied by Doak from the standpoint of copolymerization.[1] In his report, it was shown that the rate of the polymerization of styrene (St) in the presence of PA is not proportional to the square root of the initiator concentration. He explained this experimental result kinetically, by assuming that the growing chain ending in PA does not

react with PA and the termination reaction is caused only by the recombina-
tion of two radicals which end in PA units, and that other mechanisms are
the same as those of ordinary copolymerizations induced by radical
initiators.

On the other hand, from the standpoint of inhibition and retardation of
radical vinyl polymerization. Kice studied the polymerization of methyl
acrylate and methyl methacrylate (MMA) in the presence of substances
such as benzoquinone, chloranil, furfurylidene malononitrile, trinitrotol-
uene etc.[2,3] Then he presented a new polymerization rate equation which
involved the concentration of the terminators. The equation is subject to
the assumption that the radical which is produced by the reaction of a
growing chain with a terminator can react with the vinyl monomer (co-
polymerization) and terminates by the reaction with the same radical or
with a growing chain ending in a vinyl monomer unit, but does not react
with the terminator. Thus he found that the equation was in a good
accordance with his experimental results.

In the present paper, it is first reported that the rates of the polymerization
of St and MMA in the presence of PA and of five p-substituted phenyl-
acetylenes can be evaluated by using the Kice equation. The constant
$C_s = (k_s/k_p)$, where k_s is the rate constant of the reaction of a growing
chain ending in a vinyl monomer unit with the phenylacetylenes and k_p is
the propagation rate constant in the homopolymerization of the vinyl
monomer, is derived from Kice's theory for all the phenylacetylenes.
Then, it is shown that these C_s values agree well with those calculated from
the degree of polymerization of the polymers obtained in the presence of the
phenylacetylenes. Finally, the effects of p-substituents on the degradative
copolymerization of the phenylacetylenes and the vinyl monomers are dis-
cussed from the view point of Hammett's rule. In the case of the poly-
merization of St, both the polar and resonance effects of the p-substituents
influence the reaction. However, in the polymerization of MMA, the
resonance is the only factor.

EXPERIMENTAL

Materials

PA,[4] and its p-methoxy,[5] p-methyl,[6] p-chloro,[7] p-bromo,[8] and p-nitro[9,10]
derivatives were synthesized by the methods described in the literature.
The physical properties of the phenylacetylenes are shown in Table I.
As for the monomers, commercial St was purified by vacuum distillation
in a stream of nitrogen, and commercial MMA was refined by successive
steam distillations, drying with Na_2SO_4, and vacuum distillation. Com-
mercial methanol was used without purification. The benzene used for
viscosity measurements was distilled over metallic sodium after purification
by the usual method. 2,2'-Azobisisobutylonitrile (AIBN) was recrystal-
lized from ethanol (m.p. 103°C.).

TABLE I
Properties of p-Substituted Phenylacetylenes

Sub-stituent	B.p., °C./mm. Hg	M.p., °C.	Elemental analysis[a]			Ultraviolet spectrum λ_{max},[b] mμ
			C, %	H, %	Other, %	
CH$_3$O	93–95/15	—	81.52 (81.78)	6.08 (6.11)		250
CH$_3$	80–82/32	23	92.80 (93.05)	6.89 (6.95)		{240 {250
H	75/90	—	93.91 (94.07)	5.88 (5.93)		{236 {247
Cl	69–71/18	46–46.5	70.48 (70.33)	3.78 (3.69)	Cl 25.74 (25.97)	{243 {253
Br	88–91/16	64–65	53.07 (53.06)	2.62 (2.79)	Br 44.17 (44.16)	{245 {255
NO$_2$	—	150–152	65.14 (65.29)	3.40 (3.43)	N 9.44 (9.53)	287

[a] The values in parentheses are theoretical values.
[b] The solvent is ethyl alcohol.

Polymerization Procedure

The reaction mixture was prepared by dissolving the requisite amount of the phenylacetylene and AIBN in the monomer to give a total volume of 10 ml. Polymerizations were carried out in the absence of light in sealed, clean glass tubes of 15 mm. diameter. The tubes and their contents were degassed by the ordinary freezing and thawing technique under vacuum and then sealed off. They were then heated in a thermostat regulated at 60 ± 0.1°C., without shaking, for different intervals of time. After polymerization to a conversion below 10%, the reaction mixture was poured into a large amount of methanol to precipitate the polymer. The resulting polymer was filtered, washed, and then dried under vacuum. The rate of polymerization was determined gravimetrically. The number-average degree of polymerization ($\bar{P}_n$) was calculated from the data of the intrinsic viscosities [η] of the polymer in benzene at 30°C. by using the equation of Mayo et al. for polystyrene[11] and that of Baysal and Tobolsky for poly-(methyl methacrylate).[12]

For polystyrene: $\log \bar{P}_n = 3.205 + 1.37 \log [\eta]$
For poly(methyl methacrylate): $\log \bar{P}_n = 3.420 + 1.13 \log [\eta]$

Determination of the Constants C_s, k_s

From the experimental results, it is clear that the overall polymerization rates of St and MMA in the presence of phenylacetylene are not proportional to the square root of the AIBN concentration, and the constants C_s of all the phenylacetylenes obtained from the Kice theory agree approximately with those from $\bar{P}_n$. Accordingly, for the kinetic treatment, it is considered that the polymerization is composed of the elementary reac-

tions given in eqs. (1)-(8); chain transfer reactions to initiator, monomer, and polymer, are however, omitted.

$$I \longrightarrow 2R^{\cdot} \tag{1}$$

$$R^{\cdot} + M \longrightarrow P^{\cdot} \tag{2}$$

$$P^{\cdot} + M \xrightarrow{k_p} P^{\cdot} \tag{3}$$

with $R_p = k_p[P^{\cdot}][M]$

$$P^{\cdot} + S \xrightarrow{k_s} PS^{\cdot} \tag{4}$$

with $R_s = k_s[P^{\cdot}][S]$

$$PS^{\cdot} + M \xrightarrow{k_o} P^{\cdot} \tag{5}$$

with $R_o = k_o[PS^{\cdot}][M]$

$$PS^{\cdot} + P^{\cdot} \xrightarrow{k_c} \tag{6}$$

$$PS^{\cdot} + PS^{\cdot} \xrightarrow{k_z} \quad \left.\begin{array}{l} \text{Inactive} \\ \text{products} \end{array}\right\} \tag{7}$$

$$P^{\cdot} + P^{\cdot} \xrightarrow{k_t} \tag{8}$$
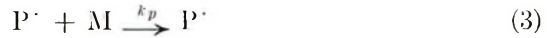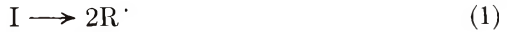
with $R_c = k_c[PS^{\cdot}][P^{\cdot}]$

$R_z = k_z[PS^{\cdot}]^2$

$R_t = k_t[P^{\cdot}]^2$

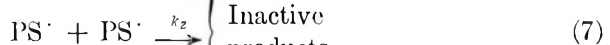Here I is the initiator, $R^{\cdot}$ the initiator-radical, M the monomer, S the phenylacetylenes, $P^{\cdot}$ a growing chain ending in a vinyl monomer unit, and $PS^{\cdot}$ a radical which ends in an S unit.

For this polymerization system, the Kice equation is

$$\frac{\phi^2[S]}{1-\phi^2}\left\{1+\left[1+\frac{c(1-\phi^2)}{\phi^2}\right]^{1/2}\right\} = \frac{k_t}{k_p k_s}\frac{R_p}{[M]}\left[1+\frac{c(1-\phi^2)}{\phi^2}\right]^{1/2}$$
$$+ \frac{k_0 k_t [M]}{k_c k_s} \tag{9}$$

where ϕ is the relative rate of the polymerization given by

$$\phi = (R_p/[M])_{[S]}/(R_p/[M])_{[S]=0}$$

and $c = k_t k_z/k_c^2$. The c value which gave a good straight line on plotting $\{\phi^2[S]/(1-\phi^2)\}\{1+[1+c(1-\phi^2)\phi^{-2}]^{1/2}\}$ against $(R_p/[M])\{1+[c(1-\phi^2)\phi^{-2}]^{1/2}\}$ was evaluated to yield $k_t/k_p k_s$ and $k_0 k_t[M]/k_c k_s$. Then by using the following rate constants reported in the literature[13,14] on the polymerization at 60°C., k_s, C_s, and k_0/k_c were determined.

$$k_p(\text{St}) = 176 \text{ l./mole-sec.}$$

$$k_t(\text{St}) = 7.2 \times 10^7 \text{ l./mole-sec.}$$

$$k_p(\text{MMA}) = 367 \text{ l./mole-sec.}$$

$$k_t(\text{MMA}) = 1.87 \times 10^7 \text{ l./mole-sec.}$$

On the other hand, according to Bagdasaryan, $\bar{P}_n$ and $[S]/[M]$ obey the following general equation:[15]

$$\frac{1}{\bar{P}_n} = \frac{1}{2}(1 + \lambda)\frac{k_t R_p}{k_p{}^2[M]^2} + \frac{k_m}{k_p} + \beta\frac{k_s[S]}{k_p[M]} \tag{10}$$

where k_m is the rate constant of the chain transfer reaction to the monomer, and

$$\lambda = k_{td}/(k_{td} + k_{tc})$$

Here k_{td} and k_{tc} are the rate constants of the disproportionation and recombination reactions in eq. (8), repectively, and β is given by

$$\beta = (1 + r)(1 + q)/2$$

where q is the ratio of PS˙ reacted with the monomer in eq. (5) to that produced by the reaction represented by eq. (4), and r is the ratio of PS˙ reacted with P˙ in eq. (6) to that inactivated by the reactions of eqs. (6) and (7). Bevington determined by tracer technique, that λ is zero for St and approximately 1.0 for MMA polymerization at 60°C.[16] On assuming $q = 0$, $r = 1$ (that is, $\beta = 1$), $\lambda(\text{St}) = 0$, and $\lambda(\text{MMA}) = 1$, eq. (10) reduces to

$$\frac{1}{\bar{P}_n} = \frac{k_t R_p}{2k_p{}^2[M]^2} + \frac{k_m}{k_p} + \frac{k_s[S]}{k_p[M]} \qquad \text{(PSt)} \tag{11}$$

$$\frac{1}{\bar{P}_n} = \frac{k_t R_p}{k_p{}^2[M]^2} + \frac{k_m}{k_p} + \frac{k_s[S]}{k_p[M]} \qquad \text{(PMMA)} \tag{12}$$

The chain transfer constants to the monomer $C_m = (k_m/k_p)$ at 60°C. were reported in the literature[11,17,18] as being C_m (St) $= 6.0 \times 10^{-5}$ and C_m (MMA) $= 1.0 \times 10^{-5}$. These C_m values, the initial concentrations of monomer and terminator (phenylacetylenes), the rate constants (k_p, k_t), and the experimental results (i.e., R_p and $\bar{P}_n$) were substituted in eqs. (11) and (12), and

$$\frac{1}{\bar{P}_n} - \left[\frac{k_t R_p}{2\,k_p{}^2[M]^2} + C_m\right]$$

or

$$\frac{1}{\bar{P}_n} - \left[\frac{k_t R_p}{k_p{}^2[M]^2} + C_m\right]$$

was plotted against the ratio of $[S]/[M]$. Then a straight line whose slope gives $C_s = (k_s/k_p)$ was obtained.

So that the concentrations of monomer and terminator could be regarded as constant within experimental error, the polymerizations were carried out to a conversion below 10%.

RESULTS AND DISCUSSION

For the polymerizations of St and MMA in the presence of PA, the initial rates of the polymerizations were not proportional to the square root of the initiator concentration, as shown in Figure 1. Therefore, it is supposed that the growing chain reacts with PA to give a comparatively stable radical. In fact, the time–conversion relations of the polymerizations showed a decrease in the rates with increase in the concentration of PA. The retardation effect of PA was greater for the polymerization of MMA than on that of St. This tendency was the same for the polymerizations in the presence of five p-substituted phenylacetylenes. All the experimental conditions and results are summarized in Tables II and III.

p-Nitrophenylacetylene had the greatest retardation effect of all the phenylacetylenes on both the St and MMA polymerizations, and p-

TABLE II
Polymerization of Styrene in the Presence of p-Substituted Phenylacetylenes (60°C.)

[St], mole/l.	Substituent in PA	[X-PA], mole/l.	[AIBN] $\times 10^3$, mole/l.	$(R_p/[St]) \times 10^6$, sec.$^{-1}$	ϕ	$[\eta]$	$\bar{P}_n$
8.71	p-CH$_3$O	0.00	3.24	5.32	1.00	1.07	1750
8.58	"	0.113	"	5.07	0.953	0.995	1590
8.45	"	0.226	"	4.82	0.906	0.942	1480
8.32	"	0.338	"	4.60	0.865	0.856	1300
8.19	"	0.451	"	4.35	0.818	0.797	1180
8.71	p-CH$_3$	0.00	0.199	1.35	1.00	2.73	6340
8.57	"	0.126	"	1.10	0.813	1.71	3340
8.43	"	0.252	"	0.860	0.635	1.53	2860
8.29	"	0.377	"	0.733	0.541	1.22	2100
8.15	"	0.503	"	0.604	0.446	1.02	1650
8.71	H	0.00	3.25	5.13	1.00	1.03	1670
8.60	"	0.117	"	4.69	0.914	0.904	1400
8.49	"	0.233	"	4.27	0.832	0.861	1310
8.38	"	0.350	"	3.91	0.762	0.765	1110
8.27	"	0.467	"	3.59	0.700	0.721	1020
8.71	p-Cl	0.00	0.195	1.37	1.00	2.62	5980
8.60	"	0.103	"	0.948	0.692	1.68	3260
8.49	"	0.205	"	0.714	0.521	1.09	1790
8.37	"	0.308	"	0.588	0.429	0.975	1550
8.26	"	0.411	"	0.488	0.356	0.775	1130
8.71	p-Br	0.00	0.195	1.56	1.00	2.54	5750
8.62	"	0.077	"	1.11	0.712	1.83	3670
8.54	"	0.155	"	0.844	0.541	1.36	2440
8.45	"	0.232	"	0.689	0.442	1.20	2060
8.36	"	0.310	"	0.569	0.365	1.00	1600
8.71	p-NO$_2$	0.00	3.24	4.71	1.00	0.942	1480
8.62	"	0.074	"	1.06	0.225	0.360	428
8.57	"	0.112	"	0.817	0.173	0.305	315
8.52	"	0.149	"	0.642	0.136	0.275	273
8.47	"	0.186	"	0.547	0.116	0.218	199

TABLE III

Polymerization of Methyl Methacrylate in the Presence of
p-Substituted Phenylacetylenes (60°C.)

[MMA], mole/l.	Substituent in PA	[X-PA], mole/l.	[AIBN] $\times 10^4$, mole/l.	$(R_p/[MMA])$ $\times 10^6$, sec.$^{-1}$	ϕ	$[\eta]$	$\bar{P}_n$
9.36	p-CH$_3$O	0.00	1.18	4.50	1.00	4.13	13100
9.22	"	0.116	"	2.17	0.482	3.93	12400
9.08	"	0.231	"	1.34	0.297	3.00	9110
8.93	"	0.347	"	1.05	0.234	2.30	6750
8.79	"	0.463	"	0.860	0.191	1.93	5540
9.36	p-CH$_3$	0.00	1.18	4.46	1.00	5.07	16500
9.21	"	0.126	"	1.75	0.393	3.06	9310
9.06	"	0.252	"	1.10	0.247	1.84	5240
8.91	"	0.377	"	0.826	0.185	1.57	4360
8.76	"	0.503	"	0.715	0.160	1.06	2820
9.36	H	0.00	1.17	3.69	1.00	4.58	14700
9.20	"	0.146	"	2.11	0.572	3.62	11300
9.05	"	0.292	"	1.38	0.375	2.85	8590
8.90	"	0.437	"	1.02	0.275	2.36	6940
8.75	"	0.583	"	0.808	0.219	2.00	5760
9.36	p-Cl	0.00	1.20	4.04	1.00	4.78	15600
9.24	"	0.140	"	1.71	0.423	3.32	10200
9.12	"	0.280	"	1.07	0.265	2.11	6110
9.00	"	0.420	"	0.833	0.206	1.81	5130
8.88	"	0.560	"	0.657	0.163	1.45	3990
9.36	p-Br	0.00	1.17	3.67	1.00	5.33	17400
9.27	"	0.077	"	2.14	0.583	3.60	11200
9.17	"	0.155	"	1.55	0.423	2.99	9070
9.08	"	0.232	"	1.11	0.303	2.36	6940
8.99	"	0.310	"	0.942	0.257	2.01	5790
9.36	p-NO$_2$	0.00	1.19	3.81	1.00	5.00	16300
9.31	"	0.035	"	1.69	0.444	4.30	13000
9.26	"	0.070	"	0.883	0.232	3.25	9980
9.22	"	0.104	"	0.650	0.171	2.70	8080
9.17	"	0.139	"	0.501	0.131	2.00	5760

methoxyphenylacetylene and PA had the least effects on the St and MMA polymerizations, respectively.

Figure 2 illustrates the results obtained by substitution of [M], [S], R_p, and ϕ in the Kice equation, eq. (9), for the polymerization of MMA in the presence of PA. It is evident that the plots of Figure 2 give a good straight line when the c value is approximately zero. Assuming $c = 0$, eq. (9) reduces to

$$2\phi^2[S]/(1 - \phi^2) = (k_t R_p/k_p k_s[M]) + (k_0 k_t[M]/k_c k_s) \qquad (13)$$

For the polymerization of MMA in the presence of five p-substituted phenylacetylenes, the plots of $2\phi^2[S]/(1 - \phi^2)$ against $R_p/[M]$ are shown in Figure 3. The slopes of the lines in Figures 2 and 3 give $k_t/k_p k_s$, then the

k_s and C_s values of all the phenylacetylenes were determined by applying the k_p and k_t values reported previously. By the same method, the k_s and C_s values of the phenylacetylenes in the polymerization of St were also determined.
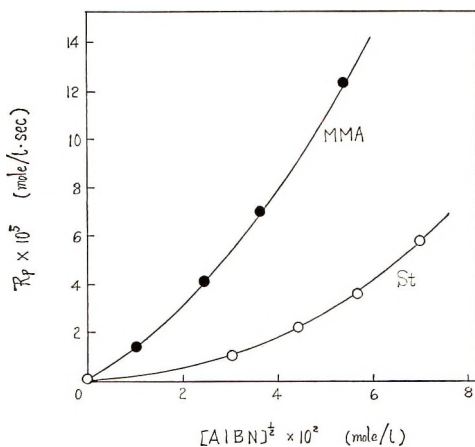

Fig. 1. Relation between overall rate and initiator concentration in the polymerizations of styrene and methyl methacrylate in the presence of phenylacetylene at 60°C. [PA] = 0.233 mole/l.; [St] = 8.49 mole/l.; [MMA] = 9.13 mole/l.
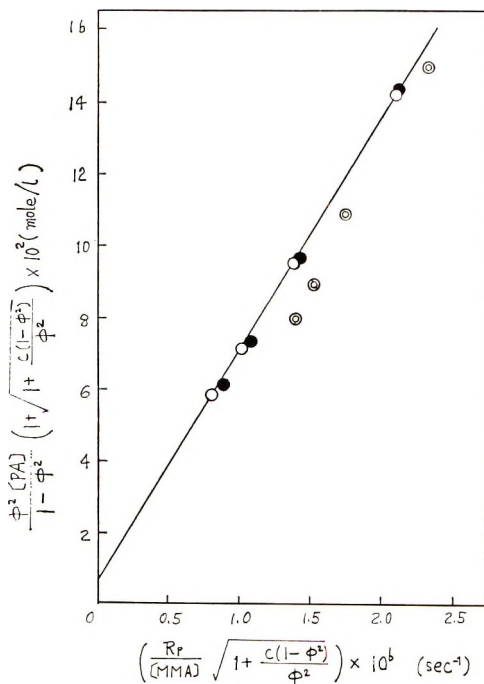

Fig. 2. Kice relationship for the polymerization of methyl methacrylate in the presence of phenylacetylene.

According to the method described in the experimental part, the relationship between the degree of polymerization and the concentration of the phenylacetylenes in the polymerization of MMA is shown in Figure 4. The reason for the negative intercepts of the lines in the figure is probably
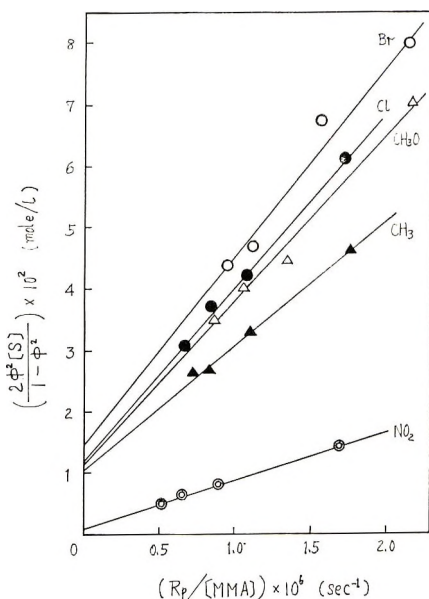

Fig. 3. Reduced Kice relationship for the polymerization of methyl methacrylate in the presence of p-substituted phenylacetylenes.
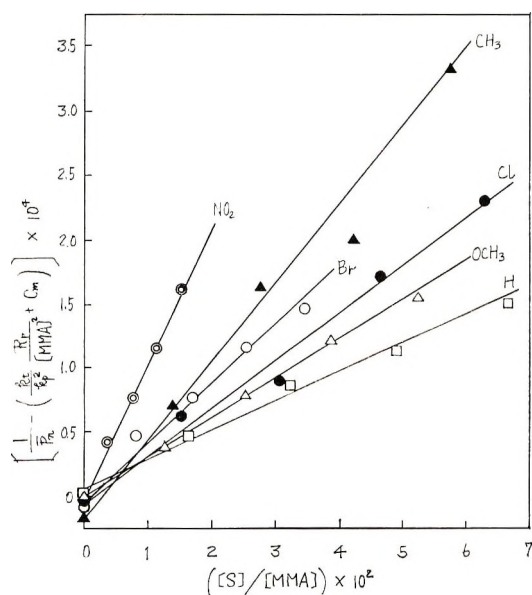

Fig. 4. Relationship between the degree of polymerization and the concentration of the p-substituted phenylacetylenes in the polymerization of methyl methacrylate.

due to the assumption of $\beta = 1$ and the inapplicability of the values of λ, k_p, k_t, or C_m employed. The slopes of the lines in Figure 4 also gave C_s value of all phenylacetylenes, and dividing the values by k_p yielded k_s values. The C_s and k_s values of the phenylacetylenes in the polymerization of St could be evaluated similarly from the degree of polymerization of the polystyrene.

The k_s and C_s values for all the phenylacetylenes in the polymerizations of St and MMA were determined by the above two different ways, and are listed in Tables IV and V. In spite of the assumption that $c = 0$, $\beta = 1$,

TABLE IV

Values of k_s and C_s of p-Substituted Phenylacetylenes in the Polymerization of Styrene at 60°C.

Substituent	k_s, l./mole-sec.		$C_s \times 10^2$	
	From $\bar{P}_n$	From R_p	From $\bar{P}_n$	From R_p
CH_3O	1.17	0.940	0.667	0.534
CH_3	1.56	0.974	0.888	0.553
H	1.73	1.65	0.983	0.943
Cl	2.96	2.71	1.68	1.54
Br	2.78	3.85	1.58	2.19
NO_2	40.7	69.6	23.1	39.5

TABLE V

Values of k_s and C_s of p-Substituted Phenylacetylenes in the Polymerization of Methyl Methacrylate at 60°C.

Substituent	k_s, l./mole-sec.		$C_s \times 10^3$	
	From $\bar{P}_n$	From R_p	From $\bar{P}_n$	From R_p
CH_3O	1.14	1.82	3.10	4.96
CH_3	2.24	2.49	6.11	6.78
H	0.818	0.790	2.23	2.15
Cl	1.38	1.47	3.77	4.01
Br	1.72	1.31	4.69	3.57
NO_2	3.93	5.42	10.7	14.8

$\lambda(St) = 0$, and $\lambda(MMA) = 1$, the constants derived from the overall polymerization rates agree well with those derived from the degrees of polymerization, as can be seen in the tables. This fact shows that the phenylacetylenes retard vinyl polymerizations by the mechanism of reactions (4)–(7) and that the rate of reaction (6) is greater than those of reactions (5) and (7). Reaction (5) corresponds to the copolymerization of the phenylacetylenes with the vinyl monomers, and this is supported by the fact that the lines in Figure 3 do not pass through the origin.

The mechanisms of reactions (4) and (5) for the polymerization in the presence of PA are considered to be as shown in eqs. (14) and (15), respectively.
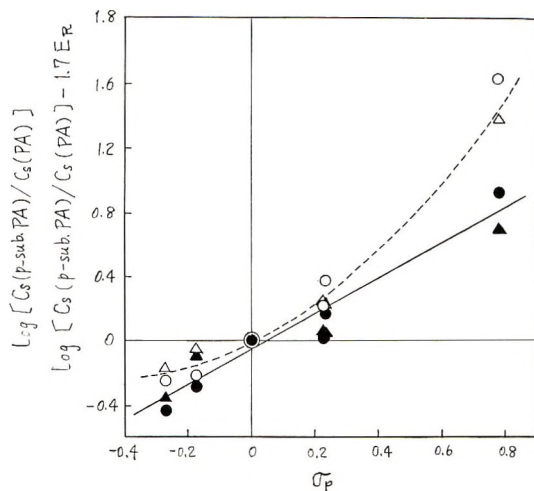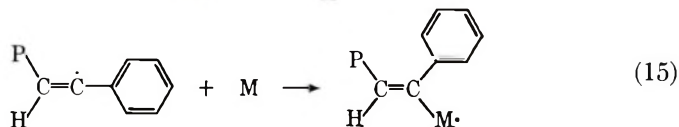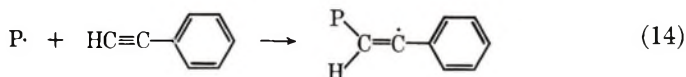
Fig. 5. Effects of *para* substituents of phenylacetylene on the degradative copoly merization of styrene: (○, △) eq. (16); (●, ▲) eq. (17); (○,●) plots obtained from R; (△,▲) plots obtained from $\bar{P}_n$.

$$P\cdot \ + \ HC\equiv C\!-\!\langle\bigcirc\rangle \ \longrightarrow \ \begin{array}{c} P \\ \diagdown \\ C=\dot{C}\!-\!\langle\bigcirc\rangle \\ \diagup \\ H \end{array} \tag{14}$$

$$\begin{array}{c} P \\ \diagdown \\ C=\dot{C}\!-\!\langle\bigcirc\rangle \\ \diagup \\ H \end{array} \ + \ M \ \longrightarrow \ \begin{array}{c} P \\ \diagdown \quad \langle\bigcirc\rangle \\ C=C \\ \diagup \quad \diagdown \\ H \quad\quad M\cdot \end{array} \tag{15}$$

The data in this paper show that the radical $-CH\!=\!\dot{C}\!-\!C_6H_5$ is less reactive in the propagation reaction than $-CH_2\!-\!\dot{C}H\!-\!C_6H_5$ and $-CH_2\!-\!\dot{C}(CH_3)\!-COOCH_3$. The reason why the radical yielded by reaction (4) has such an enhanced stability in spite of the fact that k_s is much smaller than k_p is not obvious because the electronic structure or character of $R\!-\!CH\!=\dot{C}\!-\!C_6H_5$ has never been investigated. However, if both the double
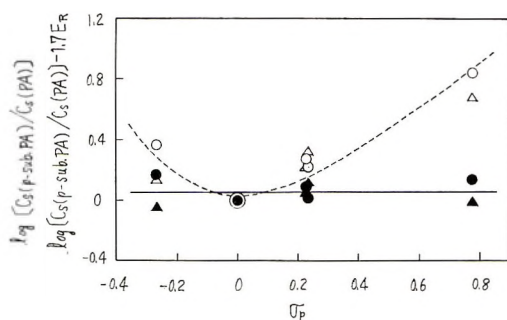

Fig. 6. Effects of *para* substituents of phenylacetylene on the degradative copolymer- ization of methyl methacrylate: (○,△) eq. (16); (●,▲) eq. (17); (○,●) plots obtained from R_p; (△, ▲) plots obtained from $\bar{P}_n$.

bonds of benzene ring and side chain of the radical are coplanar (this configuration is likely by virtue of the conjugation of their π-electrons), a bulky benzene ring and the high π-electron density around the p-orbital of the odd electron would cause to reduce its reactivity with the monomers as we can see in a molecular model of the radical.

When reaction (5) takes place, apparently β is not unity. Clearly, Tables IV and V show that C_s values obtained from eq. (13) are greater than those obtained from eqs. (11) and (12) for the polymerization in the presence of p-nitrophenylacetylene. This is because reaction (5) was taken into consideration when eq. (13) was derived, but ignored in the derivation of eqs. (11) and (12). In the latter case therefore β is unity. On the other hand, in Table IV, the C_s value of p-methylphenylacetylene obtained from eq. (13) is much smaller than that from eq. (11), for the reason that the methyl group of p-methylphenylacetylene also takes part in the reaction as a manner of hydrogen transfer to growing chain.

As Figures 5 and 6 show, the relationship between the reaction constants and the corresponding σ-values of the substituents is not expressed by the Hammett equation (14).

$$\log\ [C_s(p\text{-sub. PA})/C_s(\text{PA})] = \log[k_s(p\text{-sub. PA})/k_s(\text{PA})] = \rho\sigma \quad (16)$$

But the relationship was explained by the modified Hammett equation (17) presented by Yamamoto and Otsu for the radical reaction:[19]

$$\log\ [C_s(p\text{-sub. PA})/C_s(\text{PA})] = \rho\sigma + \gamma E_R \quad\quad (17)$$

where E_R is the resonance substituent constant and γ is a reaction constant as also is ρ. The E_R values reported for the p-methoxy, p-methyl, p-hydrogen, p-chloro, p-bromo, and p-nitro groups are 0.11, 0.03, 0.00, 0.10, 0.12 and 0.14, respectively. From Figures 5 and 6, $\gamma = 1.7$ for both the polymerizations of St and MMA, $\rho = 1.0$ for styrene polymerization and $\rho \doteqdot 0$ for methyl methacrylate polymerization were obtained. These results led us to the conclusion that the degradative copolymerization of the vinyl monomers with the p-substituted phenylacetylenes is influenced by both the polar and resonance effects of the p-substituents in the polymerization of St, and only by the resonance effect in that of MMA.

References

1. K. W. Doak, *J. Am. Chem. Soc.*, **72**, 4681 (1950).
2. J. L. Kice, *J. Am. Chem. Soc.*, **76**, 6274 (1954).
3. J. L. Kice, *J. Polymer Sci.*, **19**, 123 (1956).
4. H. Fiesselmann and K. Sasse, *Ber.*, **89**, 1786 (1956).
5. W. Manchot, *Ann.*, **387**, 280 (1912).
6. L. I. Smith and H. H. Hoehn, *J. Am. Chem. Soc.*, **63**, 1175 (1941).
7. T. H. Vaughn and J. A. Nieuwland, *J. Am. Chem. Soc.*, **56**, 1207 (1934).
8. C. Dufraisse and A. Dequesenes, *Bull. Soc. Chim. France*, **49**, 1880 (1931).
9. F. J. Alway and W. D. Bonner, *Am. Chem. J.*, **32**, 392 (1896).
10. W. B. Drewsen, *Ann.*, **212**, 150 (1882).
11. F. R. Mayo, R. A. Gregg, and M. S. Matheson, *J. Am. Chem. Soc.*, **73**, 1691 (1951).
12. B. Baysal and A. V. Tobolsky, *J. Polymer Sci.*, **9**, 171 (1952).

13. M. S. Matheson, E. E. Auer, E. B. Bevilacqua, and E. J. Hart, *J. Am. Chem. Soc.*, **73**, 1700 (1951).
14. M. S. Matheson, E. E. Auer, E. B. Bevilacqua, and E. J. Hart, *J. Am. Chem. Soc.*, **71**, 497 (1949).
15. Kh. S. Bagdasaryan, *The Theory of Radical Polymerization*, Izdatel. Akad. Nauk S.S.S.R., Moscow, 1959.
16. J. C. Bevington, H. W. Melville, and R. P. Taylor, *J. Polymer Sci.*, **14**, 463 (1954).
17. A. V. Tobolsky and J. Offenbach, *J. Polymer Sci.*, **16**, 311 (1955).
18. B. Baysal and A. V. Tobolsky, *J. Polymer Sci.*, **8**, 529 (1952).
19. T. Yamamoto and T. Otsu, *J. Polymer Sci. B*, **4**, 1039 (1966).

Preparation of p-[(S)(−)-2-Phthalimidopropionyl] Polystyrene

Z. JANOVIĆ and D. FLEŠ, *Research Institute,*
Organsko Kemijska Industrija, Zagreb, Yugoslavia

Synopsis

Samples of atactic and isotactic polystyrene were acylated with N-phthaloyl-L-alanyl chloride under the conditions of Friedel-Crafts reaction. The degree of acylation was strongly dependent on molecular weight, but not on the tacticity of polystyrene. Similarly the specific rotation of acylated polymers was not influenced by the structure of the polymer chain.

Polystyrene can, under proper conditions, undergo certain of the chemical reactions of the benzene ring. It can be nitrated, sulfonated, brominated, and can undergo the acylation and alkylation under the conditions of the Friedel-Crafts reaction.

The present work was undertaken in an attempt to prepare optically active derivatives of polystyrene and to study their properties. The preparation of p-[(S)(−)-2-phthalimidopropionyl]polystyrenes from both atactic and isotactic samples and their optical properties are described in this paper.

EXPERIMENTAL

Viscosities

Intrinsic viscosities were measured in a Cannon-Fenske capillary viscosimeter No. 100. The viscosity of sample I (Table I) was determined in toluene at a temperature of $30 \pm 0.05°$C., samples II–VI were measured in cyclohexane at $34.5 \pm 0.05°$C., and samples VII–IX in benzene at $30 \pm 0.05°$C.

Polystyrene Samples

Seven samples of atactic polystyrene having $\bar{M}_v$ between 7000 and 240,000 and two samples of isotactic polystyrene with $\bar{M}_v$ 16,000 and 55,000 (Table I) were prepared and acylated as described below. The atactic low molecular weight polymer (sample I) was prepared by polymerization of styrene monomer in the presence of stannic chloride according to the method of Staudinger.[1] Samples II–VII were prepared by suspension

TABLE I
Characteristics of the Polystyrene Samples

Sample no.	Method of polymerization and catalyst	Catalyst, %	$[\eta]$, dl./g.	$\bar{M}_v$
I	Bulk, SnCl$_4$	4.8	0.058	7,140[a]
II	Suspension, Bz$_2$O$_2$	0.8	0.204	58,980[b]
III	Suspension, Bz$_2$O$_2$	0.6	0.242	83,000[b]
IV	Suspension, Bz$_2$O$_2$	0.5	0.274	106.400[b]
V	Suspension, Bz$_2$O$_2$	0.4	0.302	129,200[b]
VI	Suspension, Bz$_2$O$_2$	0.3	0.365	188,000[b]
VII	Suspension, Bz$_2$O$_2$	0.2	0.412	240,500[b]
VIII[d]	TiCl$_4$–AlEt$_3$		0.134	16,000[c]
IX[d]	TiCl$_4$–AlEt$_3$		0.518	54,980[c]

[a] Calculated according to Trementozzi:[5] $[\eta] = 5.74 \times 10^{-5} \bar{M}_v{}^{0.76}$.
[b] Calculated according to Altares:[6] $[\eta] = 8.4 \times 10^{-4} \bar{M}_v{}^{0.5}$.
[c] Calculated according to Natta:[7] $[\eta] = 1.06 \times 10^{-4} \bar{M}_v{}^{0.735}$.
[d] Prepared by degradation of isotactic polymer with $\bar{M}_v = 990,000$.

polymerization in the presence of decreasing amounts of dibenzoyl peroxide. Isotactic polystyrenes, samples VIII and IX, were prepared by degradation of a polymer having M_v 966,000, which was prepared according to the method of Kern and co-workers.[2] The tacticity of these samples was determined by NMR technique following the procedure of Bovey and co-workers[3] and by infrared spectroscopy.[4]

N-Phthaloyl-L-alanyl Chloride. L-Alanine was converted to N-phthaloyl-L-alanyl chloride by the standard procedure.[8]

Degradation of Isotactic High Molecular Weight Polystyrene. To a solution of 8 g. of isotactic polystyrene ($\bar{M}_v$ 966,000) in 300 ml. of carbon disulfide was added at one time 8 g. of anhydrous aluminum chloride; the reaction mixture was stirred for 60 min. under reflux. Aluminum chloride was hydrolyzed with 20 ml. of hydrochloric acid in 100 ml. of ice, the solvent evaporated, and the residue dissolved in 50 ml. of benzene. The insoluble part was removed by suction filtration and the polymer precipitated with 300 ml. of methanol; yield 5.6 g. (70%); $[\mu] = 0.134$; $\bar{M}_v$ 16,600.

ANAL. Calcd. for (C$_8$H$_8$)$_n$: C, 92.31%; H, 7.69%. Found: C, 92.54%; H, 7.66%.

Sample IX was prepared in the same manner, except that the isotactic high molecular weight polystyrene was treated with aluminum chloride for 45 min.; yield 5.8 g. (72%); $[\mu]$; = 0.518: $\bar{M}_v$ 54,980.

ANAL. Calcd. for (C$_8$H$_8$)$_n$: C, 92.31%; H, 7.69%. Found: C, 92.71%; H, 7.88%.

Preparation of p-[(S)(−)-2-Phthalimidopropionyl]polystyrene. A mixture of 95 ml. of carbon disulfide and 17.85 g. (0.135 mole) of anhydrous aluminum chloride were placed in a 500-ml. three-necked flask equipped

with a mechanical stirrer, a dropping funnel, and a reflux condenser. Under rapid stirring, a solution of 16.0 g. (0.067 mole) of (S)(−)-2-phthalimidopropionyl chloride in 50 ml. of carbon disulfide was added at once. Under constant stirring, a solution of 7.2 g. of polystyrene ($\overline{M}_v$ 7140) in 75 ml. of carbon disulfide was added dropwise during 25 min., and the reaction mixture was refluxed for an additional 4 hr. Most of the carbon disulfide (120 ml.) was distilled off and the residue was hydrolyzed with 30 ml. of concentrated hydrochloric acid and 200 g. of ice and allowed to stand overnight at room temperature. Carbon disulfide was removed under diminished pressure, the aqueous layer decanted, the residue washed with two 30 ml. portions of methanol and dried *in vacuo*. The crude acylated product was dissolved in 200 ml. of acetone and precipitated by slow addition of the acetone solution into 1000 ml. of methanol; yield 12.1 g. (52.2%) of light yellow powder: $[\alpha]_D^{20} = -25.0°$ ($c = 6.93\%$ in benzene).

ANAL. Calcd.: for $[(C_8H_8)_3(C_{19}H_{16}NO_3)_2]_n$: C, 80.72%; H, 5.90%; N, 3.02% Found: C, 79.72%; H, 5.82%; N, 3.02%.

The other atactic polystyrenes were acylated by the same procedure. The acylation of isotactic samples was performed in the same manner except that the crude acylated product was dissolved in benzene instead of in acetone, in which it was insoluble.

RESULTS AND DISCUSSION

Acylation of polystyrene under the conditions of the Friedel-Crafts reaction has been studied by several authors.

Kenyon and Waugh[9] have prepared polyvinylacetophenone by condensing acetyl chloride with polystyrene under the conditions of the Friedel-Crafts synthesis. The authors have proved by thermal decomposition of the polymer in vacuum that the substitution occurred almost entirely on the *para* position of the benzene ring.

Frank[10] has studied the reaction of isocyanate with polystyrene in the presence of aluminum chloride and has found that nitrobenzene was the best solvent for this reaction. He also investigated the degree of substitution as a function of reaction time and temperature with atactic and isotactic polystyrene. Under the reaction conditions used, he did not observe the influence of tacticity on the degree of substitution.

In our studies on the acylation of polystyrenes of different molecular weight with (S)-2-phthalimidopropionyl chloride, carbon disulfide was found as the most suitable solvent. The use of nitrobenzene caused the formation of dark, insoluble products. It was further found that the highest yield of soluble acylated product for atactic polystyrene was obtained when the Friedel-Crafts reaction was carried out during a period of 4 hr. The acylation of isotactic samples VIII and IX was performed similarly, while sample IX was acylated for 2 hr. and 30 min., yielding optically active samples X and XI, respectively. The influence of molecular weight on the degree of acylation is shown in Table II. It is evident

TABLE II

Optical Rotation and Degree of Acylation of p-[(S)(−)-2-Phthalimidopropionyl]polystyrene

Sample no.	N, %	Degree of acylation X, %		Content of phthalimido propiophenone E, %	$[\alpha]_D^{20}$ in benzene	$[\alpha']_D^{20a}$	$[\alpha']_D 100/E$
		From %N	From NMR				
I	3.02	40.0	45.0	60.5	−25.0	−17.7	−29.3
II	2.49	28.5	30.0	49.3	−21.8	−15.4	−31.2
III	2.20	23.5	25.2	43.3	−19.5	−13.8	−31.8
IV	1.94	20.0	23.0	38.7	−17.7	−12.5	−32.3
V	1.69	16.6	18.8	33.7	−15.7	−11.1	−32.9
VI	1.51	14.5	15.0	30.4	−13.9	−9.8	−32.2
VII	1.37	12.5	13.1	27.0	−11.6	−8.2	−30.4
VIII	3.00	39.0	—	59.6	−24.9	−17.6	−29.5
IX	2.72	32.4	—	53.4	−23.2	−16.4	−30.7
X	2.48	27.5	—	48.2	−20.8	−14.7	−30.5
XI	0.95	7.9	—	18.4	−8.5	−6.0	−32.6

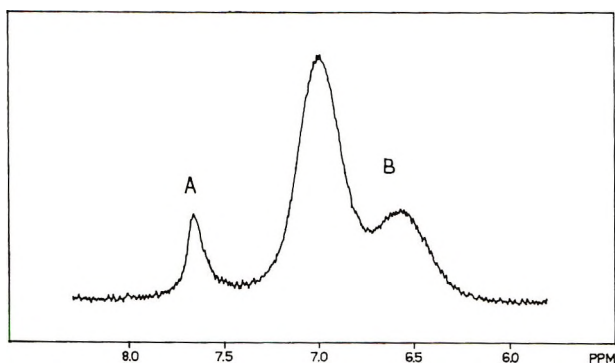[a] $[\alpha']_D = [\alpha]_D \, 3/n^2 + 2$; n is the refractive index of benzene.

Fig. 1. NMR spectrum of *p*-[(S)(−)-2-phthalimidopropionyl]polystyrene.
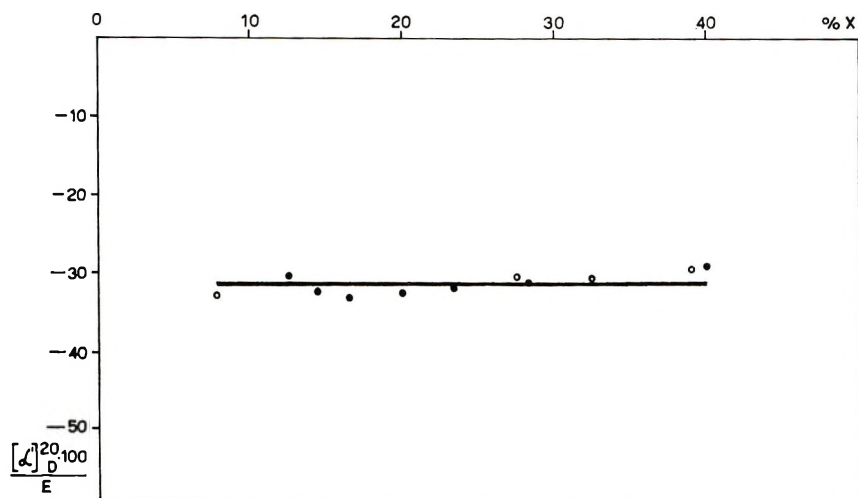

Fig. 2. Relationships between the degree of acylation and optical rotation: (●) atactic acylated PS; (○) isotactic acylated PS.

from the data obtained experimentally, that the highest degree of acylation was obtained with low molecular weight polystyrene. A probable reason for the dependence of the degree of acylation on molecular weight of polystyrene is the difference in solubility of aluminum chloride complex with high and low molecular weight polymers. It is interesting to note that Medalia and co-workers[11] did not observe the influence of molecular weight on the degree of alkylation in condensation of methyl undecanoate with polystyrene.

The degree of acylation (Table II) expressed as number of substituted styrene units per hundred styrene units was calculated either from the content of nitrogen or from NMR spectral data. Figure 1 shows the NMR spectrum of acylated polystyrene. The spectrum of the aromatic part of acylated polystyrene in acetone solution is similar to the spectrum of polystyrene (Fig. 1). The signal *A* corresponds to the benzene rings of

phthalimido groups, while other two peaks (*B*) correspond to the benzene rings of polystyrene.

The fourth column in Table II represents the content of α-phthalimido-propiophenone in the polymer and was calculated in the manner described by Minoura and Sakota.[12]

The ratio of $[\alpha']_D \times 100/E$ in the same table gives the specific rotation corrected for the refractive index of one substituted unit. The values of $[\alpha']_D \times 100/E$ are constant, although there is a relatively large random deviation of results.

By plotting the values of $[\alpha']_D \times 100/E$ versus degree of acylation X, as represented in Figure 2, the effect of the chain conformation to the optical activity can be determined. It is evident from Figure 2 that within the range of degree of acylations studied in this paper, there is no effect of chain conformation on the optical rotation of both atactic and isotactic acylated polystyrene.

Goodman[13] and Pino[14,15] have established that the effect of chain conformation on the optical activity is small when the optically active center is far from the backbone of the polymer chain. The large distance of optically active centers from the principal chain in p-[(S)(−)-2-phthalimidopropionyl]polystyrene is the obvious reason for the lack of effect of conformation to the optical activity.

References

1. H. Staudinger, M. Brunner, K. Frey, P. Garbsch, R. Signer and S. Wehrli, *Chem. Ber.*, **62**, 260 (1929).

2. R. J. Kern, H. G. Hurst, and W. R. Richard, *J. Polymer Sci.*, **45**, 195 (1960).

3. F. A. Bovey, F. P. Hood, E. W. Anderson, and L. C. Snyder, *J. Chem. Phys.*, **42**, 3900 (1965).

4. S. Krimm, *Fortschr. Hochpolymer.-Forsch.*, **2**, 51 (1960).

5. Q. A. Trementozzi, *J. Phys. Colloid. Chem.*, **54**, 1227 (1950).

6. T. Altares, Jr., D. P. Wyman, and V. R. Allen, *J. Polymer Sci. A*, **2**, 4533 (1964).

7. G. Natta and F. Danusso, *Chem. Ind. (Milan)*, **40**, 445 (1958).

8. S. Gabriel, *Chem. Ber.*, **38**, 634 (1905).

9. W. O. Kenyon and G. P. Waugh, *J. Polymer Sci.*, **32**, 83 (1958).

10. H. P. Frank, *Monatsh. Chem.*, **94**, 393 (1963).

11. A. I. Medalia, H. A. Freedman, and S. Sinha, *J. Polymer Sci.*, **40**, 15 (1959).

12. Y. Minoura and N. Sakota, *Nippon Kagaku Zasshi*, **83**, 912 (1962).

13. A. Abe and M. Goodman, *J. Polymer Sci. A*, **1**, 2193 (1963).

14. P. Pino, *Fortschr. Hochpolymer.-Forsch.*, **4**, 424 (1966).

15. P. Pino, paper presented at International Symposium on Macromolecular Chemistry, Prague 1965, Preprint 455.

# Polyaddition Reaction of Pseudoxazolones with Dimercaptans

YOSHIO IWAKURA, FUJIO TODA, YOSHINORI TORII, and REIKO SEKII, *The Department of Synthetic Chemistry, Faculty of Engineering, The University of Tokyo, Bunkyo-ku, Tokyo, Japan*

Synopsis

Polymers having thioether, thiolester, and amide linkages in each repeating unit of a polymer main chain were prepared by the polyaddition reaction of pseudoxazolones (2-isopropylidene-4-alkyl-3-oxazolin-5-ones) and dimercaptans. The polymers had inherent viscosities in a range of 0.08–0.22 and gave transparent films by solution casting.

INTRODUCTION

During a series of investigations on the polyaddition reaction, it was reported that diolefins[1] or bisaziridines[2] react with dimercaptans to form linear polysulfides of high molecular weight. In our previous paper,[3] the synthesis of polyamideamines from pseudoxazolones (2-isopropylidene-4-alkyl-3-oxazolin-5-ones, I) and primary diamines by the ring-opening polyaddition reaction was reported. It has been found that I added two moles of alkyl or aryl mercaptans to give adducts (III) in the same manner to primary amines in the presence of tertiary amines. The structure of III was established by means of infrared and NMR spectra.

I a, R_1 = Me
b, R_1 = *i*-Pr
c, R_1 = *i*-Bu

II

III
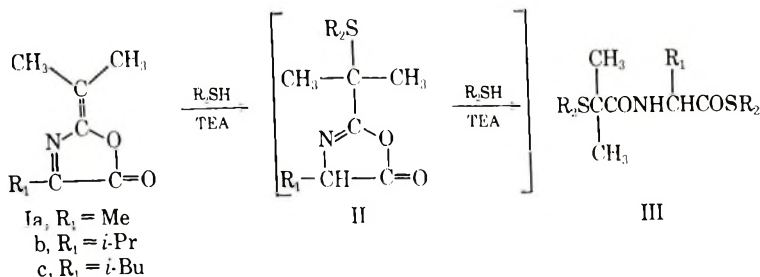
The present work deals with application of this new reaction for polymer syntheses. These polymers had a linear structure containing thioether, thiolester, and amide linkages in a polymer main chain.

EXPERIMENTAL

Materials

Thiophenol of E. P. grade (Tokyo Kasei Co.) was used for the model reaction without further purification.

Biphenyl-4,4'-dithiol was prepared by the method of Marvel[4] in 69% yield and purified by sublimation under vacuum; m.p. 180–182°C.

Phenoxybenzene-4,4'-dithiol was prepared by an analogous method[4] in 43% yield from the corresponding sulfonyl chloride and purified further by recrystallization from n-heptane; m.p. 99–101°C.

ANAL. Calcd. for $C_{12}H_{14}OS_2$: C, 61.54%; H, 4.30%; S, 27.33%. Found: C, 61.40%; H, 4.39%; S, 26.21%.

Diphenylmethane-4,4'-dithiol was synthesized in 96% yield[4] and recrystallized from the mixture of n-heptane and cyclohexane; m.p. 72–73°C.

ANAL. Calcd. for $C_{13}H_{12}S_2$: C, 67.23%; H, 5.21%; S, 27.56%. Found: C, 67.49%; H, 5.41%; S, 26.78%.

p-Xylene-α,α'-dithiol was synthesized by the method reported by Autenrieth[5] in 26% yield from p-xylylene dibromide and purified by vacuum distillation at 159–161°C./18 mm.

Tetrahydrofuran (THF) and triethylamine (TEA) were purified by distillation.

Model Reaction

A solution of 2-isopropylidene-4-methyl-3-oxazolin-5-one (Ia, 5.0 g.), thiophenol (3.1 g.), and TEA (0.5 ml.) in benzene (30 ml.) was placed in a 50 ml. ampule. The ampule was sealed and kept at 60°C. for 6 hr. After reaction, the benzene was removed under reduced pressure and then petroleum ether (40 ml.) was added to the residue. The resulting crystals were collected by filtration. The yield was 8 g. (97%); the product was recrystallized from a mixture of n-hexane and cyclohexane; m.p. 64–66°C.

ANAL. Calcd. for $C_{19}H_{21}NO_2S_2$: C, 63.50%; H, 5.89%; N, 3.90%; S, 17.81%. Found: C, 63.59%; H, 6.15%; N, 3.90%; S, 17.25%.
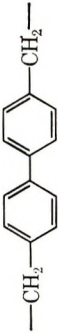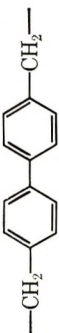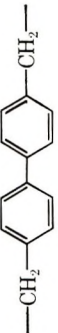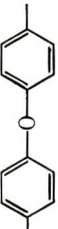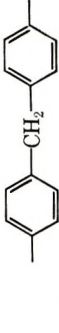
Polyaddition Reaction

For a typical polyaddition reaction, THF (10 ml.), I (0.01 mole), dithiol (0.01 mole), and TEA (0.2 ml.) were put in a 30 ml. ampule. The content of the ampule was then flushed with dry nitrogen stream, sealed and placed in a water bath kept at 60°C. for 12 hr. (in case of p-xylene-α,α'-dithiol for 24 hr.). After polymerization, polymer was precipitated by pouring the polymer solution into n-hexane and dried under vacuum for a day. Polymer XI (Table I) was synthesized at the half scale of this procedure.

Instruments

Thermogravimetric analysis was carried out in air with a Thermoflex thermogravimetric analyzer, high temperature type, (Rigaku Denki Co.) at heating rate of 10°C./min.

TABLE I
Polyaddition Reaction

| Polymer no.	R₁	R₂	Yield, %	$\eta_{inh}{}^a$	Nitrogen, % Calcd.	Found	Sulfur, % Calcd.	Found
IV	Me	(4,4'-biphenylene)	Quant.	0.14	3.92	3.92	17.57	16.88
V	Me	—CH₂—(phenylene)—(phenylene)—CH₂—	82	0.08	4.53	4.57	20.69	19.74
VI	i-Pr	(4,4'-biphenylene)	97	0.22	3.63	3.67	16.61	16.07
VII	i-Pr	—CH₂—(phenylene)—(phenylene)—CH₂—	66	0.14	4.15	4.16	18.97	17.85
VIII	i-Bu	(4,4'-biphenylene)	Quant.	0.22	3.51	3.67	16.02	15.27
IX	i-Bu	—CH₂—(phenylene)—(phenylene)—CH₂—	90	0.10	3.99	4.02	18.21	17.30
X	i-Pr	(phenylene)—O—(phenylene)	88	0.17	3.49	3.45	15.98	15.24
XI	i-Pr	—CH₂—(phenylene)—(phenylene)—CH₂—	Quant.	0.21	3.51	3.27	16.02	14.12

a Obtained at 0.5% concentration in THF at 30°C.

The x-ray diffraction pattern of the polymer film was taken with a Rigaku Denki Co., Model D2-F diffractometer, at room temperature with the use of Ni-filtered Cu Kα radiation.
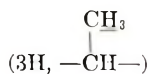
The NMR spectrum was determined with a Japan Electron Optics Lab. Co., Model 4H-100 at 100 Mc./sec. in carbon tetrachloride with tetra-methylsilane as internal standard.

RESULTS AND DISCUSSION

From the results of elemental analyses 1 mole of Ia reacted almost quantitatively with 2 moles of thiophenol. It was thought that the reaction proceeded at first by nucleophilic attack of a mercaptan molecule towards the conjugated double bond including a nitrogen atom to give an inter-mediate cyclic adduct (II), and then by ring opening with another molecule of mercaptan to give 1:2 adduct (IIIa). Tertiary amines such as TEA were known to be effective catalysts in promoting the ring-opening reac-tion of cyclic compounds with mercaptans,[2,6] because tertiary amines increase their nucleophilic reactivity. The catalytic action of TEA was also conspicuous in this addition reaction. The infrared spectrum of IIIa (Fig. 1) exhibited characteristic absorptions at 3310, 1705, 1650, and 1505 cm.$^{-1}$ which are interpreted as NH stretching, thiolester stretching vibra-tion, amide I, and amide II absorptions, respectively.[7] In the NMR spectrum IIIa showed two singlets

$$CH_3$$
$$(3H, 3H, C_6H_5SC-)$$
$$CH_3$$
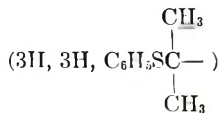
at τ 8.51 and 8.47; a doublet

$$CH_3$$
$$(3H, -CH-)$$

centered at τ 8.55; and a quartet
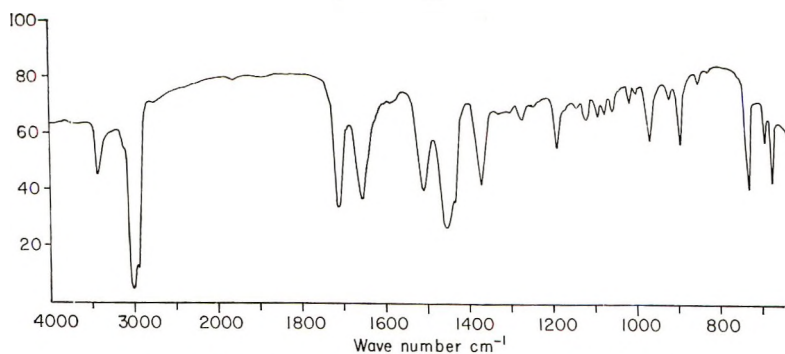
$$CH_3$$
$$(1H, -CH-)$$
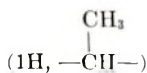
Fig. 1. Infrared spectrum of model compound (Nujol).
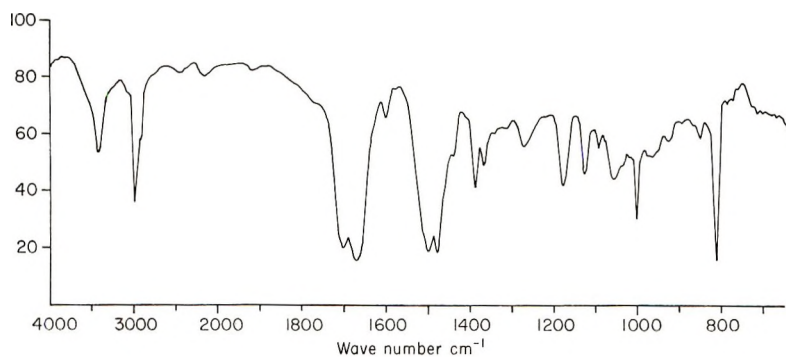
Fig. 2. Infrared spectrum of polymer VIII (film).

centered at τ 5.27 (J = 7 cps).

$$\begin{array}{cc} CH_3 & CH_3 \\ | & | \\ C_6H_5SCCONHCHCOSC_6H_5 \\ | \\ CH_3 \end{array}$$

IIIa
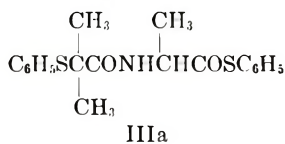
All peaks correspond well to the assigned structure.

The results of polyaddition reaction are summarized in Table I. The polyaddition reaction with aryl dimercaptans proceeded exothermally in the presence of TEA:

$$I + HS{-}R_2{-}SH \xrightarrow{\text{TEA}} \begin{array}{cc} CH_3 & R_1 \\ | & | \\ (R_2SCCONHCHCOS)_n \\ | \\ CH_3 \end{array}$$
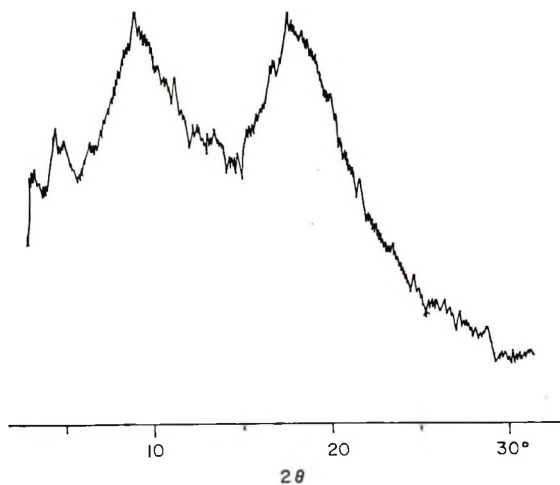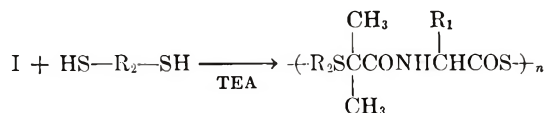
Fig. 3. X-Ray diffraction diagram of polymer VIII.

However, in the reaction with p-xylene-α,α'-dithiol, rather longer reaction time must be necessary to complete the polyaddition reaction because of the relatively low nucleophilicity of this mercaptan. The infrared spectrum of the polymer VIII is given in Figure 2. Polymers exhibited the characteristic absorption bands for νNH, thiolester, amide I, and amide II as shown in Table II, which agree well to those of IIIa.

TABLE II
Infrared Absorptions of Polymer Films

| Polymer No.	Frequency, cm.$^{-1}$			
	ν_{NH}	ν_{COS}	Amide I	Amide II
VI	3390	1695	1670	1500
VIII	3360	1695	1670	1490
IX	3360	1680	1655	1505
X	3390	1700	1675	1485
XI	3350	1695	1670	1485

Polymers were soluble in THF, dioxane, dimethylformamide, dimethyl sulfoxide, benzene, chloroform, acetone, and ethyl acetate and swelled in carbon tetrachloride; they were insoluble in methanol, n-hexane, and water. The polymers were white or slightly colored powders and could be cast to transparent brittle films from THF solution.

The x-ray diffraction diagram (Fig. 3) indicates that polymer VIII has a low degree of crystallinity. This amorphous structure might be due to the incorporation of head-to-head and head-to-tail units in the polymer chain.

The polymer melt temperature of polymer VIII was 155–160°C. Thermogravimetric analysis showed that thermal decomposition of polymer VIII occurred near 195°C. in air and about 43% of the initial weight of the polymer was lost up to 370°C. as volatile substances.

References

1. C. S. Marvel and R. R. Chambers, *J. Am. Chem. Soc.*, **70**, 993 (1948).
2. Y. Iwakura, M. Sakamoto, and M. Yoneyama, *J. Polymer Sci. A-1*, **4**, 159 (1966).
3. Y. Iwakura, F. Toda, and Y. Torii, *J. Polymer Sci. B*, **5**, 17 (1967).
4. C. S. Marvel and P. D. Caesar, *J. Am. Chem. Soc.*, **73**, 1097 (1951).
5. W. Autenrieth and F. Beuttel, *Ber.*, **42**, 4346 (1909).
6. W. Steglich, H. Tanner, and R. Hurnaus, *Chem. Ber.*, **100**, 1824 (1967).
7. L. J. Bellamy, *The Infra-red Spectra of Complex Molecules*, Wiley, New York, 1964.

Polymerization of Cyclic Iminoethers.   V. 1,3-Oxazolines with Hydroxy-, Acetoxy-, and Carboxymethyl-Alkyl Groups in the 2 Position and Their Polymers

A. LEVY* and M. LITT,† *Central Research Laboratory, Allied Chemical Corporation, Morristown, New Jersey 07960*

Synopsis

Oxazolines containing carbomethoxy-, acetoxy-, and hydroxy-alkyl groups on the side chain were prepared and polymerized. The properties of the polymers were investigated.

INTRODUCTION

Previously it had been shown[1–4] that cyclic iminoethers can be readily prepared and polymerized to high molecular weight polymers:

$$\text{(structure)} \xrightarrow{\text{H}^+} \text{(structure)}$$
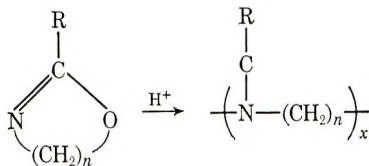
where $n = 2$ or 3 and R = aliphatic or aromatic group.   In order to modify the properties of the resulting polymers, materials were prepared that contained various functional (and reactive) groups on the side chain. We had expected that ester groups would not interfere with the polymerization,[5] and therefore we chose to make these first.   We also made a hydroxy-substituted monomer for comparison, since we knew that this group does chain transfer.[5]

DATA AND DISCUSSION

Four monomers were synthesized as representative of the classes we wanted to cover.   These classes were ester, carboxyl, and hydroxyl.

---

* Present address: Ethicon Corp., Somerville, New Jersey.

† Present address: Polymer Science Department, Case Western Reserve University, Cleveland, Ohio 44106.

Since we know carboxyl interferes strongly, and hydroxyl weakly, with polymerization[5] we shielded them by making two types of ester side chain:

$$\underset{\text{O}}{\overset{\text{O}}{\parallel}}$$

$$CH_3C{-}O{-}R \text{ and } CH_3OC{-}R$$
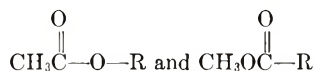
The first would produce a hydroxyl group, and the second a carboxyl group, after hydrolysis. The first polymer was then compared with the polymer produced by polymerizing the unprotected ω-hydroxy monomer. In every case, with the perchlorate salt of p-chlorophenyl oxazoline as catalyst, polymerization went to completion.

Carbomethoxy Side Chain

2-(β-Carbomethoxy)ethyl oxazoline was prepared in high yield via the following route:

$$(1)$$

$$(2)$$

$$(3)$$
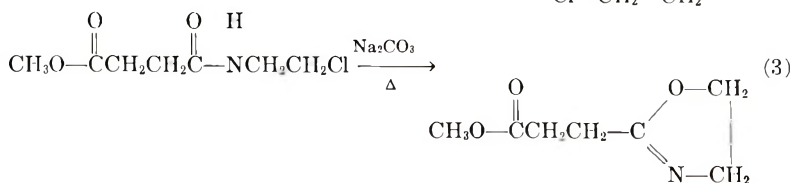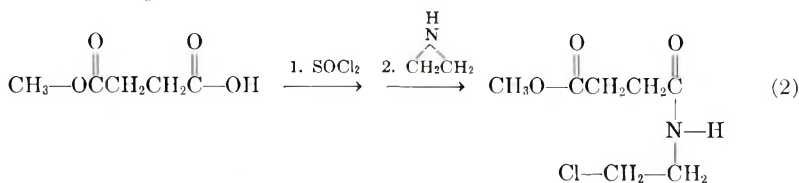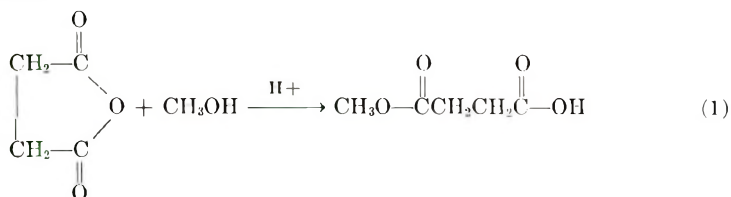
The monomer was polymerized to give a clear, colorless solid that was hard but somewhat brittle. Polymerization was carried out at monomer-to-initiator (M/I) ratios of up to 6400, and material was obtained with viscosities up to $[\eta] = 2.35$. It was soluble in cold water (precipitated hot) and alcohol and had a T_g of 31° (Clash Berg).

The polymer was then hydrolyzed with aqueous caustic to the sodium salt of the acid:
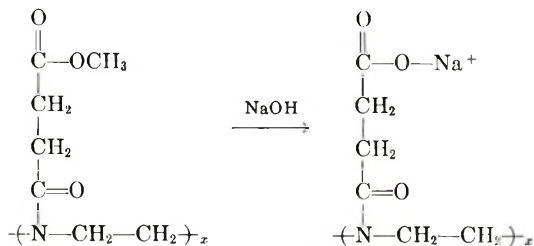
The polysalt acted as a thickening agent. It also can form insoluble complexes with a variety of metal ions (e.g., Fe^{3+}, Cu^{2+}, Co^{2+}, etc.).

Acetoxy Side Chain

2-(5-Acetoxy)pentyl oxazoline was prepared by the following route:

$$
\begin{array}{c}
\underset{\substack{CH_2 \\ | \\ CH_2 \\ \diagdown \\ CH_2-CH_2}}{\overset{\substack{O \\ \| \\ C \\ \diagup \quad \diagdown}}{\underset{}{}}} \xrightarrow[\text{2. HCl}]{\text{1. NaOH} + H_2O} HO-(CH_2)_5-\overset{O}{\overset{\|}{C}}-OH
\end{array} \qquad (1)
$$

$$
HO-(CH_2)_5-\overset{O}{\overset{\|}{C}}-OH + CH_3-\overset{O}{\overset{\|}{C}}-Cl \rightarrow CH_3-\overset{O}{\overset{\|}{C}}-O(CH_2)_5-\overset{O}{\overset{\|}{C}}-OH \qquad (2)
$$

$$
CH_3-\overset{O}{\overset{\|}{C}}-O-(CH_2)_5-\overset{O}{\overset{\|}{C}}-OH + SOCl_2 \rightarrow CH_3-\overset{O}{\overset{\|}{C}}-O-(CH_2)_5-\overset{O}{\overset{\|}{C}}-Cl \qquad (3)
$$

$$
CH_3-\overset{O}{\overset{\|}{C}}-O-(CH_2)_5-\overset{O}{\overset{\|}{C}}-Cl + \underset{\underset{H}{N}}{CH_2-CH_2} \rightarrow
$$

$$
CH_3-\overset{O}{\overset{\|}{C}}-O-(CH_2)_5-\overset{O \quad H}{\overset{\| \quad |}{C}}-N-\underset{\underset{Cl}{CH_2}}{CH_2} \qquad (4)
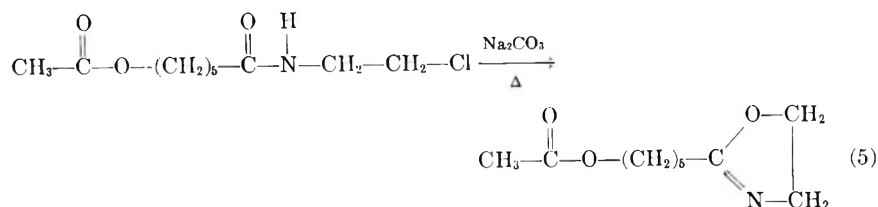$$

$$
CH_3-\overset{O}{\overset{\|}{C}}-O-(CH_2)_5-\overset{O \quad H}{\overset{\| \quad |}{C}}-N-CH_2-CH_2-Cl \xrightarrow[\Delta]{Na_2CO_3}
$$

$$
CH_3-\overset{O}{\overset{\|}{C}}-O-(CH_2)_5-\underset{\diagdown}{\overset{\diagup}{C}}\underset{N-CH_2}{\overset{O-CH_2}{|}} \qquad (5)
$$
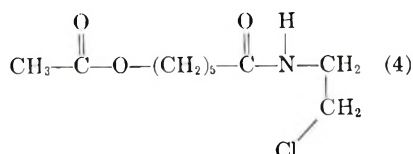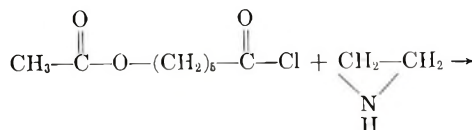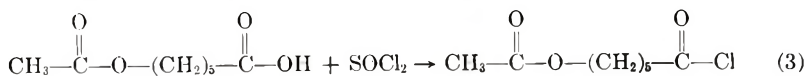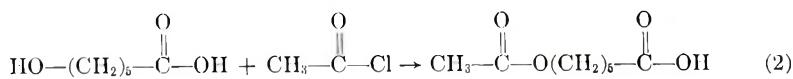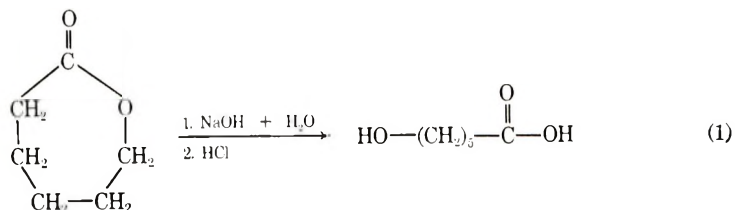
The monomer was polymerized at M/I of 120 and 1100 and gave a clear, gummy polymer in both cases. The polymer was hydrolyzed to the hydroxy-substituted polymer with sodium hydroxide in ethanol.

$$
\begin{array}{c}
O-\overset{O}{\overset{\|}{C}}-CH_3 \\
| \\
(CH_2)_5 \\
| \\
C=O \\
| \\
+N-CH_2-CH_2\!+_x
\end{array}
\xrightarrow{\text{NaOH}}
\begin{array}{c}
OH \\
| \\
(CH_2)_5 \\
| \\
C=O \\
| \\
+N-CH_2-CH_2\!+_x
\end{array}
$$
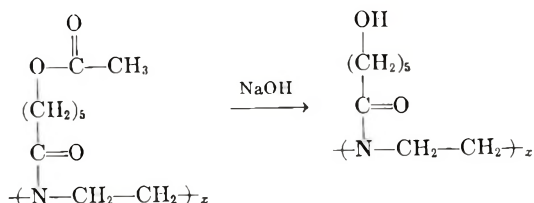
The hydrolyzed material was opaque, tough, and leathery. It became quite crystalline on standing, with a melting point of 300°C. (decomposed). It is very soluble in most polar solvents, including water.

An analogous monomer, 2-acetoxy-methyl oxazoline, was prepared from glycolic acid in a similar manner. Upon polymerization, however, at M/I of 500 or 1300 there was obtained only brittle material with an η_{sp}/c (0.5% m-cresol) of 0.34–0.37. These very low values are indicative of extensive chain transfer on the α-methylene group, probably caused by the electron-withdrawing acetoxy group. This tends to make the hydrogen atoms of the methylene group more acidic and causes chain transfer of the following type:

Similar results have been obtained with other electron-withdrawing groups, such as phenyl.[1a] The polymer was smoothly hydrolyzed to an α-hydroxy acetyl polyethylenimine. It was crystalline and had a melting point of 200°C.
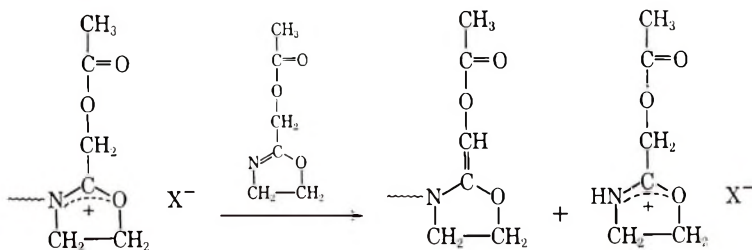
Hydroxyl Side Chain

2-(5-Hydroxypentyl)oxazoline was prepared in two steps:

$$HO{-}(CH_2)_5{-}\overset{O}{\overset{\|}{C}}{-}\overset{H}{\overset{|}{N}}{-}CH_2{-}CH_2{-}OH \quad (1)$$

$$HO{-}(CH_2)_5{-}\overset{O}{\overset{\|}{C}}{-}\overset{H}{\overset{|}{N}}{-}CH_2{-}CH_2{-}OH \xrightarrow[\Delta]{catalyst} HO{-}(CH_2)_5{-}C \quad (2)$$
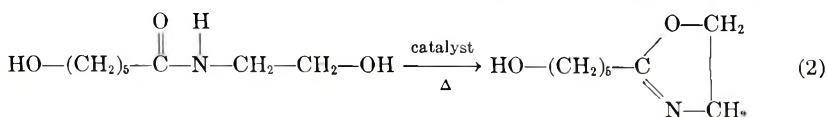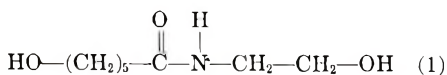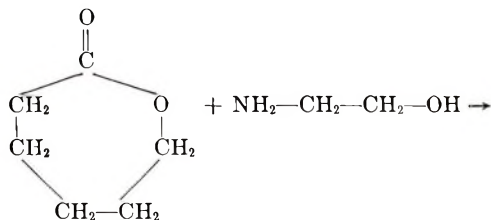
Polymerization at an M/I of 270 gave a relatively hard, amorphous material that was insoluble in every solvent tested. It swelled in many polar solvents, including water, and behaved like a crosslinked material.

We have shown that hydroxyl groups chain-transfer with growing polymer chain:[5]
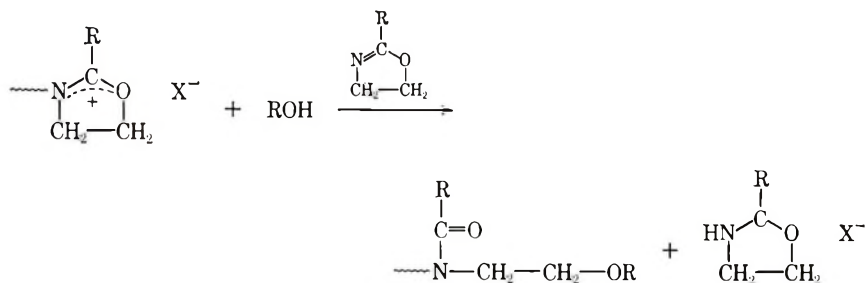
Therefore, an oxazoline containing a hydroxyl group as part of the molecule will form a giant, branched molecule:
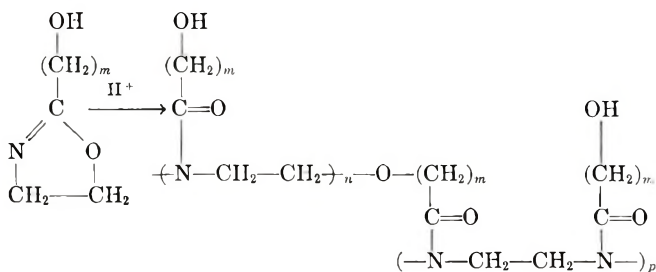
These results indicated that it could be used as a molecular-weight extender. A small amount of a hydroxy-substituted oxazoline, copolymerized with another oxazoline, should link the growing chains together, increasing the molecular weight and viscosity of the resulting polymers.

2-(5-Hydroxypentyl)oxazoline was copolymerized with 2-(i-butyl)-oxazoline at an M/I of 500. The results are shown in Table I.

TABLE I
Effect on Viscosity with Hydroxy-Substituted Oxazoline as Comonomer

Monomer	Added 2-(5-hy- droxy- pentyl) oxazo- line, %	Initiator	M/I	Time, hr.	Temp., °C.	η_{sp}/c[a]
i-Butyl oxazoline	0	PCOP[b]	500	4	120	
		"		"	160	0.61
"	~2	"	"	"	"	2.05
"	~5	"	"	"	"	Gel

[a] 0.5% in m-cresol.
[b] PCOP, 2(p-chlorophenyl)oxazolinium perchlorate.

It is obvious that small amounts of hydroxy-substituted monomers can raise viscosities (and certainly molecular weights) very easily. The polymer of highest viscosity obtained from 2-(i-butyl)oxazoline had $[\eta]$ = 2.34 (m-cresol) at an M/I of 41,000. This is about the best that can be

obtained at a temperature of 160°C. and required 25 hr. of polymerization time. By the use of a small amount of hydroxy-substituted comonomer these viscosities can be obtained in a very short time with minor modification of polymer properties.

Summary and Conclusions

Some oxazolines with ester groups on the position 2 side chains were synthesized and polymerized. There was no appreciable excess chain transfer, which was what was expected. Hydrolysis of the amorphous acetoxy alkyl polymers gave crystalline N-(ω-hydroxy acyl)poly(ethylenimines). The crystallization is probably due to two factors: the hydroxy group is smaller than the ester group, giving better packing, and the ω-hydroxy group can hydrogen-bond, giving increased interchain forces. The hydroxyl group on monomer or polymer (and, by inference, amide or phenolic groups[5]) can chain-transfer effectively during polymerization, leading to gels or high-viscosity polymers.

EXPERIMENTAL

Synthesis of Methyl Hydrogen Succinate

A mixture of 400 g. (4.0 moles) of succinic anhydride and 194 ml. (4.8 moles) of anhydrous methanol was refluxed on a steam bath. After heating for 35 min. the mixture was swirled frequently until it became homogeneous (15 min.). It was then heated for an additional 25 min.

The excess methanol was removed under reduced pressure and the warm residual liquid poured into a large evaporating dish cooled in cold water. The half-ester crystallized and was filtered by means of reduced pressure; yield 508 g. (96%); m.p. 57–58°C. (lit.: yield 96%, m.p. 57 –58°C.).[6]

Preparation of β-Carbomethoxy Propionyl Chloride

A solution of methyl hydrogen succinate (264 g., 2.0 moles) and thionyl chloride (290 ml., 4.0 moles) was warmed at 35–40°C. for 3 hr. and kept at room temperature overnight (equivalent yields have been reported from the use of only a 20% excess). The dissolved HCl and SO_2 and excess thionyl chloride were removed under reduced pressure. The β-carbomethoxy propionyl chloride was distilled at as low a pressure as possible; yield 285.1 g. (95%), b.p. 78°C. at 7 mm. (lit.:[6] yield 93%, b.p. 93°C. at 18 mm.).

Preparation of N-(β-Chloroethyl)-3-Carbomethoxy Propionamide

β-Carbomethoxy propionyl chloride (207.4 g., 1.35 moles) was dissolved in 1 liter of ether. To this was slowly added 71.5 ml. (59.3 g., 1.38 moles) of ethyleneimine in 450 ml. of ether at such a rate as to maintain reflux. The addition was complete in 5 hr. Upon chilling in a bath of solid carbon

dioxide and acetone a white solid separated. This was filtered; 187.1 g. of solid was obtained. The filtrate was evaporated to a volume of 500 ml., chilled, and refiltered to give an additional 55.7 g. of solid.

The material is extremely hygroscopic. The combined material was dried under vacuum and kept in a sealed container; yield 242.8 g. (91%).

Preparation of 2-(β-Carbomethoxyethyl) Oxazoline

N-(β-Chloroethyl)-3-carbomethoxy propionamide (239.0 g., 1.24 moles) and anhydrous sodium carbonate (95.6 g., 0.90 mole) were heated together with stirring at a pressure of 10 mm. When the pot temperature reached about 115°C., a clear, colorless liquid began to distill. When redistilled, the boiling point of the liquid was 115°C. at 10 mm.; yield 167.1 g. (86%). Elemental and infrared analyses agreed with the proposed structure.

ANAL. (for $C_7H_{11}NO_3$). Calcd.: C, 53.49%; H, 7.06%; N, 8.91%; Obsd.: C, 52.84%; H, 7.05%; N, 8.94%.

Polymerization of 2-(β-Carbomethoxy)Ethyl Oxazoline

To a cleaned, weighed, dry polymerization tube was added the initiator (p-chlorophenyl oxazolinium perchlorate) as a 2% solution in dry acetonitrile. The solvent was removed under reduced pressure, and twice-distilled monomer was distilled again through a spinning-band column directly into the tube; monomer, 38.36 g. (0.255 mole); catalyst, 0.54 ml. (0.0108 g., 0.000038 mole); $M/I = 6400$. The tube was degassed twice and sealed under reduced pressure. It was placed in an oven at 120°C. and heated for 18 hr. A clear, colorless solid formed; $[\eta] = 2.35$ in m-cresol.

Hydrolysis of Poly[N-(3-Carbomethoxy Propionyl)Ethylenimine]

The polymer (9.87 g., 0.063 mole) was dissolved in 125 ml. of water, and to it was added 2.51 g. (0.063 mole) of NaOH in 125 ml. of water. The solution was stirred at room temperature for 4 hr. and 30 min. at 100°C. An aliquot was titrated with standard acid, and it was found that all the base had been used up. The residue was evaporated to dryness to give 9.70 g. of solid. A 5% solution in water had an absolute viscosity of 92 cpoise. When an aqueous solution was mixed with various metal ions in solution, such as, Fe^{3+}, Cu^{2+}, Co^{2+}, and Zr^{2+}, a precipitate formed, indicating complex formation.

Synthesis of 6-Hydroxy-hexanoic Acid

A solution of 228 g. (2.0 moles) of caprolactone in 150 ml. of water containing a few drops of thymol blue was heated with stirring. To this was slowly added 80.0 g. (2.0 moles) of sodium hydroxide in 200 ml. of water. After it cooled, concentrated hydrochloric acid was slowly added, until the solution became red. Sodium sulfate was added, to salt out the acid, and an upper layer formed and was separated. The water layer was

extracted with ether, and the organic layer and washings were combined, dried, and evaporated to dryness, to give 247.3 g. (92%) of 6-hydroxy-caproic acid, an oil that could not be crystallized.[7]

Synthesis of 6-Acetoxy-hexanoyl Chloride

A solution of 241.4 g. (1.83 moles) of 6-hydroxycaproic acid and 261.4 ml. (287.3 g., 3.66 moles) of acetyl chloride was refluxed overnight. The excess acetyl chloride was removed under reduced pressure, leaving 329.1 g. (100%) of a pale-pink liquid. To the crude 6-acetoxycaproic acid was slowly added 268 ml. (428.4 g., 3.6 moles) of thionyl chloride. The solution was kept at 35–40°C. for 3 hr. and at room temperature over-night. The excess thionyl chloride was removed by distillation. Distil-lation of the residue under reduced pressure gave 138.6 g. (40%) of a clear, colorless, irritating liquid. The proposed structure was confirmed by infrared spectroscopy; b.p. 87–94°C. at 0.3 mm., $n_D^{23} = 1.4428$.

ANAL. (for $C_8H_{13}O_3Cl$). Calcd.: C, 50.0%; H, 6.8%; Cl, 18.4%. Obsd.: C, 49.72%; H, 6.78%; Cl, 18.7%.

Synthesis of N-(β-Chloroethyl)-6-acetoxy Hexanamide

To a solution of 38.5 g. (0.20 mole) of 6-acetoxy-hexanoyl chloride in 200 ml. of ether was slowly added 10.4 ml. (8.6 g., 0.20 mole) of ethylene-imine in 50 ml. of ether. The addition was carried out at such a rate as to maintain reflux. The ethereal solution was filtered away from the small amount of white solid and chilled in a bath of solid carbon dioxide and acetone. A white solid separated, which was collected by filtration and dried under reduced pressure. There was obtained 36.2 g. (77%) of a white solid; m.p. 37–39°C.

The reaction was repeated with 100.0 g. (0.42 mole) of acid chloride and 22.4 g. (0.52 mole) of ethyleneimine. In this run, when all of the ethyleneimine had been added, anhydrous hydrogen chloride was bubbled through the solution for 5 min. There was obtained 105.7 g. (86%) of product. Two recrystallizations from ether gave a solid; m.p. 38.5–39.5°C.

ANAL. (for $C_{10}H_{18}NO_3Cl$). Calcd.: C, 51.0%; H, 7.6%; N, 6.0%; Cl, 15.0%. Obsd: C, 50.70%; H, 7.79%; N, 6.22%; Cl, 14.7%.

Synthesis of 2-(5-Acetoxy) Pentyl Oxazoline

A mixture of 35.3 g. (0.15 mole) of N-(β-chloroethyl)-6-acetoxy hexan-amide and 11.0 g. (0.105 mole) of powdered anhydrous sodium carbonate was stirred at a pressure of 0.5 mm. Heating was begun, and after a great deal of bubbling had subsided, a clear, colorless liquid, of b.p. 114–119° at 0.5 mm., distilled. There was obtained 13.8 g. (46%) of product; the structure was confirmed by infrared spectroscopy.

The liquid was redistilled prior to polymerization; b.p. 76°C. at 0.03 mm., $n_D^{22} = 1.4559$.

Polymerization of 2-(5-Acetoxy) Pentyl Oxazoline

The monomer was distilled through a spinning-band column directly into two clean, dry, weighed polymerization tubes that already contained catalyst, the perchloric acid salt of 2-(p-chlorophenyl)oxazoline, which had been added as previously described: tube I contained 4.8 g. (0.024 mole) of monomer and 0.0564 g. (0.0002 mole) of catalyst, the M/I being 120; tube II contained 4.3 g. (0.0216 mole) of monomer and 0.00564 g. (0.00002 mole) of catalyst, the M/I being 1100. The tubes were degassed twice and sealed under reduced pressure. The samples were polymerized at 114°C. for 41.5 hr. and gave a soft, sticky polymer that flowed on standing. Polymer (I), however, was considerably softer than Polymer (II): polymer (I), $\eta_{sp}/c = 0.21$ (1.0% m-cresol); polymer (II), $\eta_{sp}/c = 1.47$ (1.0% m-cresol).

Hydrolysis of Poly[N-(6-Acetoxy Hexanoyl)Ethyleneimine]

Polymer (II) was dissolved in ethanol and filtered, to remove adhering glass. It was then refluxed for 20 min. with 0.86 g. (0.0216 mole) of sodium hydroxide; the total volume was 80 ml. After 5 min. a white solid began to precipitate and increased in thickness. The solution was allowed to cool and was filtered. The white solid was dried and identified as 0.93 g. of sodium acetate. The filtrate was treated with ether: a white solid separated and was collected by filtration; this was heated with a 50:50 mixture of ethanol and i-propanol. The insoluble portion was removed by filtration and dried; it also was sodium acetate.

Ether was added to the filtrate, and the precipitate was collected and dried. This was a leathery, white solid, which had an infrared spectrum that agreed with that of poly[N-6-hydroxy hexanoyl ethylenimine].

X-rays indicated the polymer to be quite crystalline, and DTA showed it to have a melting point of about 300°C. It was soluble in most polar solvents upon heating; $\eta_{sp}/c = 1.47$ (0.5% in m-cresol).

Synthesis of 2-Acetoxy-acetyl Chloride

Acetyl chloride (275 ml., 304.0 g., 3.9 moles) was added slowly to 152 g. (2.0 moles) of glycolic acid. The mixture was heated until no more hydrogen chloride evolved. The excess acetyl chloride was removed under reduced pressure; the residue solidified on standing. To the crude acetoxy acetic acid was added 290 ml. (476.0 g., 4.0 moles) of thionyl chloride. The solution was stirred for 3 hr. at 35–40°C. and at room temperature overnight. The excess thionyl chloride was removed by distillation, and the product was distilled under reduced pressure. There was obtained 171.2 g. (63%) of a colorless, lachrymatory material; b.p. 60°C. at 16 mm. (lit.:[3] 54°C. at 14 mm.). Its structure was confirmed by infrared spectroscopy; $n_D^{23} = 1.4240$.[8]

Synthesis of N-(β-Chloroethyl)-2-Acetoxy Acetamide

To a solution of 114.9 g. (0.84 mole) of 2-acetoxy acetyl chloride in 600 ml. of ether was added 45 ml. (36.2 g., 0.84 mole) of ethyleneimine at such a rate as to maintain reflux. The solution was chilled in a bath of solid carbon dioxide and acetone, and a white solid separated. It was collected by filtration and dried. There was obtained 147.8 g. (98%) of crude product; m.p. 58.5–64.5°C. It was recrystallized from ether; m.p. 68.5 –70.5°C.

Synthesis of 2-Acetoxymethyl Oxazoline

N-(β-Chloroethyl)-acetoxy acetamide (147.8 g., 0.82 mole) and anhydrous powdered sodium carbonate (87.2 g., 0.82 mole) were stirred together at 17 mm. At a pot temperature of 65–115°C. a clear, colorless liquid distilled in the amount 107.5 g. (92%).

A solid, which was identified as 2-hydroxyethyl oxazoline, was separated from the product by distillation. The product was redistilled; b.p. 57°C. at 0.05 mm.

ANAL. (for $C_6H_9NO_3$). Calcd.: C, 50.3%; H, 6.3%; N, 9.8%. Obsd.: C, 50.52%; H, 6.27%; N, 9.67%.

Polymerization of 2-Acetoxymethyl Oxazoline

The monomer was distilled into flamed polymerization tubes containing the p-chlorophenyl oxazolinium perchlorate added as described initially: tube I contained 5.0 g. (0.035 mole) of monomer and 0.02 g. (0.000075 mole) of catalyst, the M/I being 500, and tube II contained 6.57 g. (0.046 mole) of monomer and 0.01 g. (0.000035 mole) of catalyst, the M/I being 1300. The tubes were sealed under reduced pressure and placed in an oven at 130°C. After 30 min. the contents were both solid. They were yellow-brown and glassy and slowly soluble in water and methanol. Their structure was confirmed by infrared spectroscopy. The η_{sp}/c (0.5% m-cresol) of Polymer I was 0.34 and of Polymer II was 0.37.

Hydrolysis of Poly[N-(acetoxyacetyl)Ethylenimine]

The polymer (2.78 g., 0.0194 mole) was dissolved in 50 ml. of water and heated with 0.78 g. (0.0194 mole) of sodium hydroxide. When thymol phthalein indicator showed that all the base was used up (5 min.), the solution was evaporated to dryness. Methanol was added, and the precipitated polymer was collected by filtration and dried overnight at 50°C. The polymer (2.08 g.) was pale yellow, brittle, and water-soluble. Its structure was confirmed by infrared spectroscopy; $\eta_{sp}/c = 0.21$ (0.5% m-cresol). It was shown by x-rays to be crystalline; m.p. = 200°C., decomposed.

Synthesis of 2-(5-Hydroxypentyl)Oxazoline

N-(β-Hydroxyethyl)-6-hydroxy hexanamide (196.0 g., 1.12 moles) was flash-distilled through a column of pelletized kaolin clay heated to 275°C. at 2–3 mm. total pressure with a nitrogen bleed. The distillation took 4–5 hr. The condensate was distilled, and there was obtained 91.3 g. (52%) of oxazoline with 58.0 g. (30%) of unreacting starting material.

The oxazoline was purified by a careful distillation through a spinning-band column; b.p. 88–88.5° at 0.02 mm., $n_D^{21} = 1.4745$. The proposed structure was also confirmed by infrared spectroscopy.

ANAL. (for $C_{18}H_{15}NO_2$). Calcd.: C, 61.1%; H, 9.6%; N, 8.9%. Obsd.: C, 61.2%; H, 9.7%; N, 9.4%.

Bulk Polymerization of 2-(5-Hydroxypentyl)Oxazoline

The monomer was distilled into a clean, dry, weighed polymerization tube containing the catalyst (p-chlorophenyl oxazolinium perchlorate); M/I = 270. The tube was sealed under reduced pressure, placed in an oven, and heated at 160°C. for 4–5 hr. A clear, orange solid was obtained. The polymer, though somewhat leathery, could be cut with a knife and shattered by a mallet. It was swollen by many solvents, but it was insoluble in every one tested.

Copolymerization of 2-(i-Butyl)Oxazoline and 2-(5-Hydroxypentyl)Oxazoline

2-(i-Butyl)oxazoline, prepared as described previously,[1a] was distilled directly into flamed polymerization tubes, to which catalyst had been added. To tubes II and III (tube I was a control) the calculated amount of 2-(5-hydroxypentyl)oxazoline was added. In tube I were 5.77 g. (0.045 mole) of 2-(i-Butyl)oxazoline and 0.026 g. (0.000094 mole) of catalyst: 2-(p-chlorophenyl)oxazolinium perchlorate; M/I = 480. In tube II were 5.85 g. (0.046 mole) of 2-(i-Butyl)oxazoline, 0.15 g. (0.00096 mole) of 2-(5-Hydroxypentyl)oxazoline, ≈2 mole-%, and 0.026 g. (0.000094 mole) of catalyst; M/I = 500. In tube III were 5.78 g. (0.045 mole) of 2-(i-Butyl)oxazoline, 0.40 g. (0.00255 mole) of 2-(5-Hydroxypentyl)oxazoline, ≈5 mole-%, and 0.026 g. (0.000094 mole) of catalyst; M/I = 500.

The tubes were degassed and sealed under reduced pressure. They were placed in a bath at 100°C., and the temperature was slowly increased to 160°C. over a period of 4 hr. They were kept at 160°C for an additional 4 hr. The polymers were all cloudy, brittle solids, though polymers (II) and (III) appeared to be slightly less brittle. They were all crystalline; the η_{sp}/c (0.5% in m-cresol) of Polymer (I) was 0.61 and of Polymer (II) 2.05, and Polymer (III) was a gel.

References

1. (a) T. G. Bassiri, A. Levy, and M. Litt, *J. Polymer Sci. B*, **5,** 871 (1967). (b) A. Levy and M. Litt, *ibid.*, **5,** 881 (1967).

2. Belg. Pat. 666,828, 666, 829 (1965).

3. T. Kagiya, S. Narisawa, T. Maeda, and K. Fukui, *J. Polymer Sci. B*, **4,** 441 (1966).

4. Chem. Werke Huls, A.G., Fr. Pat.1,427,414 (1965).

5. A. Levy and M. Litt, *J. Polymer Sci. A-1*, **6,** 63 (1968).

6. J. Cason, *Org. Syn. Coll.*, **4,** 169 (1955).

7. C. Marvel, D. MacCorquodale, R. Kendall, and W. Lazier, *J. Am. Chem. Soc.*, **46,** 2838 (1924).

8. R. Anschitz and W. Bertram, *Ber.*, **36,** 467 (1903).

Radiation Grafting of Vinyl Monomers to Wool. III.   Location of the Grafted Polymer

P. INGRAM, J. L. WILLIAMS, and V. STANNETT,* *Camille Dreyfus Laboratory, Research Triangle Institute, Research Triangle Park, North Carolina,* and M. W. ANDREWS, *C.S.I.R.O. Wool Research Laboratories, Ryde, Sydney, Australia*

Synopsis

Studies of properties such as water sorption of grafted wool have shown the importance of the location of the polymer in the fiber.   Electron microscopy and low-angle x-ray diffraction studies have been used to determine the location of grafted polystyrene in wool.   Samples grafted from 15 to 800% (dry weight increase) all exhibit a large increase in contrast in the cell membranes (IR) and nuclear-remnant regions (NR) in the electron micrographs.   This is considered to be due in part to an unevenness in mechanical response to sectioning and in part to the deposition of ungrafted homopolymer in IR and NR, particularly at grafts of greater than about 100%.   Analysis of the change in the 83 A. equatorial x-ray reflection suggests that most of the grafted polymer resides in the keratinous matrix regions between the microfibrils within the cortical cells.   At larger grafts the wool still retains its basic histological character, but the increase in this spacing is no longer proportional to the amount of graft, and the deposition of polymer becomes very inhomogeneous.

INTRODUCTION

Earlier studies in this series have been concerned with the kinetics of the grafting reaction,[1,2] including the molecular weights of the grafted side chains.   In addition a study of the effect of the grafted polymer on the wool–water relationships has been undertaken.[3]   An important result of the latter study was that a similar amount of the same grafted polymer caused quite different effects on the water sorption[3,4] and in particular the drained-water content[3,4] of wool fabric.   It seemed obvious that the main difference between the samples was the actual location of the grafted polymer.   A study of methods of determining the location of the grafted polymer in the wool fiber was therefore undertaken.

It has been clear for some time that in the case of radiation grafting to fibers the polymer could be located at different depths in the fiber.   This was shown for example[5] in dyeing studies, in which polyester fibers could be made substantive to dyes in ring form, i.e. close to the surface or throughout the fiber, by changing the conditions.   In general, it would seem that the

grafting could be restricted to the surface areas of the fibers by various techniques including the following: very short contact time between the fiber and the monomer, very poor swelling conditions during grafting, and very high dose rates, to restrict the diffusion of monomer before the active centers terminated themselves. On the other hand, grafting at low dose rates and at high degrees of swelling should enable adequate diffusion of monomer and result in grafting throughout the fiber. The comments above apply to the so-called mutual grafting technique. The preirradiation method is more complex; in principle, the long reaction times should give plenty of time for the monomer to diffuse into the active centers. In the case of wool, however, ESR studies[6] have shown that with mixtures of a swelling agent, such as methanol, and monomer the swelling agent diffuses into the fiber before the bulkier monomer molecules. This causes some premature termination of the radicals; in spite of this, however, a substantial amount of grafting still takes place. One possible measure of the degree of penetration of the grafted polymer through the fiber would be the sorption isotherms. Superficial grafting should allow almost the same degree of swelling in, for example, water, whereas grafting throughout the fiber might be expected to reduce the swelling either by a bulking action or by the crosslinking action of hydrophobic regions. The water-vapor sorption isotherms of a number of wool samples grafted with a similar amount of polystyrene but under different conditions were determined. The results calculated on the weight of the wool content only are shown in Figure 1. All the grafted samples had reduced sorption values. It is interesting, however, that the two samples grafted under conditions thought to lead to a more superficial location of polymer, i.e. very high dose rates and a low degree of swelling, did indeed sorb more water than the preirradiation sample.

Studies of the location of grafted polymer in fibers are somewhat scarce. Dyeing studies have been used by Araki and his colleagues[5] with polyesters and by Stamm and his co-workers[7] with polypropylene fibers. The most complete work in the field has been reported by Arthur, Rollins, and their co-workers[8-12] with grafting to cotton and by Kaeppner and Huang[13] with rayon; excellent use was made of the electron microscope in these studies. In the case of wool itself ultraviolet microscopy was used by Horio and his co-workers[14] to locate grafted polystyrene. More recently Andrews and his co-workers[15,16] have used the electron microscope for locating polyacrylonitrile in wool fibers. In the present study electron microscopy and low-angle x-ray techniques have been used to study the location of grafted polystyrene in radiation-grafted wool fibers.

EXPERIMENTAL AND MATERIALS

The wool used for the electron microscope and x-ray studies was Beltsville Topping grade 56'S. The sample examined by M. W. Andrews was Corriedale wool. The sorption isotherm experiments were conducted on wool
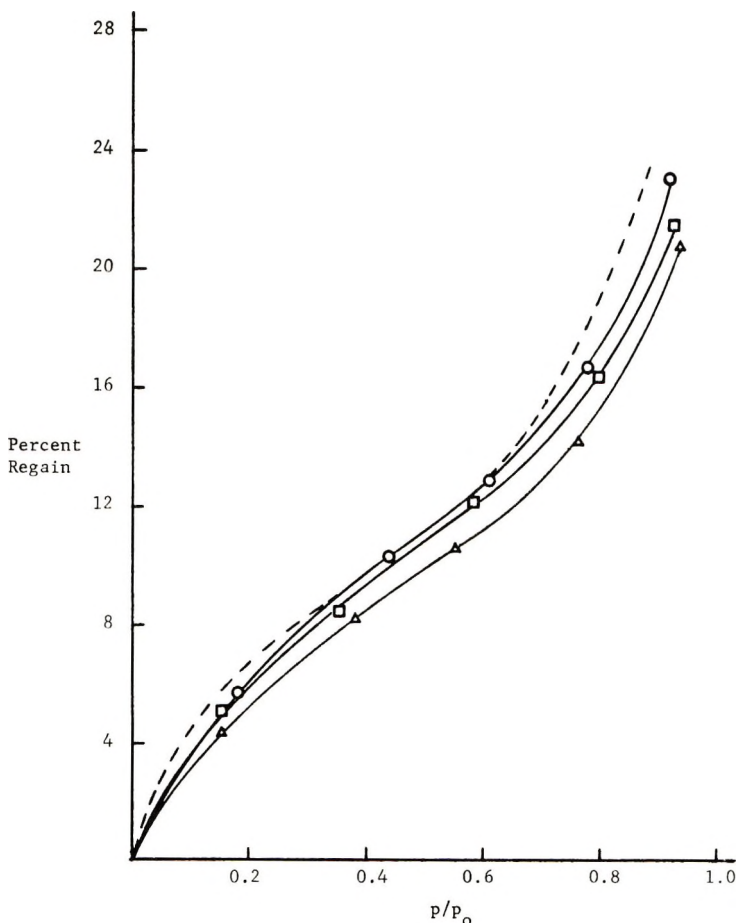
Fig. 1. Isotherms of sorption of water into polystyrene-grafted wools at 25°C.: (△) 19.4% graft, preirradiation, 18% MeOH, 4 Mrad at 0.1 Mrad/hr.; (□) 22.4% graft, mutual irradiation, 10% MeOH, 3 Mrad at 0.1 Mrad/hr.; (○) 15.4% graft, Van de Graaff, 18% MeOH, 5 Mrad. All isotherms calculated on the basis of wool only; dotted line is for untreated wool.

fabric. The grafting experiments were carried out by the methods described in the previous two papers.[1,2] The sorption isotherms shown in Figure 1 were measured with a quartz helix microbalance in the manner already described.[4]

Both native and polystyrene grafted wool samples were embedded in Epon 812 resin (Polysciences Inc., Rydal, Pa.) according to the method described by Luft.[17] After suitable cleansing and dehydration procedures short individual fibers were successively subjected to 30 min. immersions in gradually diminishing proportions of propylene oxide to embedding medium and finally were set to cure at 60°C. for 24 hr. in the Epon mixture, to which had been added a small amount of DMP 30 accelerator (Rohm and Haas, Inc., Philadelphia, Pa.). Transverse sections were then cut with a Porter-Blum

MT2 ultramicrotome (Sorvall, Inc., Norwalk, Conn.) operating at a speed of 3 mm./sec. Sections approximately 600 to 1000 A. thick (silver–gold range) were obtained by employing glass knives and subsequently picked up on 200-mesh copper grids. They were then viewed in a JELCO JEM6A electron microscope operating at 80 kv. accelerating voltage. Where appropriate, the sections could be shadowed with platinum by conventional methods.

Specimens were also examined with the use of wide- and low-angle x-ray diffraction from nickel-filtered Cu K_α radiation. About fifty fibers were aligned and mounted in front of a 0.015 in. collimator of a Statton[18] camera (manufactured by W. Wahrus, Wilmington, Del.), with which the entire range of diffraction could be obtained without moving the sample. This is partly made possible by operating under vacuum and eliminating air scattering. Thus, since all samples are run under identical (dry) conditions any errors due to moisture absorption are also eliminated. The positions of the reflections were either measured from flat plate photographs directly or with the aid of a microdensitometer; characteristic d spacings at all angles (2θ) were calculated from the Bragg equation

$$d = n\lambda/(2 \sin \theta)$$

In some experiments it was found desirable to stain the specimen. For such purposes the wool fibers were immersed in a 2% solution of osmium tetroxide[19] at pH 7.2 for various lengths of time, depending on the amount of graft, washed in distilled water for 24 hr., and dried in a vacuum oven at 30°C. Not surprisingly, the rate of diffusion of OsO_4 into the sample was reduced considerably, the higher were the amounts of polystyrene present. For example, native wool would appear to be completely stained after 24 hr., whereas a sample with 150% graft would take at least 1 wk. to attain the black color indicative of staining.

RESULTS AND DISCUSSION

Electron Microscopy

All the transverse sections of polystyrene grafted wool showed the common feature of marked increase in contrast in the cell membranes (IR) and nuclear-remnant regions (NR) over that of the untreated fibers. This fully confirms the results of Andrews and his co-workers.[15,16] Figure 2 shows untreated, unstained wool, and Figure 3 shows a section, of similar thickness, from an unstained sample containing 150% grafted polystyrene. It has also been shown quite convincingly[15] that this type of contrast effect need not be due solely to a density increase, as might be expected by comparison with stained, native, wool sections, but rather to an increase in thickness in these regions. Such an effect could be due to unequal recovery from deformation during sectioning of different components of the wool fiber (even untreated wool can show this phenomena[15]), but possibly enhanced by virtue of the deposition of polymer. Indeed, this has been shown

Fig. 2. Electron micrograph of cross section of unstained native wool ($\times 24{,}750$). The following nomenclature is used in this and subsequent micrographs: IR, intercellular regions, NR, nuclear remnants, CU, cuticle, CO, cortical cell, EM, embedding medium, H, homopolymer.

in the present investigations by shadowing the section with platinum–carbon immediately after cutting, and Figures 4 and 5 are representative micrographs of samples grafted 150 and about 800% (Corriedale wool), respectively, which have been treated in this way. Clear protrusions are seen on IR and NR (also in agreement with Andrews,[15] this was shown not to be an effect of electron bombardment). However, very little definitive information about the location of the polymer can be obtained from these results alone.

Thus, although any polystyrene homopolymer had been extracted with benzene prior to sectioning until the samples maintained constant weight, it was decided that the sections themselves should be re-extracted on the electron microscope grids. Not surprisingly, very little, if any, change in contrast was apparent (Fig. 6), compared to Figure 3, for the 150% grafted sample; however, when this same specimen (re-extracted) was then shadowed (Fig. 7) a clear, discontinuous appearance became evident along the cell membrane regions, and large portions of some nuclear remnants became removed. This indicates that a certain amount of homopolymer remained in these regions. It is even more strikingly demonstrated on

samples with nominally larger amounts of graft; for example, on the 800%
graft fibers many regions of more exaggerated appearance than the normal
histological appearance of wool can be seen (e.g., large protrusions in Figures
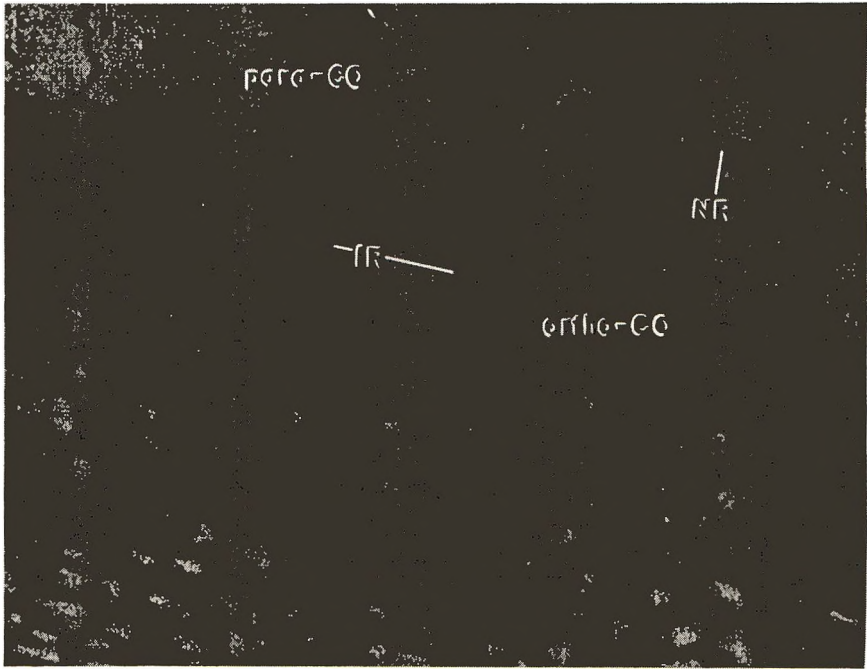

Fig. 3. Electron micrograph of cross section of unstained wool grafted 55% (×26,000).

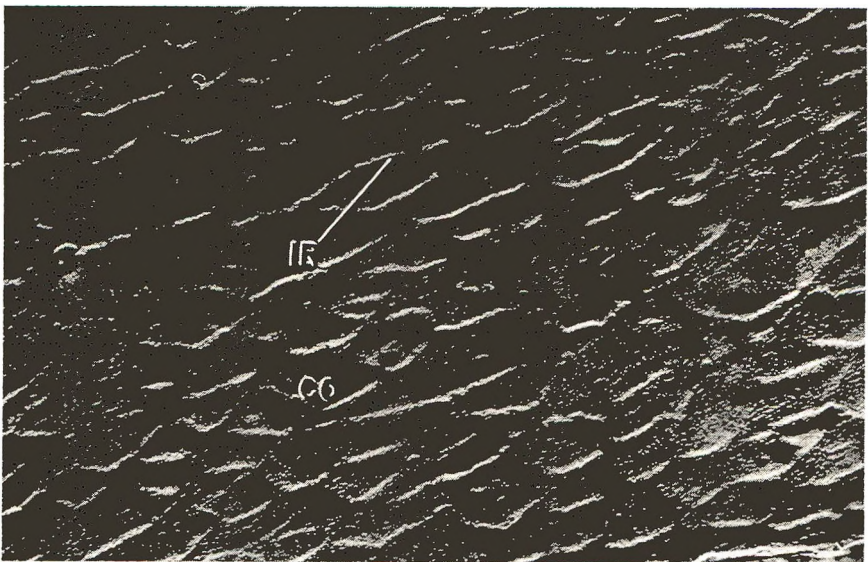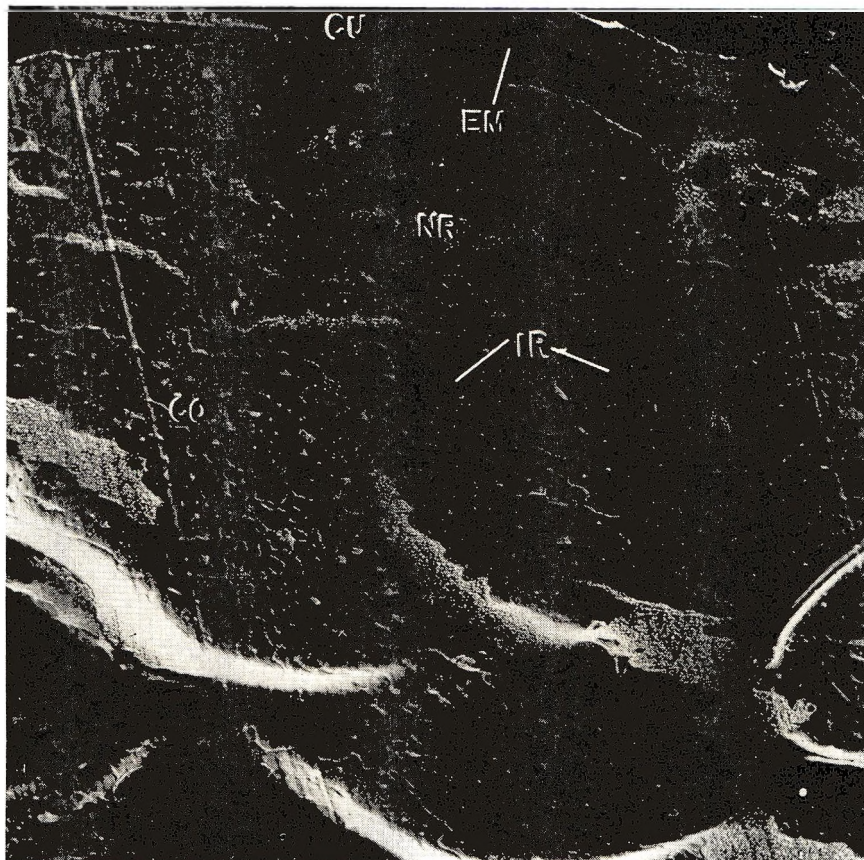Fig. 4. Electron micrograph of cross section of unstained wool grafted 150%, shadowed
with platinum–carbon at tan⁻¹ 0.8 (×16,000).

(a)

Fig. 5.   See caption p. 1903.

5a and 5b).   Furthermore, in these samples many void-like regions (Fig. 5c)
can be found, where homopolymer was either removed by the initial extrac-
tion with benzene or pulled out by the sectioning process.   The former ex-
planation seems the more likely, since there is little evidence of tearing,
rather smooth-edged holes having been formed in these cases; Figure 8 is a
further example of this.   There is also no *a priori* reason why the benzene
should not penetrate the fibers that are swollen considerably by the presence
of polystyrene.   In this connection it is pertinent to note that, although at
lower graftings the fibers were swollen in direct proportion to the amount of
graft (as determined by weighing), there was an increasingly large variation
in diameters at larger proportions of polymer content.   However, even in
cases in which extremely high graftings are obtained (for example, by using
98 to 100% formic acid as a swelling agent rather than methanol), the
sample still retains its basic wool-like histological character, but with con-
siderable unevenness of polymer deposition.   Figure 9 is a sample grafted
about 2800% in a 20% formic acid–styrene system (total dose 3.3 Mrad,
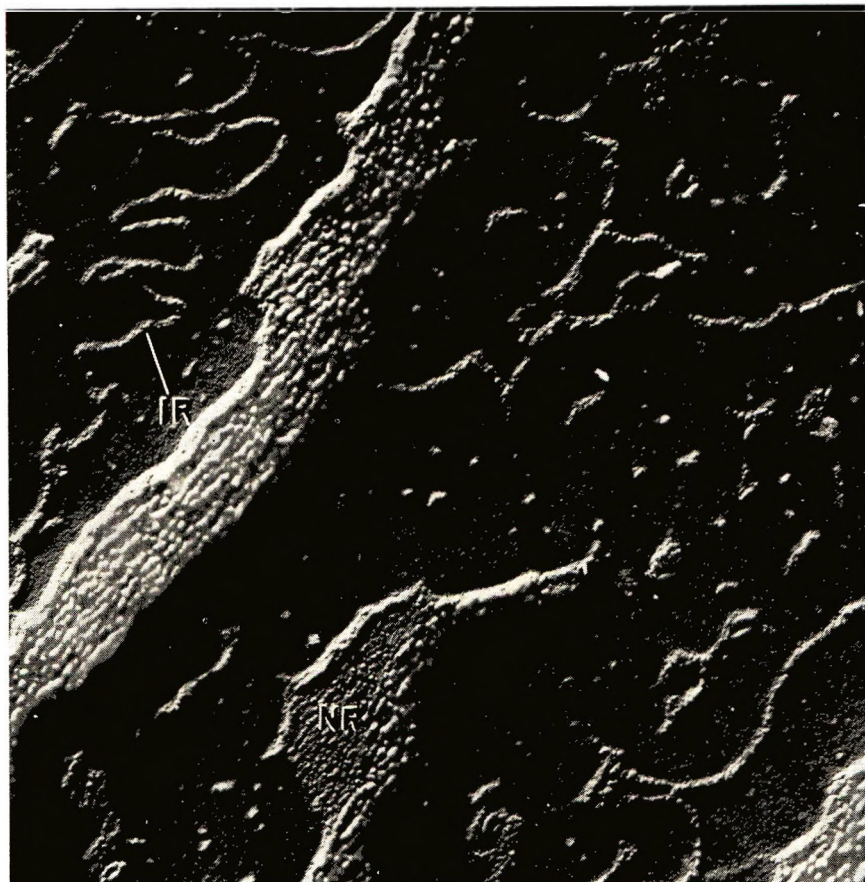
(b)

Fig. 5.   See caption p. 1903.

dose rate 0.05 Mrad/hr.; cf. Stannett et al.[1] for methanol dioxane–styrene systems). In this case island regions of polymer still remain (see Fig. 5), and also large holes where it has been removed (see Fig. 8). There was an even larger variation in diameters of individual fibers in this sample than in those grafted 800%. One can therefore infer that even within the same sample there is a considerable variation in percentage of polymer content from fiber to fiber, particularly at higher graftings.

One further experiment was performed on the sections themselves to try to determine whether there was any difference in behavior between the nuclear remnants and cell membranes and the fibrous material in the cells. Alkaline hydrolysis should digest away ungrafted portions of the wool and leave truly chemically grafted portions free for examination.[1] After 3 hr. of treatment in 5% sodium hypochlorite solution some digestion is evident (Fig. 10). However, although the cell membranes appeared to remain relatively intact (approximately the same contrast as untreated sections), no
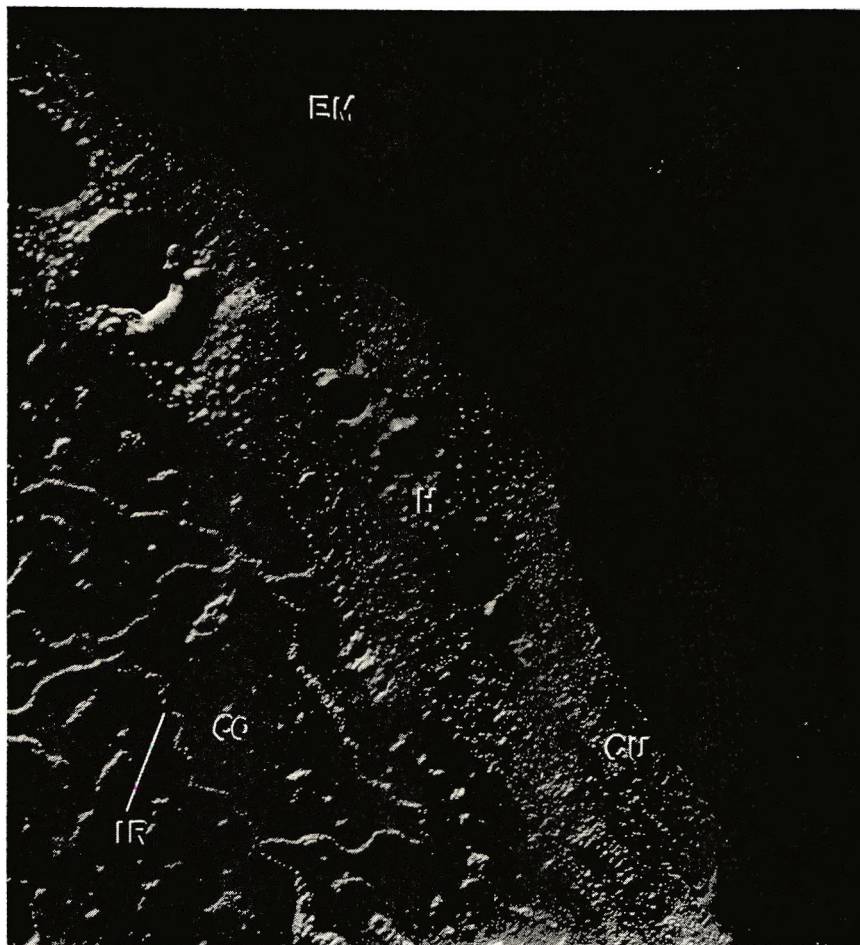
(c)

Fig. 5. Electron micrographs of wool grafted 800%, shadowed with platinum–carbon at $\tan^{-1} 0.2$: (a) $\times 7500$; (b) $\times 25,000$; (c) $\times 15,000$.

outstanding distinctions could be made between the various components, since the digestion was rather uneven.

X-Ray Measurements

Low-Angle Spacings. The staining of wool with osmium tetroxide considerably enhances the low-angle equatorial x-ray reflections.[19]   These are generally considered to arise from the packing of microfibrils and matrix in the cortical cells[20] and result in spacings of 83 A. and higher orders thereof.   If the polymeric material is associated with these regions to any significant extent, as is inferred from the electron microscopy studies, it should be seen as a change in the 83 A. reflection.   This was indeed found to be the case (Fig. 11), the spacing increasing one half as much again
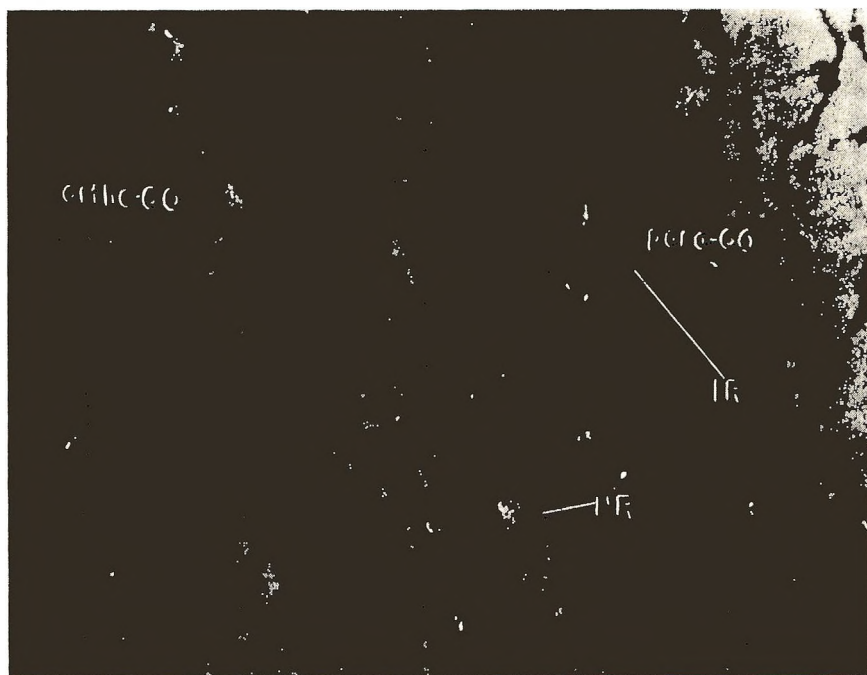
Fig. 6. Same as Figure 3, extracted with benzene on microscope grid for 24 hr. ($\times$26,000).

Fig. 7. Same as Figure 6, shadowed with platinum–carbon at $\tan^{-1}$ 0.8 ($\times$23,000).
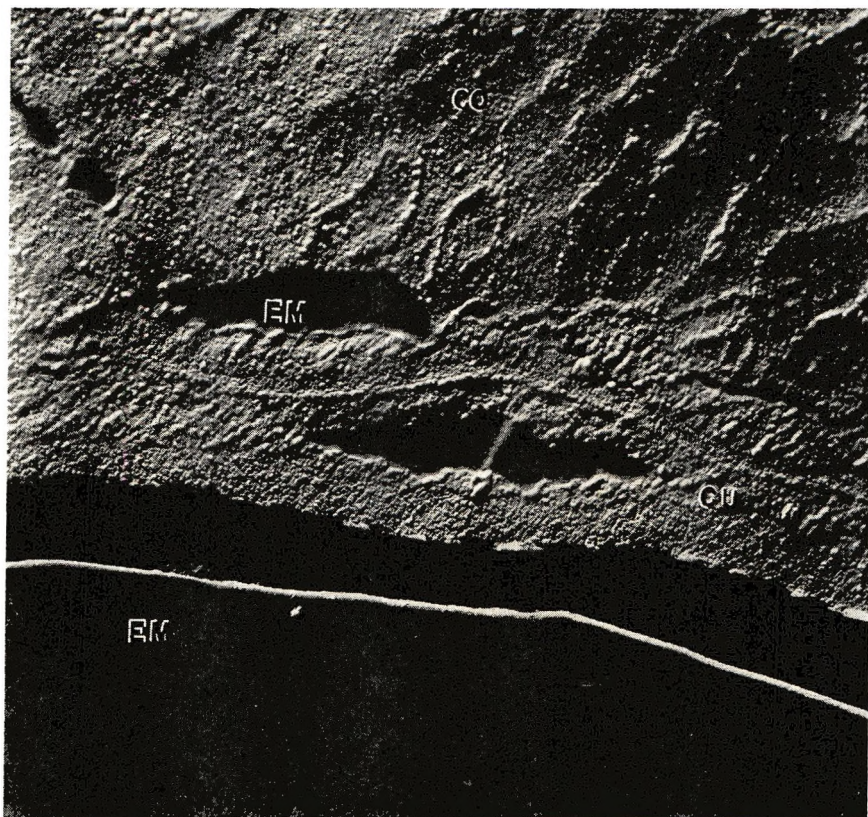
(a)

Fig. 8. See caption p. 1906.

with 150% weight increase in polymer. Figure 12 shows the measured dry weight increase versus the apparent weight increase (ΔW) due to the grafted polystyrene, calculated from the change in equatorial spacings by the formula

$$\Delta W = [(d/d_0)^2 - 1]\rho_s \times 100$$

where d_0 and d are the equatorial spacings of ungrafted and grafted specimens, respectively, and ρ_s is the density of polystyrene.[21]   The longitudinal swelling is negligible compared to the diametral swelling,[22] assuming that the disulfide bonds remain intact.[23]   There is every reason to suppose this is correct, particularly at the moderate diametral increases found here (about 50% at 150% graft[23]).   It can be seen that at least up to about 100% (by weight) graftings, the accommodation of the polystyrene is satisfactorily accounted for as residing in the matrix region between microfibrils.   In order to ascertain that the observed change in the 83 A. spacing was not in fact due to some radiation effect on the wool itself, the grafting process was simulated by using α-methylstyrene in place of the styrene monomer. Under identical conditions the α-methylstyrene will not polymerize, whereas
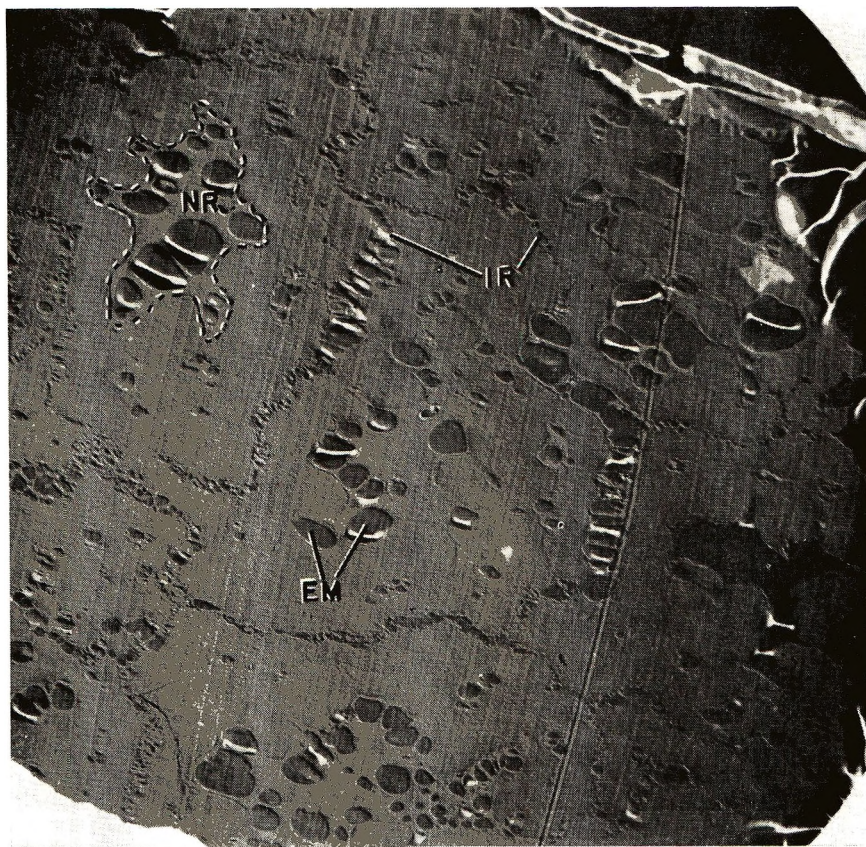
(b)

Fig. 8. Electron micrographs of wool grafted 800%, showing holes due to extraction of homopolymers, shadowed at $\tan^{-1} 0.2$: (a) small fiber, $\times 25,000$; (b) medium fiber, $\times 6000$.

the styrene will.[24]   Thus the essential parameters, such as swelling, size of monomer, and radiation dose, can be exactly duplicated and any changes due solely to the wool structure determined.   When the conditions were duplicated for approximately a 55% graft of polystyrene (35% methanol, 23% styrene, and 42% dioxane solution, 0.98 Mrad dose), there was negligible increase in weight and no change in the small-angle x-ray pattern arising from native wool.   Such a sample, therefore, serves as an excellent "control" in all work of this kind.

Wide-Angle Spacings.   Wide-angle x-ray diffraction patterns were obtained from all samples on which small-angle measurements were made. Only the prominent 9.8 A. equatorial and 5.1 A. meridional reflections characteristic of α-keratin[20] were considered in this investigation.   Figure 13 shows the changes found for various grafting experiments, including the additional "control" with α-methylstyrene.   It can be seen that there is a gradual smearing out of the two reflections with increasing amounts of

Fig. 9. Electron micrograph of wool grafted about 2800%, shadowed at $\tan^{-1}$ 0.8 ($\times 18,000$).

graft, until they are completely superimposed by halos suggesting amorphous material.   It is reasonable to assume that this simply reflects the presence of polystyrene in the fibers,[25] in spite of the slight differences (less than 1° in 2θ), occasionally observed, from atactic polystyrene (Fig. 14a). These discrepancies in the positions of the broad maxima can almost certainly be ascribed to incorrect estimates of background intensity in the films and possibly to difficulties in mounting the fibers from every sample in exactly the same position with respect to film.   However, in order to check that there were indeed no differences due to the mode of polymerization of pure homopolymer or conformation of the chemically grafted polystyrene, diffraction patterns were taken from soluble polystyrene extracted with benzene[1] (Fig. 14b) and insoluble grafted polymer (Fig. 14c) remaining after digestion[1] of ungrafted portions of wool.   No significant differences could be found between the reflections from the various polystyrenes.

CONCLUSIONS

Over the wide range of samples investigated with nominal grafts of polystyrene by weight up to 2800% the location of the polymer was found to be associated with both the matrix regions between microfibrils and the nonfibrillar regions (e.g., nuclear remnants and cell membranes).
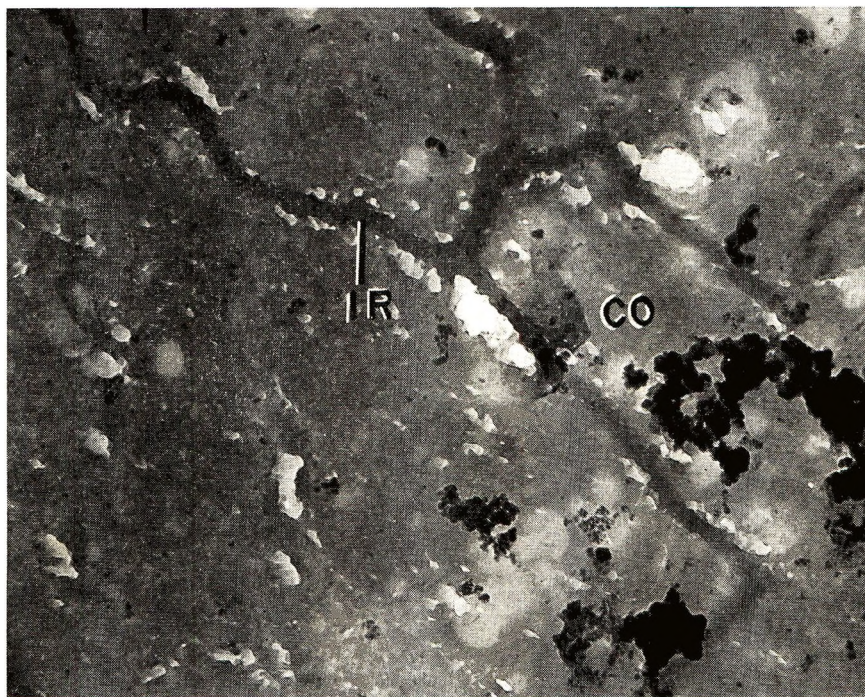
Fig. 10. Electron micrograph of wool grafted about 96%, after benzene extraction on microscope grid for 24 hr. and immersion in 5% sodium hypochlorite solution for 3 hr. (×30,000).
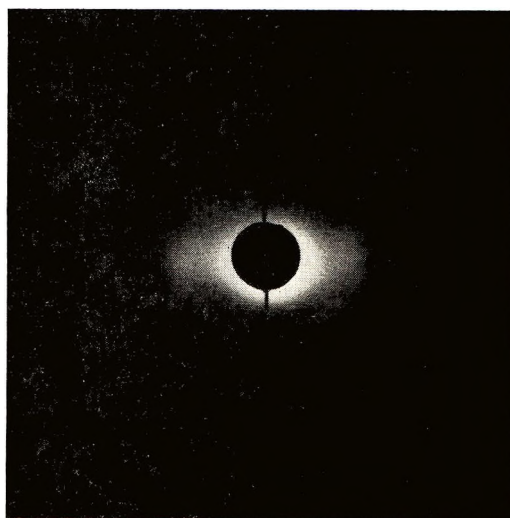
Fig. 11. Typical low-angle x-ray diffraction from polystyrene-grafted wool; sample grafted 150%. All samples in this and Figures 12 and 13 were stained with 2% OsO_4 solution.
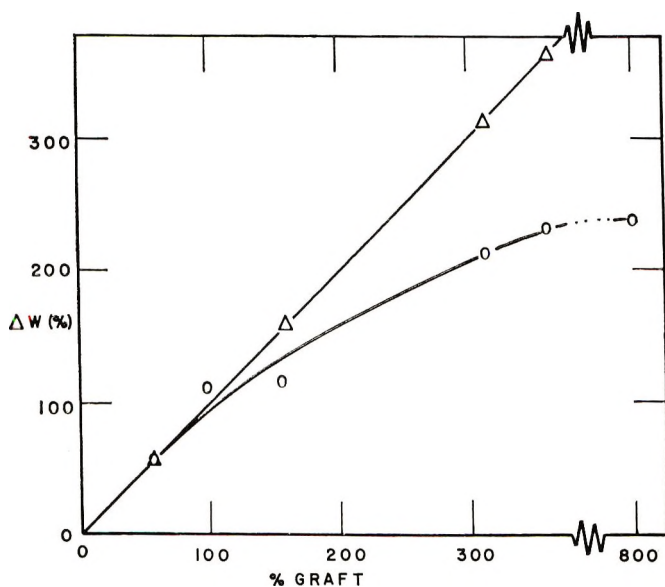
Fig. 12. Apparent weight increase (ΔW) as a function of weight percent graft: (O) calculated from change in low-angle x-ray spacings; ($\triangle$) calculated from change in diameter of fiber.
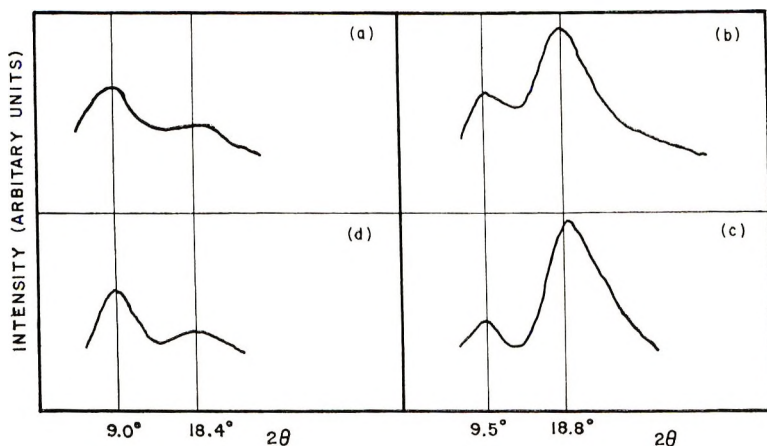
Fig. 13. Wide-angle x-ray diffraction from wool; (a) untreated; (b) with 150% polystyrene graft; (c) with 360% polystyrene graft; (d) treated with α-methylstyrene and irradiated to a dose of 0.98 Mrad. (Equatorial scans).

At low and moderate amounts of graft (<100%) the deposition of polymer was rather uniform throughout the fibers, most of the uptake being accounted for by the change in the 83 A. equatorial x-ray reflection (Fig. 12). Similar changes have been noted by Palmer[25] during the polymerization of propiolactone in wool.   This conclusion seems very reasonable in view of the affinity of the noncrystalline regions of swollen wool fibers for water and various heavy metals,[19] determined by analysis of this reflection.   Further-
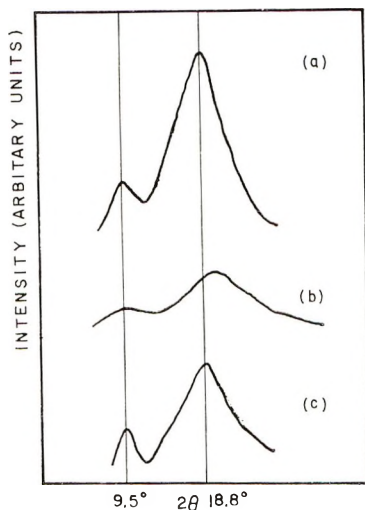
Fig. 14. Wide-angle x-ray diffraction: (a) atactic polystyrene; (b) polystyrene homopolymer extracted from wool grafted 84%; (c) grafted polystyrene remaining after digestion of ungrafted wool[6] from a sample grafted 67%.

more, electron spin resonance studies[2] show a large modification of the radical spectrum from wool during the growth of the graft. At least one of the radicals in irradiated native wool can be identified as a cystine radical due to rupture of the disulfide bonds,[26,27] and the new spectrum can also be identified as containing polystyryl radicals—again very good evidence of growth of the polymer in the "keratinous" region, since this must be the origin of most of the observed radicals. The increase in contrast of the intercellular regions in the electron micrographs, particularly at low grafts, can very likely be accounted for by the thickness effect[16] due to nonuniform mechanical response of the different fiber components[15] and a rather low amount of chemical grafting and growth of homopolymer, possibly as a result of existing voids or distortion during treatment.

At higher graftings it was possible to remove increasingly large amounts of homopolymer by extraction. The deposition of polymer was correspondingly more uneven, and wide variations in diameters from fiber to fiber were found. However, the histological appearance of the fibers remained essentially the same even at the highest graftings. This implied that the fibrous regions remained intact in spite of the increased overall uptake of polymer. The continued appearance of a strong equatorial reflection, as noted in Figure 11, supports this, and the deviation from the ideal curve in Figure 12 reflects the increasing content of homopolymer at higher grafts.

As regards the wide-angle x-ray studies, similar results were briefly reported by Palmer[25] on the uptake of propiolactone by wool by chemical grafting techniques. At graftings of less than 60% superposition of diffraction rings from polypropiolactone on the wool were observed, but at greater uptakes this polymer was said to enter the crystalline regions of the wool.

Further investigation of this effect is clearly necessary, especially concerning the influence on spacings at smaller angles ($10° > 2\theta > 5°$).

It may be remarked that one limitation of this study is that the electron microscopy has been restricted to relatively low resolutions. Techniques have now been improved such that magnifications in excess of $250,000\times$ are more readily attainable, and therefore efforts are currently being made to examine the influence of polymer growth on the separation of individually resolvable microfibrils.

In conclusion it should be emphasized that the ultimate goal of this study is to be able to correlate the actual location of the grafted polymer with the method and conditions of grafting and with the mechanical and other properties of the fibers grafted with a given polymer. It is hoped that the continuation of this research will help achieve these objectives.

References

1. V. Stannett, K. Araki, J. A. Gervasi, and S. W. McLeskey, *J. Polymer Sci. A*, **3**, 3763 (1965).

2. D. Campbell, J. L. Williams, and V. Stannett, *Advan. Chem. Ser.*, **66**, 221 (1967).

3. V. Stannett, *Am. Dyestuff Reporter*, **54**, 372 (1965).

4. J. L. Williams, V. Stannett, and A. A. Armstrong, *J. Appl. Polymer Sci.*, **10**, 1229 (1966).

5. K. Araki and co-workers, unpublished work.

6. D. Campbell, P. Ingram, J. L. Williams, and V. Stannett, *J. Polymer Sci. B*, in press.

7. R. F. Stamm, E. F. Hosterman, C. D. Felton, and C. S. H. Chen, *J. Appl. Polymer Sci.*, **7**, 753 (1963).

8. J. C. Arthur and R. J. Demint, *Textile Res. J.*, **30**, 505 (1960).

9. R. J. Demint, J. C. Arthur, A. R. Markezich, and W. F. McSherry, *Textile Res. J.*, **32**, 918 (1962).

10. F. A. Blouin and J. C. Arthur, *Textile Res. J.*, **33**, 727 (1963).

11. M. L. Rollins, A. T. Moore, W. R. Goynes, J. H. Carra, and I. V. de Gruy, *Am. Dyestuff Reporter*, **54**, 512 (1965).

12. F. A. Blouin, N. J. Morris, and J. C. Arthur, *Textile Res. J.*, **36**, 309 (1966).

13. W. M. Kaeppner and R. Y. M. Huang, *Textile Res. J.*, **35**, 504 (1965).

14. M. Herio, K. Ogami, T. Kordo, and K. Sekimoto, *Bull. Inst. Chem. Res. Kyoto Univ.*, **41**, 10 (1963).

15. M. W. Andrews, *J. Roy. Microscop. Soc.*, **84**, 439 (1965).

16. M. W. Andrews, R. L. D'Arcy, and I. C. Watt, *J. Polymer Sci. B*, **3**, 441 (1965).

17. J. H. Luft, *J. Biophys. Biochem. Cytol.*, **9**, 409 (1961).

18. W. O. Statton, *J. Polymer Sci.*, **58**, 205 (1962).

19. R. D. B. Fraser and T. P. MacRae, *Nature*, **179**, 732 (1958).

20. H. P. Lundgren and W. H. Ward, in *Ultrastructure of Protein Fibers*, Academic Press, New York, 1963.

21. J. Brandrup and E. H. Immergut, Eds., *Polymer Handbook*, Interscience, New York, 1966.

22. P. Alexander and R. F. Hudson, *Wool. Its Chemistry and Physics*, Reinhold, New York, 1954.

23. M. Feughelman and B. M. Chapman, *Textile Res. J.*, **36,** 1110 (1966).

24. J. D. Wellons and V. Stannett, *J. Polymer Sci. A*, **3,** 847 (1965).

25. K. Palmer, quoted by H. P. Lundgren, *Proc. Intern. Wool Textile Res. Conf., Australia C-374* (1955).

26. J. J. Windle, *Tech. Wool Conf. USDA*, San Francisco, May 1964, p. 74.

27. P. Kenny and C. M. Nicholls, *Proc. Intern. Wool Conf. Paris*, July 1965.

Interaction of Simple Acids with Nylon.
Part 2:   Diffusion of Simple Acids

J. MARSHALL, *Wool Industries Research Association, "Torridon," Headingley, Leeds, England*

Synopsis

The paper deals with the diffusion of two mineral acids, hydrobromic and sulfuric acids, and two simple dye acids, NOG (C.I. Acid Orange 7) and SY (C.I. Food Yellow 3), in water-swollen nylon 66. Anion self-diffusion coefficients were obtained by radiotracer techniques. The bromide ion and the SY anion self-diffusion coefficients show very little variation with concentration in the amino-dyeing region, whereas the H_2SO_4 and NOG anion diffusion coefficients are concentration-dependent. The variation of the H_2SO_4 anion diffusion coefficient with concentration is consistent with the formation of small quantities of the highly mobile bisulfate ion. The low SO_4 diffusion coefficient may be explained by the interaction of this ion with single, fixed sites in the polymer. The variation of the NOG anion diffusion coefficient with concentration does not follow a simple $D = D_0[1/(1 - \theta)]$ relationship at intermediate concentrations but the rapid increase observed as the available sites became saturated, i.e., as $\theta \to 1$, is consistent with a site saturation model.

INTRODUCTION

Apart from the work of Hayashi,[1] McGregor et al.,[2] and Brody[3] no systematic investigation has been made of the diffusion characteristics of acids in nylons. Their results indicated that diffusion coefficients of anions in nylon increased rapidly with increasing internal concentration. In the case of Naphthalene Scarlet 4R McGregor et al.[2] attributed this behavior to a proportionality between the diffusion coefficient and some power of the activity coefficient of the anion. Brody[3] has since confirmed this work.

In contrast to nylon, the diffusion of acids in keratin has been quite extensively investigated.[4–6] Since keratin contains ionizable groups similar to those in nylon, one would anticipate close resemblances in diffusion behavior in the two substrates. The results presented here indicate that many ideas developed in the work on keratin can be applied to diffusion in nylon.

It is generally accepted that acids are sorbed onto nylons in two distinct stages: first onto the limited number of amino sites present (amine-dyeing region) and then at low pH onto the amide groups (amide-dyeing or overdyeing region). The two processes should give rise to two different

diffusion mechanisms. The present work deals with diffusion in the amino region.

It is assumed the nylon exists in the zwitterion form and that the absorption of acids is equivalent to the back-titration of the carboxyl groups present in the polymer. On this model the mobility of the hydrogen ion may be explained by the well-known "free-bound" mechanism, as it was for diffusion in keratin, and this gives rise to a rapidly increasing mobility of the hydrogen ion as the sites become saturated.

This paper deals with the diffusion of the two inorganic acids monobasic HBr and dibasic H_2SO_4 and the two simple dye acids monobasic Naphthalene Orange G (C.I. Acid Orange 7), and dibasic Sunset Yellow (C.I. Food Yellow 3) in nylon 66. The anion self-diffusion coefficients were determined directly by radiotracer methods. The chemical diffusion coefficients, which refer to the movement of the acid as a whole, were measured for HBr and H_2SO_4 by desorption techniques. The hydrogen ion mobilities were obtained indirectly from the measured anion self-diffusion coefficients and chemical diffusion coefficients by application of the Nernst-Hartley formula. The full Nernst-Hartley equation must be used, since it is found that one or both of the individual ionic mobilities are concentration-dependent and, hence, the chemical diffusion coefficient will not be equal to the harmonic mean of the individual ionic self-diffusion coefficients.

EXPERIMENTAL

The nylon 66 was in staple fiber form and of average diameter 20 μ. The fibers were extracted with ether and alcohol and subjected to prolonged washings in distilled water. They were conditioned at 20°C. and 65% R.H. The amino endgroup content, 0.028 meq./g., was determined by dissolving the nylon in 70:30% phenol–methanol solution and titrating with 0.05N HCl solution with Thymol Blue as indicator.

Preparation of Dyes Containing [35]S

Naphthalene Orange G. The radioactive dye was synthesized from sulfuric acid containing [35]S (half-life, 87 days). The sulfuric acid was converted to sulfanilic, which was purified by recrystallizing from hot water. Diazotized sulfanilic acid was then coupled to β-naphthol. Any residual sulfanilic acid remaining was removed by salting out with NaCl from a slightly alkaline solution in which the dye itself is very soluble. The solution was then acidified and the dye salted out.

Sunset Yellow. Diazotized sulfanilic acid was coupled with purified Schaffer acid, any residual sulfanilic acid again being salted out with NaCl. It is impossible to salt out this dibasic dye, so the solution was converted to the free acids by means of an ion exchange resin, and the solution was boiled and evaporated down, to remove hydrochloric acid. The dyes were standardized by potentiometric and spectrophotometric methods.

Desorption Experiments

The self-diffusion coefficients and chemical diffusion coefficients were measured by the following technique.

For the self-diffusion coefficient determinations a nylon sample was equilibrated with a radioactive solution of known concentration. It was then transferred to an inactive solution of the same concentration, which was changed at suitable intervals, to prevent any significant back-diffusion. The same method was used for the four different acids. A suitable desorption apparatus is shown in Figure 1. The bromide ion concentrations were determined with a liquid counter, but solutions containing ^{35}S, which is a weak beta emitter, were neutralized, evaporated down, and then counted. The diffusion coefficient was obtained from the formula given by Crank:[7]

$$D = 0.0625a^2/t_{1/2}$$

where a is the radius of the fiber and $t_{1/2}$ is the time required for half the active material to be desorbed.
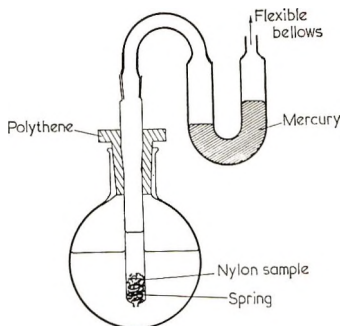
Fig. 1. Apparatus for dye sorption and desorption experiments.

The chemical diffusion coefficients were measured in a similar way. Samples were equilibrated in solutions at one concentration and then desorbed into solutions of half this concentration. By incorporating electrodes in the system the increase in external concentration was followed by conductivity measurements. The volume of the external solution was chosen so that the increase in concentration did not exceed 10%, preventing any appreciable back-diffusion.

RESULTS AND DISCUSSION

The titration curves for HBr, H_2SO_4, Naphthalene Orange, and Sunset Yellow in nylon 66 are shown in Figure 2 and indicate a tendency to approach a maximum at about 0.026 meq./g.

The variation of the individual ionic mobilities of hydrobromic acid with concentration are shown in Figure 3. The hydrogen ion mobility was calculated from the Nernst-Hartley equation:

$$D(c) = (RT/F^2) \left[\Lambda_H \Lambda_{anion}/(\Lambda_H + \Lambda_{anion}) \right]$$

$$\left[1 + (d \ln \gamma_\pm)/(d \ln c) \right] \left[(z_H + z_{anion})/z_H z_{anion} \right] \quad (1)$$

where Λ_H and Λ_{anion} are the ionic equivalent conductances, $\gamma_\pm$ the mean ionic activity coefficient, c is the internal concentration of acid in the substrate, z_H and z_{anion} are the ionic valences, and $D(c)$ is the chemical diffusion coefficient.

If Langmuir-type absorption is assumed, this may be written, for univalent ions,[6]

$$D(c) = (2\ RT/F^2) \left[\Lambda_H\ \Lambda_{anion}/(\Lambda_H + \Lambda_{anion}) \right] (2.3c/S) \quad (2)$$

where S is the slope of the experimental titration curve at a given c.

In the amine-dyeing region the bromide ion diffusion coefficient remains constant ($D_{Br} = 6 \times 10^{-11}$ cm.^{2} sec.$^{-1}$), but an increased mobility is observed in the amide region ($D_{Br} = 1 \times 10^{-10}$ cm.^{2} sec.$^{-1}$; internal concentration, 32.7×10^{-3} meq./g.). Hayashi[1] has obtained an even

Fig. 2. Variation of internal concentration with external pH.

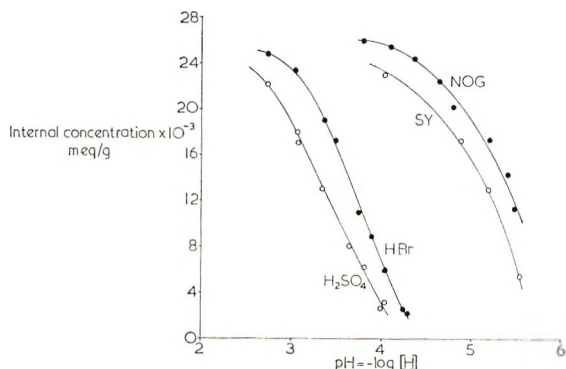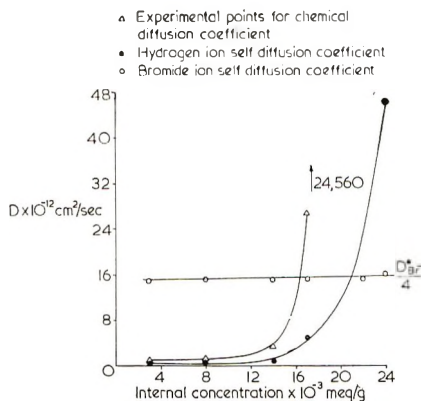Fig. 3. Diffusion coefficients of hydrobromic acid at 25°C.: ($\triangle$) experimental points for chemical diffusion coefficients; ($\bullet$) hydrogen ion self-diffusion coefficient; ($\bigcirc$) bromide ion self-diffusion coefficient.

higher value for the chloride ion than this (6.46×10^{-9} cm.^{2} sec.$^{-1}$ at an external pH of 1), but he does not state which type of nylon was used. It may have been nylon 6, in which diffusion is generally very much faster than in nylon 66.

From the experimental curve of the bromide diffusion coefficient versus concentration it is clear that there is no site saturation effect similar to that observed with the hydrogen ion or the Naphthalene Orange anion, but an enhanced bromide ion mobility is observed in the overdyeing region.

One possible explanation of this is as follows. In order to diffuse, the bromide ion has to jump from one site to another, so that in the amine-dyeing region in nylon 66, where the fixed sites are far apart and the region between the sites is of low dielectric constant, this will involve taking the ion through regions of high potential. This jump will be unfavorable, so that a low mobility will be obtained. In the amide region, where the number of sites increases with the amount of acid sorbed, the effective distance between sites decreases, so that the energy involved in a jump decreases. This will lead to an increased mobility, the mobility increasing with the number of sites.

A similar type of argument may also account for the lower mobility in nylon 66 than in keratin. Keratin contains approximately thirty times more sites, and the region between the sites is more polar, so that a jump from one site to another is more favorable, leading to a higher diffusion coefficient. The ratio of D_{Br} versus [nylon] to D_{Br} versus [keratin], or (6×10^{-11}) : (2×10^{-8}), is very much less than that obtained for uncharged molecules. Uncharged molecules, such as methanol ($D = 1 \times 10^{-7}$ cm.^{2} sec.$^{-1}$), ethanol ($D = 6 \times 10^{-8}$ cm.^{2} sec.$^{-1}$), and benzeneazophenol ($D = 2 \times 10^{-11}$ cm.^{2} sec.$^{-1}$), diffuse at about the same rate in both substrates.[8] This indicates that electrostatic effects are more important in nylon than keratin.

The hydrogen ion diffusion coefficient in contrast to the D_{Br} increases about one hundredfold over the concentration range investigated, from 3×10^{-13} cm^2. sec.$^{-1}$ at low internal concentrations to 46×10^{-12} cm.^{2} sec.$^{-1}$ at 24×10^{-3} meq./g. internal concentration.

In systems such as this, where an equilibrium exists between freely diffusible and bound immobile ions, an estimate of the "free" hydrogen diffusion coefficient may be obtained as follows:

$$Y = K_H z/(B - z) \tag{3}$$

where Y is the concentration of free H$^+$ in the polymer, K_H is the dissociation constant of the carboxyl group, B is the amino endgroup concentration, z is the concentration of bound hydrogen; the total acid sorbed is $A = z + Y$.

Now, if K_H is small, then z is much greater than y, and z approximately equals A, and the following expressions can be obtained:

$$D_F = D_T(A/Y) = (B - z)D_T/K_H \tag{4}$$
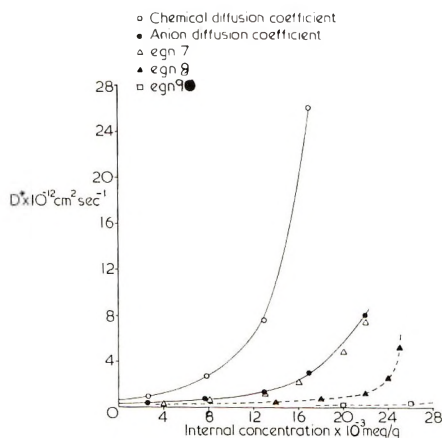
Fig. 4. Diffusion coefficients of sulfuric acid at 25°C.: (O) chemical diffusion coefficients; (●) anion diffusion coefficient; (△) eq. (7); (▲) eq. (8); (□) eq. (9).

where D_F is the "free" hydrogen diffusion coefficient, and D_T is the minimum hydrogen diffusion coefficient.

Now, with $D_T = 6 \times 10^{-13}$ cm.² sec.$^{-1}$, with $B = 26 \times 10^{-3}$ meq./g., and with $K_H = 5 \times 10^{-7}$ (calculated from HCl in the presence of NaCl) a value of $D_F = 3 \times 10^{-8}$ cm.²/sec.$^{-1}$ is obtained. The corresponding value in keratin is 2×10^{-6} cm.² sec.$^{-1}$. The assumption underlying $K_H = 5 \times 10^{-7}$ is that the "free" hydrogen ions are in a state similar to those in ordinary aqueous solutions. The mobility of the free hydrogen ion ($D_F = 3 \times 10^{-8}$ cm.² sec.$^{-1}$) is far greater than that of the bromide ion ($D_{Br} = 6 \times 10^{-11}$ cm.² sec.$^{-1}$), most of which may be considered "free." This indicates that some special mechanism of diffusion must be operating for the hydrogen ion in the polymer as compared with that of the other ions.

The extremely high hydrogen ion mobility in aqueous solution arises from the proton transfer mechanism, and a similar effect will probably also occur inside the polymer. The absolute values of the hydrogen mobilities are lower than in aqueous solution (nylon, 4000 times; keratin, 40 times) but this is to be expected, since the water even at saturation regain is in a highly dispersed state, that is, the efficiency of the protein transfer mechanism is lowered.

The Nernst-Hartley equation predicts that when one ion has a much lower mobility than the other one, the chemical diffusion is equal to twice the chemical diffusion coefficient of the slowest ion. This is observed with HBr.

The results for sulfuric acid are shown in Figure 4. With this acid both the anion and chemical diffusion coefficients are concentration-dependent. Since the chemical and anion diffusion coefficients are of similar orders of magnitude, it was impossible to calculate from the Nernst-Hartley equation the hydrogen ion mobility at low internal concentrations. Values of the

hydrogen ion mobility were obtained at higher internal concentrations, and these were found to be of the same order as those obtained with HBr.

There are two possible explanations of the increase in anion mobility with increasing concentration: either, as in the case of keratin,[5] the mobility is due to the formation of the highly mobile bisulfate ion, or the results are attributable to the saturation of the total number of positive sites available to the anion. As will be shown, it seems probable that in nylon the increase in anion mobility is due to the formation of the bisulphite ion.

Formation of Bisulfate. In this model the anion diffusion depends upon the formation of the bisulfate ion, which is considered to possess a much greater mobility than that of the sulfate ion. The equilibrium between the species may be written

$$h(A/2 - Y) = K_S Y \qquad (5)$$

$$h(B - X) = K_H X \qquad (6)$$

where h is the "free" hydrogen concentration, B is the amino endgroup concentration, A is the total acid sorbed, Y is the concentration of bisulfate ion, and X is the bound hydrogen concentration.

Following Medley,[5] an expression of the form

$$D_M = (A/Y)D_{HSO_4} = {}^1/_2 (K_H/K_S)[(x/B - X)]D_{HSO_4} \qquad (7)$$

is obtained, where D_M is the measured anion mobility.

In this treatment it is assumed that the ratio K_H/K_S has the same value as in aqueous solution, even though the individual values inside the polymer may be altered.

Site Saturation. In this model it is assumed that the activity of the bound ions is given by the term[9] $\theta/(1 - \theta)$, where θ is the fraction of occupied sites. An expression of the form

$$D = D_0[1/(1 - \theta)] \qquad (8)$$

is obtained for the variation of the self-diffusion coefficient D with concentration, where D_0 is a constant. For a divalent ion occupying two sites eq. (8) holds, but if the ion interacts only with one fixed site, eq. (8) becomes

$$D = D_0[1/(1 - \theta/_2)] = D_0[2B/(2B - A)] \qquad (9)$$

Equations (7), (8), (9) are plotted in Figure 4 with $D_{HSO_4} = 6.8 \times 10^{-10}$ cm.[2] sec.$^{-1}$, $K_H/K_S = 4 \times 10^{-3}$, and $D_0 = D_M$ (minimum) $= 2 \times 10^{-13}$ cm.[2] sec.$^{-1}$.

Equation (7), the bisulfate-formation model, fits the experimental points, whereas the site-saturation equations do not. An estimate of the amount of HSO_4^- needed to produce this increased mobility at site saturation can be calculated from eqs. (5) and (6) with $X = 25$ and $B = 26$, giving $Y/A = 5\%$; that is, 0.0013 meq./g. Therefore with nylon, in contrast to keratin, no acid sorption in excess of the terminal amino
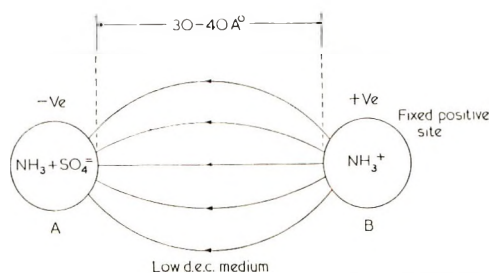
Fig. 5. Diagrammatic representation of the position of the SO_4^{2-} ion inside the polymer: d.e.c. dielectric constant.
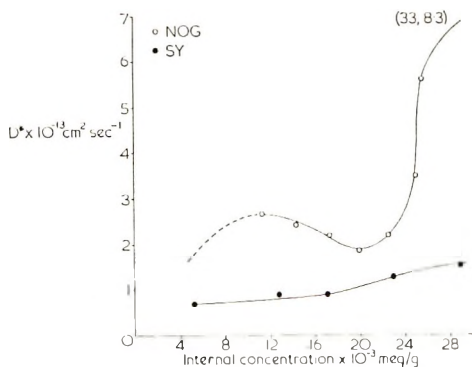
Fig. 6. Variation of anion diffusion coefficients D of NOG and SY with internal concentration at 35°C.

concentration will be observed, since the amount of bisulfate sorbed is small, within experimental error.

Whatever the explanation of the variation of D_M with internal concentration, the SO_4^{2-} mobility must be very much smaller than that of small monovalent anions at low internal concentrations (D_{SO_4} is 2×10^{-13} cm.² sec.⁻¹, as estimated from Figure 4 at low internal concentrations), when the amount of HSO_4^- present will be small, which is 300 times smaller than the corresponding bromide ion mobility. Furthermore, this cannot be merely a matter of ion size (i.e., $D \propto 1/r$), and there is no reason why site saturation should play a part, so some other explanation must be sought.

A possible explanation of this may be deduced from the absorption work carried out with simple mineral acids in nylon. From the absorption isotherms of HBr and of H_2SO_4 in nylon in aqueous and in alcohol solutions a model for the substrate may be deduced (Part I of this series).[10] The sites in the polymer are hydrated and distributed in a hydrocarbon matrix of low dielectric constant, the distance between neighboring sites being of the order of 30–40 A. A simple divalent ion such as SO_4^{2-} will be unable to neutralize completely two plus Ve sites simultaneously, since the distance between the sites is 30–40 A. The position of minimum energy is obtained when one site is completely neutralized; see Figure 5. This will leave A (in the figure) with a residual negative charge, and lines of force

will extend from A to B.   The SO_4^{2-} ion will be effectively neutralized in the region A, not because of the energy involved in the reaction $(NH_3^+ + SO_4^{2-})^-$, which will be relatively small, but because of the high-energy barrier between the residual negative charge on A and the region B.   This will give rise to a low SO_4^{2-} ion mobility.

Figure 6 shows the variation of the anionic self-diffusion coefficients with concentration for the dyes Naphthalene Orange (NOG) and Sunset Yellow (SY).   The NOG mobility increases rapidly with concentration at low internal concentrations, passes through a maximum at intermediate concentrations, decreases, and then increases rapidly again, as site saturation is approached.   The results at low concentration were estimated from the values obtained in the presence of buffer.[11]   The SY mobility increases but little with concentration, and no pronounced site saturation effect is observed.   With both dyes the anion mobility remains practically constant in the amide-dyeing region.

The rapid increase in NOG mobility with increasing concentration, as the available amino sites become saturated, may be attributed to a site saturation effect: that is, $\theta \to 1$ in eq. (8).   The simple site-saturation model cannot, however, explain the variation in mobility versus concentration observed at intermediate concentrations.   Medley[6] observed a similar phenomenon in keratin, and he attributed this to the tendency of the dye to aggregate inside the polymer, which would lead to the observed variation of mobility with concentration.   This is not altogether a satisfactory explanation, since it is difficult to reconcile with the rapid increase in mobility observed when site saturation is approached.   Whatever effect does give rise to the observed decrease in mobility must apply in both the nylon and keratin substrate.

At low internal concentrations the NOG mobility increases with increasing concentration.   Similar increases have been observed in keratin[6] and cellulose[12] and were explained in terms of electrostatic interaction with the fixed sites.   A similar type of explanation may also account for the observed phenomenon in nylon, since this has a low dielectric constant and, hence, electrostatic effects will be correspondingly higher.

Two possible mechanisms are proposed: there may be a limited number of low-energy sites which the anion approaches very closely, and, as these sites become saturated, the mobility increases, or the anion may be accelerated by interaction with the "free" hydrogen ions.   The latter appears highly improbable, since the number of "free" hydrogen ions is small in this region and there is also no indication of such an effect from the other Br^- results.

In contrast to the results for NOG, no rapid increase in SY mobility is observed when the acid concentration approaches 0.026 meq./g.   This result was checked with an isomer-exchange technique, and the same answer was obtained as with the radiotracer.   The difference in behavior between SY on the one hand and Naphthalene Scarlet 4R on the other is difficult to explain.

The kinetic properties of the dibasic dye are explainable if it is assumed that the anion interacts with fixed, single, isolated sites, but there is no evidence of this in the equilibrium work as there is for SO_4^{2-}.   The binding mechanism for the SO_4^{2-} ion was deduced from the apparent negative affinity of the anion for the polymer, but no analogous effect is obtained with the SY anion.   Table I lists the anion affinities in keratin and nylon, and it can be seen that the ratio $-\Delta\mu_{SY}/-\Delta\mu_{NOG}$ is of the same order in the two substrates.   The acid affinities for nylon were calculated from the midpoint of the free-acid titration curves (Fig. 2).   The values for keratin were calculated from the data of Medley.[6]

TABLE I

	$\Delta\mu_0$, kcal./mole			
	Wool		Nylon	
	Total	Anion	Total	Anion
NOG	11.3	5.8	16.05	6.25
SY	14.6	4.0	23.59	3.99
$-\Delta\mu_{SY}/-\Delta\mu_{NOG}$	0.69		0.64	

This indicates that the nonpolar parts of the dye are the equilibrium-determining factors in both substrates and, although no direct evaluation of the electrostatic factors can be obtained from the titration curves, it does appear that no effect similar to that with the SO_4^{2-} ion occurs with the dibasic dye anion.

The enhanced mobilities of SY and NOG obtained in the presence of salt (Fig. 7) do, however, indicate that electrostatic forces to some extent localize the dye anion, the increased mobility in the presence of salt being far greater for the dibasic anion than the monobasic one.   The SY mobility increases 35 times, and the NOG 3 times, over the salt concentration used. The effect of the salt will be to shield the dye anions from the amino sites in the polymer, and a greater effect on the divalent anion than on the
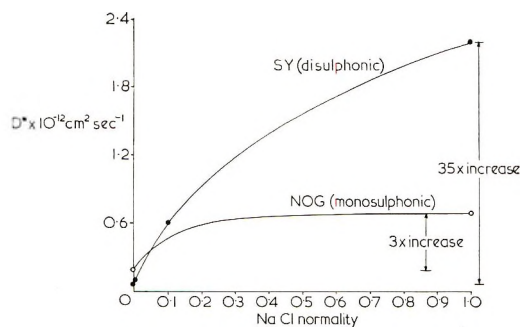
Fig. 7. Effect of salt on mobilities of dye anions in nylon under neutral conditions at 35°C.

monovalent anion would be expected.   Similar effects have been observed in keratin.[8]

In view of the conflicting evidence, the idea of interaction with single, isolated sites for the dibasic dye anion cannot be put forward with any real confidence, but it appears to be the only way of explaining the available kinetic results.

In the amide region the mobility of both dyes remains constant, as observed by McGregor et al.[2] with Naphthalene Scarlet 4R.

References

1. M. Hayashi, *Bull. Chem. Soc. Japan*, **33**, 1184 (1960).

2. R. McGregor, R. H. Peters, and J. H. Petropolous, *Trans. Faraday Soc.*, 58, 1054 (1962).

3. H. Brody, *Textile Res. J.*, **35**, 844 (1965).

4. M. L. Wright, *Trans. Faraday Soc.*, **49**, 95 (1953).

5. J. A. Medley, *Trans. Faraday Soc.*, **53**, 1380 (1957).

6. J. A. Medley, *Trans. Faraday Soc.*, **60**, 1010 (1964).

7. J. Crank, *Mathematics of Diffusion*, Clarendon Press, Oxford, 1956.

8. J. A. Medley, *Proc. 3rd Intern. Wool Textile Res. Conf. (Cirtel)*, **3**, 117 (1965).

9. R. H. Fowler and E. A. Guggenheim, *Statistical Thermodynamics*, Cambridge *Univ. Press*, London, 1949.

10. J. Marshall, *J. Polymer Sci.*, **6**, 1583 (1968).

11. J. Marshall and J. A. Medley, *Nature*, **210**, 729 (1966).

12. K. J. Hertiage, *Trans. Faraday Soc.*, **54**, 1902 (1958).

A New Transition Point of Polyacrylonitrile

SABURO OKAJIMA, MORIO IKEDA, and AKIO TAKEUCHI,
*Faculty of Technology, Tokyo Metropolitan University,
Setagaya-ku, Tokyo, Japan*

Synopsis

A polyacrylonitrile sample of molecular weight 78,000 was dissolved into a 15% solution in 70% aqueous HNO_3, spun into an undrawn model filament with diameter 0.3 mm. using a 30% aqueous HNO_3 as the coagulation bath. The fresh filament was drawn 4–16× in water at various temperatures (40, 65, and 75°C.) and then steamed at 90–180°C. Dynamic mechanical tests were carried out on these filaments at 138 cps and it was found that the steamed filaments had a new transition at about 160°C. in addition to the two well-known transitions at 60–70°C. (β) and 110°C. (α_a), although the un-steamed samples had only the two absorptions, α_a and β. This newly found transition was designated α_x. The α_x was measured at 3.5, 11, and 110 cps from which the activation energy of this relaxational motion was estimated to be 95 kcal./mole. The α_x peak height was lowered by stretching and recovered on resteaming; the change in the peak height was paralleled by the changes in the x-ray crystallinity produced by the stretching and the resteaming. These phenomena lead us to a conclusion that the region contributing to the α_x absorption is of considerably higher order than that of the α_a transition with an activation energy about 50 kcal./mole and intimately related to the crystallinity, although it cannot be connected directly to the crystalline region itself because a single crystal mat did not show the α_x.

INTRODUCTION

It is generally known[1] that polyacrylonitrile (PAN) has two transition points, α_a (85–106°C.) and β (less definitely determined), and the activation energies of the respective relaxational motions are about 50 and 20 kcal./mole.[2–5] A few authors, such as Schmieder and Wolf,[6] Cotten and Schneider,[4] and Kimmel and Andrews[1,7] have reported another transition at about 140°C. but on detailed inspection, these papers do not always agree with each other. According to Kimmel and Andrews the activation energy of their 140°C. transition is 48 kcal./mole and equal to that of the α_a transition. Cotten and Schneider's value was measured at 230–290 cps, from which about 106°C. is estimated as the value at 1 cps on the assumption of 50 kcal./mole for its activation energy. This is in accordance with the glass temperature of Schmieder and Wolf[6] or Krigbaum and Tokita;[8] therefore, Cotten and Schneider's transition is considered to be the α_a.

The present authors have found that a sample heated with high-temperature steam exhibits a transition at 160°C. (138 cps) in addition to the

α_a and β transitions; the activation energy is about 100 kcal./mole, and the transition temperature extrapolated to 1 cps is 142°C.

EXPERIMENTAL

Preparation of Sample Filaments

The acrylonitrile homopolymer used as the sample in this study was obtained through the courtesy of Asahi Chemical Industry Ltd.; it had been polymerized by using a redox catalyst, and its molecular weight was 78×10^3. The polymer was dissolved into a 15% by weight solution in 70% HNO_3 (aqueous), and spun into undrawn filament with a diameter of about 0.3 mm., 30% HNO_3 (aqueous) being used as the coagulating bath. The operations were carried out in a refrigerator at 0–5°C. in order to prevent hydrolysis of the polymer. The filament was washed thoroughly and stocked in water (fresh filament).

Dynamic Mechanical Properties

The dynamic storage modulus E', loss modulus E'' and mechanical loss tangent tan δ were measured mainly with a Vibron Model VVD-I, a type of stretching vibrometer made by Toyo Measuring Instruments Co. Ltd., at a frequency 138 cps, the temperature being raised at a rate of 1°C./ min. Measurements were made on some of the filaments with a Vibron Model VVD-II at three frequencies, 3.5, 11, and 110 cps.

X-Ray Crystallinity

The x-ray crystallinity was obtained according to the method of Takahashi and Nukushina.[9]

RESULTS AND DISCUSSION

Effect of Stretching Temperature and Steaming

The fresh filament was stretched $4\times$ in water at temperature T_w after 5 min. preheating at the same temperature; it was then air dried. A portion of the filament was then subjected to steaming at the temperature T_s for 5 min. while being kept at constant length. When T_w was 75°C., the stretched filament became milky but it recovered its transparency after the steaming. The stretching and steaming conditions are summarized in Table I.

As shown in Figure 1, E' of samples II-1–3 decreases as T_w is elevated but the difference between II-2 and II-3 is considerably larger than that between II-1 and II-2. This is bacause the glass transition of wet PAN, which is estimated to be 60–65°C., lies between T_w for II-2 and II-3.

On the tan δ curve (Fig. 2) the principal transition α_a appears at about 110°C. (II-1), 116°C. (II-2), and 120°C. (II-3) as T_w is raised. The β transition is seen faintly at about 60–70°C.

TABLE I
Condition of Preparation of Sample Series II, $v_1 = 4$

Sample no.	T_w, °C.	T_s, °C.
II-1	45	—
II-4	"	90
II-7	"	150
II-10	"	180
II-2	60	—
II-5	"	90
II-8	"	150
II-11	"	180
II-3	75	—
II-6	"	90
II-9	"	150
II-12	"	180

On steaming these samples, the E' curves shift to higher values with a rise in T_s and those of samples II-10–12 surpass the E' of samples II-1 and II-2. The α_a transition again decreases to 110°C. and remains unchanged for the steamed samples. It seems, therefore, that the strain-induced stress in samples II-2 or II-3 introduced during the stretching is eliminated by the steaming, and the amorphous chains are converted into a completely relaxed conformation. The high temperature side of the α_a peak gradually becomes prominent as T_s is elevated, and a peak can be observed clearly in samples II-10–12 as shown in Figure 2. This is a new transition which has not been reported in literature, which we will denote as α_x. A precise description of this transition is the subject of the present paper.
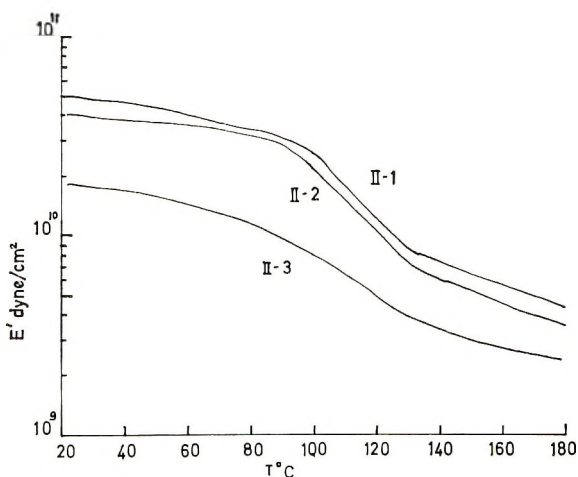
Fig. 1. Plots of E' vs. temperature of the filaments stretched 4× in water at 45°C. (II-1), 65°C. (II-2), and 75°C. (II-3). See Table I.
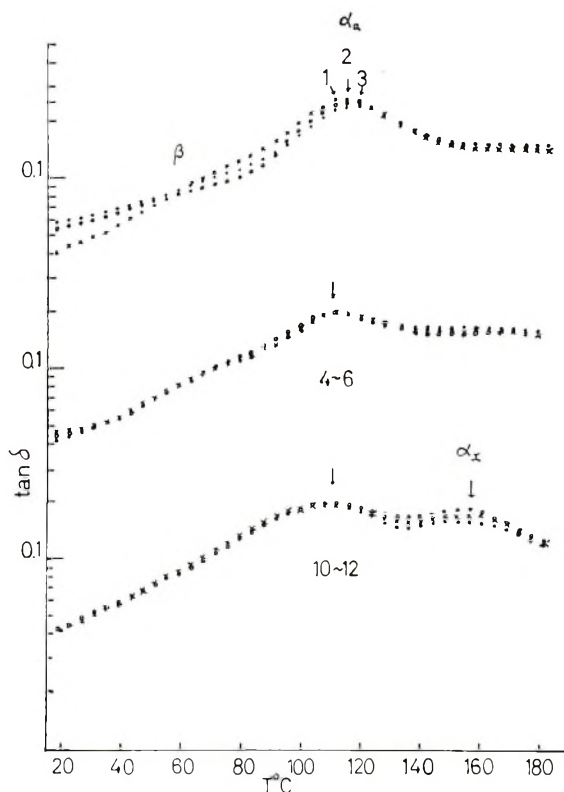
Fig. 2. Plots of tan δ vs. temperature of the filaments stretched and steamed under various conditions: (×) samples No. II-1, II-4, and II-10; (○) samples II-2, II-5, and II-11; (●) samples II-3, II-6, and II-12. See Table I.

Effect of Stretching and Heat Treatment upon α_x

The fresh filament was stretched $4\times$ (v_1) in water at $60°C$. air-dried, and again stretched v_2 in a boiling saturated solution of $(NH_4)_2SO_4$ $(108°C.)$. The total degree of stretching v was 4–16. A part of the sample at each v was subsequently steamed at $180°C.$ (Table II).

Figure 3 illustrates the change in the tan δ of these samples as a function of v and T_s. Among the odd-numbered samples, the α_x peak is observed only in sample III-1, while in the other samples it appears as a shoulder at about $160°C$. The tan δ at 140–$180°C$. decreases in order from III-1 to III-7. On the contrary, every steamed sample exhibits the α_x peak, and the peak height decreases as v increases. α_a is $110°C$. in all cases. α_x is $160°C$. in II-2, $153°C$. in II-4, but α_x cannot be determined definitely in the rest of the samples, probably because of superposition of α_a and small α_x. Hence a separation into the two peaks as illustrated in Figure 4 was made on the assumption of symmetry of the α_a curve. The results are shown in Table III in line with the apparent α_x.

It is clear from Table III that the "apparent" α_x is 153–$160°C.$, while

TABLE II

Condition of Preparation of Sample Series III, $T_w = 60°C., v_1 = 4$

Sample No.	v_2	v	T_s, °C.
III-1	—	4	—
III-2	—	4	180
III-3	2	8	—
III-4	2	8	180
III-5	3	12	—
III-6	3	12	180
III-7	4	16	—
III-8	4	16	180

the estimated "separated" α_x from Figure 4 is 155–168°C. so in both groups, the value is nearly constant and the region contributing to the α_x seems to be of similar order independent of the values of T_w and T_s. However, v has a slight effect upon the peak height, i.e., higher stretching is apt to lower the α_x.

The phenomenon that the α_x absorption becomes prominent when the fresh filament is stretched less and wet heated at high temperatures above 108°C. at an unchanged peak temperature leads us to a consideration that the fraction of α_x region increases by such treatment without changing its order.
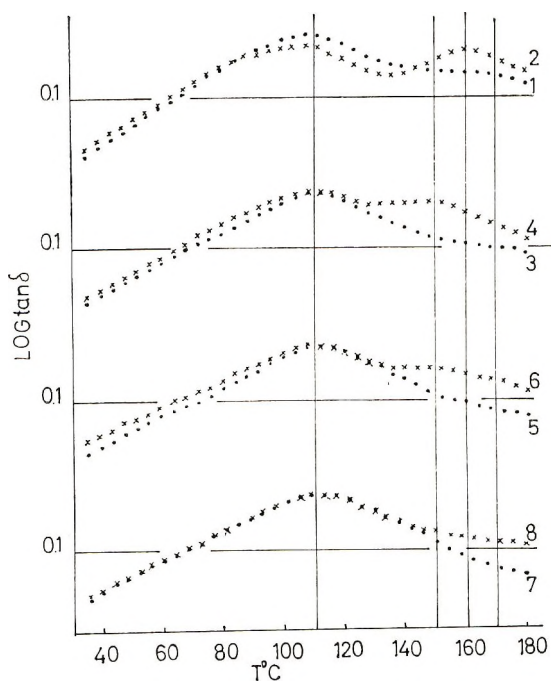
Fig. 3. Plots of tan δ vs. temperature of the samples stretched variously and steamed at 180°C. See Table II.

TABLE III

	II-10	II-11	II-12	III-2	III-4	III-6	III-8
			α_x absorption of various samples				
T_w, °C.	45	60	75	60	60	60	60
T_s, °C.	180	180	180	—	180	180	180
v	4	4	4	4	8	12	16
Apparent α_x, °C.	154	160	153	160	153	—	—
Separated α_x, °C.	160	162	164	164	155	168	—
Peak height, separated	0.09	0.09	0.07	0.11	0.08	0.05	—
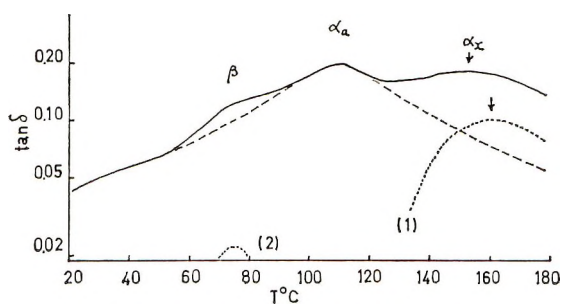
Fig. 4. Separation of the superposed peaks: (1) and (2) are the separated α_x and β, respectively.

Activation Energy of the Relaxation Process

In order to estimate the activation energy of the relaxation process, tan δ of sample III-4 was measured at frequencies f of 3.5, 11, and 110 cps, when the α_x varies as indicated in Table IV. The log f shows a good linear relationship to the reciprocal peak temperature, as shown in Figure 5, and the activation energy of each relaxation process was obtained as indicated in Table IV; thus α_x, α_a, and β at 1 cps were estimated by extrapolation.

The activation energies of the α_a and β processes are 53 and 16–19 kcal./mole, respectively, and these values are in good accord with the

TABLE IV
Transition Points Measured at Various Frequencies

Frequency, cps	α_x, °C.		α_a, °C.	β, °C.	
	Apparent	Separated		Apparent	Separated
3.5	147	145	91	40	34
11	151	148	98	52	37
110	160	152	109	80	75
1	142	142	85	22	27
Activation energy, kcal./mole	150	95	53	19	16
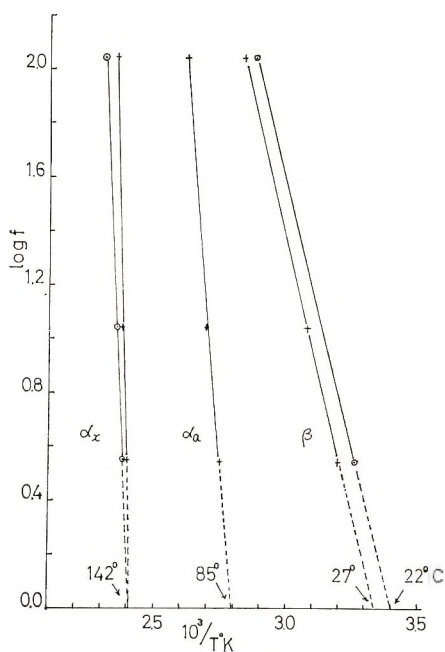
Fig. 5. Plots of log f vs. peak temperature.
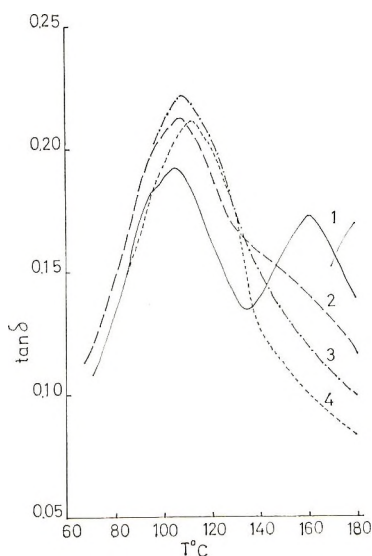
Fig. 6. Change in α_x by stretching at various v_2: (1) 1; (2) 1.5; (3) 2; (4) 3.

values in the literature.[2-5] The activation energy of the α_x relaxation process is 150 kcal./mole from the apparent α_x values, while it is 95 kcal./mole from the separated α_x and more than two times as large as the α_a's. So the region contributing to the α_x absorption is considered to be of considerably higher order than that of the α_a.
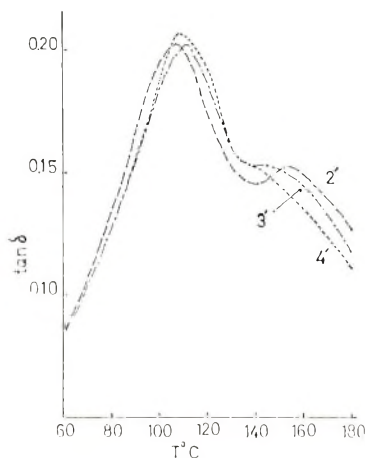
Fig. 7. Change in α_x by steaming: (2'), (3') and (4') correspond to (2), (3), and (4) in Fig. 6, respectively.
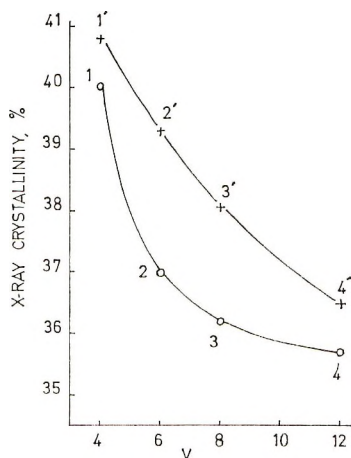
Fig. 8. Decrystallization by stretching and recrystallization by steaming. Numbers beside each point refer to Figs. 6 and 7.

Curve 1 in Figure 6 shows tan δ of sample II-11. When this filament was stretched v_2 (1.5×, 2×, and 3×) in a boiling saturated solution of $(NH_4)_2SO_4$, the curve 1 changed to curves 2, 3, and 4 with increasing v_2, and the α_x peak disappeared from curve 3 and 4 through a shoulder on curve 2. On steaming these stretched filaments, α_x again reappeared; a shoulder is seen in 3 → 3' or 4 → 4' and a peak in 2 → 2' as shown in Figure 7. Therefore the region is considered to be destroyed by stretching and regenerated again by steaming.

The x-ray crystallinity of the filament 1 in Figure 6 was 40%, and this was decreased partly by stretching in a boiling saturated $(HN_4)_2SO_4$ solution and increased again by steaming, as indicated in Figure 8. The

change in crystallinity produced by such treatments is parallel to the change in the α_x peak in Figures 6 and 7; the numbers beside the points in Figure 8 correspond to those in Figures 6 and 7. The crystallinity decreases in the order *1'*, *1*, *2'*, *3'*, *2*, *4'*, *3*, and *4*, and the change in the α_x peak heights follows the same order. Consequently it is concluded that the region developed by steaming is partly destroyed by stretching and regenerated again by steaming. Here the high stretching decelerates and the high temperature accelerates the development of the region.

Andrews and Kimmel[1,8] have reported a transition at 142°C. and illustrated it as a result of dissociation of strong dipole–dipole association of PAN. According to their calculation the activation energy is 48 kcal./mole and nearly equal to the activation energy reported in the literature of the α_a. The α_x transition agrees well with Andrews and Kimmel's transition in temperature but differs considerably in activation energy. Therefore the two transitions are probably different from each other.

The present authors also consider that the order of this region is considerably higher than that of the α_a region from the extremely high activation energy. It is associated intimately with the crystalline region but it cannot be connected directly to the crystalline region itself because an experiment carried out on a single crystal mat did not show the α_x transition. It may be a disordered region in crystalline phase.

Lately Minami et al.[10] reported the existence of a transition at about 160°C. (110 cps) and assigned it to molecular motion in the amorphous region corresponding to the glass transition temperature. The relation between this transition and the α_x is not clear at present.

References

1. R. M. Kimmel and R. D. Andrews, *J. Appl. Phys.*, **36**, 3063 (1965).
2. R. Meredith and B.-S. Hsu, *J. Polymer Sci.*, **61**, 271 (1962).
3. Y. Ishida, O. Amano, and M. Takayanagi, *Kolloid-Z.*, **172**, 129 (1960).
4. G. R. Cotten and W. C. Schneider, *Kolloid-Z.*, **192**, 16 (1963).
5. Y. Ishida, M. Matsuo, Y. Ueno, and M. Takayanagi, *Kolloid-Z.*, **199**, 67 (1964).
6. K. Schmieder and K. Wolf, *Kolloid-Z.*, **134**, 149 (1953).
7. R. D. Andrews, in *Transitions and Relaxations in Polymers* (*J. Polymer Sci. C*, **14**), R. F. Boyer, Ed., Interscience, New York, 1966, p. 261.
8. W. R. Krigbaum and N. Tokita, *J. Polymer Sci.*, **43**, 467 (1960).
9. M. Takahashi and Y. Nukushina, *Sen-i Gakkaishi*, **16**, 622 (1960).
10. S. Minami, H. Sato, and N. Yamada, *Rept. Progr. Polymer Phys. Japan*, **10**, 317 (1967).

Polypyromellitimides: Details of Pyrolysis

F. P. GAY and C. E. BERR, *Film Department,*
Experimental Station, E. I. du Pont de Nemours & Co.,
Wilmington, Delaware 19898

Synopsis

Polyimide films from 4,4′-diaminodiphenyl ether and pyromellitic dianhydride were pyrolyzed at 400–600°C. in non-oxidative systems.   Major gaseous products were carbon monoxide and carbon dioxide;   hydrogen evolution occurred above 525°C.   A mobile n-imide–isoimide equilibrium is in accord with the gas evolution data.   Carbon dioxide arises from isoimide decomposition and carbon monoxide arises from the normal imide.

In previously discussed vacuum and air pyrolyses[1-4] of aromatic polypyromellitimides, evolved gases were analyzed and kinetics were based on weight losses.   Data at advanced stages of decomposition was used and near independence of the decomposition process and temperature was assumed.   We report a more detailed study of the decomposition in vacuum.

EXPERIMENTAL

Pyrolysis

Powdered samples of polyimide film (from pyromellitic dianhydride and 4,4′-diaminodiphenyl ether) were dried and outgassed in the vacuum system (1–5 × 10^{-3} Torr) at 250°C.   The system was isolated from the pumps and the sample was dropped magnetically into the preheated pyrolysis zone.   Evolved gas was collected and removed periodically for analysis by mass spectroscopy.   In other experiments, the solid residue was also removed periodically for weighings and elemental analyses.

Sample

Within the limit of detection, the polyimide samples contained no amide groups as measured by absorption at 3.08 μ, the NH band which has a mole fraction extinction coefficient α, of 1.14.   Elemental analysis of a typical polyimide, of η_{inh} 1.0 (HNO_3, 15°C.), was as follows.

ANAL. Calcd.: C, 69.1%; H, 2.6%; N, 7.30%; O, 20.6%.   Found: C, 69.1%; H, 2.64%; N, 7.33%; O, 20.93%.

Isoimide was determined by infrared analysis by using a Perkin-Elmer model 13 infrared spectrophotometer. The 9.85 μ band was used for internal thickness and the 10.95 μ band (one of a doublet) for isoimide. The 9.85 μ band is consistent within a set of samples prepared in the same fashion but should be calibrated against the 3.25 μ band for samples of different origin. The mole fraction extinction coefficient of the 9.85 μ band, $\alpha_{9.85} = 0.717$ and that for the 10.95 μ band, $\alpha_{10.95} = 6.31$. The expression $(A_{10.95}/A_{9.85})$ (0.717/6.31) measures mole fraction of isoimide. The intensity of the 10.95 μ band allows measurements to 0.01 mole fraction of isoimide.

Polyamide acid films were cast from dimethylacetamide solutions and solvent was removed in a vacuum oven at 100°C. Films were converted to imide under nitrogen at 200, 300, 350, 400°C. until no changes in infrared spectra were observed. The 500°C. specimen was converted to imide at 300°C. and then heated at 500°C. for 3 min. under nitrogen.

Polyisoimide films were prepared by converting polyamide acid films in equivolume trifluoroacetic anhydride–pyridine baths and drying at 80°C. in a vacuum oven. Thermal conversion to normal imide was followed spectroscopically for three half lives or more.

RESULTS

This work confirms earlier observations that under anaerobic conditions the major gaseous products at 400–600°C. are carbon monoxide and carbon dioxide;[1] a variety of trace products occur at all temperatures.[2-4] At higher temperatures, hydrogen evolution becomes appreciable. Figure 1 shows CO, CO_2, and H_2 mole fractions plotted against temperature. Data were taken during the portion of the decomposition where gas evolution is approximately linear with time (e.g., 10–40 min. in Fig. 2).

Table I shows a typical set of data for gas evolution versus time for a run at 540°C. with sample collection at 30 min. intervals.

Initial high rate of evolution of carbon dioxide was found at all temperatures, persisting for 5–60 min., depending on the temperature (shorter times at higher temperatures), after which evolution settled to a steady rate to high conversion. The carbon monoxide did not show such variability.

TABLE I
Gas Evolution in Polyimide Pyrolysis (540°C.)[a]

Total exposure time, min.	Gas evolution			R_{CO_2}, mole/kg.-sec. $\times 10^4$	R_{CO}, mole/kg.-sec. $\times 10^4$
	Gas, mole $\times 10^4$	CO_2, mole $\times 10^4$	CO, mole $\times 10^4$		
30	9.9	4.56	5.05	6	6.4
60	7.895	2.34	5.14	2.96	6.5
90	8.58	2.5	5.3	3.16	6.7
120	2.63	0.58	1.55	0.73	1.9

[a] Charge, 0.439 g.; gases, 0.098 g.; residue, 0.287 g.; sublimate, 0.028 g.; mass balance, 94%.
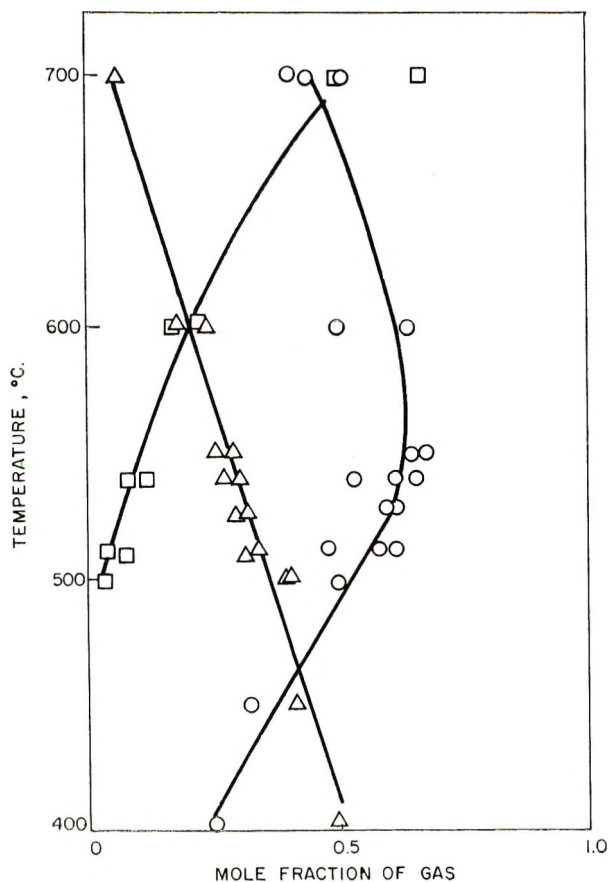
Fig. 1. Gas composition vs. temperature of pyrolysis: (O) carbon monoxide; (△) carbon dioxide; (□) hydrogen.

The derived rate parameters are given in Table II. The rate constants k are for the first-order process. The values remain constant to high percentage decomposition without compensation for the decreasing quantity of decomposing species.

TABLE II
Steady Decomposition Rates

Temp., °K	R_{CO}, mole/kg.-sec. $\times 10^4$	k_{CO}, sec.$^{-1} \times 10^4$	R_{CO_2}, mole/kg.-sec. $\times 10^4$	k_{CO_2}, sec.$^{-1} \times 10^2$
822	15.2	15.2	5.0	6.2
813	6.0	6.0	3.0	3.3
791	2.0	2.0	1.07	1.07
773	0.67	0.67	0.458	0.4
723	0.03	0.03	0.06	0.045
673	0.003	0.003	0.009	0.0051
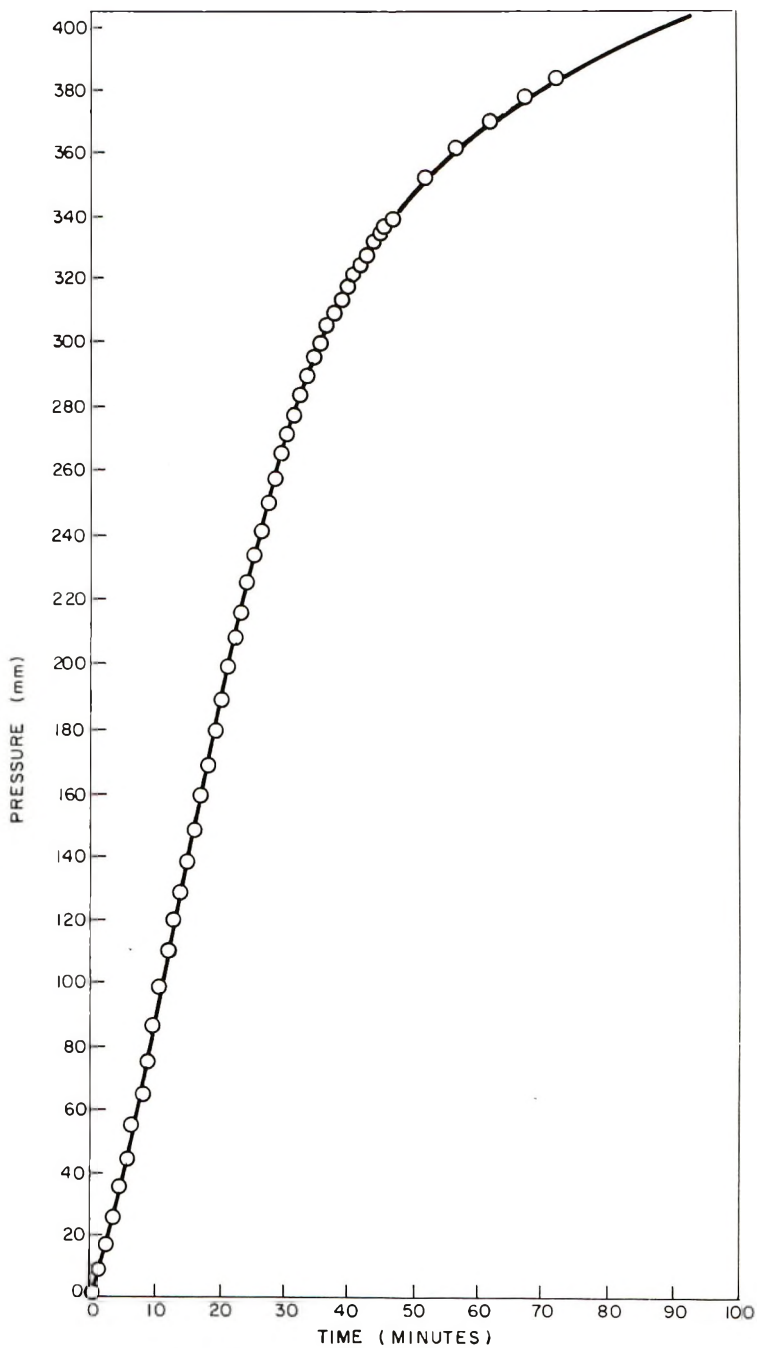
Fig. 2. Pressure vs. time at 550°C.   Total weight loss at 100 min. = 39.6%, CO and CO_2 were 55% of weight loss and 90 mole-% of gas.
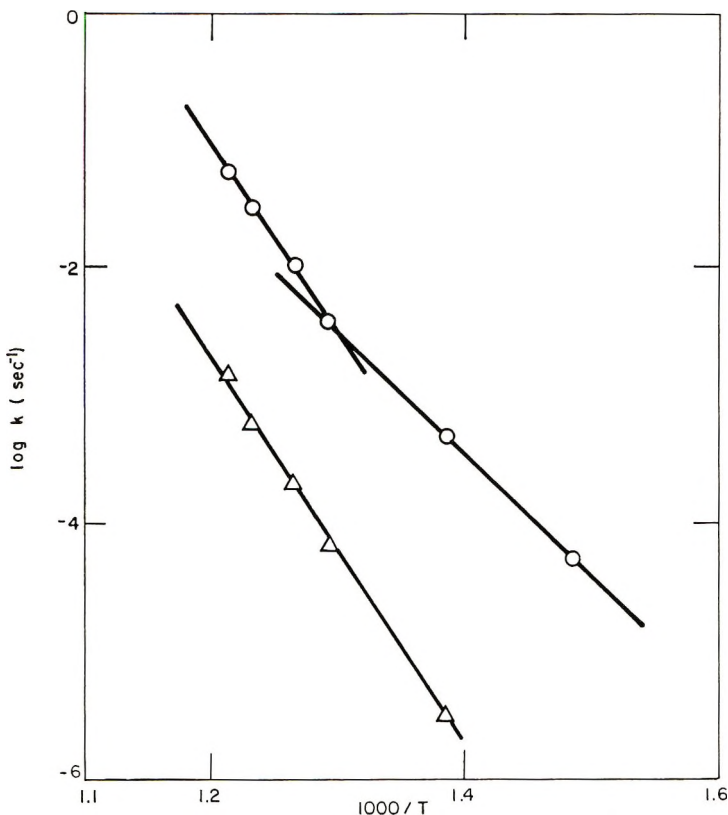
Fig. 3. Log rate constants vs. $1/T$: ($\triangle$) carbon monoxide; ($\square$) carbon dioxide, corrected isoimide concentration.

Figure 3 shows an Arrhenius plot of the rate constants for both carbon monoxide and dioxide evolution versus reciprocal temperature. The carbon monoxide curve is linear over the entire range of measurements with $\Delta H\ddagger = 69$ kcal. The carbon dioxide curve can be analyzed as two straight lines, the low temperature end with $\Delta H\ddagger = 47.9$ kcal., the high temperature end with $\Delta H\ddagger = 69$ kcal.

Initial carbon dioxide in excess of steady rate, corresponds to 1–3 mole-% of the pyromellitoyl units based on two CO_2 groups/repeat unit. Amide group analysis (and by analogy, carboxyl) can be followed into this range in control samples and was in or below this range in the pyrolysis samples. The total carbon dioxide evolved (see Table I) indicates original carboxyl cannot be the source for most or all of the carbon dioxide.
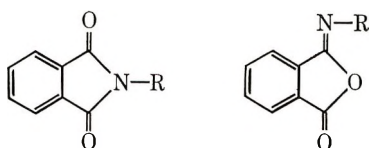
TABLE III
Change in 10.95 μ (Isoimide) Band at 400°C.

Sample time, hr.	Absorbance	
	1	2
0	0.098	0.135
1	0.107	0.12
5	0.10	0.11
10	0.11	0.10

TABLE IV
Isoimide Isomerization[a]

Temp., °C.	$t_{0.5}$, hr.	k, sec.$^{-1}$
250	100	1.9×10^{-6}
300	2	9.6×10^{-5}
350	0.083	2.3×10^{-3}

[a] $k = 10^{14.2} e^{-\frac{47000}{RT}}$.

The isoimide[5] mole fraction of the polymers was low. The kinetic data reported are for an initial isoimide mole fraction of 0.04 ($\sim CO_2$).

The total carbon dioxide evolved is much greater than the initial isoimide content and must arise from normal imide or one of its thermal products. The 10.95 μ isoimide absorption band of two samples with different initial isoimide content change on heating at 400°C. (Table III). The final isoimide mole fraction in each case was 0.02. Facile thermal conversion of isoimide to n-imide occurs. Polyisoimide samples thermally isomerize to
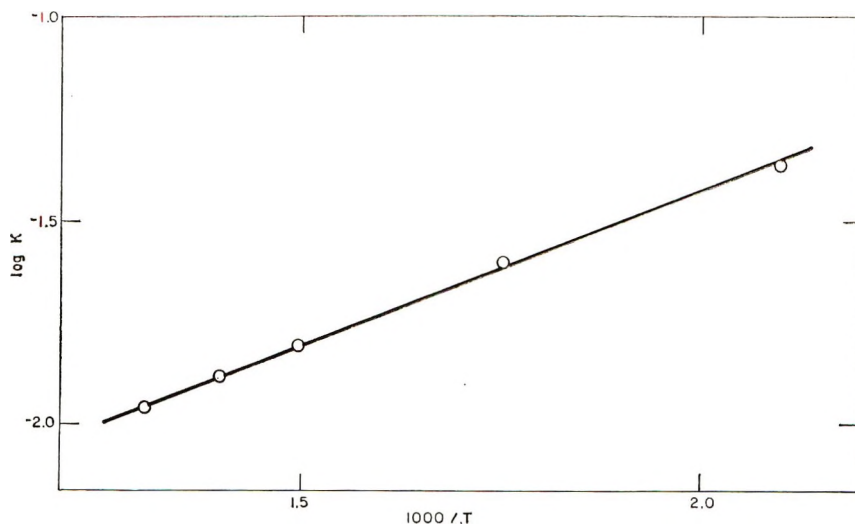
Fig. 4. Log equilibrium constant vs. reciprocal temperature for the reaction imide → isoimide.

TABLE V
Measured Equilibrium Isoimide Content of Polymers

| Temp., °C. | Mole fraction isoimide | | K |
	Measured	Calcd.[a]	
200	0.057		0.0605
300	0.028		0.0288
350	0.021		0.215
400	0.018	0.022	0.0183
450	—	0.013	0.013
500	0.012	0.011	0.011
550	—	0.0095	0.010

[a] From kinetics.

n-imide. Half lives and rates for the isomerization conversion appear in Table IV. Experimental values for equilibrium isoimide content at various temperatures are listed in Table V. A plot of log K versus $1/T$, where K = [isoimide]/[imide] (Fig. 4) yields $\Delta H = -10$ kcal.

DISCUSSION

We ascribe carbon dioxide in polyimide pyrolysis to isoimide, a minor component. High initial CO_2 evolution is attributed to isoimide initially present while the steady rate is fed by isomerization of normal imide.

Bruck has reported an activation energy of 74 kcal./mole from weight loss data. This may correspond to the decarbonylation reaction $\Delta H\ddagger$ = 69 kcal. It is not clear why the carbon dioxide forming reaction, which can account for about one third of the moles of off-gas over an appreciable temperature range, does not have more of an effect on his activation energy. Berr and Heacock did find an activation energy in the range 51–55 kcal. associated with loss of physical properties at temperatures near 400°C. It is tempting to relate this process with carbon dioxide loss.

Details of mechanisms in the solid state present a difficult problem, particularly when intractable residues prohibit a quantitative chemical group analysis as in the present case. However, mechanisms can be inferred from the measured parameters.

Values of k_{CO_2} in Figure 3 are derived from the rates, R_{CO_2} and values for isoimide contents based on Table V. If initial rates are associated with decomposition of the initial isoimide content ($N_t = 0.04$) we can obtain a value for k_{CO_2} (initial) for a unimolecular reaction. The rate constants must be the same before and after the equilibration if we are looking at the same process. One can calculate equilibrium isoimide content at various temperatures.

$$[\text{Isoimide}]_{\text{steady rate}} = [\text{Isoimide}]_{\text{initial}} R_S/R_i$$

Calculated values in Table V agree satisfactorily with measured values. From the data, isoimide is calculated to be 5.4–7.7 kcal./mole less stable

than imide in the indicated temperature range. The enthalpy change (from the slope of Fig. 4) is of the order of –10 kcal. and $\Delta S \sim -21$ e.u.

The Arrhenius factors for the decarbonylation reaction are $\Delta H\ddagger = 69.3$ kcal., $\Delta S\ddagger = +10.6$ e.u., and $A = 10^{15.9}$. The frequency factor is in the "abnormally" high region[8]—a region characteristic of decyclization (ring-opening) reactions with loose transition states. The activation energy is suggestive of the energy of a primary bond cleavage and seems appropriate for a carbonyl–nitrogen bond with an aromatic nucleus β to both atoms.

The situation with the loss of carbon dioxide is more complex. In the lower temperature portion of the Arrhenius plot, $\Delta H\ddagger = 47.9$ kcal., $\Delta S = -11.6$ e.u., and $A = 10^{11}$. The corresponding values for the isomerization, isoimide $\rightarrow$ imide, are $\Delta H\ddagger = 47$ kcal. and $A = 10^{14.2}$. The rate constants for the reverse process may be calculated from the relationship of the equilibrium constant with the forward and reverse rates

$$K = k(\text{forward})/k(\text{reverse}) = k_1/k_{-1}$$

From these values, the Arrhenius parameters can be calculated for the reaction, imide $\rightarrow$ isoimide, $\Delta H\ddagger = 41$ kcal., $A = 10^{9.9}$. At 350°C., the value of k_{-1} is 4.9×10^{-5} sec^{-1} compared to an extrapolated value of k_{CO_2} of 3.5×10^{-6}. Extrapolation of k_{-1} to 500°C. gives a value of 0.317 compared to a measured k_{CO_2} of 0.04. It seems probable that isomerization is not rate-controlling. As a consequence, the equilibrium constants are probably true constants and the decarbonation is entropy-controlled with a transition state resembling the isomerization transition state. At higher temperatures, the kinetics probably go over to steady state as primary bond breaking becomes competitive.

We have treated the data as a unimolecular process because this seems reasonable for decomposition in the solid, immobile matrix. The internal consistency of the treatment is good and external checks, such as the isoimide content are satisfactory. However, examination of Table II or Figure 2 shows that the rates R remain constant over an extended region of the decomposition—up to $\sim 75\%$ gas elimination. We attribute this psuedo-zero-order behavior to the fact that the decomposition reaction proceeds in ordered platelike domains and at specific surface regions of these domains. The surface area in such a process should change slowly so the apparent available reactive species is approximately constant.

The various factors derived give a good description of the decomposition of the polypyromellitimide at temperatures up to 600°C. The decarbonylation reaction is enthalpy-controlled and the processes involving the isoimide structure are entropy-controlled. The existence of a mobile equilibrium is not rigorously proven, but the data are self-consistent with such a picture. Complete clarification of the decomposition processes will depend on model compound work where a quantitative material balance of identified species can be obtained.

We are indebted to R. M. Ikeda and P. G. Schmidt for the infrared assignments and extinction coefficients.

References

1. J. F. Heacock and C. E. Berr, *SPE Trans.*, **5**, 105 (April 1965).

2. S. D. Bruck, *Polymer*, **5**, 435 (1964).

3. S. D. Bruck, *Polymer*, **5**, 49 (1965).

4. S. D. Bruck, paper presented at 147th National Meeting, American Chemical Society, Philadelphia, Pa., April 5–10, 1964; *Polymer Preprints*, **5**, 148 (1964).

5. W. M. Edwards, U. S. Patent 3,179,634.

6. B. E. Gowenlock, *Quart. Rev.*, **14**, 133 (1960).

Copolymerization of 4-Methyl-1,3-dioxene-4 with Maleic Anhydride and Terpolymerization with Styrene as the Third Component

WASABURO KAWAI, *Government Industrial Research Institute, Osaka, Japan*

Synopsis

Copolymerization of 4-methyl-1,3-dioxene-4 with maleic anhydride was carried out. The monomer reactivity ratio was determined to be $r_1 = 0.18$, $r_2 \sim 0$ in terminal model and $r_1 = 0.015$, $r_1' = 0.224$, $r_2 = r_2' = 0$ in the penultimate model.

Calculations of run number, linkage probabilities, and number-average chain length in the terminal model and comparison of n (mole ratio of each monomer unit content in copolymer) in each model with the experimental value was made. From these results, the obtained polymer was confirmed to be alternating. Terpolymerization of 4-methyl-1,3-dioxene-4 with maleic anhydride and styrene was also carried out. The agreement of the experimental value (titration by indicator or electroconductivity) of maleic anhydride content with the theoretical value confirms that the terpolymer has a DMS triad sequence.

INTRODUCTION

Radical copolymerizations of internal olefins with maleic anhydride have been studied by several authors.[1-3] Copolymerization of p-dioxene with maleic anhydride was investigated by Iwazuki et al., and an alternating copolymer was obtained. In the present paper, 4-methyl-1,3-dioxene-4 (I) was copolymerized with maleic anhydride to an alternating copolymer. It was found that the copolymerization process proceeded through a charge transfer complex, which was confirmed by the continuous variation method with the ultraviolet spectrometer at 340–400 mμ.

$$
\begin{array}{c}
CH_3 \\
| \\
C \\
\diagup \; \diagdown \\
O \qquad CH \\
| \qquad\quad | \\
CH_2 \qquad CH_2 \\
\diagdown \; \diagup \\
O \\
\text{I}
\end{array}
$$
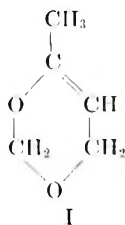
Terpolymerization with styrene as the third component was also carried out.

EXPERIMENTAL

4-Methyl-1,3-dioxene-4 was prepared according to the method described in the previous paper.[4] Copolymerization of 4-methyl-1,3-dioxene-4 with maleic anhydride was carried out in a sealed glass ampule at 50°C. without catalyst and solvent. The polymerization product was poured into methanol, and the precipitate was washed repeatedly with methanol and dried in a vacuum oven. Copolymerization of 4-methyl-1,3-dioxene-4 with styrene and terpolymerization with the three monomers were carried out in a sealed glass ampule at 50°C. by using α,α-azobisisobutyronitrile.

Compositions of these copolymers were determined by carbon–hydrogen analysis, and the results were used to estimate the monomer reactivity ratios. Estimation of maleic anhydride units in the terpolymer was carried out by the electroconductivity method or by titration $0.1N$ sodium hydroxide with phenolphthalein as indicator, after hydrolysis of the terpolymer in a dimethyl sulfoxide–water (10:1) mixture by heating on a water bath.

Measurement of the charge transfer spectra between 4-methyl-1.3-dioxene-4 and maleic anhydride was carried out in chloroform solution in the visible region by use of an ultraviolet spectrometer according to the method of Job.[5,6]

RESULTS AND DISCUSSION

Copolymerization of 4-Methyl-1,3-dioxene-4 with Maleic Anhydride

The results of bulk copolymerization of 4-methyl-1,3-dioxene-4 with maleic anhydride are tabulated in Table I. By using the results of Table
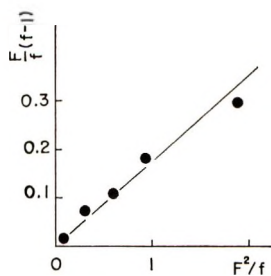
Fig. 1. Fineman-Ross plot.

I and Fineman-Ross or Mayo-Lewis integral equations,[7] the monomer reactivity ratios r_1 and r_2 were determined as indicated in Figures 1 and 2. Results are shown in Table II.

As monomer reactivity ratio (r_1,r_2), concentrations of both monomers in the feed mixtures, and molar content of both monomer units in the copolymer were known, the linkage probabilities P_{DD}, P_{DM}, P_{MD}, P_{MM} and run number R could be calculated by using the Alfrey-Goldfinger[8] or Harwood-

TABLE I

Copolymerization of 4-Methyl-1,3-dioxene-4 (M_1) with Maleic Anhydride (M_2) at 50°C. without Catalyst and Solvent

	Monomer feed			Reaction time, min.	Conversion, %	Copolymer			Copolymer				
									Found		Corrected[a]		
No.	$[M_1]_0$ mole	$[M_2]_0$ mole	$[M_1]_0 \cdot [M_2]_0$			m_1, mole-%	m_2, mole-%	m_1/m_2	C, %	H, %	C, %	H, %	η_{sp}/c[b]
1	0.0033	0.018	0.183	10	7.8	—	—	—	—	—	—	—	—
2	0.0041	0.016	0.183	15	8.1	51.31	49.68	1.033	48.76	5.73	54.65	5.10	—
3	0.0060	0.014	0.429	13	16.0	53.22	46.78	1.138	50.22	5.74	54.91	5.24	0.66
4	0.0081	0.012	0.679	9	24.5	54.02	46.92	1.151	50.38	5.73	54.94	5.26	0.39
5	0.0101	0.010	1.010	5	22.6	55.46	45.45	1.220	50.32	5.83	54.10	5.38	0.35
6	0.0120	0.008	1.50	1	18.7	56.00	44.90	1.247	50.27	5.87	55.16	5.38	0.28
7	0.0149	0.006	2.48	1	17.8	56.18	44.71	1.257	49.91	5.92	55.18	5.43	0.91

[a] The elementary analysis values were corrected for moisture absorbed in copolymer. Theoretical value of C, H content for a 1:1 alternate copolymer was C, 54.49%; and H, 5.02%.

[b] The viscosities were measured in dimethyl sulfoxide at 25°C. The concentrations of polymers were 0.238, 0.257, 0.389, 0.490, and 0.482 g./100 cc. for No.3–No.7.

TABLE II
Monomer Reactivity Ratio of 4-Methyl-1,3-dioxene-4 and Maleic Anhydride

	Fineman-Ross	Mayo-Lewis
r_1	0.18	0.20
r_2	~ 0.0	~ 0.0

Ritchey[9] equations.   The penultimate effect in copolymerization could be shown by Barb's[10] treatment ($r_2 = r_2' = 0$) to follow the equation:

$$n - 1 = \frac{r_1'x(1 + r_1x)}{1 + r_1'x} \tag{1}$$

where $x = [D]/[M]$ (ratio of concentration of each monomer in feed) and

$$n = D/M = (1/P_{DM})/(1/P_{MD}) = P_{MD}/P_{DM}$$

where n is the mole ratio of each monomer unit in the copolymer.   From plots of $n - 1$ versus x (Fig. 3), r_1' and r_1 were determined, and then $r_1 = 0.015$ and $r_1' = 0.224$ were obtained.   Theoretical values of n from the terminal model ($r_1 = 0.18$, $r_2 \sim 0$) and penultimate model ($r_1 = 0.015$, $r_1' = 0.224$, $r_2 = r_2' = 0$) were tabulated along with experimental values in Table III, and the terminal model indicated good agreement with the observed results.   On the other hand, since the run number in copolymer obtained by using the terminal model was in the range of 80–100, it was concluded the copolymers were about 1:1 alternate with a small content of
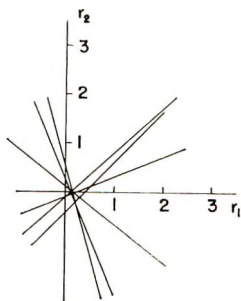
Fig. 2. Mayo-Lewis plot.
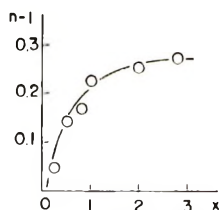
Fig. 3. Plot by Barb equation.

TABLE III

Calculations of Run Number, Linkage Probabilities, and Number-Average Chain Length in the Terminal Model and Comparison of n in Each Model with Experimental Values

| No. | [D]/[M] | Terminal model | | | | | | | $n =$ P_{MD}/P_{DM} | Penultimate model n | Experimental value $n = m_1/m_2$ |
		R	P_{DM}	P_{MD}	P_{DD}	P_{MM}	$\langle D \rangle^a$	$\langle M \rangle^a$			
2	0.183	98.4	0.959	0.990	0.041	0.009	1.04	1.01	1.032	1.039	1.033
3	0.429	96.3	0.905	1.029	0.095	0.000	1.11	0.97	1.137	1.088	1.138
4	0.675	94.3	0.873	1.005	0.127	0.000	1.14	0.99	1.151	1.133	1.151
5	1.01	91.7	0.827	1.009	0.174	0.000	1.21	0.99	1.220	1.187	1.220
6	1.50	88.1	0.787	0.981	0.213	0.019	1.27	1.02	1.247	1.257	1.247
7	2.48	81.8	0.728	0.915	0.272	0.085	1.37	1.09	1.257	1.370	1.257

$^a \langle D \rangle = [D(\%)]/(R/2)$ (number-average chain length of D sequence); $\langle M \rangle = [M(\%)]/(R/2)$ (number-average chain length of M sequence).[9]

Fig. 4. Charge transfer spectra between 4-methyl-1,3-dioxene-4 and maleic anhydride in chloroform (f_m denotes mole fraction of maleic anhydride). Solvent, chloroform; concentration of maleic anhydride, 0.486 mole/l.; concentration of 4-methyl-1,3-dioxene-4, 0.5101 mole/l.
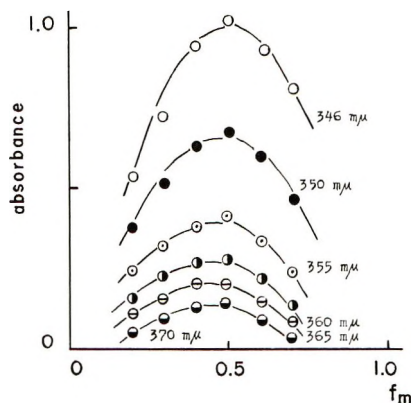
DD sequences, as indicated by number-average chain lengths $\langle D \rangle$ and $\langle M \rangle$.

To clarify the mechanism of alternate copolymerization spectrometrically, the charge transfer spectrum in various concentrations of 4-methyl-1,3-dioxene-4 and maleic anhydride in chloroform were measured by the continuous variation method[5] as shown in Figure 4. From the results, it was confirmed that in the initial step in copolymerization a charge-transfer 1:1 complex is formed between 4-methyl-1,3-dioxene-4 and maleic anhydride, of the same type as assumed by Iwazuki et. al.[2] in copolymerization of p-dioxene and maleic anhydride, i.e., a complex of the electron donor–acceptor type. It was also noted that in the present work the chloroform solution became yellow or brown on prolonged standing.

Terpolymerization of 4-Methyl-1,3-dioxene-4, Maleic Anhydride, and Styrene

Since it is well known that copolymerization of maleic anhydride with styrene produces an alternate copolymer, the 1:1:1 alternate terpolymer
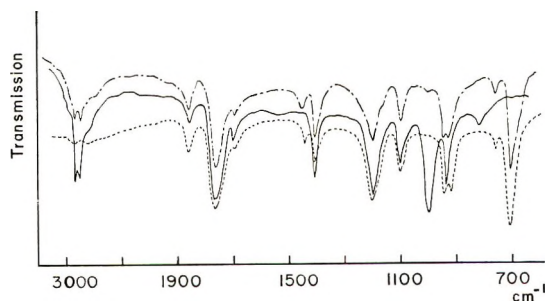
Fig. 5. Infrared spectra of copolymers and terpolymer: (——) DM copolymer; (- -) SM copolymer; (– · –) terpolymer.

TABLE IV

Terpolymerization of 4-Methyl-1,3-dioxene-4, Maleic Anhydride, and Styrene at 50°C. Catalyzed by α,α-Azobisisobutyronitrile

No.	M_1, mole	M_2, mole	M_3, mole	Mole ratios		Conversion, %	Reaction time, min.	Maleic anhydride content in terpolymer, mmole/g.[a]	
				M_1/M_2	M_3/M_2			By indicator	By electro-conductivity
1	0.005	0.005	0.040	1.0	8.0	7.60	20	3.90	—
2	0.010	0.010	0.030	1.0	3.0	28.5	15	3.03	3.34
3	0.015	0.015	0.020	1.0	1.33	10.6	15	3.45	3.60
4	0.020	0.020	0.010	1.0	0.50	44.3	15	3.40	—
5	0.005	0.025	0.030	0.2	1.20	48.4	9	3.33	3.38
6	0.010	0.020	0.030	0.5	1.50	58.4	13	3.00	3.36
7	0.020	0.010	0.030	2.0	3.0	9.46	20	3.91	3.97
8	0.025	0.005	0.030	5.0	6.0	5.78	29	3.10	—

[a] Maleic anhydride content in terpolymer composed of $(SMD)_n$ is 3.31 mmole/g.

Fig. 6. Infrared spectra of hydrolyzed and lactonized terpolymer: (———) lactonized (– · –) hydrolyzed.

may be formed in terpolymerization of 4-methyl-1,3-dioxene-4, maleic anhydride, and styrene. The results of terpolymerization are tabulated in Table 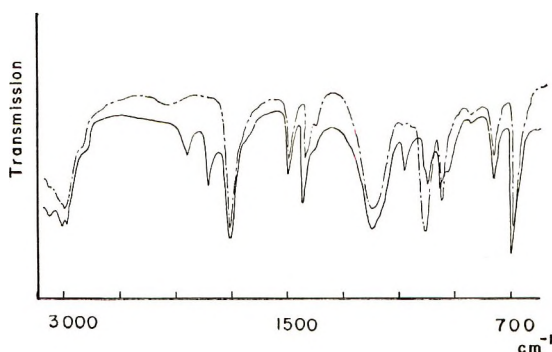IV. After hydrolysis of terpolymer, quantitative determination of carboxylic group showed that the terpolymer was approximately formed by SMD sequences. The infrared spectra of copolymers and the terpolymer are shown in Figure 5. In the maleic anhydride–styrene copolymer, the relative optical density I_{760}/I_{700} due to the MSM triad decreased as described by Harwood,[10] but in the terpolymer it increased markedly. It

TABLE V
Monomer Reactivity Ratios

Combination	r_1	r_2
DS	0.05 (r_{DS})	2.5 (r_{SD})
MS	~0.00 (r_{MS})	0.019 (r_{SM})[a]
DM	0.18 (r_{DM})	~0.00 (r_{MD})

[a] Data of Ang and Harwood.[12]

TABLE VI
Linkage Probabilities and Composition Ratios in Terpolymer

No.[a]	Linkage probabilities[b]						Composition ratio in terpolymer, D:M:S
	P_{DM}	P_{MS}	P_{SM}	P_{MD}	P_{SD}	P_{DS}	
1	0.0334	1.00	0.862	1.00	0.0065	0.961	1:0.98:2.1
2	0.0835	1.00	0.939	1.00	0.0071	0.876	1:0.96:1.9
3	0.1972	1.00	0.968	1.00	0.0074	0.802	1:0.98:1.8
5	0.1870	1.00	0.976	1.00	0.0015	0.806	1:0.99:1.8
6	0.1540	1.00	0.969	1.00	0.0366	0.840	1:0.93:1.75
7	0.0822	1.00	0.928	1.00	0.0141	0.909	1:0.98:1.95
8	0.0425	1.00	0.868	1.00	0.0318	0.919	1:0.89:2.0

[a] Experiment numbers correspond to those in Table IV.
[b] As example, the linkage probability P_{DM} was calculated by the following equation:
$P_{DM} = 1/\{[D]/[M]r_{DM} + 1 + [S]/[M](r_{DM}/r_{DS})\}$, where [D], [M], and [S] indicate concentrations of 4-methyl-1,3-dioxene-4, maleic anhydride, and styrene, respectively, in the feed mixture.

is not evident whether the increase of I_{760}/I_{700} in the terpolymer was due to DMS triad or SS diad in SSM or SSD triad sequences.

The presence of DMS triad sequence was apparently supported by the agreement of the experimentally determined (titration by indicator or electroconductivity) maleic anhydride content in the terpolymer with the theoretical value as SMD triad sequence. However, calculation of the composition in terpolymer by eqs. (2) and (3)[11] by using monomer reactivity ratios from Table V and linkage probabilities from Table VI indicated that the terpolymers had a 1:1:2 composition on the average, and this may support the presence of SS diad in terpolymer.

$$\frac{D}{M} = \frac{P_{MD}P_{SD} + P_{SM}P_{MD} + P_{MS}P_{SD}}{P_{DM}P_{SM} + P_{SD}P_{DM} + P_{DS}P_{SM}} \tag{2}$$

$$\frac{D}{S} = \frac{P_{MD}P_{SD} + P_{SM}P_{MD} + P_{MS}P_{SD}}{P_{DS}P_{MS} + P_{MD}P_{DS} + P_{DM}P_{MS}} \tag{3}$$

Hydrolysis of Terpolymer

In order to ascertain the presence of 4-methyl-1,3-dioxene-4 unit in terpolymer, ca. 1 g. of polymer (sample No. 5) was hydrolyzed by 1 cc. concentrated hydrochloric acid and 5 cc. water in 20 cc. dimethyl sulfoxide for 20 hr. on a steam bath. The reaction mixture was poured into water; the polymer precipitated was collected and dried at 80°C. The infrared spectrum of the hydrolyzed polymer is shown in Figure 6. It was found that anhydride (1765, 1845 cm.$^{-1}$) and ether linkages (1075 cm.$^{-1}$) in the original terpolymer were completely hydrolyzed and absorptions characteristic of carboxylic acid (1700 cm.$^{-1}$) and alcohol (1000 cm^{-1}) appeared in the hydrolyzed polymer. The polymer was easily soluble in methanol.

The lactonization of the hydrolyzed terpolymer was carried out by reacting ca. 0.5 g. of polymer and a few drops of concentrated sulfuric acid in 10 cc. dimethyl sulfoxide for 100 hr. at 65°C. The infrared spectrum of the lactonized polymer is also shown in Figure 6. The absorption of alcohol at 1000 cm.$^{-1}$ decreased and moreover, absorptions at 1770 and 1850 cm.$^{-1}$ appeared; and these may be considered to be due to β-lactone and γ-lactone, although these absorptions were near to that of the carboxylic anhydride group. However, the lactonized polymer still had free carboxylic acid group.
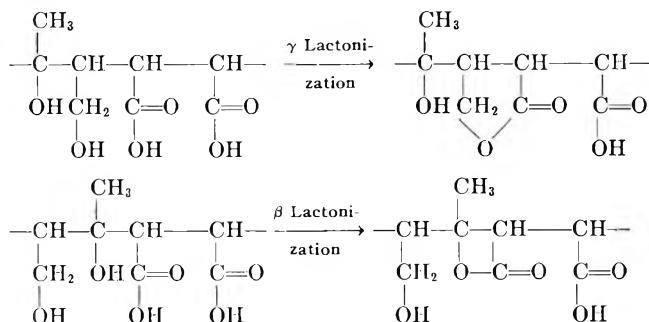
References

1. S. Iwazuki and Y. Yamashita, *Kōgyo Kagaku Zasshi*, **67**, 1467, 1470 (1964).

2. S. Iwazuki and Y. Yamashita, *Makromol. Chem.*, **89**, 205 (1965).

3. S. Murahashi and S. Nozakura, *Kōbunshi Kagaku*, **23**, 361 (1966); *ibid.*, **22**, 739 (1965); *Bull. Chem. Soc. Japan*, **38**, 1560 (1965).

4. W. Kawai, *J. Polymer Sci.*. in press.

5. P. Job, *Ann. Chim.* [9] **10**, 113 (1928).

6. H. H. Jaffe and M. Orchin, *Theory and Applications of Ultraviolet Spectroscopy*, 1962, p. 581.

7. F. R. Mayo and F. M. Lewis, *J. Am. Chem. Soc.*, **66**, 1594 (1944).

8. T. Alfrey and G. Goldfinger, *J. Chem. Phys.*, **12**, 205 (1944).

9. H. J. Harwood and W. M. Ritchey, *J. Polymer Sci. B*, **2**, 601 (1964).

10. H. J. Harwood, *Angew. Chem.*, **77**, 1124 (1965).

11. G. E. Ham, *Copolymerization*, Interscience, New York, 1964, p. 38.

12. T. L. Ang and H. J. Harwood, paper presented at 147th American Chemical Society Meeting, Philadelphia, April 1964.

Charge Transfer Complexes of *N*-Ethylcarbazole and Poly-*N*-Vinylcarbazole

A. REMBAUM, A. M. HERMANN, and R. HAACK, *Jet Propulsion Laboratory, California Institute of Technology, Pasadena, California 91103*

Synopsis

Poly-*N*-vinylcarbazole and its monomeric analog, i.e., *N*-ethylcarbazole, act as donors in charge transfer complexes with such electron acceptors as iodine, tetracyanoethylene, and tetracyanoquinodimethane. Poly-*N*-vinylcarbazole and *N*-ethylcarbazole are also capable of accepting electrons from an alkali metal such as sodium. A study of the spectral properties of both types of complexes showed that the monomer can both accept and donate electrons to a greater extent than the corresponding unit segment of the polymer chain. Equilibrium constants are presented for both cases, and estimates of the ionization potential of *N*-ethylcarbazole and related compounds are made from the characteristic charge transfer frequencies. Good agreement between these values and those calculated from molecular orbital theory is outlined.

INTRODUCTION

Charge transfer complexes of a great variety of organic compounds have been reviewed in detail by Briegleb[1] and Andrews and Keefer.[2] The continued interest in this area is evidenced by the large number of reports in the recent literature.[3] However, relatively little information exists concerning charge transfer complexes in which either the donor or the acceptor consists of a polymeric species. Recently the studies of electronic transport properties of organic materials have been extended to polymers such as polystyrene, isomeric polyvinylnaphthalenes, polybiphenylenes, and poly-*N*-vinyl carbazole complexed with quinones and other reagents of high electron affinity.[4-6] Similarly the conductivity of polyethylene,[7] poly-*N*-vinylcarbazole,[8] polyvinylpyridine,[9] and polyphenylenes[10] complexed with iodine was investigated in detail. Smets and co-workers[11] studied the donor–acceptor complexes of 2,4-dinitropolystyrene and *p*-dimethyl aminopolystyrene as well as their monomeric homologs with napthalenic hydrocarbons and amines. Little difference was noted between the polymeric materials and their low molecular weight homologs. To our knowledge, only in one case was a detailed spectrophotometric study made in which the equilibrium constant of the polymeric complex was compared with that of the corresponding complex of the unit segment; Sugiyama and Kamigawa[12] have carried out an investigation of absorption maxima and equilibrium constants for charge transfer complexes formed between polyvinylpyridines and

quinones and the measured optical properties were compared with mono-meric molecules similar to the unit segments. In the above investigations, as well as in those of Smets and co-workers, the polymeric and the mono-meric complexes were found to be unstable and their absorption spectra underwent considerable changes with time and concentration. Further-more, the charge transfer bands exhibited by the polymeric complexes did not coincide with those of the monomeric complexes with which they were compared.

In the work described below, a spectrophotometric study was carried out with poly-N-vinylcarbazole (PVCA) complexed with iodine, tetracyano-ethylene (TCNE), and tetracyanoquinodimethane (TCNQ). The results were compared with those obtained by the use of the monomeric analog, i.e., N-ethylcarbazole (NECA) complexed with the same acceptors.

With the exception of TCNQ complexes, our materials were characterized by excellent stability. The polymeric as well as the monomeric complexes exhibited identical spectra independent of concentration. It was found that in every case the equilibrium constant determined by the use of the Benesi-Hildebrand method[13] was higher for the monomer than for the polymer.

An analogous phenomenon of charge transfer from an alkali metal to an aromatic polymer was compared with electron transfer to its monomeric analog. As in the previous case, the electron transfer occurred to a greater extent with the monomer than with the polymer.

EXPERIMENTAL

Reagents

N-Ethylcarbazole (NECA) from Aldrich Chemical Company was re-crystallized in presence of charcoal from methanol three times and vacuum-dried at 40°C., m.p. 68–69°C. (literature m.p. 68°C.).

Poly-N-vinylcarbazole (PVCA) from Borden Chemical Company was precipitated from benzene with methanol and vacuum-dried at 50°C. The intrinsic viscosity ($[\eta]$ = 0.8 dl./g.) was determined in benzene at 25.0°C.

N-Methylpyrrole from Aldrich Chemical Company was vacuum-distilled from potassium hydroxide immediately before using.

Tetracyanoethylene (TCNE) was recrystallized from ethyl acetate followed by vacuum sublimation.

Tetracyanoquinodimethan (TCNQ) was used as received from E. I. du Pont de Nemours Company.

All absorption measurements were carried out with spectrophotometric grade methylene chloride as the solvent.

Spectrophotometric Analysis

Spectra were obtained by means of a Cary 14 Spectrophotometer using 10 mm. fused silica cells with spacers (1 mm. optical path). Absorption

maxima were recorded immediately after filling cells in order to reduce evaporation effects.

Desired iodine concentrations for sample and reference cell solutions were obtained by taking 5-cc. aliquots from 25-cc. stock solutions. Spectra were taken 30–60 min. after preparation of the charge transfer complex solution. The same iodine stock solutions were used for spectral determinations with the polymer and monomer. The solutions of other acceptors were used in the same manner as the iodine solution.

RESULTS

Optical Spectra

In Figure 1 are shown absorption spectra of NECA–I and PVCA–I complexes both taken at identical concentrations in methylene chloride. Included in this figure is the spectrum of pure NECA which does not absorb to any significant extent in the region of the charge transfer band, namely at 402 mμ. Figure 1 also shows that at lower concentrations (approximately $5 \times 10^{-3}M$) the charge transfer band is not observable. It should be noted that the absorbance of NECA–I is greater than the absorbance of PVCA–I at identical concentrations.

The 1:1 stoichiometry of both the polymeric and monomeric complexes is shown in Figure 2; it is seen here that the absorbance is maximum at 50 mole-% of iodine. The data in Figure 2 were taken on maintaining the total number of molecules (donor plus acceptor) in the optical cell constant.

Similar results to those obtained with iodine were also found during the spectrophotometric study of the same donors with other acceptors. Figure 3 shows the charge transfer bands of NECA–TCNE, PVCA–TCNE, NECA–TCNQ, and NECA–I. In the same figure the spectrum of a similar donor, namely N-methylpyrrole complexed with iodine, is included for purposes of comparison.
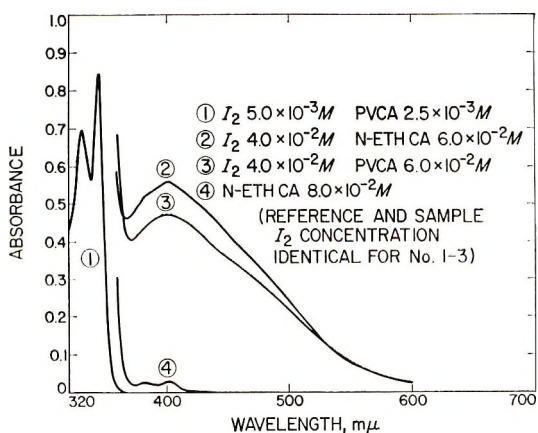

Fig. 1. Optical absorption spectra of PVCA–1 and NECA–I charge transfer complexes in methylene chloride.
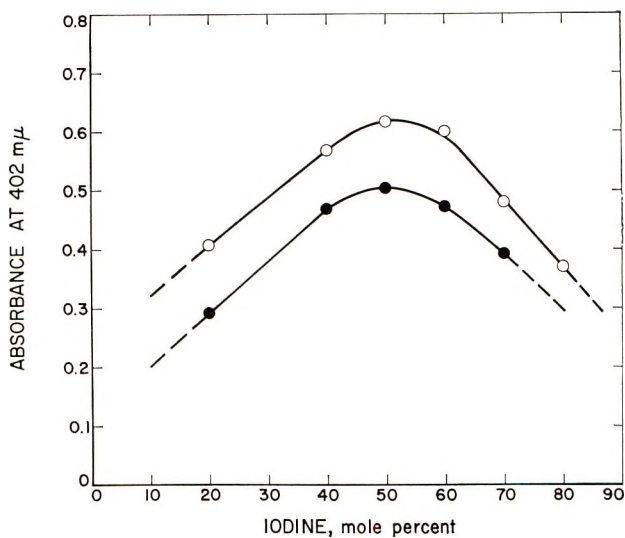
Fig. 2. Variation of absorbance with molar percentage of iodine for PVCA–I and NECA–I charge transfer complexes at 402 mμ (100 mole-% of iodine corresponds to 0.1M solution).

The appearance of a new charge transfer band in the PVCA–I complex is very evident when iodine vapor is diffused into a film of PVCA (Fig. 4a). The similarity of this spectrum taken in the solid state (film) with the one measured in methylene chloride indicates that the solvent does not influence the charge transfer absorption spectrum to a significant extent. The shoulder at about 510 mμ is due to a small amount of uncomplexed iodine in the film. This conclusion comes from the comparison of Figure 4a with Figure 4b, the latter representing the spectrum of pure iodine in methylene chloride.

Equilibria

Equilibrium constants (k) and molar extinction coefficients (ϵ) were calculated from Benesi-Hildebrand plots.[13] The value of k and ϵ obtained for NECA and PVCA complexed with iodine, TCNE, and TCNQ are given in Table I. In these cases where the equilibrium constant could be measured accurately, it was found to be higher for the monomer than for the polymer. The equilibrium constant for the PVCA–I complex could not be determined unambiguously due to the limited solubility of PVCA in methylene chloride and the high absorbance of iodine at high concentration in the range 350–540 mμ (Fig. 4b). This did not permit the use of donor or acceptor in excess. The λ_{max} of TCNQ complexes of NECA and PVCA remained unchanged with time and concentration; however the extinction coefficient of TCNQ complexes of PVCA did decrease with time, and care was therefore taken to measure the intensity of absorption immediately after sample preparation.

Fig. 3. Absorption spectra of NECA–TCNE, PVCA–TCNE, NECA–TCNQ, NECA–I and N-methylpyrrole–I in methylene chloride: (1) TCNE 2.0 × 10⁻³M, NECA 4.0 × 10⁻²M, optical path 1 cm.; (2) TCNE 8.0 × 10⁻³M, PCVA 3.08 × 10⁻²M, optical path 1 cm.; (3) TCNE 1.0 × 10⁻²M, NECA 1.2 × 10⁻¹M, optical path 1 cm.; (4) I₂ 4.0 × 10⁻²M, NECA 6.0 × 10⁻²M, optical path 0.1 cm.; (5) I₂ 1.0 × 10⁻³M, N-methylpyrrole 1.05 × 10⁻³M, optical path 0.1 cm.
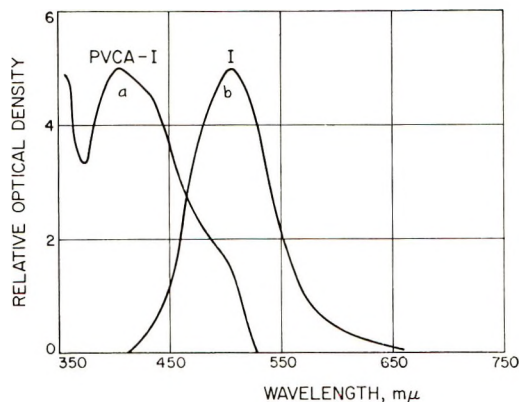
Fig. 4. Optical absorption spectra of (a) PVCA–I$_2$ in film form (iodine concentration 5–10% by weight); (b) pure iodine in dichloromethane.

In the reaction of NECA and PVCA with sodium involving an electron transfer from the alkali metal to the aromatic hydrocarbon, both NECA and PVCA act as electron acceptors. In this reaction the equilibrium constant was also found to be smaller for the polymer than for the monomer.

TABLE I

Equilibrium Constants and Molar Extinction Coefficients of NECA and PVCA Complexes with Various Acceptors

Donor	Donor concentration range, mole/l.	Acceptor	Acceptor concentration, mole/l.	λ_{max}, mμ	ϵ_{max}	k (at room temperature), l./mole
NECA	4.0×10^{-2}–9.6×10^{-2}	TCNE	2.0×10^{-3}	600	1090	5.85
PVCA	3.1×10^{-2}–6.2×10^{-2}	TCNE	8.0×10^{-3}	600	1060	1.30
NECA	2.5×10^{-1}–4.0×10^{-1}	I$_2$	1.0×10^{-2}	402	7100	0.33
NECA	2.4×10^{-1}–3.0×10^{-2}	TCNQ	1.0×10^{-3}	590	2770	2.87
PVCA	1.2×10^{-1}–3.0×10^{-2}	TCNQ	2.0×10^{-3}	595	1310	1.19

TABLE II

Equilibrium Constants for Electron Transfer from Sodium to NECA and PVCA

Donor (in excess)	Acceptor	Acceptor concentration, mole/l.	ϵ_{max}	λ_{max}	k (at $-80°$C.), l./mole
Na	NECA	1.6×10^{-2}	15,600	393	2.2
Na	PVCA	2.0×10^{-1}	—	393	0.031

Details for the determinations of these equilibrium constants at $-80°C$. are described in previous papers,[14,15] and the values of the equilibrium constant k are given in Table II. Since the concentration of radical ions (and consequently the absorbance) decreases with increase of temperature,[14] measurements at higher temperatures become less reliable. This, along with the possibility of chain scission of the polymer precluded determinations of k at higher temperatures.

CONCLUSIONS

A comparison of absorption spectra of a polymeric donor–acceptor complex with its monomeric homolog presents a number of difficulties, one of which is the fact that side reactions might be taking place during complex formation. Spectral shifts and instability could be due partly to reactions between donor and acceptor or to the presence of impurities.

It is believed that the systems studied here, in particular PVCA–I, NECA–I, PVCA–TCNE, and NECA–TCNE, represent well defined systems. The absence of side reactions and impurities was ascertained by the examination of infrared spectra of these materials complexed with iodine. The infrared absorption spectra in the range of 3–15 μ of NECA–I and PVCA–I was found to be identical to both monomeric and polymeric donors. In addition, no other products than the donor and acceptor could be detected by thin layer chromatography in all the cases investigated here. In spite of the fact that the extinction coefficient of the NECA–TCNQ and PVCA–TCNQ complexes decreased slowly with time, measurements on both at the same initial time also led to the same result, namely that the equilibrium constants for the monomer was higher than for the polymer. The reason for this observation could be due to one or more of the following factors: (1) difference in the ionization potentials between the monomer and the corresponding unit segment of the polymeric chain; (2) charge repulsion or attraction in the polymer chain; (3) steric hindrance due to chain configuration.

The first factor does not seem likely, since the λ_{max} of the charge transfer band is the same for the above monomeric and polymeric donor acceptor complexes.

Figure 2 indicates that charges introduced through complex formation do not play a significant role since the curves are reasonably symmetrical. This would not be expected in the case of considerable coulomb attraction or repulsion forces. The latter would be very much greater at high iodine concentration than at low iodine concentration. Thus it appears that the main reason for the weaker charge transfer interactions in polymers is predominately a result of steric hindrance.

The present study permits the calculation of the ionization potential of pyrrole, N-methylpyrrole, and N-ethylcarbazole applying the semiempirical relation for iodine complexes proposed by McConnel et al.[16] together with the experimentally determined charge transfer frequencies. The results of these calculations are shown in Table III. In Table III are also recorded

TABLE III

	Pyrrole	N-Methyl-pyrrole	Indole	N-Methyl-indole	Carbazole	N-Methyl-carbazole	N-Ethyl-carbazole
$\lambda_{CT-Iodine}$, mμ	360	362	—	—	—	—	402
Coefficient of β for the highest occupied molecular orbital[a]	0.618	0.618	0.534	0.432	0.539	0.370	—
I_{mo}, e.v.[b]	8.18	8.18	7.92	7.53	7.93	7.40	>7.40[e]
$I_{CT-Iodine}$, e.v.[d]	8.20	8.12	—	—	—	—	7.75
$I_{measured}$, e.v.							
(By electron impact)[e]	8.97	—	—	—	—	—	—
(By UV and photoionization)[f]	8.20	—	—	—	—	—	—

[a] The parameters for the Coulomb and resonance integrals for pyrrole, indole, and carbazole were: $\alpha_N = \alpha_c + \beta_c$ and $\beta_{N-C} = 0.9\beta$, respectively. The parameters for methyl pyrrole, methyl indole, and methyl carbazole were: $\alpha_N = \alpha_c + 0.5\beta_c + 6.24$, according to Wacks and Dibeler.[17]

[b] Calculated on the basis of $I_{mo} = 3.14 \times$ (coefficient of β) + 6.24, according to Wacks and Dibeler.[17]

[c] The MO calculations were performed for N-methylcarbazole. The ionization potential of N-ethylcarbazole is anticipated to be slightly higher than N-Methyl carbazole due to the likely larger inductive effect of the ethyl over the methyl group.

[d] Calculated on the basis of $\nu_{CT} = 0.94 I_{CT-Iodine} - 0.42$, according to McConnell et al.[18]

[e] Data of Baba et al.[18]

[f] Data of Watanabe and Nakayama.[19]

the coefficients of the resonance integral β for the highest occupied molecular orbitals calculated by the simple HMO technique with the parameters shown in Table III. The equation of Wacks and Dibeler[17] provides an estimate of ionization potentials from the coefficients of β, and it is seen (Table III) that these estimates are in good agreement with the ionization potential values derived from the charge transfer frequencies. In the only case where the ionization potential was determined by direct measurement, namely for pyrrole, the ultraviolet and photoionization technique gave an identical value to that based on the charge transfer frequency.

References

1. G. Briegleb, *Electronen-Donator-Acceptor-Komplexe*, Springer-Verlag, Berlin, 1961.

2. L. J. Andrews and R. M. Keefer, *Molecular Complexes in Organic Chemistry*, Holden-Day, San Francisco, 1964.

3. A. Rembaum, Z. M. Hermann, and Y. Matsunaga, *Electronic Properties of Monomeric and Polymeric Charge Transfer Complexes*, in press.

4. W. Slough, *Trans. Faraday Soc.*, **58**, 2360 (1962).

5. A. Taniguchi, S. Kanda, T. Nogaito, S. Kasabayashi, H. Mikawa, and K. Ito, *Bull. Chem. Soc. Japan*, **37**, 1386 (1964).

6. J. H. Lupinski and K. D. Kopple, *Science*, **146**, 1038 (1964).

7. N. A. Bakh, A. K. Vannikow, A. D. Grishina, and S. V. Nizhnig *Usp. Khim.* **34**, No. 10, 1733 (1965).

8. A. M. Hermann and A. Rembaum, *Electrical Conduction Properties of Polymers* (*J. Polymer Sci. C*, **17**), A. Rembaum and R. F. Landel, Eds., Interscience, New York, 1966, p. 107.

9. S. B. Mainthia, P. L. Kronick, and M. M. Labes, *J. Chem. Phys.*, **41**, 2206 (1964).

10. S. B. Mainthia, P. L. Kronick, H. Ur, E. F. Chapman, and M. M. Labes, paper presented at 144th American Chemical Society Meeting, Los Angeles, April 1963; *Polymer Preprints*, **4**, No. 1, (1963).

11. G. Smets, V. Balogh, and Y. Castille, in *Macromolecular Chemistry* (*J. Polymer Sci. C*, **4**), M. Magat, Ed., Interscience, New York, 1964, p 1467

12. H. Sugiyama and H. Kakagawa, *J. Polymer Sci. A-1*, **4**, 2281 (1966).

13. H. A. Benesi and J. H. Hildebrand, *J. Am. Chem. Soc.*, **71**, 2703 (1949).

14. A. Rembaum, A. Eisenberg, R. Haack, and R. F. Landel, *J. Am. Chem. Soc.*, **89**, 1062 (1967); F. E. Stewart and A. Rembaum, *J. Macromol. Sci. Chem.*, **A1** (6), 1143 (1967).

15. A. M. Hermann, A. Rembaum, and R. Carper, *J. Phys. Chem.*, **71**, 2661 (1967).

16. H. McConnell, J. S. Ham, and J. R. Platt, *J. Chem. Phys.*, **21**, 66 (1953).

17. M. E. Wacks and V. H. Dibeler, *J. Chem. Phys.*, **31**, 1557 (1959).

18. H. Baba, Y. Omura, and V. Higasi, *Bull. Chem. Soc. Japan*, **29**, 521 (1956).

19. K. Watanabe and T. Nakayama, ASTIA Report No. 152934.

A Study of the Enzymic Degradation of CMC and Other Cellulose Ethers

M. G. WIRICK, *Research Center, Hercules Incorporated,*
Wilmington, Delaware 19899

Synopsis

Accelerated enzymic degradation of a series of six sodium carboxymethylcelluloses (CMC) varying in degree of substitution (DS) from 0.41 to 2.45 demonstrated that stability improves with increasing substitution, the DS 2.45 sample being essentially refractory to enzyme attack. The concentration of completely unsubstituted anhydroglucose (AHG) units in these samples, determined by acid hydrolysis followed by a glucose assay, is less at all substitution levels than would be expected from the relative etherification rates of the C_2, C_3, and C_6 hydroxyls reported in the literature. Assuming random distribution of the unsubstituted AHG units, the frequency of single (1U) and multiple adjacent (xU) sequences can be predicted. Consideration of the extent of enzymic degradation, expressed in terms of the decrease in average molecular chain length deduced from $[\eta]$ measurements, indicated that in CMC chain scission occurs only at xU sites. A limited comparison of the performance of methyl-, hydroxyethyl-, and hydroxypropylcelluloses under identical conditions revealed that, by contrast, in these ethers enzyme-induced chain scission is possible not only at xU but also adjacent to 1U. The hydroxyalkyl and methyl groups appear to offer approximately equivalent protection against enzyme attack.

INTRODUCTION

A previous paper[1] described a study of the enzymic hydrolysis of a series of hydroxyethylcellulose (HEC) samples, varying in moles of combined substituent from 1.9 to 3.7, in which the rate and extent of degradation were correlated with the frequency and distribution of completely unsubstituted (U) anhydroglucose (AHG) units. This report covers a similar study of sodium carboxymethylcellulose (CMC) in comparison with a limited number of samples of other cellulose ethers.

EXPERIMENTAL

Samples

A total of 11 cellulose derivatives were considered, including six CMC's, three HEC's, one methylcellulose (MC), and one hydroxypropylcellulose (HPC). The characteristics of these samples are summarized in Table I. Substitution is expressed in terms of the degree of substitution (DS, the average number of substituted hydroxyl groups per AHG unit), the substi-

TABLE I

Description of Cellulose Ethers Used in Enzymic Degradation Study

Sample no.	Cellulosic	DS	MS	SI	M_0[a]	Predicted tot. U	Measured tot. U	Per 1000 AHG units										
								1U	2U	3U	4U	5U	6U	7U	8U	9U	10U	11U
(1)	(2)	(3)	(4)	(5)	(6)	(7)	(8)	(9)	(10)	(11)	(12)	(13)	(14)	(15)	(16)	(17)	(18)	(19)
1	CMC	0.41	—	38.0	195	633	620	90	56	34	21.3	13.2	8.2	5.1	3.2	2.0	1.2	0.8
2	CMC	0.79	—	70.0	225	370	300	147	44.1	13.2	4.0	1.2	0.36	0.1	—	—	—	—
3	CMC	0.89	—	75.2	233	315	248	140	33.0	8.6	2.1	0.52	0.13	<0.10	—	—	—	—
4	CMC	0.97	—	80.0	240	274	200	130	25.3	5.1	1.0	0.21	<0.10	—	—	—	—	—
5	CMC	1.30	—	89.9	266	135	101	81	8.2	0.8	0.1	<.10	—	—	—	—	—	—
6	CMC	2.45	—	99.9	358	<1	≈1	1	—	—	—	—	—	—	—	—	—	—
7	HEC	1.1[b]	1.92	81.9	247	270	181	125	22.0	3.9	0.70	0.13	—	—	—	—	—	—
8	HEC	1.2[b]	2.25	88.5	261	227	115	89	10.3	1.15	0.13	—	—	—	—	—	—	—
9	HEC	1.6[b]	3.70	95.8	325	113	42	38	1.6	<0.10	—	—	—	—	—	—	—	—
10	MC	1.85[c]	—	92.1	188	54	79	68	5.3	0.42	<0.10	—	—	—	—	—	—	—
11	HPC	2.1[d]	4.2	99.7	406	—	≈3	3	—	—	—	—	—	—	—	—	—	—

[a] Average weight of substituted AHG unit.
[b] Estimated.
[c] Nominal value.
[d] Clarke and Conner.[2]

tution index (SI, the percentage of substituted AHG units) and, where applicable, the molar substitution (MS, moles of substituent per mole of AHG units). The unit molecular weight M_0 (weight of AHG unit plus that of average amount of substituent) is listed for each ether in column 6.
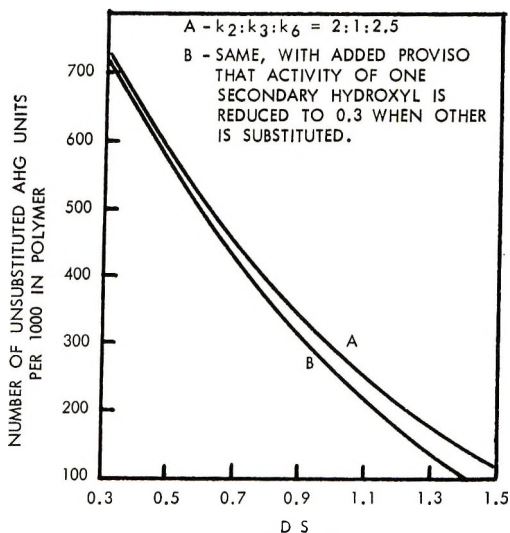

Fig. 1. Predicted incidence of unsubstituted AHG units in CMC from relative reaction rates of hydroxyl groups. See Croon and Purves.[3]
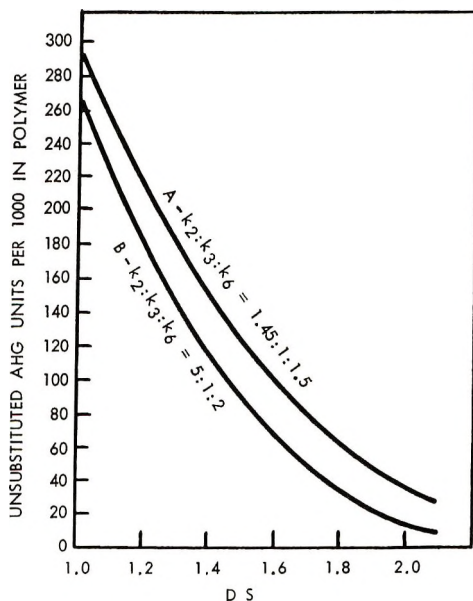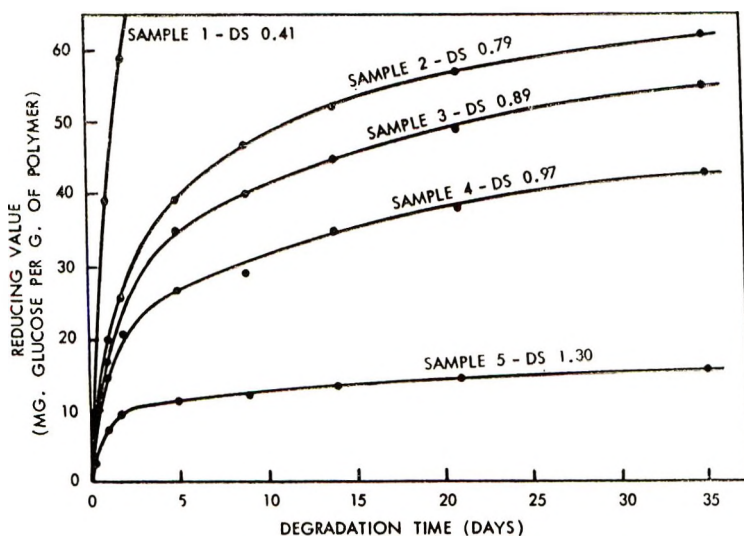

Fig. 2. Predicted incidence of unsubstituted AHG units in MC from relative reaction rates of hydroxyl groups. See (curve A) Smith and Smith[4] and (curve B) Croon.[5]

Fig. 3. Progress of enzymic degradation of CMC samples of varying substitution as indicated by reducing-ends measurements.

The predicted frequency of U per 1000 AHG units in these samples (column 7) is based on reported relative reaction rates of the various available hydroxyl groups; see Figure 1, curve B, Figure 2, curve A, and, in Wirick,[1] Figure 1, upper curve. The actual measured concentration of U (column 8) was determined by complete acid hydrolysis followed by a glucose assay, whereas the predicted frequency of sequences of adjacent unsubstituted AHG units per 1000 AHG units (1U, 2U, 3U, etc.; see columns 9–19) was estimated from the total measured U, assuming random distribution; see Wirick,[1] Figure 3.

Procedure

The average chain length or degree of polymerization, DP, of these samples, both before and after degradation, was estimated from the following relationships at 25°C.:

$$\text{CMC, } [\eta]_{0.1N\ NaCl} = 1.8 \times 10^{-2}\ \overline{DP}_w^{0.79} \quad \text{(Brown et al.[6])}$$
$$\text{MC, } [\eta]_{H_2O} = 2.92 \times 10^{-2}\ \overline{DP}_n^{0.905} \quad \text{(Savage[7])}$$
$$\text{HEC, } [\eta]_{H_2O} = 1.1 \times 10^{-2}\ \overline{DP}_w^{0.87} \quad \text{(Brown et al.[8])}$$
$$\text{HPC, } [\eta]_{H_2O} = 1.17 \times 10^{-2}\ \overline{DP}_w^{0.90} \quad \text{(Stow[9])}$$

As in earlier work,[1] a 2:1 $\overline{DP}_w / \overline{DP}_n$ ratio was assumed. Intrinsic viscosity, reducing-ends measurements, acid hydrolyses, and glucose analyses were made by methods previously described.[1]

As before, the commercially available celluloytic enzyme complex, Cellase 1000 (Wallerstein Laboratories, Staten Island, N.Y.), derived from *Aspergillus niger*, was used as the degrading agent either under the standard or accelerated conditions listed below:

	Polymer concn., % by wt.	Enzyme concn. (based on polymer)	Temp., °C.
Standard	2	400 ppm	25
Accelerated	1	1%	37

In both cases the cellulose ethers were studied in aqueous solution at pH 6 (phthalate buffer), protected by a biocide (Ottasept extra, 4-chloro-3,5-xylenol, 100 ppm). It was demonstrated that 72 hr. of treatment under the accelerated conditions resulted in degradation equivalent to 8.5 mo. at the standard conditions.

RESULTS AND DISCUSSION

By the standard enzymic degradation technique the performances of a series of CMC samples of varying degrees of substitution were compared by following the change in reducing-ends value (Fig. 3) and intrinsic fluidity (Fig. 4). Because both of these parameters can be related to molecular chain breaks, it is obvious that polymer stability improves with increasing DS and that the rate of scission is rapid at first and then slows as an apparent asymptotic limit is approached. This behavior was observed earlier in the case of HEC.[1] At a sufficiently high substitution level CMC appears to be essentially refractory to enzyme attack (Fig. 4, sample 6).

Results of accelerated enzymic degradation studies of four CMC's, three HEC's, one MC, and one HPC are summarized in Table II in terms of decrease in DP and liberation of glucose. The observed number of chain breaks (column 13) represents the difference between the number of molecules per 1000 AHG units in the original (column 8) and degraded (column 12) samples. Although Cayle[10] and Holden and Tracey[11] concluded that cellulase effects chain scission between pairs of contiguous unsubstituted AHG units in CMC, the data in Table II indicate that enzyme attack (column 17) probably occurs at sequences of three or
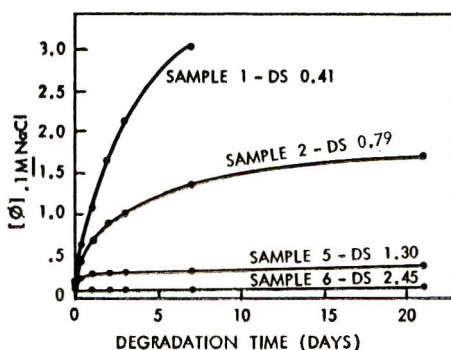

Fig. 4. Effect of enzymic degradation on intrinsic fluidity of CMC samples of varying substitution.

TABLE II

Glucose Liberated from, and Molecular Chain Breaks in, Cellulose Ethers Subjected to Enzymic Degradation

Sample no.	Cellulosic	SI	G/A[a]	$[\eta]$	Original			$[\eta]$	After enzymic degradation			Obs. chain breaks	Per 1000 AHG units[c]			Indicated sequences attacked by enz.
					$\overline{DP}_w$	$\overline{DP}_n$	M/A[b]		$\overline{DP}_w$	$\overline{DP}_n$	M/A[b]		1U	$2U^+$	$3U^+$	
(1)	(2)	(3)	(4)	(5)	(6)	(7)	(8)	(9)	(10)	(11)	(12)	(13)	(14)	(15)	(16)	(17)
1	CMC	38.0	183	4.9	1180	590	1.7	0.19	20	10	100	98.3	90	146	90	$3U^+$
2	CMC	70.0	27.5	6.9	1820	910	1.1	0.82	124	62	16.1	15.0	147	63	18.9	"
5	CMC	89.9	7.8	7.5	2020	1010	1.0	3.9	890	445	2.2	1.2	81	9.2	1.0	"
6	CMC	99.9	3.5	10.8	3200	1600	0.6	9.8	2860	1430	0.7	0.1	≈1	0.0	0.0	"
7	HEC	81.9	32.6	4.2	920	460	2.2	0.25	36	18	55.5	53.3	125	26.8	4.8	$2U^+$; some 1U
8	HEC	88.5	18.5	5.0	1140	570	1.8	0.48	76	38	26.3	24.5	89	11.6	1.3	"
9	HEC	95.8	6.9	1.8	350	175	5.7	0.70	118	59	17.0	10.3	38	1.7	0.1	"
10	MC	92.1	5.1	4.75	—	275	3.6	0.86	—	41.5	24.1	20.5	68	5.8	0.5	$2U^+$; many 1U
11	HPC	99.7	—[d]	4.0	650	325	3.1	3.0	470	235	4.2	1.1	≈3	0	0	1U

[a] Molecules of glucose per 1000 AHG units.

[b] Molecules per 1000 AHG units.

[c] $2U^+$, number of sequences 2 or more AHG units in length; $3U^+$, number of sequences 3 or more AHG units in length.

[d] None detected.

more (3U$^+$) adjacent unsubstituted units (compare figures in columns 13 and 16).

Holden and Tracey[11] and Savage[12] postulated enzymic chain scission adjacent to isolated unsubstituted AHG units in MC. The current results substantiate this view, not only for MC, but also for hydroxyalkylcellulose. Previously reported data[1] indicated, however, that in the case of HEC the rate of polymer chain breaks is much higher at multiple adjacent sequences
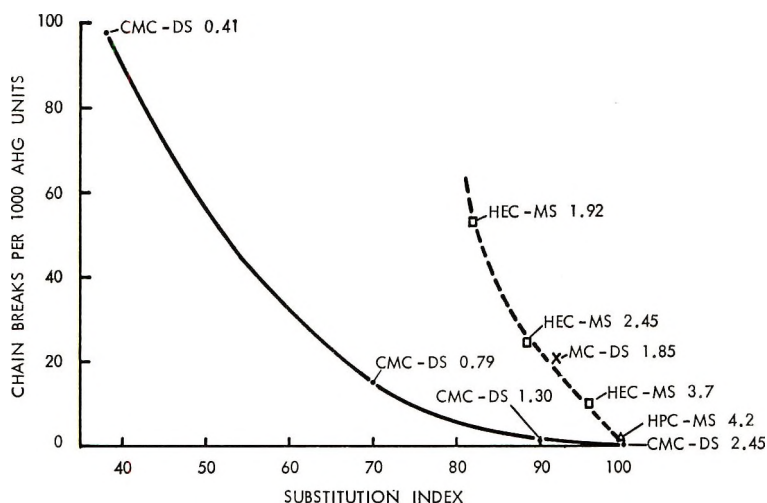

Fig. 5. Effect of substitution on resistance of various cellulose ethers to enzymic degradation.
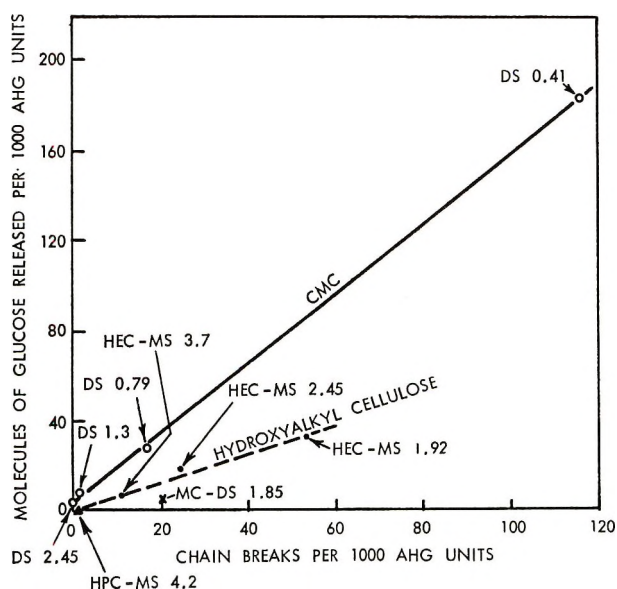
Fig. 6. Glucose released during enzymic degradation of various cellulose ethers.

(2U, 3U, etc.) than adjacent to isolated unsubstituted units. Presumably this is also true of MC. The enzyme-induced chain scission in the HPC included in this study must necessarily have occurred primarily adjacent to single, unsubstituted AHG units, since the total concentration of unsubstituted units is so low.

Estimated chain breaks are plotted as a function of SI in Figure 5. It is apparent that the resistance of CMC to enzymic degradation is better than that of any of the other cellulose ethers studied at all levels of substitution. The hydroxyalkyl derivatives present an approximately homogeneous pattern of behavior, as illustrated by the broken line, essentially equivalent to that characteristic of MC.

The glucose released during enzymic degradation (Table II, column 4) is depicted graphically as a function of chain breaks (Table II, column 13) in Figure 6. In the case of the CMC samples (1 and 2) of lower substitution, for which the data are most meaningful, the ratio of molecules of glucose released to number of chain breaks observed is approximately 2:1. This ratio lends weight to the conclusion that in this cellulose ether chain scission takes place only at xU sequences.

In the case of HEC a molecule of glucose is released for every 1.7 chain breaks, whereas for MC the ratio is 1:4. No glucose has ever been detected in enzymically degraded HPC in our laboratory.

CONCLUSIONS

In the case of those cellulose ethers (CMC, HEC, and MC) for which such information is available, there is poor agreement between the frequency of completely unsubstituted AHG units estimated from reaction rates reported in the literature and that determined by acid hydrolysis (see Table I, columns 7 and 8). Fewer unsubstituted units are present than expected in all derivatives except MC.

For HEC excellent agreement between the expected and observed frequencies of unsubstituted AHG units is obtained, if the relative reaction rate for the formation of polyethylene oxide side chains, reported by Croon and Lindberg,[13] is reduced from 20 to 10.[1] It is obvious, however, that the substitution pattern of HPC is quite different from that of HEC, probably because of the formation of secondary, rather than primary hydroxyls, when the alkylene oxide adds to cellulose in the synthesis of the former. At an MS level of approximately 4 the concentration of unsubstituted AHG units in HPC is only one tenth that in HEC. However, at an MS of approximately 3, HEC contains no more unsubstituted units than MC at a DS of 1.85.

As previously reported[1] for HEC, unsubstituted AHG units in the polymer chain appear to be the foci of enzyme attack; thus, the SI appears to

be a better criterion of resistance to enzymic degradation than either DS or MS.

The protective or enzymic blocking effect of various substituents varies appreciably at the same substitution level. Of those studied the carboxymethyl group is the most effective; in CMC chain scission appears to occur only at sequences of three or more $(3U^+)$ adjacent, unsubstituted AHG units. A sample of DS 2.45 $(SI \approx 99.9)$ was completely resistant to enzyme attack. As previously reported,[1] enzymic chain scission in HEC proceeds relatively rapidly at multiple adjacent unsubstituted sites $(2U^+)$ and much more slowly at sites adjacent to isolated, unsubstituted AHG units. Apparently the degradations of MC and of HPC progress in the same fashion, but their rates and ultimate extents of degradation are lower because the level of substitution is higher, as is normal for the common commercial types of these two ethers.

The foregoing discussion is predicated on the random distribution of unsubstituted AHG units in cellulose ethers and, accordingly, on the tacit assumption of uniform substitution. Since these products are prepared commercially by a heterogeneous reaction mechanism, non-uniform distribution of substituents is to be expected. The greater the degree of non-uniformity, the greater the possible error in predicting the incidence of sequences of unsubstituted AHG units and the average $\overline{DP}_n$ of enzymically degraded samples from intrinsic-viscosity measurements.

Therefore, the proposed relationships between the apparent frequency of enzyme-induced chain breaks and the points of enzyme attack on the polymer chain relative to the possible distribution of completely unsubstituted AHG units is open to question. Thus, chain scission in CMC may occur primarily at sequences of two or more adjacent, unsubstituted AHG units, instead of at three or more, as indicated by the statistical approach. Nevertheless, it does appear that in water-soluble cellulose ethers at a given SI level the sodium carboxymethyl group offers appreciably greater protection against viscosity loss due to enzymic degradation than any of the other substitutents studied. Whether or not this behavior is related to its ionic nature has not been established.

References

1. M. G. Wirick, *J. Polymer Sci.*, **6**, 1705 (1968).

2. J. F. G. Clarke and A. Z. Conner, Hercules Incorporated, Research Center, unpublished data.

3. I. Croon and C. B. Purves, *Svensk. Papperstid.*, **62**, 876 (1959).

4. B. F. Smith and F. Smith, reported by A. B. Savage, Encyclopedia of Polymer Science and Technology, Vol. 3, Interscience, New York, 1965, p. 500.

5. I. Croon, *Svensk. Papperstid.*, **61**, 919 (1958).

6. Interpolated relationship from data reported by W. Brown, D. Henley, and J. Öhman, *Arkiv Kemi*, **22**, 189 (1964).

7. A. B. Savage, in Encyclopedia of Polymer Science and Technology, Vol. 3, Interscience, New York, 1965, p. 504, Table 7.

8. W. Brown, D. Henley, and J. Öhman, *Makromol. Chem.*, **64**, 49 (1963).

9. F. S. Stow, Hercules Incorporated, Research Center, unpublished data.

10. T. Cayle, *Wallerstein Lab. Commun.*, **25**, 349 (1962).

11. M. Holden and M. V. Tracey, *Biochem. J.*, **47**, 407 (1950).

12. A. B. Savage, *Ind. Eng. Chem.*, **49**, 99 (1957).

13. I. Croon and B. Lindberg, *Svensk. Papperstid.*, **59**, 794 (1956).

Metal Coordination Polymers. I. Synthesis and Thermogravimetric Analysis of Beryllium Phosphinate Polymers

P. J. SLOTA, JR., L. P. FREEMAN, and N. R. FETTER, *Naval Weapons Center, Corona, California 91720*

Synopsis

The preparation, properties, infrared, DTA, and TGA data are given for beryllium dimethyl-, tetramethylene-, di-*n*-butyl-, di-*n*-pentyl-, di-*n*-heptyl-, methylphenyl-, diphenyl-, and bispentafluorophenylphosphinates. Synthesis of dimeric beryllium acetylacetonyl phenyl-[*o*-methylcarboranyl (B_{10})]phosphinate is reported. The beryllium phosphinates were prepared by the reaction of beryllium acetylacetonate with the appropriate phosphinic acid.

INTRODUCTION

Metal-phosphinate-bridged coordination polymers of beryllium(II),[1–3] zinc(II),[3–6] chromium(III),[1,7–10] cobalt(II),[4,6,11] and iron(II),[10] have been synthesized. Beryllium diphenyl and dimethyl phosphinates[1–3] were shown to be very intractable and insoluble materials; however, the thermal stability of beryllium diphenyl phosphinate was the highest reported for the various phosphinates studied. It was also shown that tractable linear metal phosphinate polymers, such as $(Zn[OP(C_6H_5)(CH_3)O]_2)_x$,[5] and such as cobalt and zinc di-*n*-butylphosphinates,[4,6] which were soluble in organic solvents, could be prepared and had interesting polymer properties. These results prompted us to make a more comprehensive study of the beryllium phosphinate system, the effort being directed to the preparation of tractable polymers having good thermal characteristics. The beryllium phosphinates prepared in this investigation were made by the reaction between beryllium acetylacetonate and a phosphinic acid, in the absence of a solvent[2,3]:

$$Be(AcCHAc)_2 + 2R_2P(O)OH \rightarrow [Be(OPR_2O)_2]_x + 2AcCH_2Ac,$$
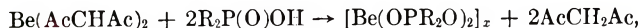
where $AcCH_2Ac$ represents acetylacetone, and R is CH_3, $n\text{-}C_4H_9$, $n\text{-}C_5H_{11}$, $n\text{-}C_7H_{15}$, C_6H_5, or C_6F_5. In one case R_2 was tetramethylene $[(CH_2)_4]$. Two mixed phosphinic acids, $C_6H_5(CH_3)P(O)OH$ and $o\text{-}CH_3CB_{10}H_{10}C\text{-}(C_6H_5)P(O)OH$, were also used. Details of the synthesis, general properties, and results of a thermogravimetric study of the polymers are presented below.

EXPERIMENTAL

Apparatus

Molecular weight data were obtained with either the Mechrolab Model 303 or the Hewlett-Packard Model 502 osmometer. Infrared spectra were obtained with a Beckman IR5 infrared spectrophotometer with sodium chloride optics. Mass spectra were recorded with a Consolidated Electrodynamics Corp. Model 21–130 mass spectrometer. All differential thermal analyses (DTA) were carried out on a du Pont Model 900 thermal analyzer, and thermogravimetric analyses (TGA) were done on a du Pont Model 950 thermal balance. Elemental analyses were performed by Schwarzkopf Microanalytical Laboratory, Woodside, New York.

In the preparation of the beryllium phosphinate polymers two different reaction setups were used. Method A used a thin-wall 20 mm. (o.d.) Pyrex reaction tube that extended 150 mm. from the tip of a water-cooled cold finger. In Method B the reaction tube was modified by having a liquid collection bulb sealed onto the Pyrex tube 200 mm. from the bottom. The cold finger was 250 mm. from the bottom of the tube. The volatile products that were not stopped by the cold finger were collected in a $-196°C$. trap. In both setups the apparatus could be filled with dry nitrogen or evacuated to less than 1.0 mm. pressure. Volatile products were transferred quantitatively by means of a high-vacuum system.

Commercial Reagents

Beryllium acetylacetonate, obtained from Alfa Inorganics, Inc., was triply sublimed at 100°C. immediately before use. Di-n-butylhydrogen phosphite (Peninsular ChemResearch, Inc.) and diphenylphosphinous chloride (Victor Chemicals) were used as received.

Synthesis of the Phosphinic Acids

Since the degree of polymerization obtained in a condensation reaction can be adversely affected by small amounts of impurities, considerable effort was made to prepare the phosphinic acids used in this investigation in a high state of purity. It was found that the purity of an acid could be greatly improved by converting it to the phosphinyl chloride ($R_2P(O)Cl$) with the use of thionyl chloride[12] and then hydrolyzing[13,14] a constant boiling fraction of the chloride with distilled water. This method was used in the preparation of $(n\text{-}C_4H_9)_2P(O)OH$, $(n\text{-}C_5H_{11})_2P(O)OH$, and $(C_6H_5)_2P(O)OH$. A brief description of the syntheses of the phosphinic acids used in this investigation is given below.

Dimethylphosphinic Acid, $[(CH_3)_2P(O)OH]$. The acid was prepared by the reaction of $(CH_3)_2P(S)\text{--}P(S)(CH_3)_2$ with 30% hydrogen peroxide, m.p. 89–90°C.[15]

Di-n-butylphosphinic Acid, $[(n\text{-}C_4H_9)_2P(O)OH]$. This compound was prepared in a 70% yield by the oxidative hydrolysis of $(n\text{-}C_4H_9)_2PN(C_2H_5)_2$

in n-hexane with dilute nitric acid. Conversion to $(n\text{-}C_4H_9)_2P(O)Cl$, b.p. 81°C. at 0.12 mm. Hg, by means of thionyl chloride and recrystallization of the hydrolyzed product from n-hexane gave the pure acid, m.p. 69–70°C. (lit.[16] 70.5–71°C.). The aminophosphine was prepared by making an n-hexane solution of n-butyllithium react with $(C_2H_5)_2NPCl_2$ in diethyl-ether.[17]

Tetramethylenephosphinic Acid, $(CH_2)_4P(O)OH$. This five-membered heterocyclic phosphinic acid[18,19] was readily prepared in high yield (73%) by the following new method. The dropwise addition of 2.5 ml. of 30% hydrogen peroxide dissolved in 10 ml. of diethyl ether to 1.812 g. (14.8 mmole) of $(CH_2)_4PCl$ in 25 ml. of ether (0°C.) gave, after removal of the solvent, 1.8 g. of white solid. Recrystallization of the solid from n-hexane gave 1.3 g. of colorless needle-like crystals, m.p. 54.5–55°C., in accordance with the literature reports.[18,19]

Di-n-pentylphosphinic Acid, $(n\text{-}C_5H_{11})_2P(O)OH$. This acid was prepared by hydrolysis of $(n\text{-}C_5H_{11})_2P(O)Cl$, b.p. 125°C. at 0.1 mm. Hg, with distilled water. A zone-refined sample (52 passes) melted at 68–70°C. A sample of the original acid upon repeated recrystallization from an ethanol–water solution melted at 70–71°C. (lit.[14] 68–69°C.). The $(n\text{-}C_5H_{11})_2P$-$(O)Cl$ was obtained from the reaction of $(n\text{-}C_5H_{11})_2PHO$ with thionyl chloride.[13] Neutralization equivalent $(n\text{-}C_5H_{11})_2P(O)OH$: found 214; calcd. 206.

Di-n-heptylphosphinic Acid, $(n\text{-}C_7H_{15})_2P(O)OH$. The acid was prepared in a 66% yield by the method described for $(n\text{-}C_4H_9)_2P(O)OH$. Recrystallization from absolute ethanol gave a white solid, m.p. 78–79°C. (lit.[14] 77–78°C.). Neutralization equivalent: found 260; calcd. 262.

Phenyl(methyl)phosphinic Acid, $C_6H_5(CH_3)P(O)OH$. This acid was prepared by first hydrolyzing $C_6H_5(CH_3)P(O)OCH_3$ with a 3% NaOH solution and then acidifying the mixture with concentrated hydrochloric acid.[20] Repeated recrystallization of the product from ethanol and then benzene gave hard white crystals, m.p. 137.5–139.5°C. (lit. 133–134°C.[20] 135–136°C.[5]).

Diphenylphosphinic Acid, $(C_6H_5)_2P(O)OH$. This acid was prepared by treating $(C_6H_5)_2PCl$ with dilute nitric acid solution. As a further purification step the phosphinic acid was converted to $(C_6H_5)_2P(O)Cl$, with thionyl chloride, and a constant boiling fraction of the chloride was hydrolyzed with distilled water. Recrystallization of the product from absolute ethanol gave hard white crystals, m.p. 196–198°C. (lit. values range from 187 to 196°C.).

Bis(pentafluorophenyl)phosphinic Acid, $(C_6F_5)_2P(O)OH$. The synthesis of this compound will be described elsewhere.

Phenyl(o-methylcarboranyl)phosphinic Acid, $CH_3CB_{10}H_{10}C(C_6H_5)P(O)$-OH. A 200 ml. Pyrex tube (sealed under high vacuum) containing 3.2 g. (10.1 mmole) of $CH_3CB_{10}H_{10}C(C_6H_5)P(O)Cl$ and 2 ml. of distilled water was heated in an oven at 105°C. for 38 hr. When the cooled reaction tube was opened under high vacuum, the volatile fraction contained 0.179 mmole of

TABLE I
Beryllium Phosphinate Preparations

Product	Reactants concn., mmoles		Ac-CH₂Ac isolated, mmole	Reaction conditions				Properties of Polymers		
	Be(AcCHAc)₂·R₂P(O)OH			Step 1[a]		Step 2[b]				
		OH		°C.	hr.	°C.	hr.	Phys.	Soly.	M_n
Be[OP(CH₃)₂O]₂[c,d]	15.21	30.30	30.14	25–180	10.0	170	6.5	Hard, white solid	Insol.[e]	
"a"	22.89	45.77	44.14	25–180	9.0	155–180	4.0	" "	"	
Be[OP(CH₂)₄O]₂[d]	3.50	7.00	6.90	25–160	5.5	130–210	1.5	Hard, tan solid	Insol.[e]	
Be[OP(n-C₄H₉)₂O]₂[d]	12.36	24.72	24.55	25–180	6.0	180–190	2.0	Forms soft, flexible, colorless films	Hydrocarbons	50,000
Be[OP(n-C₅H₁₁)₂O]₂[d]	7.09	14.15	13.44	25–200	11.0	200–215	0.5	" "	"	26,000
Be[OP(n-C₇H₁₅)₂O]₂[d]	10.16	20.32	19.86	25–170	4.5	165–205	4.0	Colorless, hard wax	"	16,900
Be[OP(C₆H₅)(CH₃)O]₂[f]	5.20	10.43	10.23	25–165	8.0	155–180	3.0	Amber, glassy solid	benzene	30,000
Be[OP(C₆H₅)₂O]₂[f]	12.40	24.81	24.58	25–175	6.0	170–200	4.0	Hard, white solid	insol.[g]	
Be[OP(C₅F₅)₂O]₂[d]	0.53	1.05	1.02	25–195	1.8	210	0.3	Glassy solid	N-methyl-2-pyrolidone	
Be(AcCHAc)[OP(C₆H₅)]-(CB₁₀H₁₀CCH₃)O]₂[d]	0.164	0.328	0.88	25–100	0.7	100–200	1.3	Hard, tan solid[h] (m.p. 248-9°C)	Chloroform hydrocarbons	808 (dimer)

[a] Reaction mixture heated in atmosphere of dry nitrogen (temperature recorded is that of the oil bath).
[b] Same as in footnote (a), followed by heating at ≈1.0 mm. Hg.
[c] Number-average molecular weights, benzene solvent.
[d] Reaction method A.
[e] Insoluble in nonprotonic solvents.
[f] Reaction method B.
[g] Insoluble in organic protonic and nonprotonic solvents.
[h] Recrystallized from mixture of n-heptane and toluene to give colorless crystals.

hydrogen and 6.8 mmole of hydrogen chloride (in solution). Recrystallization of the solid reaction product in diethylether gave 769 mg. of a hard, colorless, crystalline solid, m.p. 212–214°C.

ANAL. Calcd. for $C_9H_{19}B_{10}P$: C, 36.22%; H, 6.42%; B, 36.26%; P, 10.38%. Found: C, 36.69%; H, 6.62%; B, 36.09%; P, 10.58%. Neut. equiv.: calcd. 298, found 293.

Addition of aniline to a chloroform solution of the phosphinic acid gave the anilide derivative; m.p. 228°C.

ANAL. Calcd. for $C_{15}H_{26}B_{10}NP$: C, 46.01%; H, 6.69%; B, 27.63%; N, 3.58%; P, 7.91%. Found: C, 45.55%; H, 7.43%; B, 27.30%; N, 3.26%; P, 7.62%. Neut. equiv.: calcd. 392, found 396.

Synthesis of Phosphinate Polymers

The polymers were made by heating a mixture containing stoichiometric amounts of triply sublimed beryllium acetylacetonate and the corresponding phosphinic acid. In these reactions the temperature of the mixture was slowly raised (oil bath) in an atmosphere of dry nitrogen until the acetylacetone that was formed refluxed vigorously (≈ 130°C.). After refluxing for at least 1 hr. the acetylacetone was removed from the reaction tube. The mixture was then heated under vacuum (≈ 1.0 mm.) to about 200°C., to insure complete reaction or removal of acetylacetone, or both. Two methods were used to remove the bulk of the acetylacetone from the reaction tube. In method A the following procedure was repeated several times. The mixture was heated to approximately 130°C. and cooled to ambient temperature, and the system was slowly evacuated. The acetylacetone collected in a -196°C. trap. In method B the acetylacetone was

TABLE II
Analytical Data for Beryllium Phosphinates

$Be[OP(CH_3)_2O]_2$	Calcd.:	C, 24.62; H, 6.20; P, 31.76
	Found:	C, 25.61; H, 6.60; P, 31.25
$Be[OP(CH_2)_4O]_2$	Calcd.:	C, 38.87; H, 6.52; P, 25.07; Be, 3.65
	Found:	C, 40.08; H, 6.65; P, 24.68; Be, 3.89
$Be[OP(n\text{-}C_4H_9)_2O]_2$	Calcd.:	C, 52.88; H, 9.99; P, 17.05; Be, 2.48
	Found:	C, 52.07; H, 9.83; P, 17.32; Be, 3.05
$Be[OP(n\text{-}C_5H_{11})_2O]_2$	Calcd.:	C, 57.26; H, 10.57; P, 14.77; Be, 2.15
	Found:	C, 57.33; H, 10.39; P, 14.91; Be, 1.89
$Be[OP(n\text{-}C_7H_{15})_2O]_2$	Calcd.:	C, 63.24; H, 11.37; P, 11.65; Be, 1.70
	Found:	C, 63.30; H, 11.67; P, 11.25; Be, 2.09
$Be[OP(C_6H_5)(CH_3)O]_2$	Calcd.:	C, 52.67; H, 5.05; P, 19.41; Be, 2.89
	Found:	C, 53.37; H, 5.49; P, 19.26; Be, 2.21
$Be[OP(C_6F_5)_2O]_2$	Calcd.:	C, 35.89; F, 47.31; P, 7.71; Be, 1.12
	Found:	C, 37.19; F, 44.26; P, 7.70; Be, 1.14
$Be(AcCHAc)[OP(C_6H_5)\text{-}$	Calcd.:	C, 41.46; H, 6.21; P, 7.68; Be, 2.22; B, 26.68
$(CB_{10}H_{10}CCH_3)O]$	Found:	C, 41.18; H, 6.25; P, 8.40; Be, 2.03; B, 26.38

distilled from the reaction tube at atmospheric pressure into a glass bulb sealed to the reaction tube. The experimental data for the preparation and characterization of the beryllium phosphinates are shown in Table I. Analytical results are given in Table II.

Thermogravimetric Studies of Beryllium Phosphinate Polymers

The thermogravimetric analyses (TGA) were scanned at 5°C./min. in static vacuum, nitrogen, and ambient air until weight loss was constant.

The thermal balance was attached to a vacuum manifold fitted with a -196°C. trap to collect volatile materials for later mass spectral and infrared analyses. The balance and vacuum line were evacuated to approximately 0.1 mm. before heating, and the entire system was sealed during the heating cycle. Weight losses were measured from the start of heating.

The nitrogen was used directly from the tank at a rate of 1 ft.^{3}/hr., and the air runs were made with balance open to the atmosphere. Sample sizes varied from approximately 20–60 mg. and were powdered but unsieved. Some of the polymers were waxy solids and had to be loaded onto the balance pan in large lumps. These remarks also apply to the isothermal runs shown in Table III.

TABLE III
Isothermogravimetric Analysis of Beryllium Phosphinate Polymers in Air[a]

Compound	Temp., °C.	Heat. time, hr.	Sample wt., mg.	Wt. loss, mg.	Avg. loss rate, mg./hr.
$(Be[OP(CH_3)_2O]_2)_x$	400	3.3	15.2	0.0	0.0
	400	2.3	14.6	2.3	1.0
	320	24.0	29.6	0.0	0.0
$(Be[OP(n-C_4H_9)_2O]_2)_x$	330	4.0	6.10	1.2	0.25
$(Be[OP(CH_2)_4O]_2)_x$	350	17.0	37.5	0.0	0.0
	375	20.7	35.0	1.8	0.086
$(Be[OP(n-C_5H_{11})_2O]_2)_x$	300	4.2	33.0	2.0	0.48
$(Be[OP(n-C_7H_{16})_2O]_2)_x$	310	23.5	28.0	4.7	0.20
$(Be[OP(CH_3)(C_6H_5)O]_2)_x$	400	10.2	25.2	8.5	0.83
$(Be[OP(C_6H_5)_2O]_2)_x$	500	1.5	34.8	20.5	
	430	3.4	33.0	20.0	
	390	3.3	51.5	1.0	0.30
$(Be[OP(C_6F_5)_2O]_2)_x$	385	3.5	27.0	7.0	2.0

[a] All in air except compound with data of first line, which was in nitrogen.

The differential thermal analyses (DTA) were run in 2 mm. capillary tubes containing approximately 10 mg. of undiluted sample. The sample cell was flushed with nitrogen, and the samples were scanned at 20°C./min. from room temperature to 500°C.

RESULTS

The temperature-scanned TGA and DTA data are summarized in Table IV. Although exact measurements of the condensibles were not made,

estimates based on mass spectra were made in some cases and are indicated in the appropriate column.   The selection of the point of initial weight loss was difficult to estimate in some runs, so the temperature at 10 and 50% weight loss plus the total weight loss, in milligrams, is given in Table IV. In some runs, under vacuum, material sublimed onto the cold portion of the thermal balance and, when contamination could be avoided, the materials were scraped off and infrared spectra taken.   These sublimates are listed in the appropriate column in Table IV and their identity confirmed by comparison with spectra of authentic samples.

The results of the isothermal studies are given in Table III.   In those samples where the weight loss rate was linear, they are given in milligrams per hour.   The total weight losses and exposure times are also listed.

DISCUSSION

General Characteristics of the Beryllium Phosphinates

The beryllium phosphinate coordination polymers synthesized in our investigation differed greatly in their physical properties.   The diphenyl and dimethyl phosphinates were intractable, insoluble, white powders, in agreement with the observation of Block and his co-workers[2,3] and, as found with the corresponding zinc phosphinates,[5] the physical properties of $(Be[OP(C_6H_5)(CH_3)O]_2)_x$ are not intermediate between $(Be[OP(C_6H_5)_2O]_2)_x$ and $(Be[OP(CH_3)_2O]_2)_x$.   For example, the first is a benzene-soluble resin-like material, whereas the latter two are hard, easily powdered solids, insoluble in organic solvents.

Previous work[6] has shown that the initial point of weakness in the metal phosphinates lies with carbon–phosphorus bonds of the pendant groups and not with the inorganic, bridged backbone.[21]   Zinc diphenylphosphinate undergoes thermal decomposition initially to give benzene.[6]   We found this to be the case with the corresponding beryllium diphenylphosphinate; however, with the alkyl derivatives the parent phosphinic acids were obtained along with alkanes and alkenes.   In order to make workable beryllium phosphinate polymers with less thermally reactive organic substituents, attempts to prepare the tetramethylene, perfluorophenyl, and phenyl(o-methylcarboranyl)phosphinate derivatives were made.   The tetramethylene and bisperfluorophenylphosphinates are friable, resin-like materials.   They are insoluble in hydrocarbon and halocarbon solvents and display only very limited solubilities in a wide range of polar organic solvents.   One exception was found: beryllium bisperfluorophenylphosphinate did dissolve in hot N-methyl-2-pyrrolidone, but it is not known whether the polymer chain was broken in the process.   It has not been possible to study the properties of the phenyl(o-methylcarboranyl)phosphinate, since the reaction gave the dimer $(AcCHAcBe[OP(C_6H_5)(CB_{10}H_{10}-CCH_3)O])_2$, where only one acetylacetonate on beryllium was substituted by a bridging phosphinate group.   The reasons for this unique behavior

TABLE IV
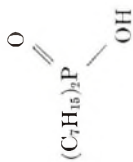### Thermogravimetric Analyses of Beryllium Phosphinate Polymers

Compound	Cond.	Sample wt., mg.	10% wt., loss	50% weight loss	Tot. wt. loss,[a] mg, %	Condensibles	Sublimates	DTA temp., °C. Endo.	m.p. endo.
$(Be[OP(CH_3)_2O]_2)_x$	air	17.3	522		7.2, 41.5				
	N_2	13.5	540	600	7.2, 53.4	methane hydrogen	$(CH_3)_2P(=O){-}OH$	280	465
	vac.	28.0	400	465	28.0, 100				
$(Be[OP(n\text{-}C_4H_9)_2O]_2)_x$	N_2	41.5	410	477	36.5, 88.0				
	vac.	40.7	415	475	40.7, 100	ca. 50:50 mixt. n-butane + 1-butene	$(C_4H_9)_2P(=O){-}OH$	35	452

$(Be[OP(n\text{-}C_5H_{11})_2O]_2)_x$	air	44.2	457	515	16.3, 37.0			
	N_2	30.0	445	500	17.5, 58.4			
	vac.	53.8	445	475		ca. 50:50 mixt. n-pentane + 1-pentane		
$(Be[OP(n\text{-}C_7H_{15})_2O]_2)_x$	N_2	49.5	420	483	42.5, 86.0		67	
	vac.	45.0	—[b]	—[b]	45.0, 100	50:50 mixt.	441	
$(Be[OP(CH_2)_4O]_2)_x$	N_2	17.5	515	600	8.4, 48	n-heptane + 1-heptane	384	
	vac.	38.8	455	520	34.4, 87.6	1-butene		

(continued)

TABLE IV, *Continued*

Compound	Cond.	Sample wt., mg.	10% wt. loss	50% weight loss	Tot. wt. loss,[a] mg., %	Condensibles	Sublimates	Endo.	m.p. endo.
$(Be[OP(CH_3)(C_6H_5)O]_2)_z$	air	31.7	500	violent oxidation at 550°C.					
	N_2	31.2	525	600	25.0, 82.0		$(CH_3)(C_6H_5)P\!\!\underset{\backslash OH}{\overset{O}{\parallel}}$	160	>500
	vac.	68.5	465	530	68.5	benzene + toluene			
$(Be[OP(C_6H_5)_2O]_2)_z$	air	24.0	545	650	12.0, 50.0				
	N_2	34.0	610	630	18.4, 54.2			208, 290, 450	
	vac.	51.8	548	595	39.7, 76.7	benzene	sublimate not identified		>500
$(Be[OP(C_6F_5)_2O]_2)_z$	N_2	60.0	470	510	51.5, 86.0			78, 263	>500
	vac.	44.8	300	490	44.8, 100	perfluoro-benzene			

[a] First figure, mg.; second, %.
[b] Thermocouple failed during run.

are not known, but perhaps it is due to the bulky nature of the phosphinate group.

In contrast to the phosphinates discussed above, beryllium di-n-butyl-, di-n-pentyl-, and di-n-heptyl phosphinates are colorless, waxy materials that readily dissolve in hydrocarbon solvents. The molecular weights of these polymers and of the methyl(phenyl)phosphinate (membrane or vapor-pressure osmometry) were >10,000. A sample of beryllium di-n-butylphosphinate that had been extracted with benzene had a molecular weight of ≈50,000. More complete molecular weight data are given in Table I.

Very little data have been collected on the physical characteristics of these materials. However, it can be stated that thin films of the di-n-butyl- and di-n-pentylphosphinate polymers are flexible, the di-n-heptylphosphinate is a hard wax, and thin sheets of the methyl(phenyl) derivative are glassy.

The major infrared absorption bands for these beryllium phosphinates are listed in Table V. The spectra all have two or three very strong absorption bands assigned to P—O stretching in the region 1167–1067 cm.$^{-1}$. These are lower than the P—O stretching frequencies, 1125–1175 cm.$^{-1}$, observed for metal complexes of tertiary phosphine oxides[22] but are close to the P—O stretching frequencies ≈1130 and ≈1055 cm.$^{-1}$ in cobalt dimethyl, methyl (phenyl), and diphenylphosphinates reported by Coates and Golightly.[11] Beryllium tetramethylene phosphinate does not show an absorption at 1370 cm.$^{-1}$, which would have indicated a methyl group. This indicated that the $(CH_2)_4P$ ring remained intact during the preparation of the polymer.

Thermogravimetric Studies of the Beryllium Phosphinate Polymers

Rose and Block[5] observed only benzene from the decomposition of $(Zn-([OP(C_6H_5)_2O]_2)_x$ at 500°C. in nitrogen and suggested that the $Zn(O—OP)_2$ backbone was not ruptured; however, our studies under vacuum reveal the presence of sublimates as soon as 10% decomposition is reached. These sublimates appear to be phosphinic acids corresponding to the acid used to make the polymer. It should also be noted that in most cases under vacuum all of the sample left the balance pan, suggesting complete degradation of the polymer into volatile components. One of the exceptions to this observation was $[Be(OP(C_6H_5)_2O)_2]_n$, which had a weight loss of 77%, and which yielded a sublimate that could not be characterized from its infrared spectrum. It is perhaps fortuitous that Block et al.[2] studied a diphenylphosphinic acid polymer, for it may be the only one prepared that does not undergo complete backbone cleavage.

It is possible that the mode of decomposition of the diphenyl phosphinate polymers described by Rose and Block[5] is unique. In the mechanism proposed by these authors the cleavage of a phenyl group as benzene results in the crosslinking of two adjacent metal phosphinate chains through a *para*-disubstituted phenyl group.

TABLE V
Infrared Absorption Frequencies of[a] Be(OPRR'O)$_2$ Polymers in the Region 3600–650 cm^{-1}

R,R': CH$_3$[b,e]	(CH$_2$)$_4$[b,e]	n-C$_4$H$_9$[d]	n-C$_5$H$_{11}$[d]	n-C$_7$H$_{15}$[d]	CH$_3$, C$_6$H$_5$[b,e]	C$_6$H$_5$[b,e]	C$_6$F$_5$[b,c]	C$_6$H$_5$, CB$_{10}$H$_{10}$CCH$_3$[b]
3049 w	2924 w	2964 s	2959 s	2933 w	3106 w	3054 w	3064 w	3096 vw
3008 w	2857 w	2875 m	2874 m	2870 m	3067 w	1595 w	3008 w	2967 vw
2920 w	1447 w	1469 m	1468 m	1469 m	3003 w	1487 m	2955 w	2068 s
2842 w	1410 m	1461 sh	1458 m	1409 w	2732 w	1443 s	2342 w	1595 s
2335 w	1347 w	1410 w	1445 m	1379 w	2688 w	1313 w	1779 w	1493 s
2316 w	1339 w	1381 w	1410 w	1247 w	1621 m	1284 w	1648 m	1259 s
1594 m	1267 s	1330 w	1377 w	1227 w	1481 m	1259 s	1598 s	1152 s
1484 m	1232 m	1281 w	1280 w	1197 m	1425 m	1168 vs	1522 ms	1106 s
1435 s	1149 vs	1223 m	1242 w	1135 vs	1344 w	1138 vs	1489 vs	1029 m
1309 w	1117 vs	1142 vs	1215 m	1083 vs	1337 w	1083 vs	1441 m	1001 w
1258 w	1067 vs	1080 vs	1140 vs	889 m	1297 m	1024 s	1397 m	957 w
1164 vs	1052 vs	1003 w	1085 vs	870 m	1134 bvs	941 m	1357 m	932 w
1152 vs	1024 s	969 w	993 w	813 vbm	1066 bvs	926 m	1301 m	879 w
1085 vs	880 vs	887 w	900 w	667 vbs	1027 s	762 vs	1200 bvs	847 w

1022 m	867 s	869 w	881 w	966 m	756 ssh	1143 bvs	780 ms
996 m	766 s	814 bm	870 w	886 bs	734 s	1108 bvs	772 m
926 w	747 bvs	674 bvs	827 bm	786 bs	728 ssh	1104 bvs	765 m
764 bs	699 bvs		797 bw	719 bs	692 s	1092 msh	751 ms
758 bs	657 bvs		710 bvs		672 s	1025 w	730 mb
734 bs						985 s	699 ms
722 bs						925 w	688 m
692 bs						854 m	670 m
674 bs						843 m	650 mb
671 bs						754 s	
						745 s	
						723 s	
						691 s	

a Abbreviations: v, very; w, weak; m, medium; s, strong; b, broad; sh, shoulder.
b Nujol mull.
c Kel-F mull.
d Thin film.

The residue we obtained from pyrolysis in nitrogen showed a strong infrared absorption at 710 cm.$^{-1}$, which may be assigned to a 1,3,5 trisubstituted aromatic ring, but none at 800 cm.$^{-1}$ assigned to *para* disubstitution.[23] Furthermore, the weight loss of 54.2% benzene (see Table IV) agrees closely with the 52.0% weight loss of three phenyl groups from (Be-[OP(C$_6$H$_5$)$_2$O])$_{2x}$. The residue may be a three-dimensional network with the structure
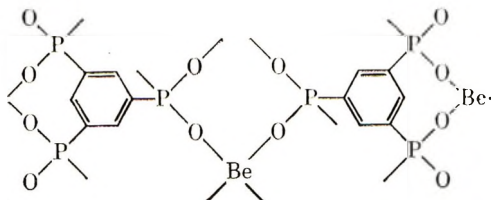
This type of trade-off is not observed in the beryllium straight-chain alkylphosphinate polymers. The yield of approximately 50:50 mixtures of alkane and alkene from the decompositions of (Be[OP(n-C$_4$H$_9$)$_2$O]$_2$)$_x$, (Be-[OP(n-C$_5$H$_{11}$)$_2$O]$_2$)$_x$, and (Be[OP(n-C$_7$H$_{15}$)$_2$O]$_2$)$_x$ suggests a mechanism by which an alkyl radical promotes the cleavage of a second alkyl radical in a stepwise manner, as shown by the dibutyl phosphinate, for example:
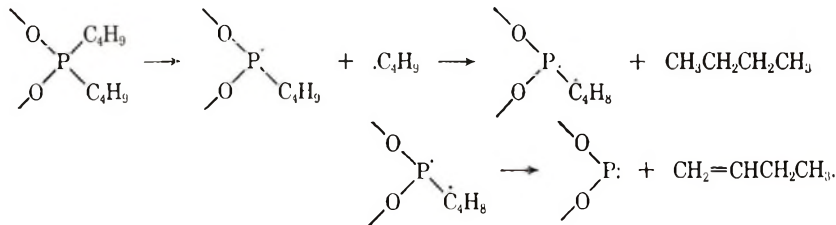
The resulting phosphorus atom is apparently sufficiently unstable to cause backbone rupture.

The beryllium tetramethylenephosphinate polymer, (Be[OP(CH$_2$)$_4$O]$_2$)$_x$, which is considerably more stable than the corresponding beryllium di-n-butylphosphinate, requires for decomposition the cleavage of two P—C bonds to give the only observed hydrocarbon, 1-butene. In this case the decomposition may also occur stepwise with hydrogen shift:
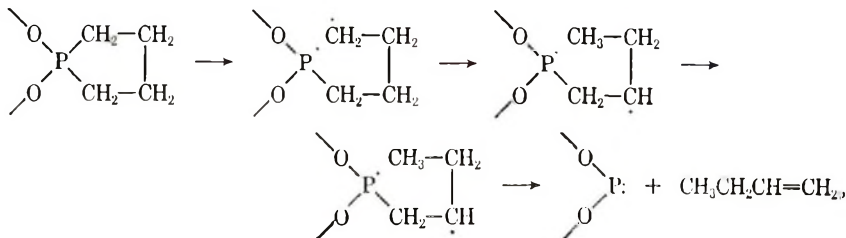

Or the formation of 1-butene could occur by means of β-hydrogen elimination and reduction via the resulting phosphine:
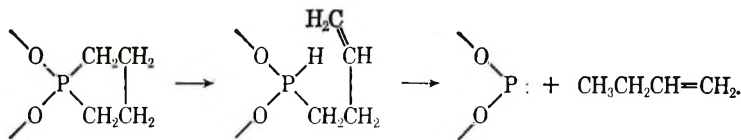
The odor of phosphine in the TGA residues of the beryllium dialkylphosphinates suggests that the latter process occurs, but to what extent is not known.

Beryllium dimethylphosphinate also represents a unique case in which the evolved gases are methane and hydrogen. Although dimethylphosphinic acid sublimes from the decomposition in the same manner as the other straight-chain alkyl phosphinate polymers, the mechanism of the formation of methane and hydrogen does not appear to be as straightforward as the one suggested for the higher alkyl groups. A difference in the decomposition mechanism may also account for the greater stability of $(Be[OP(CH_3)_2O]_2)_x$ than of the other straight-chain alkyl phosphinates.

The presence of toluene among the decomposition products of $(Be[OP(CH_3)(C_6H_5)O]_2)_x$ suggests that a methyl and phenyl radical combine;
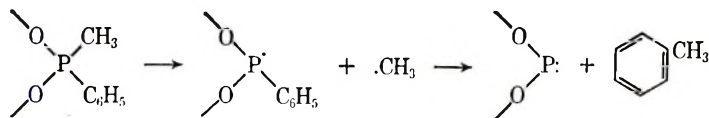
It is suggested that decomposition starts by methyl, rather than phenyl, cleavage, because this polymer has a stability more like $(Be[OP(CH_3)_2O]_2)_x$ than $(Be[OP(C_6H_5)_2O]_2)_x$.

The DTA data in Table IV show that most of the polymers had high melting points near the onset of decomposition. Even the waxy straight-chain beryllium dialkylphosphinates had sharp melting point endotherms. Both $(Be[OP(C_6H_5)(CH_3)O]_2)_x$ and $(Be[OP(C_6H_5)_2O]_2)_x$ decomposed before melting, the latter compound remaining a sintered solid up to 700°C. The exact nature of the well-defined low-temperature endotherms has not been determined, but the changes do not involve the physical appearance of the polymers.

Although making weight-loss measurements in ambient air may lead to ambiguous results because of weight gains by oxidation, this atmosphere appears to be more realistic for assessing a polymer's long-term thermal stability in actual use. For this reason all but one of the isothermal studies listed in Table III were carried out in air. In general, most polymers showed some weight loss above 350°C.; particularly disappointing was $[Be(OP(C_6H_5)_2O)_2]_x$, which lost weight rapidly above 400°C., but which appeared to be rather stable in nitrogen. It should also be noted that weight losses in air under isothermal conditions tend to occur at lower temperatures than 10% points on the temperature-scanned thermograms run in air.

References

1. B. P. Block, E. S. Roth, C. Schaumann, and L. Ocone, *Inorg. Chem.*, **1**, 860 (1962).

2. B. P. Block, S. H. Rose, C. W. Schaumann, E. S. Roth, and J. Simkin, *J. Am. Chem. Soc.*, **84**, 3200 (1962).

3. B. P. Block and C. W. Schaumann, U.S. Pat. 3,245,953 (Apr. 12, 1966).

4. V. Crescenzi, V. Giancotti, and A. Ripamonti, *J. Am. Chem. Soc.*, **87**, 391 (1965).

5. S. H. Rose and B. P. Block, *J. Polymer Sci. A-1*, **4**, 573 (1966).

6. S. H. Rose and B. P. Block, *J. Polymer Sci. A-1*, **4**, 583 (1966).

7. B. P. Block, J. Simkin, and L. Ocone, *J. Am. Chem. Soc.*, **84**, 1749 (1962).

8. A. J. Saraceno and B. P. Block, *Inorg. Chem.*, **3**, 1699 (1964).

9. A. J. Saraceno and B. P. Block, *J. Am. Chem. Soc.*, **85**, 2018 (1963).

10. H. E. Podall and T. L. Iapalucci, *J. Polymer Sci. B*, **1**, 457 (1963).

11. G. E. Coates and D. S. Golightly, *J. Chem. Soc.*, **1962**, 2523.

12. C. S. Gibson and J. D. A. Johnson, *J. Chem. Soc.*, **1928**, 92.

13. R. H. Williams and L. A. Hamilton, *J. Am. Chem. Soc.*, **74**, 5418 (1952).

14. R. H. Williams and L. A. Hamilton, *J. Am. Chem. Soc.*, **77**, 3411 (1955).

15. H. Reinhardt, D. Bianchi, and D. Mölle, *Ber.*, **90**, 1656 (1957).

16. G. M. Kosolapoff and R. M. Watson, *J. Am. Chem. Soc.*, **73**, 4101 (1951).

17. A. B. Burg and R. I. Wagner (to American Potash and Chemical Corp.), U.S. Pat. 2,934,564 (1960).

18. B. Helferich and E. Aufderhaar, *Ann.*, **658**, 100 (1962).

19. R. Schmutzler, *Inorg. Chem.*, **3**, 421 (1964).

20. H. J. Harwood and D. W. Grisley, *J. Am. Chem. Soc.*, **82**, 423 (1960).

21. F. Giordano, L. Randaccio, and A. Ripamonti, *Chem. Comm.*, **1967**, 19.

22. F. A. Cotton, R. D. Barnes, and E. Bannister, *J. Chem. Soc.*, **1960**, 2199.

23. L. J. Bellamy, The Infrared Spectra of Complex Molecules, Wiley, New York, 1958, pp. 78, 79.

The Optical Rotation of Gelatin Films

I. H. COOPES, *Research Laboratory, Kodak (Australasia) Pty. Ltd., Coburg, Victoria, Australia*

Synopsis

Optical rotation measurements of a series of relatively thick gelatin films prepared under a variety of drying conditions were made. The technique permits rotation measurements to be made during the drying process. It is found that the temperature and humidity of the drying air do not significantly affect the rotation of the films at temperatures below about 25°C. wet bulb. Above this temperature the rotation drops sharply. Films containing formaldehyde and mucochloric acid as hardeners tend to have lower rotations than unhardened films. Various types of gelatin show differences in the gel state, but not when dried. The results of these experiments indicate that in general gelatin tends to acquire the same level of ordered structure during drying, regardless of the drying conditions and type of gelatin. This tendency is inhibited only by high temperatures or the establishment of stable intermolecular crosslinks by hardeners.

INTRODUCTION

The characteristically high optical rotation of gelatin has been used in many studies of configurational changes in the gelatin molecule. The variation of rotation with temperature in gelatin solutions was interpreted by Cohen[1] as being due to a transition from the helical configuration of collagen at low temperatures to a random coil configuration at higher temperatures. Pchelin and his co-workers,[2,3] in studies of the rotation–temperature curves of gelatin sols and gels, found no discontinuities at the melting points of the gels and concluded that the setting mechanism and optical rotation were not directly related. A similar conclusion could be drawn from the work of Janus,[4,5] who found that the setting of gels was basically an intermolecular crosslinking process, whereas the development of rigidity was related to the assumption of the helical conformation by the gelatin molecule. The variation in rotation would be associated with the latter process.

Drake and Veis[6] followed the optical rotation and viscosity as functions of temperature and time for α and γ gelatins. The results obtained led these workers to propose an intermolecular refolding mechanism involving the interaction of chain segments of the same molecule. Piez and Carrillo[7] found that the helices formed in gelatin consisted predominantly of two chains, which might be either from the same or from different molecules. In single-chain molecules helix formation was found to be a concentration-

dependent reaction, and this was interpreted as involving interchain association.

Most investigations of gelatin molecular structure have been carried out with solutions of low to moderate concentrations. The general opinion seems to be that helix formation is primarily an intramolecular process. The position with respect to the molecular conformation of substantially dry gelatin is less clear. Robinson and Bott[8] studied the optical rotation and infrared spectra of solutions and dry films of gelatin. Their results indicated that films dried from gels had a high helical content whereas films dried from hot sols had a largely random molecular conformation.

When a gelatin solution sets to a gel, the gelatin molecules become bonded together by weak intermolecular crosslinks, presumably consisting of hydrogen bonds. With the passage of time the gel becomes more rigid, and this is accompanied by increased negative optical rotation and the development of a degree of ordered structure, as indicated by x-ray diffraction measurements.[9] When the gel is dried, it contracts vertically (horizontal contraction, although present, is normally small) and forms an ordered structure whose crystallites are oriented in a direction parallel to the surface of the film.[10] However, films formed by drying a solution at elevated temperatures show no such orientation. There is still no exact model of the structural changes that take place during gelation and drying. Although a distinction is usually made between intermolecular crosslinking and collagen-fold formation, the two phenomena seem to be inextricably interrelated. The gelatin molecule has an inherent tendency to assume the collagen fold conformation, which must require some interaction between segments of the polypeptide chains. However, even at low concentrations intermolecular and intramolecular contacts are equally probable,[11a] and there is a strong tendency of molecules to form double-chain helices.[6,7] Thus collagen fold formation must involve the formation of at least some intermolecular crosslinks.

There is a further level of ordered structure formed in films, viz. crystallites, which appear to consist of aggregates of gelatin molecules more or less in the collagen fold configuration. The assumption of the collagen fold by gelatin molecules plays an essential role in the development of these higher levels of structure in gelatin films.

The present work aims at studying the process of collagen fold formation in films in order to gain insight into the development of structure. A series of experiments has been designed, in which the change in helical content of gelatin films is followed by means of optical rotation measurements during the drying process, and in which the effects of varying the experimental conditions are observed.

EXPERIMENTAL

Apparatus

The optical rotation measurements were made with a Bellingham and Stanley Model A Polarimeter with filtered sodium light. The analyzer was

equipped with a micrometer adjustment that enabled readings to be made to 0.002°, but in practice it was found that reproducibility was about ±0.009° without a sample and ±0.010° with a film sample. With thick films the actual measured rotation was generally in the range 0.6–1.7°. Some of these films caused serious distortion of the transmitted light, making readings difficult and resulting in errors substantially greater than those given above.

The films were dried in a Köttermann Climatic Test Cabinet, which could be adjusted to a wide range of temperatures and humidities to accuracies of ±0.5°C. and ±2.5% relative humidity, respectively. The air-circulating system provided a gentle flow of air across the surfaces of the film samples.

Preparation of Films

The gelatin used in this work was a commercial acid-processed pigskin gelatin. The viscosity and pH of a 1% solution at 40°C. were 1.07 cpoise and 5.02, respectively.

The gelatin was soaked in water overnight, heated to 50°C., and made up to a 10% solution. 15 ml. of solution were poured into a mold approximately 7.4 cm. square, the base of which was a glass plate, giving a covering of 270 g. of gelatin per square meter. The mold was placed in a refrigerator at 9°C. for 30 min. and then placed in the Köttermann Cabinet at the appropriate temperature and humidity. The film was allowed to equilibrate in the cabinet for at least 30 min. before the first optical rotation measurement was made.

Procedure for Measurements

The optical rotation of the films was measured by placing the sample in the light beam as close to the analyzer as was practicable and making a series of six readings. Three readings were made with the film in its initial orientation and then three more after the film had been rotated through 90° in a plane perpendicular to the path of the polarized light. The polarimeter was placed close to the Köttermann Cabinet so as to expose the films to room conditions for the shortest possible time.

The rotation data are given in terms of specific rotation $[\alpha]_D$, defined as

$$\frac{\text{(measured rotation in deg.)}/\text{(grams gelatin per vol. sample in cc.)}}{\text{(distance in dm.)}}$$

Times were measured from the moment the gelatin solution was poured into the mold.

Measurements of a gel contained in an airtight cell of path length 20 mm. were also made. As in the case of the films, measurements were made with the cell in two orientations at 90° to each other.

RESULTS

Films were prepared as described above and dried in the Köttermann Cabinet under various conditions of temperature and humidity, ranging

from 16 to 38°C. and from 40 to 75% relative humidity, and optical rotations were measured during drying (Fig. 1). On a few occasions anomalously high readings were obtained. With one sample (at 26°C. wet bulb) a high rotation was observed in one position; when rotated through 90° it gave a normal reading. This was an unusual case, since the readings in the two orientations were normally very similar. It is possible that the very high rotation was due to tensions between the film and the glass base, leading to a temporary anisotropy. It may be noted that in the case of the 26°C. sample the experiment was carried out in duplicate, and there is no doubt about the validity of the curve in Figure 1.
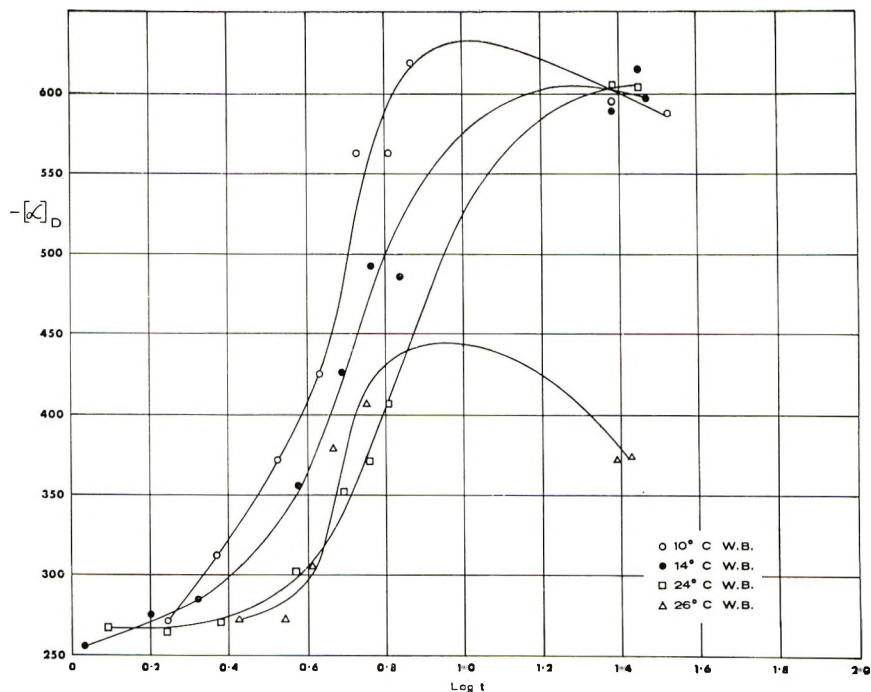
Fig. 1. Specific rotation plotted against logarithm of time, in hours, for gelatin films dried under various conditions of temperature and humidity. W. B., wet bulb.

The films dried at 21°C. and 50% relative humidity were weighed after each polarimeter reading; then the moisture contents were calculated and plotted against time (Fig. 2).

Measurements were made of films hardened with 1, 5, and 10% of formaldehyde (based on the weight of dry gelatin) and dried at 21°C. and 50% relative humidity. The results for the formaldehyde-hardened films are shown in Figure 3. The curves obtained from films hardened with mucochloric acid were similar. Experiments were also carried out to determine the effect of variations in the temperature and humidity of drying air on the rotation of hardened films (Fig. 4).
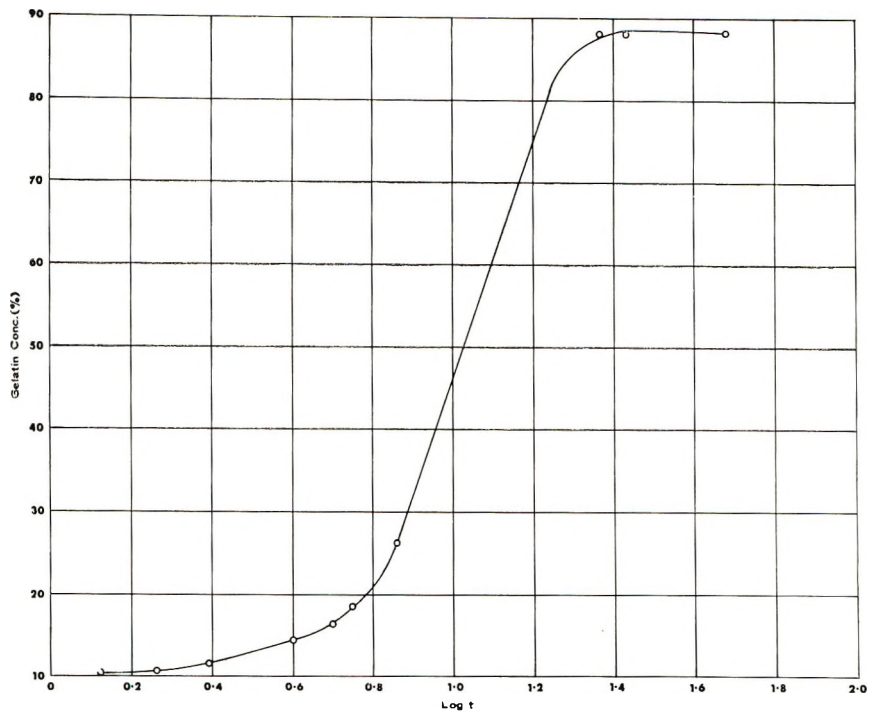
Fig. 2. Gelatin concentration plotted against logarithm of time, in hours, for a gelatin film dried at 21°C. and 50% relative humidity.

It may be noted that the temperature of the film will be equal to the wet-bulb temperature of the drying air in the early stages but toward the end will rise to the dry-bulb temperature of the air.

A series of measurements of a 10% gel was made, and the change in rotation with time was compared with that of a film, both samples being maintained at 21°C. (Fig. 5).

DISCUSSION

Nature of Drying Process

In the present experiments the gelatin sample is initially in the form of a 10% gel. As drying proceeds, the optical rotation of the film begins to change much more rapidly than in the case of the 10% gel of unchanged moisture content. The higher rate of change of rotation in the films is obviously caused by bringing the polypeptide chains closer together and thus assisting the formation of the collagen fold. The slope of the curve of $[\alpha]_D$ versus log t tends to reach a maximum at values of log t between 0.6 and 0.8, corresponding to times of 4–6 hr. after the initial preparation of the film. Figure 2 indicates that at this stage the gelatin concentration in the film will be between about 15 and 22%. This appears to be the optimum condition for helix formation. As drying proceeds further, the slope
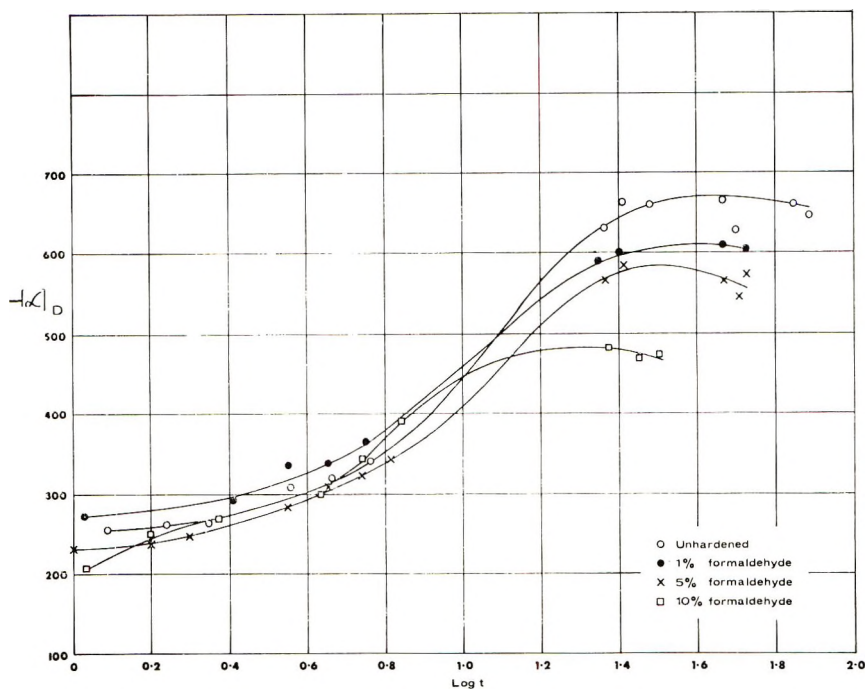
Fig. 3. Specific rotation plotted against logarithm of time, in hours, for formaldehyde-hardened gelatin films dried at 21°C. and 50% relative humidity.

levels off to a maximum of between $-600°$ and $-650°$. At the stage where the rate of increase in optical rotation starts to decline, the gel structure has probably become so rigid that changes in the conformation of the molecules are severly restricted. It has been found that after the drying process has been completed, the rotation of the film does not change significantly over periods of up to a week. These films are relatively slow drying, because of their thickness, and this may permit a higher degree of ordered structure than is obtained in thinner films.

The results illustrated in Figure 1 indicate that the maximum rotation does not vary significantly with temperature and humidity over a wide range, and it is only when the temperature rises to between 24 and 26°C. wet bulb that the rotation begins to decline appreciably. At the higher temperatures the drying takes place with the film largely in the sol form, and the molecules are unable to assume the helical conformation.

In addition to the work already described in this paper experiments have been carried out on several different types of gelatin, in both gel and dry-film form. As films the gelatins showed no significant differences in optical rotation, but in the gel form quite substantial differences were observed. The highest negative rotation was manifested by the gelatin used in the main body of this work, viz. an acid-processed pigskin gelatin, whereas that giving the lowest rotation was an alkaline-processed calfskin gelatin. The difference in specific optical rotation between these two materials was of the
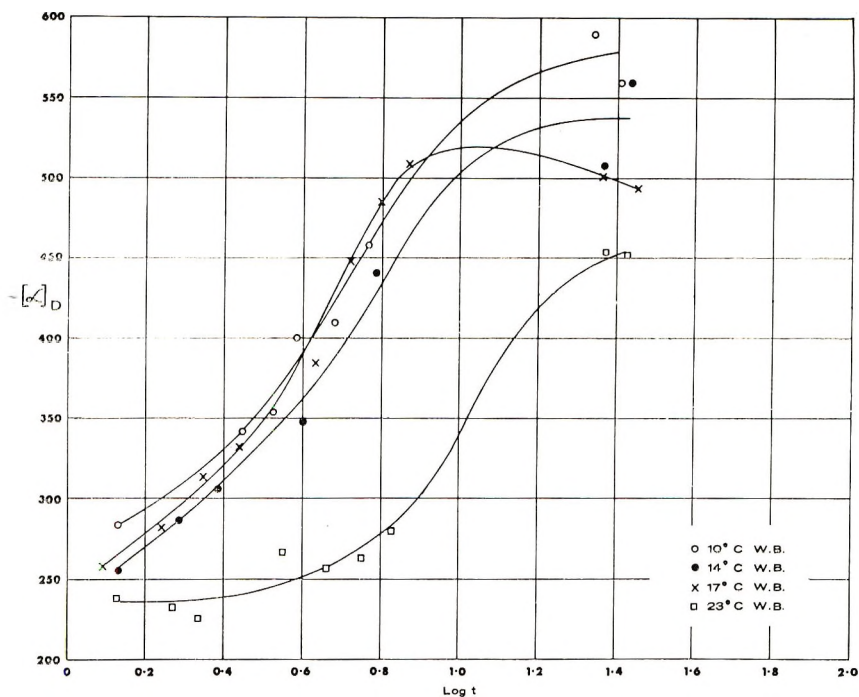
Fig. 4. Specific rotation plotted against logarithm of time, in hours, for films hardened with 5% formaldehyde and dried under various conditions of temperature and humidity. W. B., wet bulb.

order of 35%. Little information is available on the molecular composition of the various gelatins investigated, although work in progress in this laboratory is designed to obtain more data on this point. However, it is interesting to note that the pigskin gelatin had the highest viscosity (1.07 cpoise for a 1% solution at 40°C.) and thus probably the highest molecular weight, while the lime-processed calfskin gelatin had the lowest viscosity (0.85 cpoise). It may be that the pigskin gelatin has a higher proportion of two-chain (β) and three-chain (γ) molecules than does the calfskin gelatin; Veis has indicated[11b] that in general acid-processed gelatins have more covalent crosslinks than alkaline-processed gelatins. If this is true, then gelatins with more multichain molecules may initially form helices more rapidly. However, the structure achieved in the dry state is much the same for various types of gelatin, regardless of these molecular differences.

Effect of Hardeners

The effect of hardeners, or chemical crosslinking agents, on the structure of gelatin films is of considerable interest, since many of the uses of gelatin require some degree of hardening. It was therefore thought to be of interest to study the effects on optical rotation of two common organic hardeners, formaldehyde and mucochloric acid. The results showed that hardener
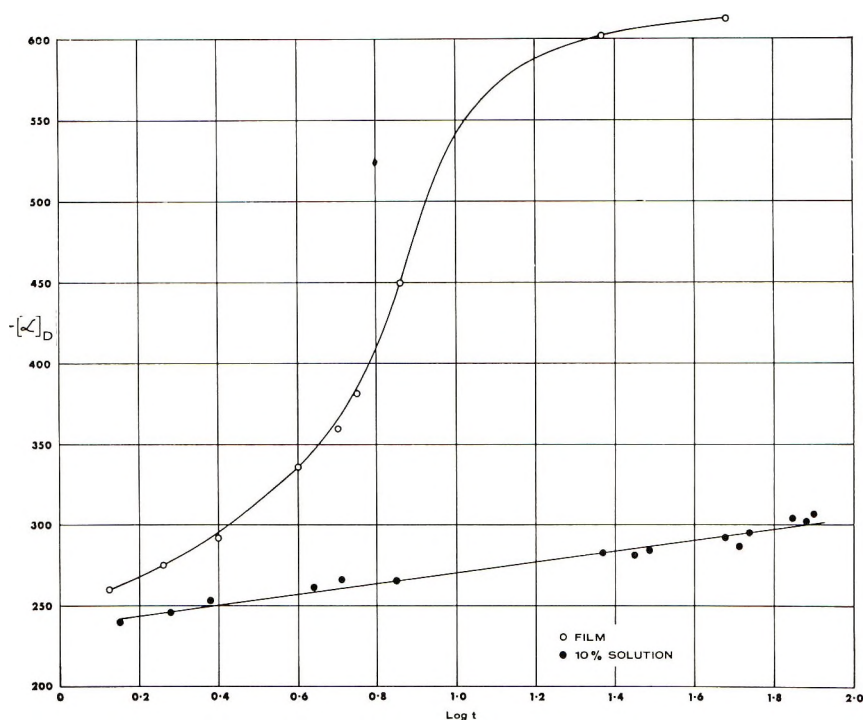
Fig. 5. Specific rotation plotted against logarithm of time, in hours, for a film dried at 21°C. and 50% relative humidity and a 10% gel maintained with constant moisture content at 21°C.

concentrations of greater than 1% of the dry weight of gelatin caused considerable depression of the optical rotation.   It was also found that for a given hardener concentration the rotation tended to drop as the temperature of the drying air was raised, contrasting with the behavior of unhardened films in the same temperature range.   These two effects may be explained by restrictions on the rearrangement of the polypeptide chains, resulting from the formation of stable interchain crosslinks by the hardeners, which stabilize the chains in a comparatively random structure and inhibit the natural tendency to the assumption of the collagen fold. Hardening that takes place before drying has been substantially completed must be regarded as a hindrance to the formation of a well-ordered structure in the film.

References

1. C. Cohen, *J. Biophys. and Biochem. Cytol.*, **1**, 203 (1955).

2. V. A. Pchelin, V. N. Izmailova, and V. P. Merzlov, *Dokl. Akad. Nauk SSSR*, **150**, 1307 (1963).

3. V. A. Pchelin, V. N. Izmailova, and V. P. Merzlov, *Vysokomolekul. Soedin.*, **5**, 1429 (1963).

4. J. W. Janus, *Recent Advances in Gelatin and Glue Research*, G. Stainsby, Ed., Pergamon Press, New York, 1956, p. 214.

5. J. W. Janus, B. E. Tabor, and R. L. R. Darlow, *Kolloid-Z.*, **205,** 134 (1965).

6. M. P. Drake and A. Veis, *Biochem.*, **3,** 135 (1964).

7. K. A. Piez and A. L. Carrillo, *Biochem.*, **3,** 907 (1964).

8. C. Robinson and M. J. Bott, *Nature*, **168,** 325 (1951).

9. O. Gerngross, K. Herrmann, and K. Lindemann, *Kolloid-Z.*, **60,** 276 (1932).

10. E. M. Bradbury and C. Morton, *Proc. Roy. Soc.*, **A214,** 183 (1952).

11. A. Veis, *The Macromolecular Chemistry of Gelatin*, Academic Press, New York–London, 1964; (a) p. 359; (b) p. 216.

Polylactones Derived from Polymethacrolein and Styrene–Methacrolein Copolymerizations

W. E. SMITH, G. E. HAM,* H. D. ANSPON, S. E. GEBURA,† and
D. W. ALWANI,‡ *Gulf Research and Development Company, Kansas City Laboratory, Merriam, Kansas 66202*

Synopsis

Emulsion polymerization of methacrolein produces a polyacetal which can be converted through the action of sodium hydroxide to an alternating copolymer of methallyl alcohol and sodium methacrylate. Support for the alternating structure was gained primarily through a study of the polylactone formed through subsequent acidification of the sodium salt. Thus, the poly(methallyl alcohol–sodium methacrylate) copolymer was acidified under selected conditions to give a soluble polylactone containing 14.2 mole-% of residual acid and hydroxyl groups. This number agrees quite closely with the value of 13.5 mole-% which one would predict from the random cyclization of a true alternating copolymer. Cyclization of a random copolymer of poly(methallyl alcohol–sodium methacrylate) in a random fashion would have resulted in a value of about 36.8 mole-%. The results also support both the 1,2 vinyl polymerization of methacrolein and a nonrandom attack of the polymethacrolein by base. In a completely separate set of experiments, the value of r_1 and r_2 for the copolymerization of styrene (M_1) and methacrolein (M_2) were determined to be 0.22 ± 0.02 and 0.88 ± 0.02, respectively.

INTRODUCTION

Methacrolein, one of the more reactive vinyl monomers, undergoes either polymerization or copolymerization with a variety of catalysts including peroxides,[1] boron trifluoride,[2] sodium naphthalene,[3] alkali metal nitrites,[4] organometallics,[5] sodium metal,[6] or by heat[7] alone. Polymers containing methacrolein units have been modified through reaction with such materials as hydrogen cyanide,[8] sodium hydroxide,[9] hydrogen,[10] acid anhydrides,[11] and hexamethylenetetramine.[12] Although this list of references is far from complete, it illustrates the versatility of methacrolein, in both polymerization and post-polymerization reactions. Despite this versatility, only scant attention has been directed toward elucidating the basic chemistry associated with this monomer.

Therefore, this contribution is offered to present some new and interesting experimental facts on: (a) polylactones derived from polymethacrolein

---

and (b) styrene–methacrolein copolymerizations. Moreover, the data derived from a study of polylactones derived from polymethacrolein will be shown to contribute strong evidence for the 1,2 vinyl polymerization of methacrolein, as well as yielding information on the nature of the reaction of polymethacrolein with base. Finally, we have attempted to put methacrolein in its proper perspective with respect to its reactivity with other monomers and, more specifically, in relation to its relative reactivity with the styrene radical. The latter discussion is based on the well-known concepts of relative reactivity ratios, r_1 and r_2, and Q, and e values.

EXPERIMENTAL

Reagents

Methacrolein (99 wt.-%) was dried over calcium chloride, filtered, and fractionated to obtain a fraction boiling at 67°C. Gas chromatography showed this material to have a purity of 99.9 wt.-%, with the main impurities being isobutyraldehyde and a trace of acetone.

Styrene monomer was washed with 5 wt.-% sodium hydroxide solution, dried over anhydrous magnesium sulfate, and distilled. The fraction boiling at 45°C./20 mm. Hg was collected for polymerization.

All other reagents were used, as received, from the suppliers.

Methacrolein Homopolymerizations

Methacrolein was polymerized under a nitrogen atmosphere in a 1-liter, three-necked flask. A solution of 3.0 g. of sodium lauryl sulfate in 500 ml. of deionized water was purged with nitrogen and heated to 60°C. with stirring. About 100 ml. of a 2 wt.-% potassium persulfate solution was poured into the flask; then, during the next hour, 100 g. of freshly distilled methacrolein was added while the temperature was maintained at 65–70°C. Conversion of monomer to polymer, as determined by solids content, was 97 wt.-%. The product was a relatively unstable emulsion, and the polymer was readily isolated by a single freeze–thaw cycle followed by filtration. After several washes with deionized water and methanol, the polymer was dried in vacuo at 50°C. This polymer had an inherent viscosity of 0.18 dl./g. in dimethylformamide at 29°C.

Methacrolein was also mass polymerized in sealed tubes at temperatures from 25 to 65°C. by use of 0.06 wt.-% azobisisobutyronitrile as the initiator. The product was clear, colorless, and tough; in contrast to the emulsion, it contained a predominance of free aldehyde groups.

Polymethacrolein Modification

Polymethacrolein was reacted with aqueous sodium hydroxide (the Cannizzaro reaction) in a stirred autoclave. The charge—polymethacrolein, 70 g.; sodium hydroxide, 44 g.; and deionized water, 1000 ml.—was purged with nitrogen and then heated to 170°C for 3 hr. The product,

TABLE I

Influence of Time and Temperature of Acidification on Lactone Content

Sample no.	Time, hr.	Temperature, °C.	Neutralization equivalent, mg./meq.	Lactonization, mole-%
1	1	55	440	66.0
2	2	55	459	67.8
3	3	55	489	70.5
4	4	55	508	71.7
5	4.5	55	528	72.6
6	1.0	100	991	85.8

poly(methallyl alcohol–sodium methacrylate), was soluble in water and gave a viscous, pale-yellow solution.

The Cannizzaro product was divided into two portions. The first portion was heated to 50–52°C. and stirred gently while a sufficient quantity of a 20 wt.-% solution of sulfuric acid was added slowly to a pH of 0.1. Upon addition of the acid, the polymer precipitated as a white, easily filterable solid. Samples of this polymer were withdrawn as a function of aging time. The second portion of the Cannizzaro product was heated to
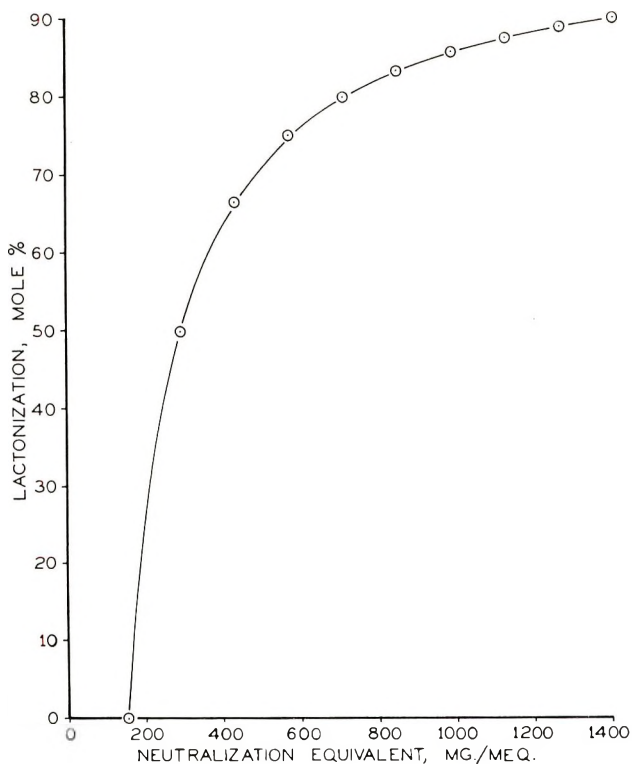
Fig. 1. Lactone content as a function of neutralization equivalent.

100°C., acidified to a pH of 0.1, and aged for 1 hr. The samples were dried overnight under vacuum at 50°C. Moisture analyses, both on a moisture balance and by Karl Fischer titrations, showed that the polymers contained about 1.0 wt.-% water. All of the polymers were soluble in cold dimethylformamide.

The amount of "free" acid remaining in the various samples of poly-lactone was determined through potentiometric titrations in pyridine by using tetrabutylammonium hydroxide dissolved in a 3:1 mixture of benzene and isopropanol as the titrant. Typical non-aqueous titration curves with sharp endpoints were obtained. The data, expressed as neu-tralization equivalents, or milligrams of polymer/milliequivalent of acid, are given in Table I; calculated lactone contents are also given. Neu-tralization equivalents can be conveniently converted to lactone contents by using the curve shown in Figure 1.

Styrene (M1)–Methacrolein (M2) Copolymerizations

Comonomer and azobisisobutyronitrile (0.100 wt.-%) mixtures were made up with the use of freshly distilled monomers which had been pre-viously purged with nitrogen. These samples were sealed into 14 mm. i.d. Pyrex tubes under a blanket of nitrogen. The tubes were placed in a cir-culating air oven at 60 ± 1°C. for 6 hrs. Copolymers were precipitated in a large excess of methanol; after being heated on a steam bath for 5 hr., they were isolated from the methanol by filtration, then soaked in fresh methanol for 2 days, again isolated by filtration, and dried *in vacuo* at 55°C. for 3 days. Table II lists compositions of the copolymers de-termined from carbon analyses, plus conversions and feed compositions. The conversion of monomers to polymer did not exceed 8.4 wt.-%.

TABLE II
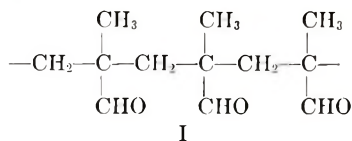Styrene (M_1)–Methacrolein (M_2) Copolymerization Data
($T = 60 \pm 1°C.$)

Monomer feed M_2, mole-%	Copolymer m_2, mole-%	Conversion, wt.-%
0.056	0.186	8.4
0.100	0.305	5.8
0.301	0.475	6.8
0.497	0.609	6.3
0.650	0.714	6.6
0.802	0.805	5.7
0.900	0.888	4.4

DISCUSSION OF RESULTS

Methacrolein Homopolymerizations

Methacrolein may be transformed readily into a polymer of a moderate molecular weight (ca. 10,000) by reaction at 25–65°C. with azobisiso-

butyronitrile. According to infrared analysis, the product—which is clear, colorless, and tough—appears to have the simple formula I,

$$-CH_2-\underset{\underset{CHO}{|}}{\overset{\overset{CH_3}{|}}{C}}-CH_2-\underset{\underset{CHO}{|}}{\overset{\overset{CH_3}{|}}{C}}-CH_2-\underset{\underset{CHO}{|}}{\overset{\overset{CH_3}{|}}{C}}-$$

I

that is to say, the pendant aldehyde groups predominate; only a few acetal linkages exist. The product is probably random in steric configuration although by analogy with poly(methyl methacrylate) prepared under similar conditions, it may have a somewhat higher syndiotactic content than would be expected from statistical considerations alone.
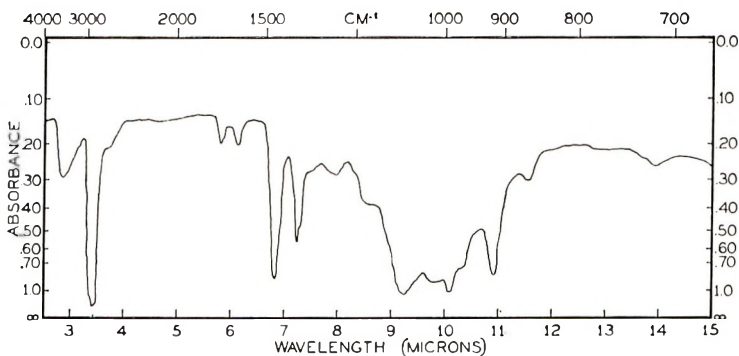
Fig. 2. Infrared spectrum of polymethacrolein.

Polymerization of methacrolein in emulsion at 65–70°C. with potassium persulfate as the initiator and sodium lauryl sulfate as emulsifier leads to a quite different product. An infrared spectrum of this type polymer, as taken in a Nujol mull, is recorded in Figure 2. The strong ether absorbance (9.25 μ), the moderately strong hydroxyl absorbance (2.9 μ), and the extremely weak carbonyl absorbance (5.8 μ) indicate the presence of stretches of cyclic ether groups terminated by hydroxyl groups, as represented by the structure II:

II
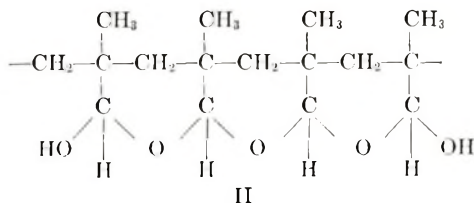
Structures like this have been previously reported for both polymethacrolein[13] and polyacrolein.[14] Such a structure would seem to require some stereoregularity in order to form, but molecular models show that the six-membered rings may be accommodated by either syndio- or isotactic

configurations. The syndiotactic form of the polyacetal is probably favored because it possesses the least amount of interaction of 1,3 axial methyl groups.

Polymethacrolein Modification

To investigate the possibilities of polylactone formation, a Cannizzaro reaction on polymethacrolein was run, followed by acidification. Treating the emulsion-polymerized polymethacrolein with caustic at 170–172°C. gave essentially quantitative conversion to poly(methallyl alcohol–sodium methacrylate), as seen by the spectrum in Figure 3. Absorbance was strong for sodium methacrylate groups at about 6.45 μ and equally strong for hydroxyl groups at about 2.9 μ; absorbances because of residual carbonyl (5.8 μ) and cyclic ether (9.25 μ) groups are extremely weak. More evidence for the completeness of the Cannizzaro reaction is gained from the experimental fact that a potentiometric titration showed that almost exactly one-half mole of sodium carboxylate groups was formed per mole of original aldehyde groups.

Acidification of the Cannizzaro product led to the ready formation of a high proportion of the polyactone structure as evidenced by a combination
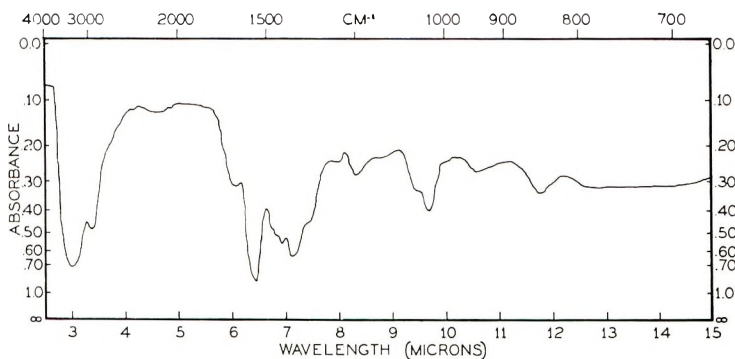

Fig. 3. Infrared spectrum of poly(methallyl alcohol–sodium methacrylate).
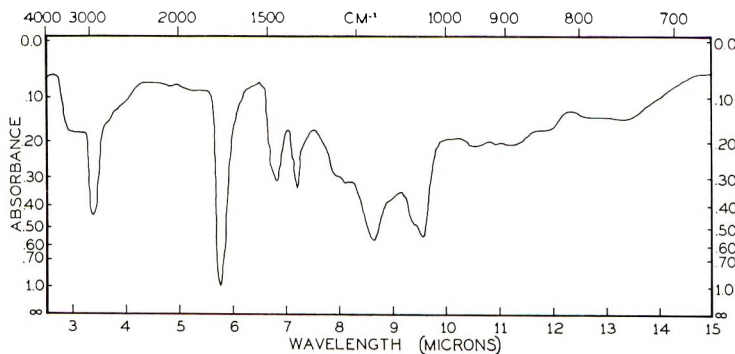

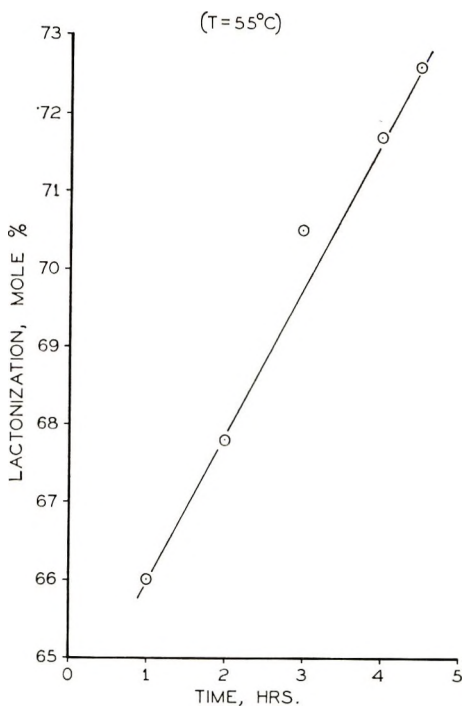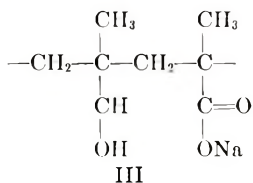Fig. 4. Infrared spectrum of the partial polylactone derived from polymethacrolein.

Fig. 5. Effect of aging time on lactone content.

of evidence from infrared spectra, a typical one being shown in Figure 4, and polymer solubility. That is to say, a strong absorption band exists at 5.8 μ, the frequency where δ-lactones are known to absorb; and all of the polymers were completely soluble in cold dimethylformamide, thus indicating very little, if any, inter-molecular reaction or crosslinking. This evidence strongly suggests an alternating structure for the poly(methallyl alcohol–sodium methacrylate) intermediate of the type III:

$$
\begin{array}{cc}
\mathrm{CH_3} & \mathrm{CH_3} \\
| & | \\
-\mathrm{CH_2-C-CH_2-C-} \\
| & | \\
\mathrm{CH} & \mathrm{C=O} \\
| & | \\
\mathrm{OH} & \mathrm{ONa} \\
\end{array}
$$

III

The regularity in structure probably relates to the ordered arrangement of ether groups in the precursor. Schulz et al.[15] have pointed out that a semiacetal-like intermediate (similar to the structure shown as II) is first formed when two molecules of a simple aldehyde react.

Let us now turn our attention to the extent of the lactonization reaction and its interpretation. When the poly(methallyl alcohol–sodium methacrylate) was acidified at 55°C. and allowed to age at the same temperature, the lactone content of the precipitated polymer increased from 66 mole-%

after 1 hr. to 72.6 mole-% after 4.5 hr. This is shown along with other data in Figure 5. The situation changes with reaction temperature; thus, when a sample of poly(methallyl alcohol–sodium methacrylate) solution was neutralized at 100°C. and aged at that temperature for 1 hr. the polymer was found to contain 85.8 mole-% lactone groups. Flory[16] presented a straightforward analysis of the proportion of isolated units to be expected when random coupling or elimination of 1,3 substituents occurs in a uniform 1,3 polymer. Applied to the present case, the number of residual acid and alcohol units under these conditions is predicted to be $1/e^2$ or 13.5 mole-%. The experimental value of 14.2 mole-% (100.0–85.8) obtained in this work is in excellent agreement with the predicted value and supports the idea that the poly(methallyl alcohol–sodium methacrylate) has an alternating structure which subsequently lactonizes in a random fashion.

If the methallyl alcohol and sodium methacrylate groups were randomly distributed in equimolar proportions along the polymer chains, hypothetically one would expect the following species in an individual chain: AB, AA, BA, BB, where A represents alcohol and B represents salt groups. Thus, half of the combinations present could lactonize (with some unit isolation), whereas the other half could not. This situation is a special case of the general treatment of Merz et al.[17] for copolymers, which states that "the proportion of isolated units is an inverse function of the probability of finding reactable pairs adjacent (1,3) to one another." More precisely, here, the proportion of isolated units equals $1/\exp\{P_{ab} + P_{ba}\}$ of $1/e = 36.79\%$. Alfrey et al.[18] have derived an expression for predicting the amount of lactonization to be expected from a hydrolyzed copolymer of vinyl acetate and acrylic acid which can also be applied to this situation and which gives identical results. Of course, the calculated figure is far too high for the experimental value obtained, so random placement of the alcohol and salt groups may be ruled out.

Although the possibility of head-to-head and tail-to-tail placements in polymethacrolein and derived products has not been mentioned, such possibilities probably can be neglected. This is not surprising, since no unequivocal evidence exists for such placements in the polymerization of conjugated monomers, such as methacrolein. Monomers of low conjugations, such as vinyl acetate, have been shown to undergo about 2% head-to-head placement.[19]

In summary, the structure of the polylactone can be represented by structures IV and V.

IV
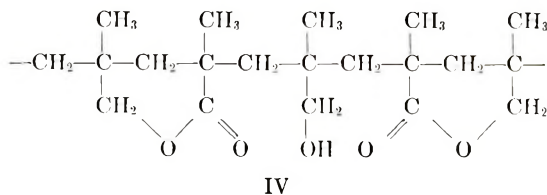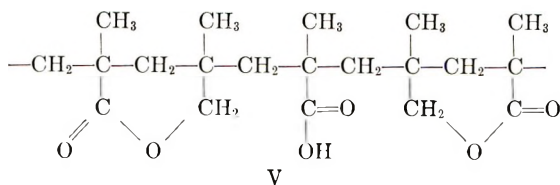
Without interchange reactions, which apparently do not occur under the conditions used, the percentage of isolated units approaches $1/e^2$ or 13.5%.

Styrene (M1)–Methacrolein (M2) Copolymerizations

How methacrolein behaves in copolymerization has received little attention. Haas and Simon[20] copolymerized methacrolein with acrylonitrile and reported that $r_1 = 2.0$ and $r_2 = 0.06$. Young[21] presumably used these values and calculated $Q = 1.75$ and $e = -0.01$. Schulz and co-workers[22] copolymerized methacrolein with methacrylonitrile in dimethylformamide solution and reported r_1 as equal to 1.78 ± 0.06 and r_2 as equal to 0.40 ± 0.04. Values of $Q = 1.59$ and $e = 0.36$ were calculated from these data.

Acrolein has also been studied.[22,23] Copolymerizations were carried out with acrylonitrile and acrylamide in both water and dimethylformamide solution; important differences in reactivity ratios were noted. These differences were attributed to changes in the partition of the monomers between the aqueous phase and precipitated polymer phase in the aqueous copolymerizations, as contrasted with the homogeneous copolymerization in dimethylformamide solution. Acrolein was also copolymerized with methacrylonitrile, 2-vinylpyridine, vinyl acetate, and methyl acrylate by these workers.

Schulz[23] attempted to calculate Q and e values for acrolein and methacrolein from these data, but his task was most difficult because the comonomers chosen were electropositive in character, except for 2-vinylpyridine. The 2-vinylpyridine presented experimental difficulties which did not allow calculation of meaningful Q and e values. Accordingly, Q values ranging from 0.20 to 0.99 and e values from 0.56 to 0.69 (an exception, 0.05, from acrylamide copolymerization) were obtained for acrolein and a Q value of 1.59 and an e value of 0.36 were obtained for methacrolein. Employing the data of Haas,[20] Schulz calculated Q to be 1.70 and e to be 0.26 for methacrolein.

It was desirable to endeavor to reach a more accurate evaluation of Q and e for methacrolein by using a definitely electronegative monomer, styrene, in copolymerization studies. The electron-withdrawing character of the carbonyl group is well established and styrene with its electron-rich double bond should allow good assessment of these parameters. Accordingly, mass copolymerizations of styrene and methacrolein were conducted at 60°C. in the presence of azobisisobutyronitrile and interrupted at low conversion by precipitation in methanol. Further details are described in the experimental section. The results of the copolymeriza-
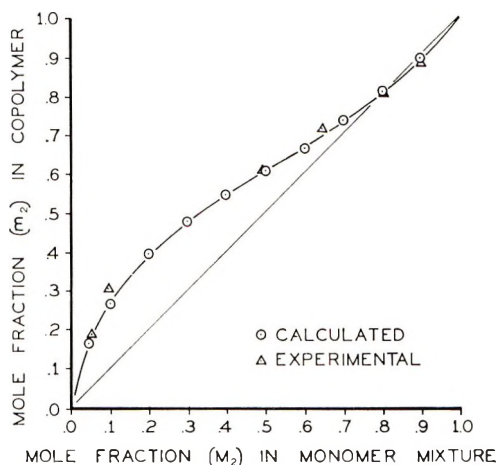
Fig. 6. Instantaneous copolymer composition as a function of monomer composition for the system styrene (M_1)–methacrolein (M_2), AIBN, 60°C.

tions were shown previously in Table II. Values for r_1 and r_2 were determined by curve-fitting of the data plotted in Figure 6 by the method of least squares. The best fit of the data for the system styrene–methacrolein was obtained when: r_1 (styrene) $= 0.22 \pm 0.02$, r_2 (methacrolein) $= 0.88 \pm 0.02$.

Calculation of e by means of the equation

$$e_2 = e_1 \pm (-\ln r_1 r_3)^{1/3}$$

yielded 0.48 and calculation of Q by the equation

$$Q_2 = Q_1/r_1 e^{-e_1(e_1 - e_2)}$$

yielded 1.63 based on styrene ($Q = 1.0$, $e = -0.8$).

TABLE III

Influence of α-Methyl Substitution on Q and e Values for Several Acrylic Monomers[a]

Monomer	e	Q
Acrolein	0.65	0.67
Methacrolein	0.48[b]	1.63[b]
Acrylonitrile	1.20	0.60
Methacrylonitrile	0.81	1.12
Methyl acrylate	0.60	0.42
Methyl methacrylate	0.40	0.74
Acrylic acid	0.77	1.15
Methacrylic acid	0.65	2.34
Acrylamide	1.30	1.18
Methacrylamide	1.24	1.46

[a] Data of Ham.[24]

[b] This work.

It is of interest to compare the values of Q and e for acrolein and methacrolein. In common with other systems, the presence of α-methyl substitution lowers e and increases Q (see Table III). The results strongly indicate the electropositive nature of acrolein and methacrolein arising from the electron-withdrawing character of the carbonyl group. Substantial conjugation, as seen from the high values of Q, is also indicated.

The relative reactivity of methacrolein with that of a number of other monomers[24] in competition with styrene is listed in Table IV. Methacrolein is 4.5 times as reactive as is styrene for a styrene radical and is very

TABLE IV
Relative Reactivities of Several Monomers Toward the Styrene Radical
(M_1 = styrene)[a]

M_2	$1/r_1$
Methacrylic acid	6.7
Methacrolein	4.5[b]
Acrylic acid	4.0
Methacrylonitrile	4.0
Acrylonitrile	2.5
Methyl methacrylate	1.9
Methyl acrylate	1.3

[a] Data of Ham.[24]
[b] This work.

close to the top of the list of the monomers listed. α-Methyl substitution enhances reactivity toward styrene in every case selected and the reactivity toward the styrene radical is in the order:

$$-COOH > -CHO > -CN > -COOCH_3$$

References

1. Monsanto Chem. Co., U.S. Pat. 2,889,311 (1959).

2. I. V. Andreeva, M. M. Koton, and K. A. Kovaleva, *Vysokomol. Soedin.*, **4**, 528 (1962).

3. M. M. Koton, I. V. Andreeva, and Yu. P. Getmanchuk, *Dokl. Akad. Nauk SSSR*, **155**, 836 (1954).

4. Shell Development Co., U.S. Pat. 2,809,185 (1957).

5. Asahi Kasei Kogoyo Kabushiki Kaisha, Belgium Pats. 603,087 and 603,088 (1961).

6. Badische Anilin- and Soda-Fabrik Akt.-Ges., German Pat. No. 889,227 (1953).

7. Dow Chemical Co., U.S. Pat. 2,256,152 (1941).

8. Monsanto Chem. Co., U.S. Pat. 2,833,743 (1958).

9. General Tire and Rubber, U.S. Pat. 2,999,830 (1961).

10. Monsanto Chem. Co., U.S. Pat. 2,893,979 (1959).

11. E. I. Du Pont de Nemours and Co., U.S. Pat. 3,000,862 (1961).

12. General Tire and Rubber, U.S. Pat. 2,651,624 (1953).

13. R. C. Schulz, *Kunststoffe*, **47**, 303 (1957).
14. E. I. Du Pont de Nemours and Co., U.S. Pat. 3,118,860 (1964).
15. R. C. Schulz, H. Vielhaber, and W. Kern, *Angew. Chem.*, **70**, 316 (1958).
16. P. J. Flory, *J. Am. Chem. Soc.*, **61**, 1518 (1939).
17. E. Merz, T. Alfrey, and G. Goldfinger, *J. Polymer Sci.*, **1**, 75 (1946).
18. T. Alfrey, C. Lewis, and B. Magel, *J. Am. Chem. Soc.*, **71**, 3793 (1949).
19. P. J. Flory and F. S. Leutner, *J. Polymer Sci.*, **3**, 880 (1948).
20. H. C. Haas and M. S. Simon, *J. Polymer Sci.*, **9**, 399 (1953).
21. L. J. Young, *J. Polymer Sci.*, **54**, 411 (1961).
22. R. C. Schulz, E. Kaiser, and W. Kern, *Makromol. Chem.*, **58**, 160 (1962).
23. R. C. Schulz, H. Cherdron, and W. Kern, *Makromol. Chem.*, **28**, 197 (1958).
24. G. E. Ham, *Copolymerization*, Interscience, New York, 1964.

NOTES

Preparation of Optically Active Polymethyl Vinyl Carbinol

INTRODUCTION

A number of works concerning the preparation of optically active polymers have been reported. Up to now optically active polymers have been obtained according to the following methods:[1-4] (*1*) polymerization of optically active monomers, (*2*) asymmetric induced polymerization of optically inactive monomers, (*3*) asymmetric selective polymerization of racemic monomers, (*4*) reactions of optically inactive polymers with optically active, low molecular weight compounds, (*5*) separation of polymers obtained from racemic monomers into fractions having optical activity of opposite sign, and (*6*) reactions of optically inactive polymers containing functional groups, producing asymmetric carbon atoms.

In this work the preparation of an optically active polymer according to the last method was attempted. The asymmetric reduction of optically inactive polymethyl vinyl ketone (hereinafter abbreviated to PMVK) was carried out with lithium borneoxyl aluminohydride,

$$\left[LiAl \left(O - \bigtriangleup \hspace{-0.2em}\bigcirc \right)_n H_{4-n} \right]$$
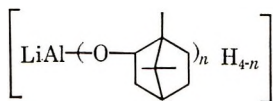
as a reducing agent, and polymethyl vinyl carbinol (hereinafter abbreviated to PMVC) was obtained.

The PMVC was optically active, and its rotatory dispersion was found to fit the simple Drude equation over a range between 450 and 589 mμ, and the λ_c values were 169 and 173 mμ. The rotatory power of the PMVC increased with an increase in the molar ratio of *d*-camphor to LiAlH$_4$.

As a reference reduction, the reduction of methyl ethyl ketone (hereinafter abbreviated to MEK) was carried out in diethyl ether with lithium borneoxyl aluminohydride, which was prepared from LiAlH$_4$ and *d*-camphor, and optically active methyl ethyl carbinol (hereinafter abbreviated to MEC) was obtained. The optical rotatory dispersion of MEC was measured over a range between 280 and 480 mμ and was found to fit the simple Drude equation, and the λ_c values were 173 and 171 mμ.

EXPERIMENTAL

Reagents

THF and diethyl ether were dried over calcium chloride for several days, refluxed with the sodium wire, and used immediately after distillation. LiAlH$_4$ and *d*-camphor were commercially obtained reagents, and they were used without further purification. The value of [α] for the *d*-camphor used was +42.4 in ethanol. MEK was distilled by means of a fractionating column packed with fine stainless-steel coils.

Preparation of Polymethylvinylketone (PMVK)

The polymerization of 80 ml. of methyl vinyl ketone, which had been distilled under N$_2$ (760 mm. Hg), was carried out in 250 ml. of acetone with 4.5 g. of AIBN as catalyst,

at about 52°C. under N₂. The PMVK was purified by precipitation from THF with water. The PMVK obtained was soluble in acetone and THF but insoluble in water. The intrinsic viscosity [η] of the polymer was 0.261 in THF at 30°C.

Asymmetric Reduction of Methylethylketone (MEK)

A solution of d-camphor in diethyl ether was added dropwise to a vigorously stirred solution of LiAlH₄ in diethyl ether over a period of 30 min. in a three-necked flask. After the addition was complete, the reaction mixture was stirred and heated under reflux for 1 hr., and an ether solution of MEK was added dropwise to the vigorously stirred reaction mixture. After the addition was complete, the reaction mixture was stirred and heated under reflux for 2 hr. and allowed to stand overnight at room temperature. A 10% aqueous solution of hydrochloric acid was added to the reaction mixture. The ether layer was separated, and the aqueous layer was extracted with ether.

After combining, the ether solution was distilled off, and the residue was distilled under reduced pressure to give a volatile distillate. The fractional distillation of this volatile part was carried out twice with a fractionating column consisting of a tube with a side arm packed tightly with fine stainless-steel coils, and MEC of b.p. 99.5–100°C. was obtained. The MEC obtained was purified further by gas chromatography with a 6.4 m. polyethylene glycol column at 130°C. and helium at an inlet pressure of 1.4 kg./cm.², and it was found that the product consisted of only one compound.

Asymmetric Reduction of Polymethylvinylketone

A solution of d-camphor in diethyl ether was added dropwise to a vigorously stirred solution of LiAlH₄ in THF over a period of 30 min. in a three-necked flask. After the addition was complete, the reaction mixture was stirred and heated under reflux for 1 hr., and a THF solution of PMVK was added dropwise to the vigorously stirred reaction mixture. After the addition was complete, the reaction mixture was stirred and heated under reflux for 2 hr. and allowed to stand overnight at room temperature. A 10% aqueous solution of hydrochloric acid was added to the reaction mixture and stirred, to separate the polymer. The polymer obtained was purified by precipitation from ethanol with petroleum ether. The precipitation was carried out until the rotatory dispersion of the polymer showed a constant value. The optical rotatory properties were determined with a spectropolarimeter, Shimazu Model QV-50, equipped with a xenon lamp source. The viscosity measurements of these polymers were made in an Ubbelohde capillary viscometer at 30°C.

Measurement of Reduction Percentage of PMVC

The reduction percentage of PMVC was determined by infrared spectral analysis. The infrared spectrum of PMVC was measured with the use of a KBr disk on a photospectrometer, Perkin-Elmer Model 337. The reduction percentage, R, was obtained from the following equation:

$$R = (1 - C_{PMVC}/C_{PMVK} \ C) \times 100$$

where C is the absorption intensity of the carbonyl group of the polymer. It is the ratio of the peak intensity at 1715 cm.⁻¹, due to the carbonyl group, to that at 2925 cm.⁻¹ due to the methylene group.

RESULTS AND DISCUSSION

Preparation of Optically Active Methylethylcarbinol

The asymmetric reduction of MEK was carried out with LiAlH₄ and d-camphor, and the MEC obtained was optically active. The results and experimental conditions are summarized in Table I. The absolute value of [α] for MEC increased with increasing molar ratio of d-camphor to LiAlH₄: i.e., $1 \rightarrow 2 \rightarrow 3$.

TABLE I

Asymmetric Reduction of Methyl Ethyl Ketone (MEK) with LiAlH$_4$ and *d*-camphor

Reduction conditions[a]				Methyl ethyl carbinol (MEC)				Optical purity,[c] %
Run no.	Camph.-/LiAlH$_4$	LiAlH$_4$/MEK	(H)-/MEK	b.p., °C.	n_D^{24}	Yield, %	$[\alpha]_D^{15}$ [b]	
A	0	1.5	6	99.5–100	1.3968	57.1	0	—
B	1	1.5	4.5	99.5–100	1.3969	78.8	−0.26	1.9
C	2	1.5	3	99.5–100	1.3962	60.5	−0.30	2.2
D	3	1.5	1.5	99.5–100	1.3962	60.5	−0.31	2.3
E[d]	2	1	2	99.5–100	1.3975	67.6	+2.50	18.0

[a] At 0–25°C. for 20 hr. in diethyl ether.
[b] Observed at 1 = 0.2 dm. (neat).
[c] Calculated from (−)-MEC $[\alpha]_D^{25}$ − 13.5°; Lenox and Lucas.[5]
[d] Bothner-By.[6]

Bothner-By[6] has reported that the value of [α] for the MEC obtained in similar conditions is +2.5, but Portoghese[7] has found that the optically active MEC could not be obtained by the same method.   Bothner-By has expressed his agreement with Portoghese's results concerning the absence of asymmetric induction in the d-camphor–LiAlH$_4$ reduction of MEK and pinacolone.   From these results he[7] thought that AlH$_4^{\ominus}$ could act as the reducing species even in the presence of a substantial quantity of alkoxyhydride anion, since Al(OR)H$_3^{\ominus}$ is not as effective a reducing agent.[8]
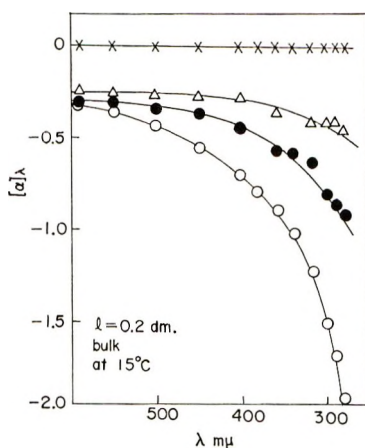
Fig. 1. Rotatory dispersions of optically active methyl ethylcarbinol (MEC). d-Camphor/LiAlH$_4$: (×) run A, = 0; (△) run B, = 1; (●) run C, = 2; (○) run D, = 3.
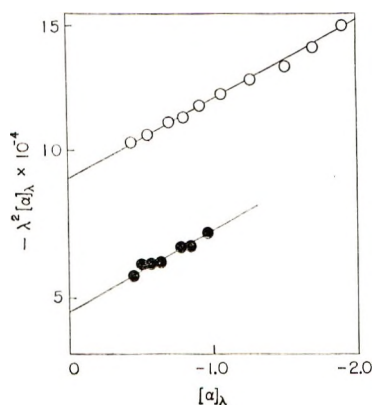
Fig. 2. Simple Drude dispersions of optically active methylethylcarbinol (MEC), simple Drude equation $[\alpha] = A/\lambda^2 - \lambda_c^2$. d-Camphor/LiAlH$_4$: (●) run C, 2 λ_c = 173 mμ; (○) run D, 3, λ_c = 171 mμ.

In this work the [α] for the resulting MEC, which was found to be pure by gas chromatography, lay in the range between −0.26 and −0.31 for runs B, C, and D, and therefore the optical purity of l-MEC was calculated to be approximately 2%.

The rotatory dispersion curves of the MEC obtained were measured over a range between 280 and 480 mμ as shown in Figure 1. The rotatory dispersion curves were found to fit the simple Drude equation, as shown in Figure 2.   The λ_c values were 173 mμ for run C and 171 mμ for run D.
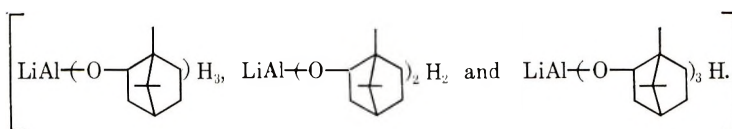
The formation of
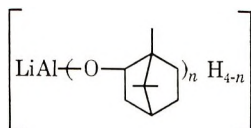
increased with increasing molar ratio of d-camphor to LiAlH$_4$. From the relationship between the value of [α] for the MEC and the molar ratio of d-camphor to LiAlH$_4$ it was thought that
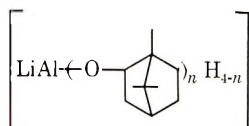
reacted with MEK as the reducing agent. It consists[9] of

Preparation of Optically Active Polymethylvinylcarbinol

The asymmetric reduction of PMVK was carried out with LiAlH$_4$ and d-camphor, and optically active PMVC was obtained. The polymer was purified by repeating the reprecipitation until the value of [α] became constant.

In Table II the relationship between the values of [α] for the resulting PMVC and

TABLE II
Asymmetric Reduction of Polymethyl Vinyl Ketone[a] (PMVK) with LiAlH$_4$ and d-Camphor

| Run no.	Reduction conditions[b]			Polymethyl vinyl carbinol (PMVC)		
	Camph./ LiAlH$_4$	LiAlH$_4$/ PMVK	(II)/ PMVK	[η][c]	Reduct.,[d] %	$[α]_D^{15}$[e]
A-3	0	0.75	3	0.345	87.6	0
B-3	1	1	3	0.349	84.1	−1.6
C-3	2	1.5	3	0.085	62.7	−9.2
D-3	3	3	3	0.155	62.6	−12.3

[a] [η] of PMVK was 0.261 in THF at 30°C.
[b] At 0–25°C. for 20 hr. in THF.
[c] Measured in ethanol at 30°C.
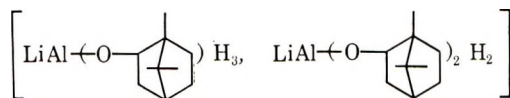[d] Calculated from infrared spectra.
[e] Measured in ethanol.

the molar ratio of d-camphor to LiAlH$_4$ is shown. The increase in the values of [α] for the PMVC with increase in the molar ratio of d-camphor to LiAlH$_4$ (i.e., 1 → 2 → 3) was observed, although the reduction percentage differed in each case. That is, the value of [α] for the PMVC obtained in the reduction with
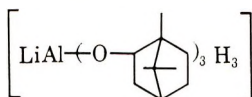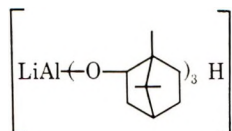
was largest (run D-3), and that for the PMVC obtained in the reduction with

$$\left[\text{LiAl} \left(\text{O} - \bigcirc \right) \text{H}_3 \right]$$
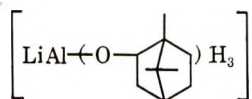
was smallest (run B-3).   It was thought that

$$\left[\text{LiAl} \left(\text{O} - \bigcirc \right) \text{H}_3, \quad \text{LiAl} \left(\text{O} - \bigcirc \right)_2 \text{H}_2 \right]$$

and

$$\left[\text{LiAl} \left(\text{O} - \bigcirc \right)_3 \text{H} \right]$$

would be formed, although the ratio between them might vary, depending on the ratio of d-camphor to LiAlH$_4$.   They would act as the reducing agent for the asymmetric syntheses, but LiAlH$_4$ would also take part in the reduction.

As shown in Table II, the PMVC obtained in run D-3 had the largest optical rotatory power in spite of the lowest reduction percentage and, on the other hand, the PMVC obtained in run B-3 had the lowest optical rotatory power in spite of the largest reduction percentage.   It was thought from this that

$$\left[\text{LiAl} \left(\text{O} - \bigcirc \right)_3 \text{H} \right]$$
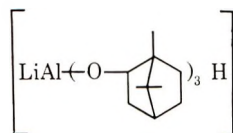
was a strong agent for the asymmetric induction but a weak one for the reduction.

The rotatory dispersion curves of the PMVC obtained are shown in Figure 3.   They are found to fit the simple Drude equation, as shown in Figure 4.   The λ_c values were 169 mμ for run C-3 and 173 mμ for run D-3.   These values are similar to those of optically active MEC (173 and 171 mμ).   Therefore the optical activity was thought to be due to PMVC itself and not to any impurity present.

TABLE III
Asymmetric Reduction of Polymethyl Vinyl Ketone[a] (PMVK)
with LiAlH$_4$ and d-camphor

| Run no. | Reduction conditions[b] | | | Polymethyl vinyl carbinol (PMVC) | | |
	Camph./ LiAlH$_4$	LiAlH$_4$/ PMVK	(H)/ PMVK	$[\eta]$[c]	Reduct.,[d] %	$[\alpha]_D^{15}$[e]
D-1	3	1	1	0.165	57.7	−2.7
D-2	3	2	2	0.113	54.1	−6.3
D-3	3	3	3	0.115	62.6	−12.3

[a] $[\eta]$ of PMVK was 0.261 in THF at 30°C.
[b] At 0–25°C. for 20 hr. in THF.
[c] Measured in ethanol at 30°C.
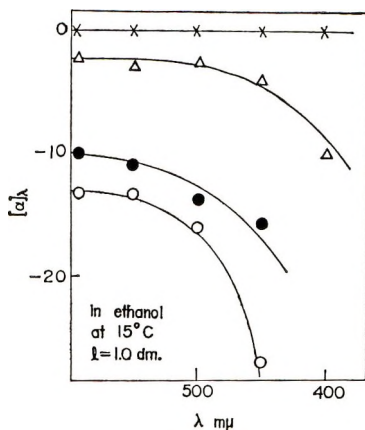[d] Calculated from infrared spectra.
[e] Measured in ethanol.

Fig. 3. Rotatory dispersions of optically active polymethyl vinyl carbinol (PMVC). d-Camphor/LiAlH$_4$ and c values (in grams per 100 ml.): ($\times$) run A-3, O, 0.33; ($\triangle$) run B-3, 1, 0.53; ($\bullet$) run C-3, 2, 1.0; ($\bigcirc$) run D-3, 3, 1.0.
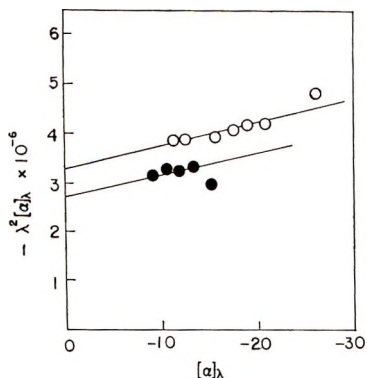

Fig. 4. Simple Drude dispersions of optically active polymethyl vinyl carbinol (PMVC), simple Drude equation $[\alpha] = A/\lambda^2 - \lambda_c^2$. d-Camphor/LiAlH$_4$: ($\bullet$) run C-3, 2, $\lambda_c = 169$ mμ; ($\bigcirc$) run D-3, 3, $\lambda_c = 173$ mμ.
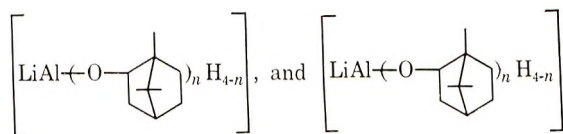
The asymmetric reductions in runs D-1, D-2, and D-3 were carried out with a constant molar ratio of LiAlH$_4$ to d-camphor, the amounts of the reducing agent being varied. As shown in Table III, the values of $[\alpha]$ for the PMVC increased with increasing amounts of camphor and LiAlH$_4$, but no correlation was observed between $[\alpha]$ and the extent of reduction, because the composition of
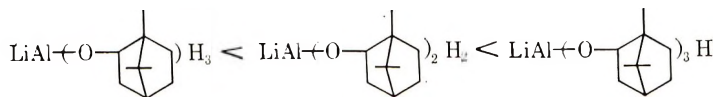
$$\left[\text{LiAl} \left(\text{O} - \begin{array}{c} \end{array} \right)_n \text{H}_{4-n} \right]$$
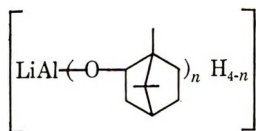
would not be constant.

Mechanism of Asymmetric Induction

In the reduction of a ketone with LiAlH$_4$ and d-camphor there are three possible reduction systems: LiAlH$_4$ alone, a mixture of LiAlH$_4$ and

$$\left[\text{LiAl} \leftarrow \text{O} - \bigodot)_n \text{H}_{4\text{-}n} \right], \text{ and } \left[\text{LiAl} \leftarrow \text{O} - \bigodot)_n \text{H}_{4\text{-}n} \right]$$

alone.   It was thought that in the reduction of MEK and PMVK with LiAlH$_4$ and d-camphor the reduction system would be the second one described above, and that the asymmetric inducing power of the reducing agents was in the following order:
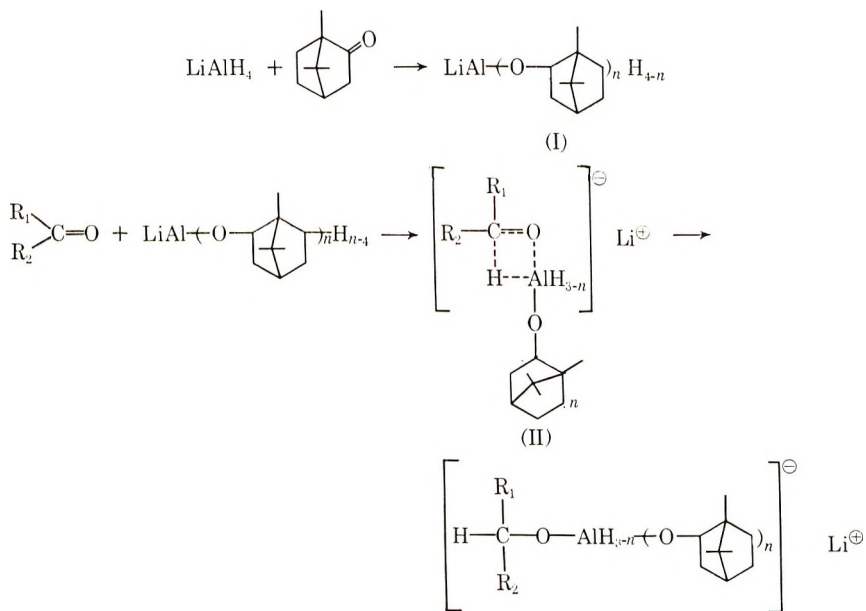
$$\text{LiAl} \leftarrow \text{O} - \bigodot) \text{H}_3 < \text{LiAl} \leftarrow \text{O} - \bigodot)_2 \text{H}_2 < \text{LiAl} \leftarrow \text{O} - \bigodot)_3 \text{H}$$

However, the reduction power was in the opposite order for the asymmetric inducing power.

Haubenstock and Eliel[9] have reported that the reducing agent is

$$\left[\text{LiAl} \leftarrow \text{O} - \bigodot)_n \text{H}_{4\text{-}n} \right]$$
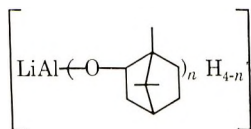
in the reduction of $trans$-3,3,5-trimethylcyclohexanone with LiAlH$_4$ and d-camphor. Therefore, the mechanism of the asymmetric reduction reaction of ketones with LiAlH$_4$ and d-camphor may be written as follows:

$$\text{LiAlH}_4 + \bigodot \text{O} \longrightarrow \text{LiAl} \leftarrow \text{O} - \bigodot)_n \text{H}_{4\text{-}n}$$

(I)

$$\begin{array}{c} R_1 \\ R_2 \end{array} \!\! C = O + \text{LiAl} \leftarrow \text{O} - \bigodot)_n H_{n\text{-}4} \longrightarrow \left[\begin{array}{c} R_1 \\ | \\ R_2 - C = O \\ | \\ H \text{-}\text{-}\text{-} \text{AlH}_{3\text{-}n} \\ | \\ O \\ \bigodot)_n \end{array} \right]^{\ominus} \text{Li}^{\oplus} \longrightarrow$$

(II)

$$\left[\begin{array}{c} R_1 \\ | \\ H - C - O - \text{AlH}_{3\text{-}n} \leftarrow \text{O} - \bigodot)_n \\ | \\ R_2 \end{array} \right]^{\ominus} \text{Li}^{\oplus}$$

The reduction of ketones with

$$\left[\text{LiAl} \!\left(\text{O} \!-\!\!\left<\!\!\raisebox{2pt}{\tiny$\boxplus$}\!\!\right>\!\right)_n \text{H}_{4-n} \right]$$

(I)
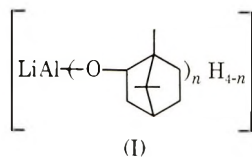
seems to involve the formation of two new bonds in the transition state (II):[10]   first, a bond between a hydrogen from the reagent and the carbon of the carbonyl group and, second, a bond between the metal of the hydride and the oxygen of the carbonyl group.

In the transition state the attack of the hydride anion on the oxygen of the carbonyl group will be influenced by the asymmetric group

$$\left[\left(\!\!-\!\text{O} \!-\!\!\left<\!\!\raisebox{2pt}{\tiny$\boxplus$}\!\!\right>\!\right) \right]$$
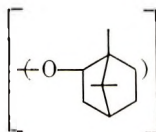
and thus the asymmetric induction will occur.

References

1. Y. Minoura, *J. Syn. Org. Chem. Japan*, **19**, 589 (1961).
2. J. Furukawa, *J. Syn. Org. Chem. Japan*, **22**, 2 (1964).
3. R. C. Schulz and E. Kaiser, *Advan. Polymer Sci.*, **4**, 236 (1965).
4. P. Pino, *Advan. Polymer Sci.*, **4**, 393 (1966).
5. P. J. Lenox and H. J. Lucas, *J. Am. Chem. Soc.*, **73**, 41 (1951).
6. A. A. Bothner-By, *J. Am. Chem. Soc.*, **73**, 846 (1951).
7. P. S. Portoghese, *J. Org. Chem.*, **27**, 3359 (1962).
8. H. C. Brown and R. F. Mcfarlin, *J. Am. Chem. Soc.*, **80**, 5372 (1958).
9. H. Haubenstock and E. L. Eliel, *J. Am. Chem. Soc.*, **84**, 2363 (1962).
10. O. R. Vail and D. M. S. Wheeler, *J. Org. Chem.*, **27**, 3803 (1962).

Yugi Minoura
Hidemassa Yamaguchi

Department of Applied Chemistry
Faculty of Engineering
Osaka City University
Osaka, Japan

Thermal and Mechanical Properties of Some Polysulfonates

Introduction

The formation of simple sulfonates from arylsulfonyl chlorides and phenols is well known and application of the reaction to the formation of polymers has been reported.[1-3] We prepared polysulfonates based on 1,3-benzene and 3,3'-benzophenone disulfonyl chlorides and 4,4'-isopropylidene diphenol in order to examine their thermal and mechanical properties. Of further interest was a polysulfonate based on a phosphorus-bearing disulfonyl chloride and a comparison of its properties with those of an analog based upon 3,3'-dichlorosulfonyl benzophenone.

Results and Discussion

The polysulfonates (Table I) were prepared by interfacial condensation with the use of methylene chloride as a solvent for the sulfonyl chloride and aqueous alkali for 4,4'-isopropylidene diphenol. Catalytic amounts of a quaternary ammonium salt, triethylbenzylammonium chloride, were utilized in the reaction as reported by Goldberg and Scardiglia.[1] The polysulfonates were generally obtained in good yields on adding the entire reaction mixture or, in some cases, just the organic phase to isopropyl alcohol. In the case of polysulfonates 2 and 3 based upon 1,3-benzenedisulfonyl chloride and 3,3'-dichlorosulfonyl benzophenone, one additional precipitation from methylene chloride solution by its addition to isopropyl alcohol gave analytically pure materials (Table I). A homopolymer 1 (Table I) based on 1,3-benzenedisulfonyl chlorine and resorcinol was also prepared, but it was not characterized due to insolubility. The polymer melt temperature was similar to that reported earlier by Thomson and Ehlers.[2]

The reaction mixture obtained from the reaction of bis(m-chlorosulfonyl phenyl) methylphosphine oxide and 4,4'-isopropylidene diphenol contained a crystalline white solid, which was essentially insoluble in both the organic and aqueous phases. On the basis of its elemental analysis and molecular weight it was tentatively formulated as a cyclic sulfonate (structure I). The infrared spectrum of the crystalline product failed to indicate the presence of hydroxy or sulfonic acid absorptions.

The PMR spectrum of I lent further support to the proposed cyclic structure, in that two overlapping singlets centered at τ 8.48, accounting for six protons, were observed. These absorptions are attributed to protons associated with the two methyl groups of the isopropylidene unit. Furthermore, two overlapping singlets were observed centered at τ 3.14, accounting for eight protons, and attributed to the protons associated with the two para-substituted phenylene groups. These results indicate non-equivalence of both the two methyl groups and the two para-substituted phenylene groups. The non-equivalence of the respective groups could be the result of their configuration in the proposed cyclic structure I.* The protons associated with the methyl group attached to phosphorus and those of the two meta-substituted phenylene groups gave the expected absorptions, a doublet centered at τ 7.84 and a complex multiplet centered at τ 1.84, respectively.

The crystalline solid (I) accounted for 20% of the starting materials. A low molecular weight amorphous polysulfonate (4) was recovered from the methylene chloride phase of the reaction mixture and accounted for 52% of the starting materials (Table I).

---

* In contrast the PMR spectrum of 4,4'-isopropylidene diphenol in CDCl₃ exhibits a singlet at τ 8.4 (isopropylidene group, 6 protons) and a typical AB pattern for the para-substituted phenylene groups (8 protons) centered at τ_B 3.28 and τ_A 2.88 (J_{AB} = 9.0 cps). A singlet at τ 5.34 accounted for two protons associated with the hydroxyl groups.

I
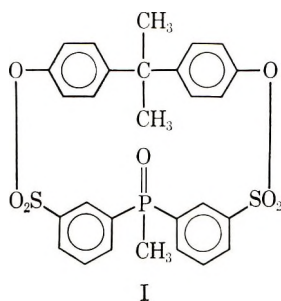
The polysulfonates (2, 3, and 4) were soluble in methylene chloride, dimethylformamide, and tetrahydrofuran at room temperature. The polymers (2 and 3) became sticky when treated at room temperature with benzene, ethyl alcohol, and acetonitrile. By using solution or melt-press techniques somewhat brittle films can be formed from polysulfonates 2 and 3. Films prepared from the polysulfonate (3) bearing the benzophenone moiety yellowed after several days at room temperature.

Polysulfonates (2 and 3) were analyzed by gel permeation chromatography. Tetrahydrofuran was used as the carrier solvent. Both polymers had bimodal molecular weight distributions. The distribution ratios, A_w/A_n were 19.8 and 29.2 for polymers 2 and 3, respectively. The ratios, excluding the low molecular weight fractions, were 2.67 and 2.02 for polymers 2 and 3, respectively. The intrinsic viscosities (Table I) are similar to those obtained by Goldberg and Scardiglia.[1] Thomson and Ehlers[2] obtained an inherent viscosity of 0.42 at a concentration of 0.25 g./dl. in DMF for a polysulfonate with an $\bar{M}_w$ of 50,000. The inherent viscosity of polymer 2 was 0.67 at a concentration of 0.25 g./dl. in THF, indicating an $\bar{M}_w$ in the range of a high polymer. The molecular weight of the amorphous polysulfonate (4) was determined in methyl ethyl ketone by vapor pressure osmometry to be 1609, corresponding to 2.8 recurring structural units.
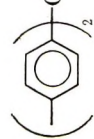
The polysulfonate (2) (Table I) was found by x-ray diffraction to be amorphous, while the polymer (3) based on chlorosulfonated benzophenone possessed some crystalline character. The crystalline and amorphous nature of the products from the reaction of bis-(m-chlorosulfonylphenyl) methylphosphine oxide with 4,4′-isopropylidene diphenol was also ascertained by x-ray diffraction.

In most cases the infrared absorption spectra of the polysulfonates exhibited the characteristic stretching vibrations for the sulfonate linkage (1185 and 1390 cm.$^{-1}$). However, in the case of the amorphous phosphorus-bearing polysulfonate and also the crystalline cyclic by-product (I) the phosphoryl absorption occurs in the same region (1195–1165 cm.$^{-1}$) as the symmetrical stretching vibration for the sulfonate linkage and consequently no definite assignment can be made for the latter.
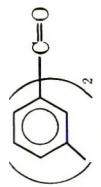
The thermal stability of the polysulfonates was evaluated by thermal gravimetric analysis (TGA) in dry air (Fig. 1). All the polysulfonates examined showed an initial relatively rapid weight loss between ca. 350 and 400°C. The polysulfonate (3) based on chlorosulfonated benzophenone and 4,4′-isopropylidene diphenol was the most thermally stable polymer of the three examined. Polysulfonates 2 and 3 underwent weight losses of ca. 28 and 20%, respectively, between 350 and 400°C. If one assumes that cleavage occurs at the sulfonate linkage with the evolution of sulfur dioxide as postulated by Thomson and Ehlers,[2] the observed weight losses for 2 and 3 compare favorably with the calculated values, 30 and 24%, respectively, assuming complete desulfurization. The polysulfonate (3) prepared from chlorosulfonated benzophenone and 4,4′-isopropylidene diphenol failed to show any differences when heated in dry air or in nitrogen.

The low molecular weight, amorphous polysulfonate (4) based on bis-(m-chlorosulfonylphenyl) methylphosphine oxide was least stable. In addition, the actual weight loss (32% by weight) up to 400°C. was significantly greater than that calculated for com-

TABLE I

Polysulfonates $+O_2S-Ar-SO_2-O-Ar'-O+_x$ Prepared by Interfacial Polycondensation with Methylene Chloride as the Organic Solvent[a]

Polymer no.	Reactants		Yield, %	Polymer melt temperature, °C	Polysulfonate					
	Sulfonyl chloride Ar (mole)	Phenol Ar' (mole)			Analysis, calcd. (found)				[η][b]	Crystallinity (x-ray diffraction)
					C, %	H, %	P, %	S, %		
1	(dimethylphenyl) (0.04)	(methylphenyl) (0.04)	78	145–200	—	—	—	—	—	—
2	(dimethylphenyl) (0.20)	(bisphenol, —C(CH₃)₂—) (0.20)	98 82[c]	185–205	58.59 (58.40)	4.21 (4.18)	—	14.90 (15.00)	0.36	Amorphous

No.	Structure			Yield[b]	[η]	M.p., °C	C	H	N	P		Form
3	(C=O)₂ ... C(CH₃)₂ (0.19) (0.19)			91	81°	185–215	62.90 (62.04)	4.15 (4.15)	— —	12.00 (12.08)	0.27	8% Crystalline[d]
4	(O=P–CH₃)₂ ... C(CH₃)₂ (0.02) (0.02)			52		174–196	59.14 (58.68)	4.43 (5.14)	5.45 (5.38)	11.28 (11.70)	—[e] —	Amorphous

[a] The reactions were carried out in the presence of a slight excess of sodium hydroxide, 2.5% in excess of that required to neutralize the theoretical amount of hydrogen chloride available. In addition, 2 drops of an aqueous 60% triethylbenzylammonium chloride were used for each 0.01 mole of reactant.

[b] Intrinsic viscosity values were obtained from determinations made in THF at 30°C.

[c] Yield after one precipitation from methylene chloride solution by addition to isopropyl alcohol.

[d] The value represents a relative per cent crystallinity and was determined according to a reported procedure.[4]

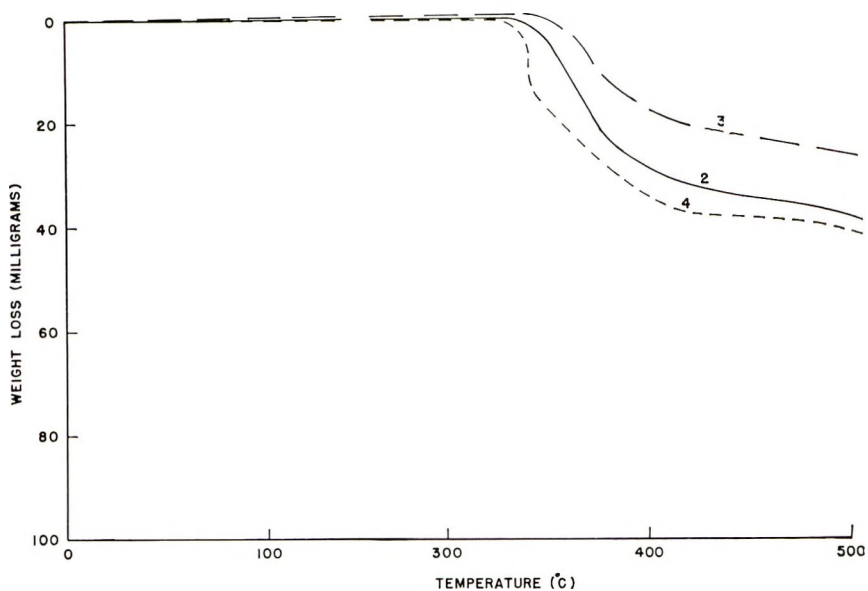[e] The molecular weight, as determined in THF by vapor phase osmometry, was 1609.

Fig. 1. Thermogravimetric curves of polysulfonates 2, 3, and 4 (Table I) to 500°C. at 6°C./min. in dry air.

plete desulfurization assuming sulfur dioxide evolution (22.5% by weight). This higher weight loss may be due to a concurrent reaction involving cleavage of the carbon–phosphorus bond. Berlin and Butler have reviewed[5] the cleavage of carbon–phosphorus bonds in tertiary phosphine oxides and report that under basic conditions and elevated temperatures cleavage may occur. Furthermore, they reported that the presence of electron-withdrawing groups on substituents attached to phosphorus apparently weaken the carbon–phosphorus bond. It is effects of this latter nature that may be influencing the stability of the phosphorus-bearing polysulfonate (4). The cyclic phosphorus-bearing sulfonate (I) gave a thermogram similar to that of its amorphous low molecular weight analog.

The thermomechanical spectra of polysulfonates prepared from the reaction of 3,3'-dichlorosulfonyl benzophenone and 1,3-benzenedisulfonyl chloride with 4,4'-isopropylidene diphenol are compared in Figures 2 and 3 with that for 4,4'-isopropylidene diphenol polycarbonate (Lexan). The glass transition temperature (T_g) of the polysulfonate based on chlorosulfonated benzophenone is 395°K. compared to Lexan at 421°K. The T_g of the polysulfonate based on 1,3-benzenedisulfonyl chloride is not clearly defined by the logarithmic decrement data of Figure 3 because this material was overcritically damped at temperatures above 375°K. This is probably due to its broad molecular weight distribution. The T_g appears to be at approximately 385°K. These T_g values agree well with softening temperatures reported by Goldberg for polysulfonates of similar structure.

Lexan, as well as both polysulfonates, have β transition temperatures in the range of 177–185°K. (Fig. 3). The structural unit common to all three polymers is the 4,4'-bisphenoxy isopropylidene group. Therefore, it is probable that the β transition is due to some motion of this group. The magnitude of the logarithmic decrement at the β transition temperature decreases from Lexan to the polysulfonate based on chlorosulfonated benzophenone. These differences may be due to the decreasing concentration of the 4,4'-bisphenoxy isopropylidene group in the repeat unit of the polymers.

The shear storage modulus is higher for the polysulfonates than for Lexan throughout the glassy region (Fig. 2), indicating that the polysulfonates are less flexible than Lexan.
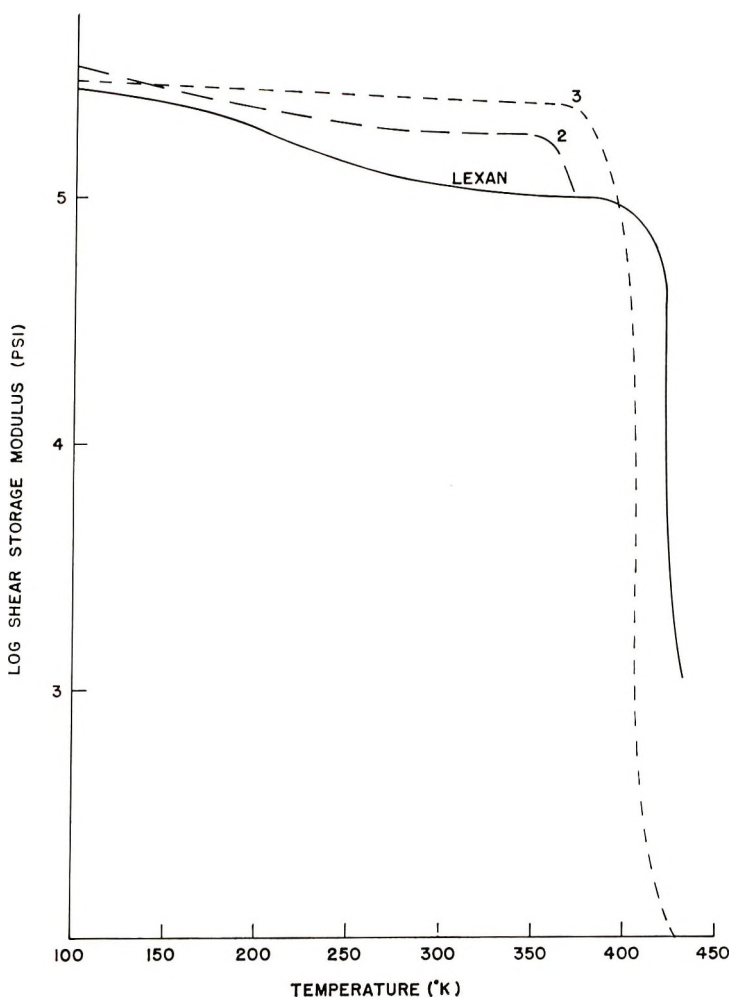
Fig. 2. Shear storage modulus of Lexan polycarbonate and polysulfonates 2 and 3 as a function of temperature.

Experimental

Melting and boiling points are uncorrected. Elemental analyses were carried out by Galbraith Laboratories, Inc., Knoxville 21, Tennessee. Infrared absorption spectra were obtained with a Perkin-Elmer spectrophotometer, Model 337. Molecular weight distribution determinations were carried out on a Waters Associates gel permeation chromatography unit. Molecular weights determined by vapor pressure osmometry were determined by using a Mechrolab vapor pressure osmometry, Model 301. Thermogravimetric analyses were performed on an American Instrument Co. Thermo-Grav in dry air and nitrogen. Samples were heated at the rate of 6°C./min. from 25 to 500°C. PMR spectra were determined on a Varian A-60 spectrometer with TMS as an internal standard. Chemical shifts are given on the τ scale in ppm relative to TMS ($\tau = 10.00$ ppm).

4,4'-Isopropylidene diphenol (bisphenol A) was purified by recrystallization from toluene (70 g./l.). Material melting at 155.5–158.5°C. was used in our work. Re-
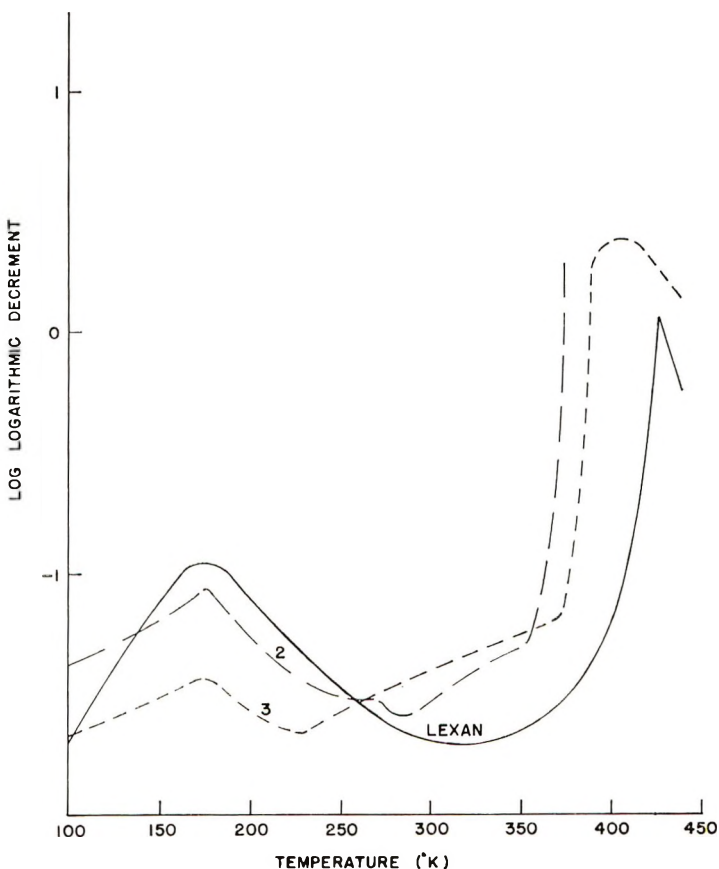
Fig. 3. Logarithmic decrement of Lexan polycarbonate and polysulfonates 2 and 3 as a function of temperature.

sorcinol was purified (m.p. 110-111°C.) by recrystallization from benzene (100 g./1500 ml.). Diphenylmethyl phosphine oxide, m.p. 107-112°C., was prepared in 77.7% yield by treatment of triphenylmethylphosphonium iodide with aqueous 40% sodium hydroxide. Triethylbenzylammonium chloride was obtained by refluxing equimolar amounts of triethylamine and benzyl chloride in acetone for 48 hr.

Preparation of 1,3-Benzenedisulfonyl Chloride. The disulfonyl chloride was prepared in 83.5% yield by using a procedure analogous to that reported[6] for benzenesulfonyl chloride. The crude disulfonyl chloride was purified by adding its concentrated chloroform solution to hexane. The filtered and dried product melted at 59-60.5°C. (reported[7] m.p. 63°C.).

Preparation of 3,3'-Dichlorosulfonyl Benzophenone. Benzophenone (92 g., 0.5 mole) was added in 30 min. to stirred freshly distilled chlorosulfonic acid (1175 g., 10.1 mole) at room temperature. Upon completing the addition, the reaction mixture was heated at 120°C. for 20 hr. The cooled dark amber reaction mixture was added to crushed ice and a cream-colored, finely divided solid precipitated which was dissolved in 1500 ml. of chloroform. The organic and aqueous layers were separated, and the latter was extracted two times with chloroform (50 ml. portions). The combined chloroform layers were washed consecutively with aqueous 10% sodium bicarbonate, cold water, and aqueous saturated sodium chloride. The dried chloroform layers were washed consecu-

tively with aqueous 10% sodium bicarbonate, cold water, and aqueous saturated sodium chloride. The dried chloroform solution was distilled at reduced pressure to remove solvent and left a residual oil that solidified on storage *in vacuo* overnight. The crude chlorosulfonated benzophenone (145.7 g.) melted at 118–133°C. Recrystallization once from a chloroform–hexane mixture and twice from chloroform gave 88 g. (42%) of analytically pure 3,3'-dichlorosulfonyl benzophenone, m.p. 139.5–141°C. (reported[8] m.p. 137–138°C.). Infrared absorptions (KBr) occurred at 1670 (s), 1590 (m), 1380 (s), 1275 (s), 1192 (s), 1175 (s), 982 (m), 743 (s), 713 (m), 636 (m), 583 (s), and 548 (s) cm.$^{-1}$.

ANAL. Calcd. for $C_{13}H_8Cl_2O_5S_2$: C, 41.17%; H, 2.13%; Cl, 18.70%; S, 16.91%; mol. wt. 379.2. Found: C, 40.94%; H, 2.14%; Cl, 18.89%; S, 16.81%; mol. wt. 385.5 (determined cryoscopically in benzene).

Preparation of Bis-(*m*-Chlorosulfonylphenyl) Methylphosphine Oxide. The above procedure was repeated with the use of 21.6 g. (0.1 mole) of diphenyl methylphosphine oxide and 175 g. (1.5 mole) of chlorosulfonic acid. The crude chlorosulfonated phosphine oxide (24.5 g.), a tan solid, melted at 157–162°C. Recrystallization of the crude product from benzene in the presence of decolorizing charcoal followed by two additional recrystallizations from benzene gave bis-(*m*-chlorosulfonylphenyl) methylphosphine oxide* (19.4 g.), m.p. 165–170°C. Infrared absorptions (KBr) occurred at 1420 (m), 1390 (s), 1320 (m), 1180 (s), 1128 (m), 1090 (m), 894 (m), 788 (m), 760 (m), 684 (m), 660 (m), 600 (m), 582 (m), 555 (s), 530 (m) and 513 cm.$^{-1}$.

ANAL. Calcd. for $C_{13}H_{11}Cl_2O_5PS_2$: Cl, 17.16%; P, 7.50%. Found: Cl, 17.14%; P, 7.36%.

General Procedure for the Preparation of Polysulfonates by Interfacial Polycondensation. The procedure reported by Goldberg and Scardiglia in two patents[1] was used in our work. In a typical example, a solution of the aryl disulfonyl chloride (0.02 mole) in 75 ml. of methylene chloride was added dropwise in ca. 1 hr. to a solution of the diphenol (0.02 mole) in 75 ml. of water containing 4 drops of aqueous 60% triethylbenzylammonium chloride and 0.041 mole of sodium hydroxide. The reaction was carried out at ca. 25–35°C. by using a Waring Blendor to obtain efficient mixing. After completing the addition, the reaction mixture was stirred for 2.5–3 hr. and then added to 500 ml. of cold isopropyl alcohol to precipitate the polysulfonate. The filtered product was then washed consecutively with water, isopropyl alcohol and ether. The crude polymer was precipitated once from methylene chloride solution by addition to isopropyl alcohol, washed as described above, and finally dried to constant weight *in vacuo*. The results obtained in the preparation of several polysulfonates are summarized in Table I.

Interfacial Polycondensation of Bis-(*m*-Chlorosulfonylphenyl) Methylphosphine Oxide with 4,4'-Isopropylidene Diphenol. The general procedure described above was repeated with the use of 0.02 mole of the chlorosulfonated phosphine oxide and 0.02 mole of 4,4'-isopropylidene diphenol. After 3 hr., the reaction mixture consisting of two liquid phases and a white solid was filtered. The filter cake was washed with fresh methylene chloride and dried to give 2.3 g. of crude crystalline cyclic sulfonate (I). The crude product (I) was precipitated from its solution in tetrahydrofuran by addition to petroleum ether. It melted at 313–318°C. The PMR spectrum of (I) in DMSO-d$_6$ solution gave the following absorptions: τ 8.48 [(CH$_3$)$_2$C—, two overlapping singlets, 6 protons], 7.84 (CH$_3$-P, doublet, J_{PCH} = 14 cps, 3 protons), 3.14 (*p*-C$_6$H$_4$O—, two overlapping singlets, 8 protons) and 1.84 ppm (*m*-C$_6$H$_4$SO$_2$—, complex multiplet, 8 protons).

---

* The *meta* substitution of the sulfonyl chloride group on the phenyl ring was not proven unequivocally. The point of substitution (*meta*) was based to some degree upon reported[5,9] results involving the nitration and chlorosulfonation of aryl phosphine oxides. In these latter cases *meta* substitution is the predominant course.

ANAL.   Calcd. for $C_{28}H_{25}O_7PS_2$ (I):   C, 59.14%; H, 4.43%; P, 5.45%; S, 11.28%; mol. wt. 568.   Found: C, 59.29%; H, 5.15%; P, 5.53%; S, 11.79%; mol. wt. 533 (determined in THF by vapor phase osmometry).

The methylene chloride aqueous filtrate from the main reaction mixture was added to isopropyl alcohol to precipitate the amorphous polysulfonate (4), 5.9 g. after washing and drying (Table I).

Mechanical Properties

The thermomechanical spectra of the polysulfonates and Lexan polycarbonate were obtained using a torsion pendulum.   Samples for use in the torsion pendulum were prepared by placing 4 g. of the powdered polymer in a $6 \times 0.38 \times 0.035$ in. stainless steel frame supported by Rexo Ferrotype plate.   The sample was separated from these plates with 5 mil Teflon sheets.   This assembly was placed in a Wabash press at 180°C. in the case of the polysulfonate (2) (Table I) and 200°C. in the case of polymer 3 (Table I). The assembly was heated for 4 min. with the top platen just touching the top plate of the assembly.   A 0.25 ton load on a 2 in. diameter ram was applied to the sample for 1 min.   A 6 ton load on a 2 in. diameter ram was next applied and then removed from the press.   The sample was removed from the frame at 100°C. in order to prevent cracking.   The resulting samples were slightly yellow and rather opaque.   A $3 \times 1 \times 0.125$ in. sample of each polymer was prepared in the same manner using the appropriate amount of material and frame.

References

1. E. Goldberg and F. Scardiglia, U.S. Pat. 3,236,808 (1966); U.S. Pat. 3,236,809 (1966).

2. D. Thomson and G. Ehlers, *J. Polymer Sci. A*, **2**, 1051 (1964).

3. P. W. Morgan, *Condensation Polymers by Interfacial and Solution Methods*, Interscience, New York, 1965, Chapt. 8.

4. D. R. Petersen, Research Report SL 87902, The Dow Chemical Co., Midland, Michigan, 1957.

5. D. Berlin and G. Butler, *Chem. Rev.*, **60**, 243 (1960).

6. H. Gilman and A. H. Blatt, Eds., *Organic Synthesis Collective Volume I*, Wiley, New York, 1941, p. 84.

7. T. Zincke and O. Krüger, *Ber.*, **45**, 3472 (1912).

8. A. Lapworth, *J. Chem. Soc.*, **73**, 405 (1898).

9. J. E. Herweh, *J. Org. Chem.*, **31**, 2422 (1966).

J. L. WORK
J. E. HERWEH

Research and Development Center
Armstrong Cork Company
Lancaster, Pennsylvania 17604

ERRATUM

Cyclocopolymerization of Dicyclic Dienes and Maleic Anhydride to Fused Ring Systems

(article in *J. Polymer Sci. A-1*, **5**, 1845, 1967)

By KLAUS MEYERSEN and JEAN Y. C. WANG, *Mellon Institute, Pittsburgh, Pennsylvania 15213*

The first sentence of the Introduction on page 1845 should read: Cyclocopolymerization with *cis,cis*-1,5-cyclooctadiene is the only reported case of a cyclocopolymerization of maleic anhydride (MA) and cyclic dienes.